DISCRETE SEMICONDUCTORS

Semiconductor Sensors

Data Handbook SC17
CD-ROM included
1998

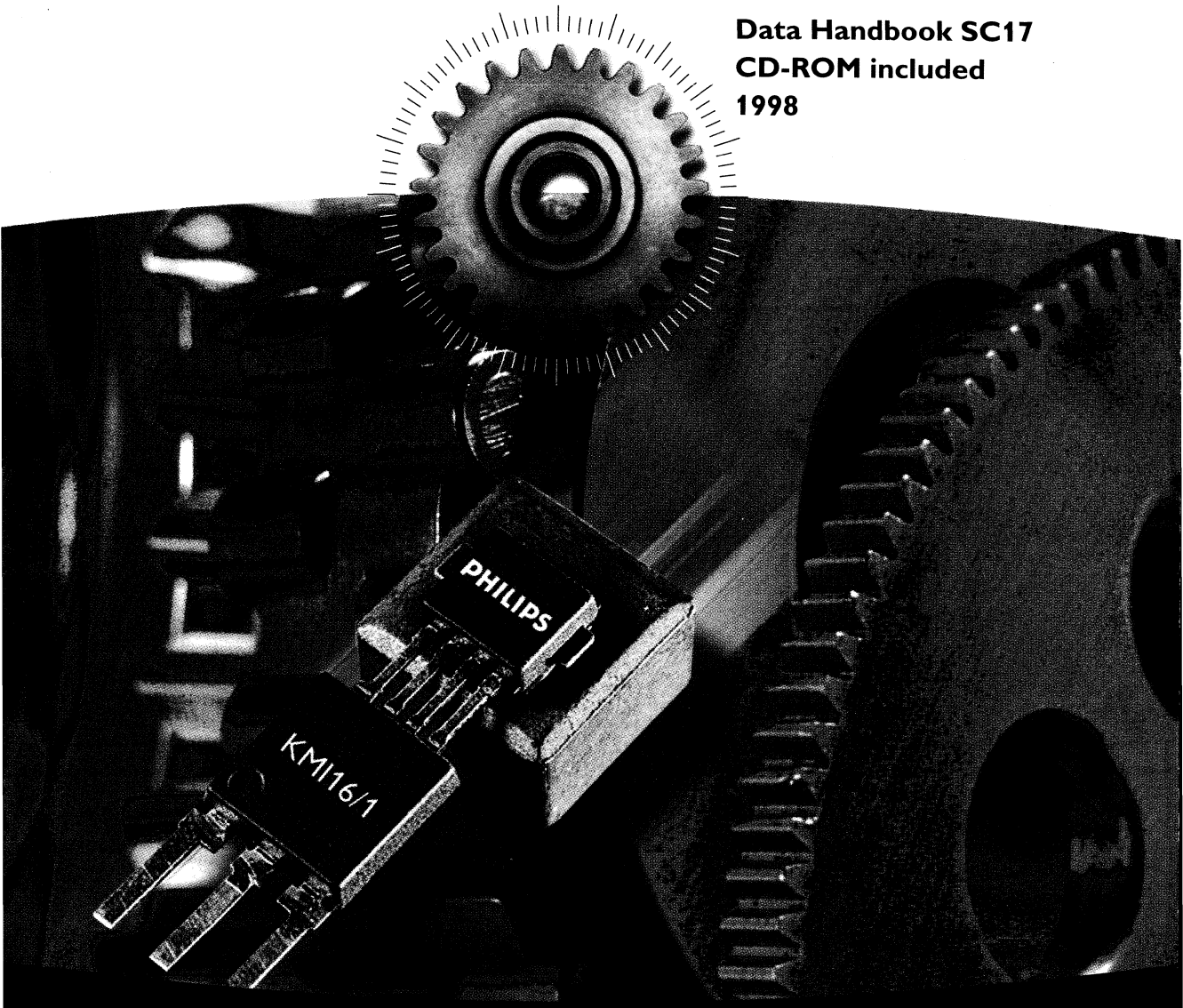

PHILIPS

Let's make things better.

http://www.semiconductors.philips.com

QUALITY ASSURED

Our quality system focuses on the continuing high quality of our components and the best possible service for our customers. We have a three-sided quality strategy: we apply a system of total quality control and assurance; we operate customer-oriented dynamic improvement programmes; and we promote a partnering relationship with our customers and suppliers.

PRODUCT SAFETY

In striving for state-of-the-art perfection, we continuously improve components and processes with respect to environmental demands. Our components offer no hazard to the environment in normal use when operated or stored within the limits specified in the data sheet.

Some components unavoidably contain substances that, if exposed by accident or misuse, are potentially hazardous to health. Users of these components are informed of the danger by warning notices in the data sheets supporting the components. Where necessary the warning notices also indicate safety precautions to be taken and disposal instructions to be followed. Obviously users of these components, in general the set-making industry, assume responsibility towards the consumer with respect to safety matters and environmental demands.

All used or obsolete components should be disposed of according to the regulations applying at the disposal location. Depending on the location, electronic components are considered to be 'chemical', 'special' or sometimes 'industrial' waste. Disposal as domestic waste is usually not permitted.

Semiconductor Sensors

CONTENTS

DEFINITIONS

Data sheet status	
Objective specification	This data sheet contains target or goal specifications for product development.
Preliminary specification	This data sheet contains preliminary data; supplementary data may be published later.
Product specification	This data sheet contains final product specifications.
Limiting values	
Limiting values given are in accordance with the Absolute Maximum Rating System (IEC 134). Stress above one or more of the limiting values may cause permanent damage to the device. These are stress ratings only and operation of the device at these or at any other conditions above those given in the Characteristics sections of the specification is not implied. Exposure to limiting values for extended periods may affect device reliability.	
Application information	
Where application information is given, it is advisory and does not form part of the specification.	

LIFE SUPPORT APPLICATIONS

These products are not designed for use in life support appliances, devices, or systems where malfunction of these products can reasonably be expected to result in personal injury. Philips customers using or selling these products for use in such applications do so at their own risk and agree to fully indemnify Philips for any damages resulting from such improper use or sale.

INDEX

Semiconductor Sensors Index

Types added to the range since the last issue of data handbook SC17 are shown in bold print.

REPLACEMENT/WITHDRAWAL TYPE

The following type number was in the previous issue of this data handbook, but not in the current version:

TYPE NUMBER	REASON FOR DELETION
KM110B/1	Discontinued

SELECTION GUIDE

MAGNETIC FIELD SENSORS

TYPE[1]	FIELD RANGE (kA/m)	SENSITIVITY $\frac{mV/V}{kA/m}$	BRIDGE RESISTANCE (kΩ)	PACKAGE	PAGE
KMZ10A	−0.5 to +0.5	16	1.2	SOT195	80
KMZ10A1; note 2	−0.05 to +0.05	22	1.3	SOT195	85
KMZ10B	−2.0 to +2.0	4	2.1	SOT195	91
KMZ10C	−7.5 to +7.5	1.5	1.4	SOT195	96
KMZ11B1	−0.2 to +0.2	4	2.1	SOT96 (SO8)	-
KMZ41	H = 100; note 3	2.8	2.5	SOT96 (SO8)	101
KMZ50	−0.2 to +0.2	16	2	SOT96 (SO8)	105
KMZ51	−0.2 to +0.2	16	2	SOT96 (SO8)	109

Notes

1. In air, 1 kA/m corresponds to 1.25 mT.
2. Field range and sensitivity with switched H_x-field for detection of low magnetic fields.
3. Recommended field strength.

SENSORS FOR CONTACTLESS ROTATIONAL SPEED MEASUREMENT AND REFERENCE-/MARK DETECTION

TYPE	SENSING DISTANCE (mm)	FREQUENCY RANGE (Hz)	TARGET	PACKAGE	PAGE
KMI15/1	2.5	0 to 25000	note 1	SOT453B	142
KMI15/2	2.5	0 to 25000	note 2	SOT453A	152
KMI15/4	2.0	0 to 25000	note 1	SOT453C	158
KMI16/1	2.0	0 to 25000	note 2	SOT477B	168

Notes

1. Ferromagnetic target wheel.
2. Magnetized target wheel.

SENSORS FOR CONTACTLESS ANGULAR POSITION MEASUREMENT

TYPE	ANGLE RANGE (DEG)	OUTPUT			PACKAGE	PAGE
		VALUE	TYPE	UNIT		
KM110BH/2130	30	0.5 to 4.5	linear	V	hybrid	194
KM110BH/2190	90	0.5 to 4.5	sinusoidal	V	hybrid	194
KM110BH/2270	70	4 to 20	sinusoidal	mA	hybrid	200
KM110BH/2430	30	0.5 to 4.5	linear	V	hybrid	209
KM110BH/2470	70	0.5 to 4.5	sinusoidal	V	hybrid	209
UZZ9000	180	0.5 to 4.5	linear	V	SO24	218

TEMPERATURE SENSORS

TYPE	TEMPERATURE RANGE (°C)	RESISTANCE		SENSOR ACCURACY		PACKAGE	PAGE
		R (Ω)	at T_{amb} (°C)	°C	at T_{amb} (°C)		
KTY81-110	−55 to +150	990 to 1010	25	±1.3	25	SOD70	142
KTY81-120	−55 to +150	980 to 1020	25	±2.5	25	SOD70	142
KTY81-121	−55 to +150	980 to 1000	25	±1.3	25	SOD70	142
KTY81-122	−55 to +150	1000 to 1020	25	±1.3	25	SOD70	142
KTY81-150	−55 to +150	950 to 1050	25	±6.3	25	SOD70	142
KTY81-151	−55 to +150	950 to 1000	25	±3.2	25	SOD70	142
KTY81-152	−55 to +150	1000 to 1050	25	±3.2	25	SOD70	142
KTY81-210	−55 to +150	1980 to 2020	25	±1.3	25	SOD70	253
KTY81-220	−55 to +150	1960 to 2040	25	±2.5	25	SOD70	253
KTY81-221	−55 to +150	1960 to 2000	25	±1.3	25	SOD70	253
KTY81-220	−55 to +150	2000 to 2040	25	±1.3	25	SOD70	253
KTY81-250	−55 to +150	1900 to 2100	25	±6.3	25	SOD70	253
KTY81-251	−55 to +150	1900 to 2000	25	±3.2	25	SOD70	253
KTY81-252	−55 to +150	2000 to 2100	25	±3.2	25	SOD70	253
KTY82-110	−55 to +150	990 to 1010	25	±1.3	25	SOT23	264
KTY82-120	−55 to +150	980 to 1020	25	±2.5	25	SOT23	264
KTY82-121	−55 to +150	980 to 1000	25	±1.3	25	SOT23	264
KTY82-122	−55 to +150	1000 to 1020	25	±1.3	25	SOT23	264
KTY82-150	−55 to +150	950 to 1050	25	±6.3	25	SOT23	264
KTY82-151	−55 to +150	950 to 1000	25	±3.2	25	SOT23	264
KTY82-152	−55 to +150	1000 to 1050	25	±3.2	25	SOT23	264
KTY82-210	−55 to +150	1980 to 2020	25	±1.3	25	SOT23	274
KTY82-220	−55 to +150	1960 to 2040	25	±2.5	25	SOT23	274
KTY82-221	−55 to +150	1960 to 2000	25	±1.3	25	SOT23	274
KTY82-222	−55 to +150	2000 to 2040	25	±1.3	25	SOT23	274
KTY82-250	−55 to +150	1900 to 2100	25	±6.3	25	SOT23	274
KTY82-251	−55 to +150	1900 to 2000	25	±3.2	25	SOT23	274

Semiconductor sensors — Selection guide

TYPE	TEMPERATURE RANGE (°C)	RESISTANCE		SENSOR ACCURACY		PACKAGE	PAGE
		R (Ω)	at T_{amb} (°C)	°C	at T_{amb} (°C)		
KTY82-252	−55 to +150	2000 to 2100	25	±3.2	25	SOT23	274
KTY83-110	−55 to +175	990 to 1010	25	±1.3	25	SOD68	284
KTY83-120	−55 to +175	980 to 1020	25	±2.5	25	SOD68	284
KTY83-121	−55 to +175	980 to 1000	25	±1.3	25	SOD68	284
KTY83-122	−55 to +175	1000 to 1020	25	±1.3	25	SOD68	284
KTY83-150	−55 to +175	950 to 1050	25	±6.6	25	SOD68	284
KTY83-151	−55 to +175	950 to 1000	25	±3.3	25	SOD68	284
KTY83-152	−55 to +175	1000 to 1050	25	±3.3	25	SOD68	284
KTY84-130	−40 to +300	970 to 1030	100	±4.8	100	SOD68	293
KTY84-150	−40 to +300	950 to 1050	100	±8.0	100	SOD68	293
KTY84-151	−40 to +300	950 to 1000	100	±4.0	100	SOD68	293
KTY84-152	−40 to +300	1000 to 1050	25	±4.0	100	SOD68	293
KTY85-110	−40 to +125	990 to 1010	25	±1.3	25	SOD80	299
KTY85-120	−40 to +125	980 to 1020	25	±2.6	25	SOD80	299
KTY85-121	−40 to +125	980 to 1000	25	±1.3	25	SOD80	299
KTY85-122	−40 to +125	1000 to 1020	25	±1.3	25	SOD80	299
KTY85-150	−40 to +125	950 to 1050	25	±6.6	25	SOD80	299
KTY85-151	−40 to +125	950 to 1000	25	±3.3	25	SOD80	299
KTY85-152	−40 to +125	1000 to 1050	25	±3.3	25	SOD80	299

Internet World Wide Web Home Page

WHAT IS IT?

Welcome to our place in cyberspace.

The Discretes Group now has its own home page within Philips Semiconductors. Explore our Web pages and take a look at our product offering of advance Discrete Applications and Products.

In addition we offer you the latest information on Products, News, Support, Employment and Offices.

HOW TO REACH US

For access to the Philips Semiconductors Home Page go to the World Wide Web location:

http://www.semiconductors.philips.com

You can find us in the Product category of Discretes.

FAX-on-DEMAND System

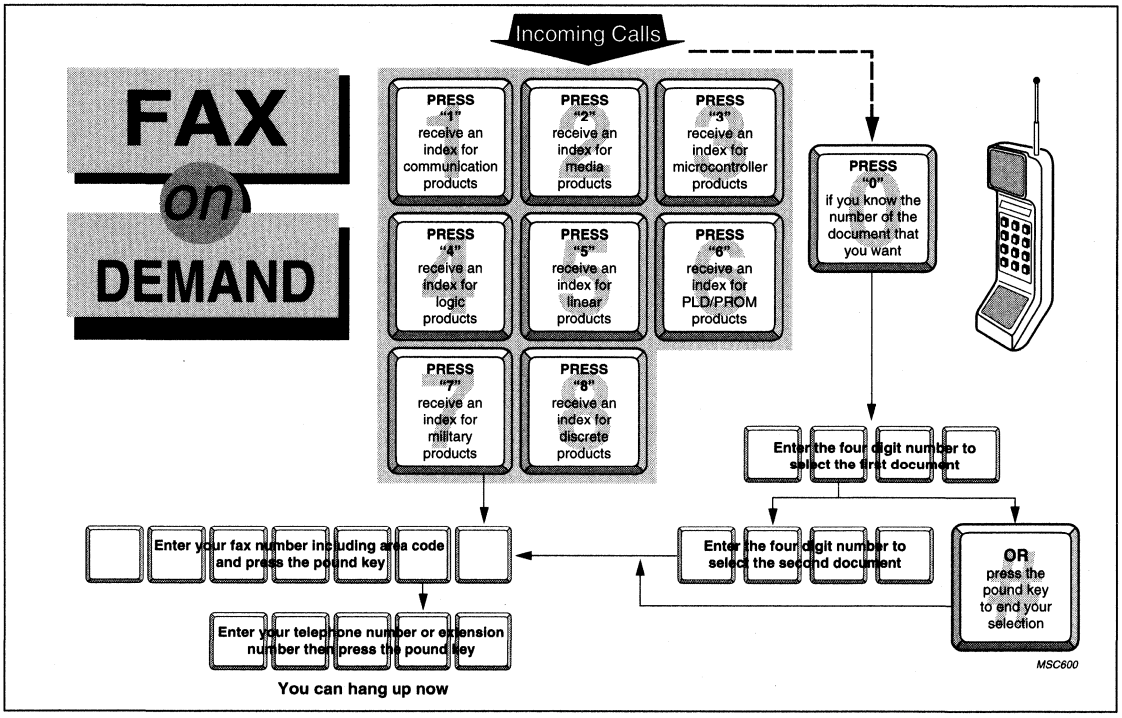

WHAT IS IT?

The FAX-on-DEMAND system is a computer facsimile system that allows customers to receive selected documents by fax automatically.

HOW DOES IT WORK?

To order a document, you simply enter the document number. This number can be obtained by asking for an index of available documents to be faxed to you the first time you call the system.

Our system has a selection of the latest product data sheets from Philips with varying page counts. As you know, it takes approximately one minute to FAX one page. This isn't bad if the number of pages is less than 10. But if the document is 37 pages long, be ready for a long transmission!

Philips Semiconductors also maintains product information on the World-Wide-Web. Our home page can be located at:

http://www.semiconductors.philips.com

WHO DO I CONTACT IF I HAVE A QUESTION ABOUT FAX-ON-DEMAND?

Contact your local Philips sales office.

FAX-ON-DEMAND PHONE NUMBERS

United Kingdom, Ireland	44-181-730-5020
France	33-1-40-996060
Italy	39-167-295502
North America	1-800-282-2000

LOCATIONS SOON TO BE IN OPERATION

- Hong Kong
- Japan
- The Netherlands.

GENERAL
MAGNETIC FIELD SENSORS

GENERAL INTRODUCTION

Contents

- Operating principles
- Philips magnetoresistive sensors
- Flipping
- Effect of temperature on behaviour
- Using magnetoresistive sensors
- Further information for advanced users
  - The MR effect
  - Linearization
  - Flipping
  - Temperature compensation.

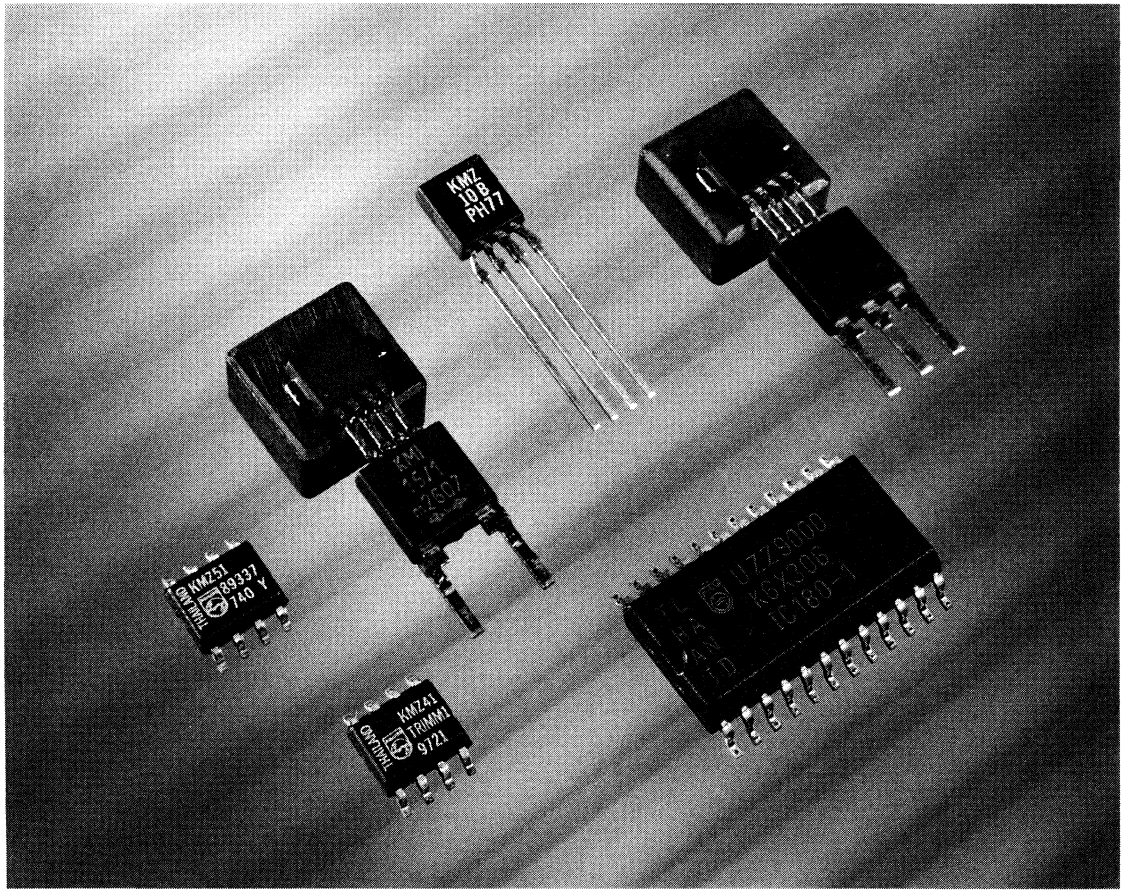

The KMZ range of magnetoresistive sensors is characterized by high sensitivity in the detection of magnetic fields, a wide operating temperature range, a low and stable offset and low sensitivity to mechanical stress. They therefore provide an excellent means of measuring both linear and angular displacement under extreme environmental conditions, because their very high sensitivity means that a fairly small movement of actuating components in, for example, cars or machinery (gear wheels, metal rods, cogs, cams, etc.) can create measurable changes in magnetic field. Other applications for magnetoresistive sensors include rotational speed measurement and current measurement.

Examples where their properties can be put to good effect can be found in automotive applications, such as wheel speed sensors for ABS and motor management systems and position sensors for chassis position, throttle and pedal position measurement. Other examples include instrumentation and control equipment, which often require position sensors capable of detecting displacements in the region of tenths of a millimetre (or even less), and in electronic ignition systems, which must be able to determine the angular position of an internal combustion engine with great accuracy.

Finally, because of their high sensitivity, magnetoresistive sensors can measure very weak magnetic fields and are thus ideal for application in electronic compasses, earth field correction and traffic detection.

If the KMZ sensors are to be used to maximum advantage, however, it is important to have a clear understanding of their operating principles and characteristics, and how their behaviour may be affected by external influences and by their magnetic history.

Operating principles

Magnetoresistive (MR) sensors make use of the magnetoresistive effect, the property of a current-carrying magnetic material to change its resistivity in the presence of an external magnetic field (the common units used for magnetic fields are given in Table 1).

Table 1 Common magnetic units

1 kA/m = 1.25 mTesla (in air)
1 mT = 10 Gauss

The basic operating principle of an MR sensor is shown in Fig.2.

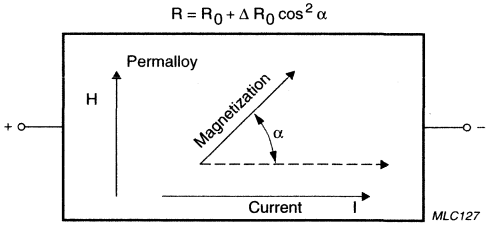

Fig.2 The magnetoresistive effect in permalloy.

Figure 2 shows a strip of ferromagnetic material, called permalloy (20% Fe, 80% Ni). Assume that, when no external magnetic field is present, the permalloy has an internal magnetization vector parallel to the current flow (shown to flow through the permalloy from left to right). If an external magnetic field H is applied, parallel to the plane of the permalloy but perpendicular to the current flow, the internal magnetization vector of the permalloy will rotate around an angle α. As a result, the resistance of R of the permalloy will change as a function of the rotation angle α, as given by:

$$R = R_O + \Delta R_O \cos^2 \alpha \qquad (1)$$

R_o and ΔR_o are material parameters and to achieve optimum sensor characteristics Philips use Ni19Fe81, which has a high R_o value and low magnetostriction. With this material, ΔR_o is of the order of 3%. For more information on materials, see Appendix 1.

It is obvious from this quadratic equation, that the resistance/magnetic field characteristic is non-linear and in addition, each value of R is not necessarily associated with a unique value of H (see Fig.3). For more details on the essentials of the magnetoresistive effect, please refer to the Section "Further information for advanced users" later in this chapter or Appendix 1, which examines the MR effect in detail.

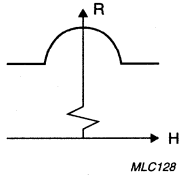

Fig.3 The resistance of the permalloy as a function of the external field.

In this basic form, the MR effect can be used effectively for angular measurement and some rotational speed measurements, which do not require linearization of the sensor characteristic.

In the KMZ series of sensors, four permalloy strips are arranged in a meander fashion on the silicon (Fig.4 shows one example, of the pattern on a KMZ10). They are connected in a Wheatstone bridge configuration, which has a number of advantages:

- Reduction of temperature drift
- Doubling of the signal output
- The sensor can be aligned at the factory.

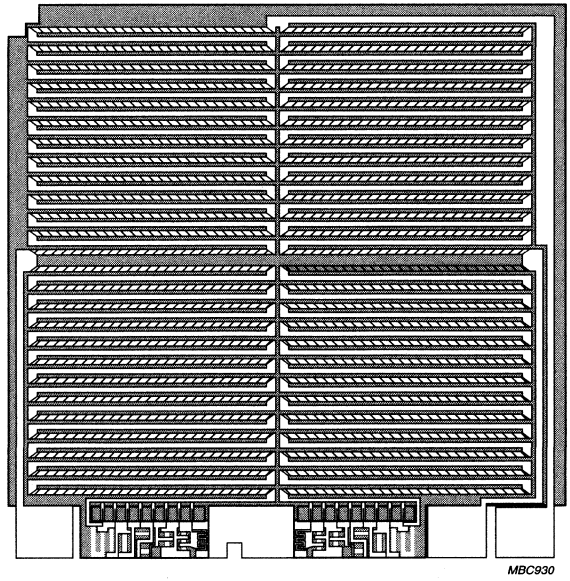

Fig.4 KMZ10 chip structure.

Two further resistors, R_T, are included, as shown in Fig.5. These are for trimming sensor offset down to (almost) zero during the production process.

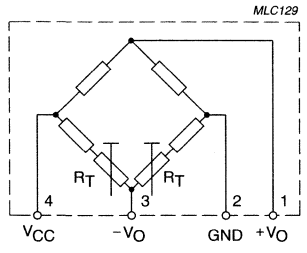

Fig.5 Bridge configuration with offset trimmed to zero, by resistors R_T.

For some applications however, the MR effect can be used to its best advantage when the sensor output characteristic has been linearized. These applications include:

- Weak field measurements, such as compass applications and traffic detection;
- Current measurement; and
- Rotational speed measurement.

For an explanation of how the characteristic is linearized, please refer to the Section "Further information for advanced users" later in this chapter.

Philips magnetoresistive sensors

Based on the principles described, Philips has a family of basic magnetoresistive sensors. The main characteristics of the KMZ sensors are given in Table 2.

Table 2 Main characteristics of Philips sensors

SENSOR TYPE	PACKAGE	FIELD RANGE (kA/m)[1]	V_{CC} (V)	SENSITIVITY $\frac{(mV/V)}{(kA/m)}$	R_{bridge} (kΩ)	LINEARIZE MR EFFECT	APPLICATION EXAMPLES
KMZ10A	SOT195	−0.5 to +0.5	≤9	16.0	1.2	Yes	compass, navigation, metal detection, traffic control
KMZ10A1[2]	SOT195	−0.05 to +0.05	≤9	22.0	1.3	Yes	
KMZ10B	SOT195	−2.0 to +2.0	≤12	4.0	2.1	Yes	current measurement, angular and linear position, reference mark detection, wheel speed
KMZ11B1	SO8	−2.0 to +2.0	≤12	4.0	2.1	Yes	
KMZ10C	SOT195	−7.5 to +7.5	≤10	1.5	1.4	Yes	
KMZ41	SO8	H = 100[3]	≤12	2.8	2.5	No	angular measurement
KMZ50	SO8	−0.2 to +0.2	≤8	16.0	2.0	Yes	compass, navigation, metal detection, traffic control
KMZ51	SO8	−0.2 to +0.2	≤8	16.0	2.0	Yes	

Notes

1. In air, 1 kA/m corresponds to 1.25 mT.
2. Data given for operation with switched auxiliary field.
3. Recommended field strength.

Flipping

The internal magnetization of the sensor strips has two stable positions. So, if for any reason the sensor is influenced by a powerful magnetic field opposing the internal aligning field, the magnetization may flip from one position to the other, and the strips become magnetized in the opposite direction (from, for example, the '+x' to the '–x' direction). As demonstrated in Fig.6, this can lead to drastic changes in sensor characteristics.

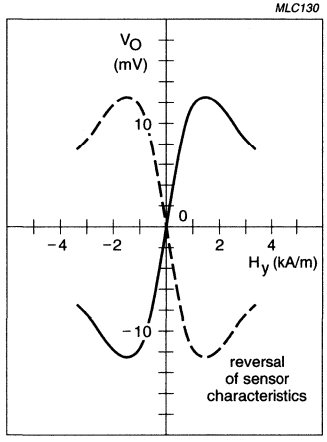

Fig.6 Sensor characteristics.

The field (e.g. '$-H_x$') needed to flip the sensor magnetization, and hence the characteristic, depends on the magnitude of the transverse field 'H_y': the greater the field 'H_y', the smaller the field '$-H_x$'. This follows naturally, since the greater the field 'H_y', the closer the magnetization's rotation approaches 90°, and hence the easier it will be to flip it into a corresponding stable position in the '–x' direction.

Looking at the curve in Fig.7 where H_y = 0.5 kA/m, for such a low transverse field the sensor characteristic is stable for all positive values of H_x and a reverse field of ≈1 kA/m is required before flipping occurs. At H_y = 2 kA/m however, the sensor will flip even at smaller values of 'H_x' (at approximately 0.5 kA/m).

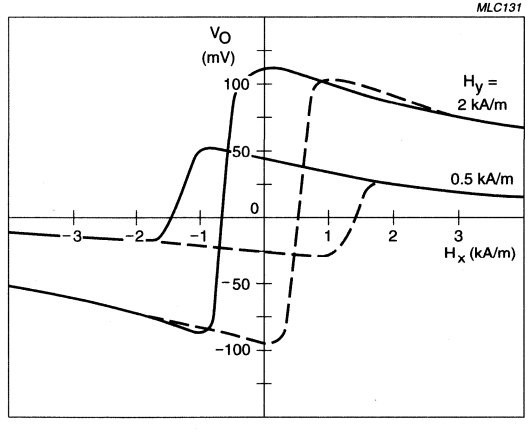

Fig.7 Sensor output 'V_o' as a function of the auxiliary field 'H_x' for several values of transverse field 'H_y'.

Figure 7 also shows that the flipping itself is not instantaneous, because not all the permalloy strips flip at the same rate. In addition, it illustrates the hysteresis effect exhibited by the sensor. For more information on flipping, see the Section "Further information for advanced users" later in this chapter and Appendix 1 on the magnetoresistive effect.

Effect of temperature on behaviour

Figure 8 shows that the bridge resistance increases linearly with temperature, due to the bridge resistors' temperature dependency (i.e. the permalloy) for a typical KMZ10B sensor. The data sheets show also the spread in this variation due to manufacturing tolerances and this should be taken into account when incorporating the sensors into practical circuits.

In addition to the bridge resistance, the sensitivity also varies with temperature. This can be seen from Fig.9, which plots output voltage against transverse field 'H_y' for various temperatures. Figure 9 shows that sensitivity falls with increasing temperature (actual values for given for every sensor in the datasheets). The reason for this is rather complex and is related to the energy-band structure of the permalloy strips.

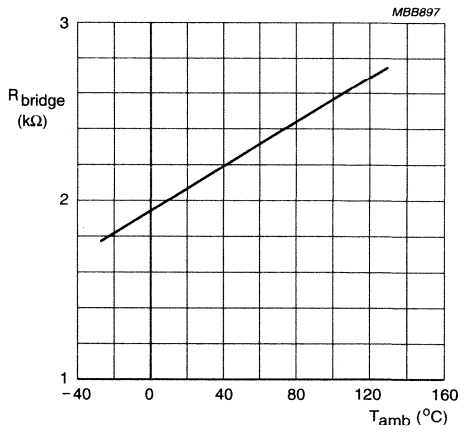

Fig.8 Bridge resistance of a KMZ10B sensor as a function of ambient temperature.

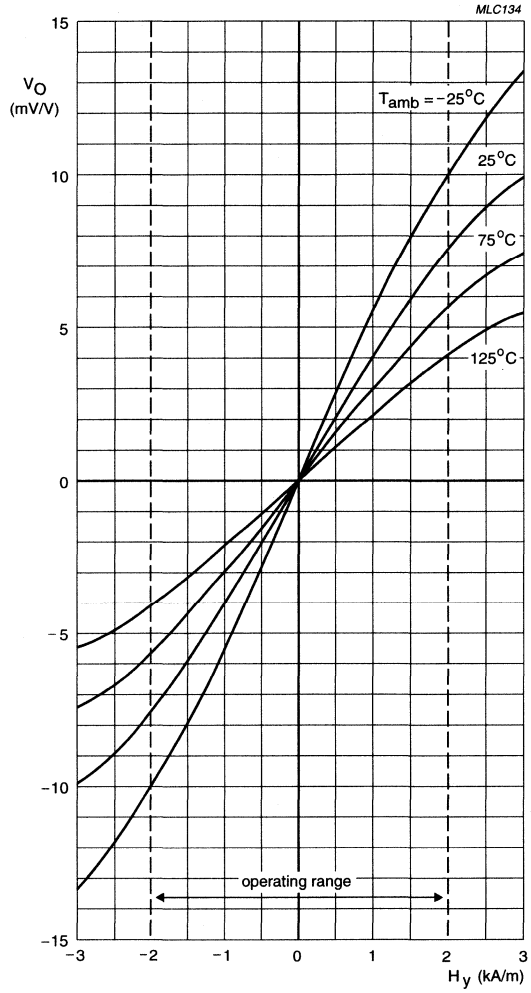

Fig.9 Output voltage 'V_o' as a fraction of the supply voltage of a KMZ10B sensor as a function of transverse field 'H_y' for several temperatures.

Figure 10 is similar to Fig.9, but with the sensor powered by a constant current supply. Figure 10 shows that, in this case, the temperature dependency of sensitivity is significantly reduced. This is a direct result of the increase in bridge resistance with temperature (see Fig.8), which partly compensates the fall in sensitivity by increasing the voltage across the bridge and hence the output voltage. Figure 8 demonstrates therefore the advantage of operating with constant current.

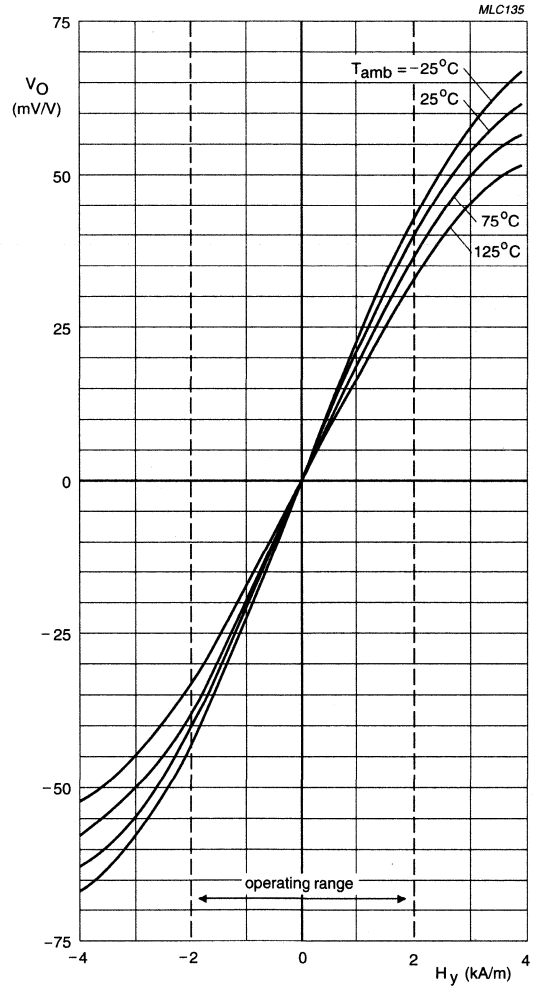

Fig.10 Output voltage 'V_o' of a KMZ10B sensor as a function of transverse field 'H_y' for several temperatures.

Using magnetoresistive sensors

The excellent properties of the KMZ magnetoresistive sensors, including their high sensitivity, low and stable offset, wide operating temperature and frequency ranges and ruggedness, make them highly suitable for use in a wide range of automotive, industrial and other applications. These are looked at in more detail in other chapters in this book; some general practical points about using MR sensors are briefly described below.

Analog application circuitry

In many magnetoresistive sensor applications where analog signals are measured (in measuring angular position, linear position or current measurement, for example), a good application circuit should allow for sensor offset and sensitivity adjustment. Also, as the sensitivity of many magnetic field sensors has a drift with temperature, this also needs compensation. A basic circuit is shown in Fig.11.

In the first stage, the sensor signal is pre-amplified and offset is adjusted. After temperature effects are compensated, final amplification and sensitivity adjustment takes place in the last stage. This basic circuit can be extended with additional components to meet specific EMC requirements or can be modified to obtain customized output characteristics (e.g. a different output voltage range or a current output signal).

Philips magnetoresistive sensors have a linear sensitivity drift with temperature and so a temperature sensor with linear characteristics is required for compensation. Philips KTY series are well suited for this purpose, as their positive Temperature Coefficient (TC) matches well with the negative TC of the MR sensor. The degree of compensation can be controlled with the two resistors R7 and R8 and special op-amps, with very low offset and temperature drift, should be used to ensure compensation is constant over large temperature ranges.

Please refer to part 2 of this book for more information on the KTY temperature sensors; see also the Section "Further information for advanced users" later in this chapter for a more detailed description of temperature compensation using these sensors.

Using magnetoresistive sensors with a compensation coil

For general magnetic field or current measurements it is useful to apply the 'null-field' method, in which a magnetic field (generated by a current carrying coil), equal in magnitude but opposite in direction, is applied to the sensor. Using this 'feedback' method, the current through the coil is a direct measure of the unknown magnetic field amplitude and it has the advantage that the sensor is being operated at its zero point, where inaccuracies as result of tolerances, temperature drift and slight non-linearities in the sensor characteristics are insignificant. A detailed discussion of this method is covered in Chapter "Weak field measurements".

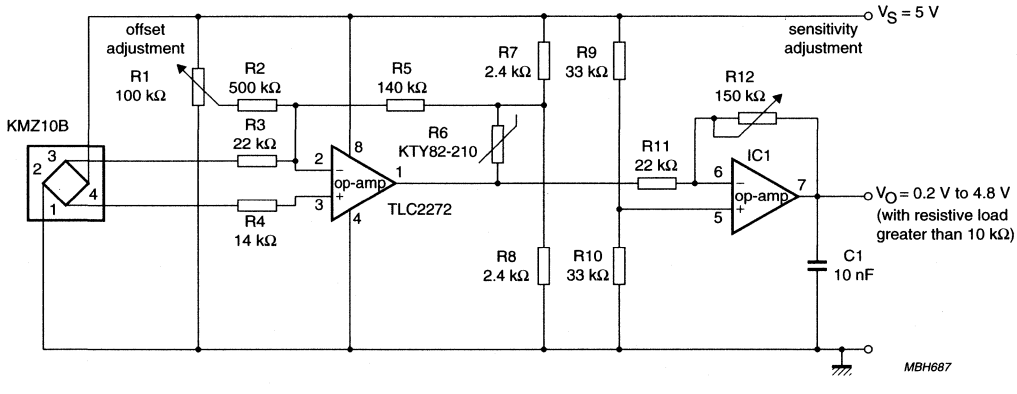

Fig.11 Basic application circuit with temperature compensation and offset adjustment.

Further information for advanced users

THE MR EFFECT

In sensors employing the MR effect, the resistance of the sensor under the influence of a magnetic field changes as it is moved through an angle α as given by:

$$R = R_O + \Delta R_O \cos^2 \alpha \quad (2)$$

It can be shown that

$$\sin^2 \alpha = \frac{H^2}{H_O^2} \text{ for } H \leq H_O \quad (3)$$

and

$$\sin^2 \alpha = 1 \text{ for } H > H_O \quad (4)$$

where H_o can be regarded as a material constant comprising the so called demagnetizing and anisotropic fields.

Applying equations (3) and (4) to equation (2) leads to:

$$R = R_O + \Delta R_O \left(1 - \frac{H^2}{H_O^2} \right) \text{ for } H \leq H_O \quad (5)$$

$$R = R_O \text{ for } H > H_O \quad (6)$$

which clearly shows the non-linear nature of the MR effect.

More detailed information on the derivation of the formulae for the MR effect can be found in Appendix 1.

LINEARIZATION

The magnetoresistive effect can be linearized by depositing aluminium stripes (Barber poles), on top of the permalloy strip at an angle of 45° to the strip axis (see Fig.12). As aluminium has a much higher conductivity than permalloy, the effect of the Barber poles is to rotate the current direction through 45° (the current flow assumes a 'saw-tooth' shape), effectively changing the rotation angle of the magnetization relative to the current from α to $\alpha - 45°$.

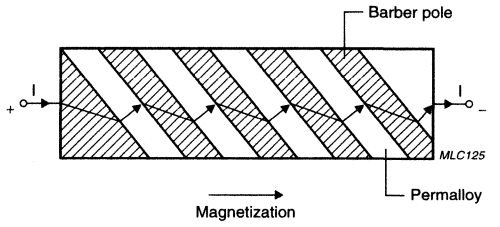

Fig.12 Linearization of the magnetoresistive effect.

A Wheatstone bridge configuration is also used for linearized applications. In one pair of diagonally opposed elements, the Barber poles are at +45° to the strip axis, while in another pair they are at –45°. A resistance increase in one pair of elements due to an external magnetic field is thus 'matched' by a decrease in resistance of equal magnitude in the other pair. The resulting bridge imbalance is then a linear function of the amplitude of the external magnetic field in the plane of the permalloy strips, normal to the strip axis.

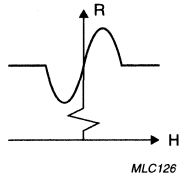

Fig.13 The resistance of the permalloy as a function of the external field H after linearization (compare with Fig.6).

For sensors using Barber poles arranged at an angle of +45° to the strip axis, the following expression for the sensor characteristic can be derived (see Appendix 1 on the MR effect):

$$R = R_O + \frac{\Delta R_O}{2} + \Delta R_O\left(\frac{H}{H_O}\right)\sqrt{1-\frac{H^2}{H_O^2}} \quad (7)$$

The equation is linear where $H/H_o = 0$, as shown in Fig.7. Likewise, for sensors using Barber poles arranged at an angle of –45°, the equation derives to:

$$R = R_O + \frac{\Delta R_O}{2} - \Delta R_O\left(\frac{H}{H_O}\right)\sqrt{1-\frac{H^2}{H_O^2}} \quad (8)$$

This is the mirror image of the characteristic in Fig.7. Hence using a Wheatstone bridge configuration ensures the any bridge imbalance is a linear function of the amplitude of the external magnetic field.

FLIPPING

As described in the body of the chapter, Fig.7 shows that flipping is not instantaneous and it also illustrates the hysteresis effect exhibited by the sensor. This figure and Fig.14 also shows that the sensitivity of the sensor falls with increasing 'H_x'. Again, this is to be expected since the moment imposed on the magnetization by 'H_x' directly opposes that imposed by 'H_y', thereby reducing the degree of bridge imbalance and hence the output signal for a given value of 'H_y'.

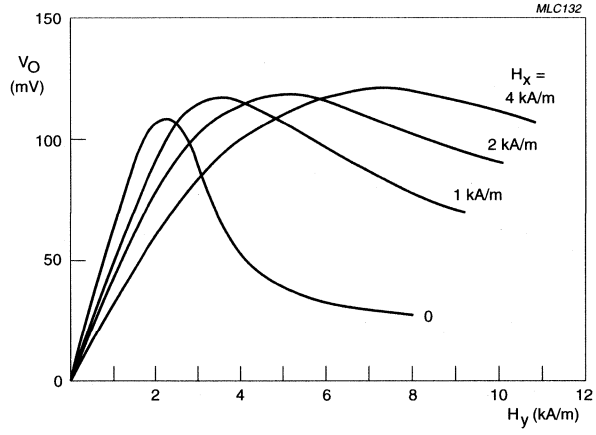

Fig.14 Sensor output 'V_o' as a function of the transverse field 'H_y' for several values of auxiliary field 'H_x'.

The following general recommendations for operating the KMZ10 can be applied:

- To ensure stable operation, avoid operating the sensor in an environment where it is likely to be subjected to negative external fields ('$-H_x$'). Preferably, apply a positive auxiliary field ('H_x') of sufficient magnitude to prevent any likelihood of flipping within he intended operating range (i.e. the range of 'H_y').
- Before using the sensor for the first time, apply a positive auxiliary field of at least 3 kA/m; this will effectively erase the sensor's magnetic 'history' and will ensure that no residual hysteresis remains (refer to Fig.6).
- Use the minimum auxiliary field that will ensure stable operation, because the larger the auxiliary field, the lower the sensitivity, but the actual value will depend on the value of H_d. For the KMZ10B sensor, a minimum auxiliary field of approximately 1 kA/m is recommended; to guarantee stable operation for all values of H_d, the sensor should be operated in an auxiliary field of 3 kA/m.

These recommendations (particularly the first one) define a kind of Safe Operating ARea (SOAR) for the sensors. This is illustrated in Fig.15, which is an example (for the KMZ10B sensor) of the SOAR graphs to be found in our data sheets.

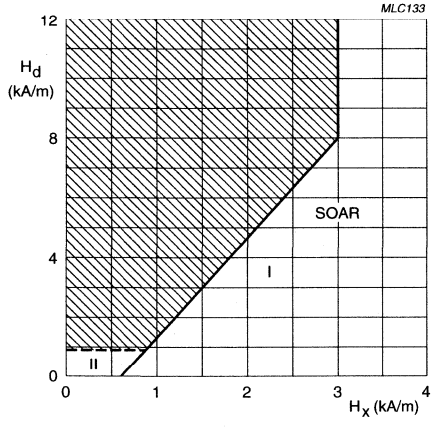

Fig.15 SOAR of a KMZ10B sensor as a function of auxiliary field 'H_x' and disturbing field 'H_d' opposing 'H_x' (area I).

The greater the auxiliary field, the greater the disturbing field that can be tolerated before flipping occurs. For auxiliary fields above 3 kA/m, the SOAR graph shows that the sensor is completely stable, regardless of the magnitude of the disturbing field. It can also be seen from this graph that the SOAR can be extended for low values of 'H_y'. In Fig.15, (for the KMZ10B sensor), the extension for $H_y < 1$ kA/m is shown.

Temperature compensation

With magnetoresistive sensors, temperature drift is negative. Two circuits manufactured in SMD-technology which include temperature compensation are briefly described below.

The first circuit is the basic application circuit already given (see Fig.11). It provides average (sensor-to-sensor) compensation of sensitivity drift with temperature using the KTY82-210 silicon temperature sensor. It also includes offset adjustment (via R1); gain adjustment is performed with a second op-amp stage. The temperature sensor is part of the amplifier's feedback loop and thus increases the amplification with increasing temperature.

The temperature dependant amplification A and the temperature coefficient TC_A of the first op-amp stage are approximately:

$$A = \frac{R_5}{R_3}\left(1 + \frac{2R_T}{R_7}\right) \text{ for } R_8 = R_7$$

$$TC_A = \frac{TC_{KTY}}{1 + \frac{R_7}{2R_T}} \text{ for } R_8 = R_7$$

R_T is the temperature dependent resistance of the KTY82. The values are taken for a certain reference temperature. This is usually 25 °C, but in other applications a different reference temperature may be more suitable.

Figure 16 shows an example with a commonly-used instrumentation amplifier. The circuit can be divided into two stages: a differential amplifier stage that produces a symmetrical output signal derived from the magnetoresistive sensor, and an output stage that also provides a reference to ground for the amplification stage.

To compensate for the negative sensor drift, as with the above circuit the amplification is again given an equal but positive temperature coefficient, by means of a KTY81-110 silicon temperature sensor in the feedback loop of the differential amplifier.

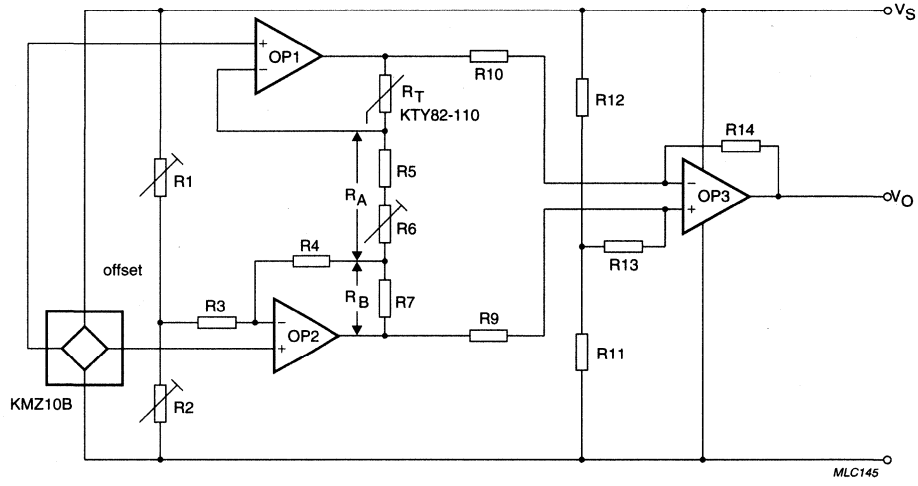

Fig.16 KMZ10B application circuit with instrumentation amplifier.

The amplification of the input stage ('OP1' and 'OP2') is given by:

$$A1 = 1 + \frac{R_T + R_B}{R_A} \quad (9)$$

where R_T is the temperature dependent resistance of the KTY82 sensor and R_B is the bridge resistance of the magnetoresistive sensor.

The amplification of the complete amplifier can be calculated by:

$$A = A1 \times \frac{R_{14}}{R_{10}} \quad (10)$$

The positive temperature coefficient (TC) of the amplification is:

$$TC_A = \frac{R_T \times TC_{KTY}}{R_A + R_B + R_T} \quad (11)$$

For the given negative 'TC' of the magnetoresistive sensor and the required amplification of the input stage 'A1', the resistance 'R_A' and 'R_B' can be calculated by:

$$R_B = R_T \times \left(\frac{TC_{KTY}}{TC_A} \times \left(1 - \frac{1}{A1} \right) - 1 \right) \quad (12)$$

$$R_A = \frac{R_T + R_B}{A1 - 1} \quad (13)$$

where TC_{KTY} is the temperature coefficient of the KTY sensor and TC_A is the temperature coefficient of the amplifier. This circuit also provides for adjustment of gain and offset voltage of the magnetic-field sensor.

WEAK FIELD MEASUREMENTS

Contents:

- Principles of weak field sensing
- Philips sensors for weak field measurement
- Application examples
- Test modules.

Principles of weak field sensing

Measurement of weak magnetic fields such as the earth's geomagnetic field (which has a typical strength of between approximately 30 A/m and 50 A/m), or fields resulting from very small currents, requires a sensor with very high sensitivity. With their inherent high sensitivity, magnetoresistive sensors are extremely well suited to sensing very small fields.

Philips' magnetoresistive sensors are by nature bi-stable (refer to Appendix 2). 'Standard' techniques used to stabilize such sensors, including the application of a strong field in the x-direction (H_x) from a permanent stabilization magnet, are unsuitable as they reduce the sensor's sensitivity to fields in the measurement, or y-direction (H_y). (Refer to Appendix 2, Fig. A2.2).

To avoid this loss in sensitivity, magnetoresistive sensors can instead be stabilized by applying brief, strong non-permanent field pulses of very short duration (a few µs). This magnetic field, which can be easily generated by simply winding a coil around the sensor, has the same stabilizing effect as a permanent magnet, but as it is only present for a very short duration, after the pulse there is no loss of sensitivity. Modern magnetoresistive sensors specifically designed for weak field applications incorporate this coil on the silicon.

However, when measuring weak fields, second order effects such as sensor offset and temperature effects can greatly reduce both the sensitivity and accuracy of MR sensors. Compensation techniques are required to suppress these effects.

OFFSET COMPENSATION BY 'FLIPPING'

Despite electrical trimming, MR sensors may have a maximum offset voltage of ±1.5 mV/V. In addition to this static offset, an offset drift due to temperature variations of about 6 $(\mu V/V)K^{-1}$ can be expected and assuming an ambient temperature up to 100 °C, the resulting offset can be of the order of 2 mV/V.

Taking these factors into account, with no external field a sensor with a typical sensitivity of 15 mV/V $(kA/m)^{-1}$ can have an offset equivalent to a field of 130 A/m, which is itself about four times the strength of a typical weak field such as the earth's geomagnetic field. Clearly, measures to compensate for the sensor offset value have to be implemented in weak field applications.

A technique called 'flipping' (patented by Philips) can be used to control the sensor. Comparable to the 'chopping' technique used in the amplification of small electrical signals, it not only stabilizes the sensor but also eliminates the described offset effects.

When the bi-stable sensor is placed in a controlled, reversible external magnetic field, the polarity of the premagnetization (M_x) of the sensor strips can be switched or flipped between the two output characteristics (see Fig.17).

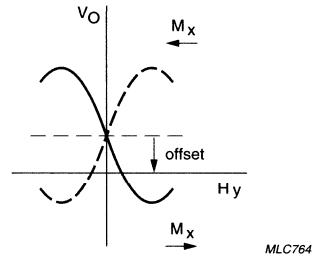

Fig.17 Butterfly curve including offset.

This reversible external magnetic field can be easily achieved with a coil wound around the sensor, consisting of current carrying wires, as described above. Depending on the direction of current pulses through this coil, positive and negative flipping fields in the x-direction ($+H_x$ and $-H_x$) are generated (see Fig.18). Although in principle the flipping frequency need not be an exact figure, design hints are given in the Section "Typical drive circuit".

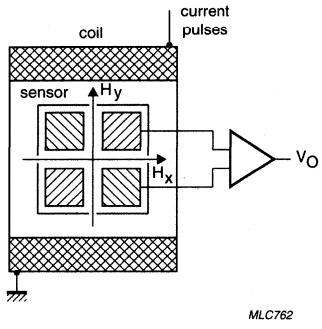

Fig.18 Flipping coil.

Flipping causes a change in the polarity of the sensor output signal and this can be used to separate the offset signal from the measured signal. Essentially, the unknown field in the 'normal' positive direction (plus the offset) is measured in one half of the cycle, while the unknown field in the 'inverted' negative direction (plus the offset) is measured in the second half. This results in two different outputs symmetrically positioned around the offset value. After high pass filtering and rectification a single, continuous value free of offset is output, smoothed by low pass filtering. See Figs 19 and 20.

Offset compensation using flipping requires additional external circuitry to recover the measured signal.

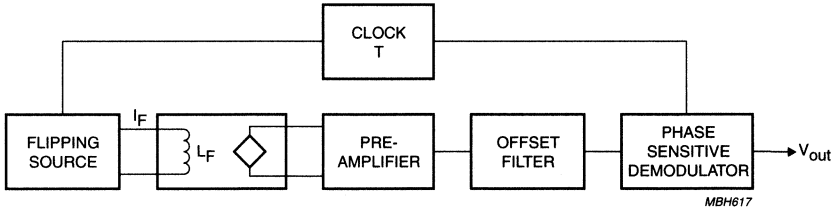

Fig.19 Block diagram of flipping circuit.

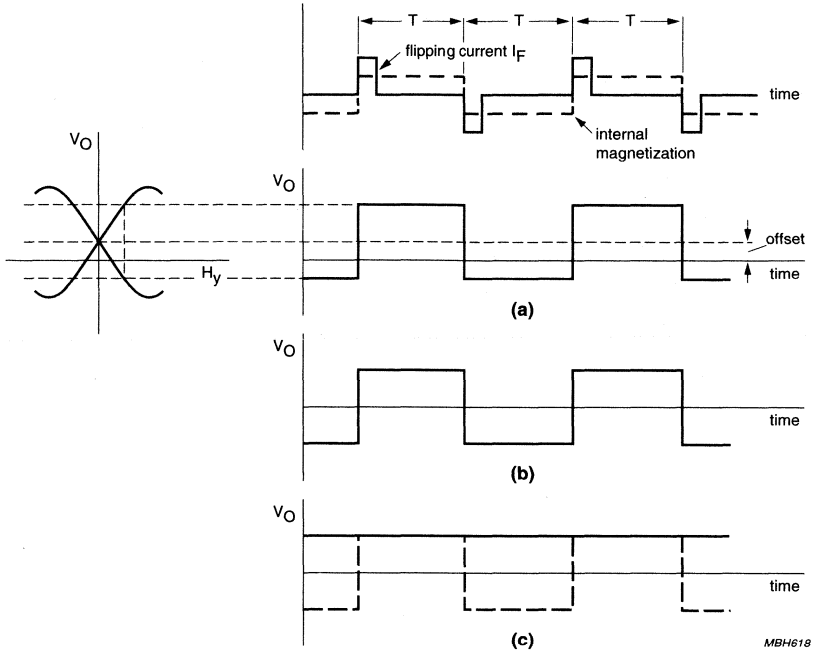

Fig.20 Timing diagram for flipping circuit (a) output voltage; (b) filtered output voltage; (c) output voltage filtered and demodulated.

SENSOR TEMPERATURE DRIFT

The sensitivity of MR sensors is also temperature dependent, with sensitivity decreasing as temperature increases (Fig.21).The effect on sensor output is certainly not negligible, as it can produce a difference of a factor of three within a –25 °C to +125 °C temperature range, for fields up to 0.5 kA/m. This effect is not compensated for by the flipping action described in the last section.

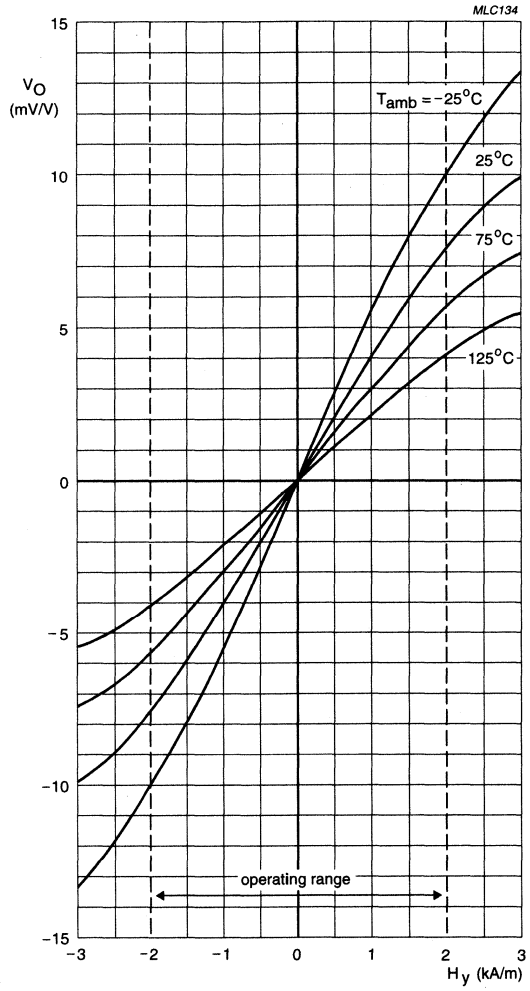

Fig.21 Output voltage 'V_o' as a fraction of the supply voltage for a KMZ10B sensor, as a function of transverse field 'H_y', at several temperatures.

The simplest form of temperature compensation is to use a current source to supply to the sensor instead of a voltage source. In this case, the resulting reduction in sensitivity due to temperature is partially compensated by a corresponding increase in bridge resistance.

Thus a current source not only improves the stability of the output voltage 'V_o', and reduces the variation in sensitivity to a factor of approximately 1.5 (compared to a factor of three using the voltage source). However, this method requires a higher supply voltage, due to the voltage drop of the current source.

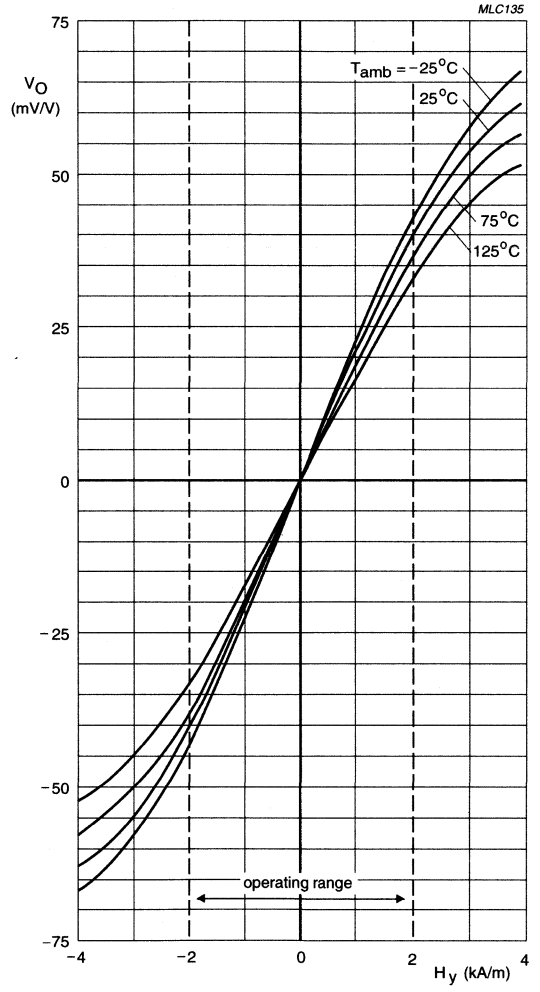

Fig.22 Output voltage 'V_o' of a KMZ10B sensor as a function of transverse field 'H_y' using a current source, for several temperatures.

The optimal method of compensating for temperature dependent sensitivity differences in MR measurements of weak fields uses electro-magnetic feedback. As can be seen from the sensor characteristics in Figs 21 and 22, sensor output is completely independent of temperature changes at the point where no external field is applied (the null-point). By using an electro-magnetic feedback set-up, it is possible to ensure the sensor is always operated at this point.

To achieve this, a second compensation coil is wrapped around the sensor perpendicular to the flipping coil, so that the magnetic field produced by this coil is in the same plane as the field being measured.

Should the measured magnetic field vary, the sensor's output voltage will change, but the change will be different at different ambient temperatures. This voltage change is converted into a current by an integral controller and supplied to the compensation coil, which then itself produces a magnetic field proportional to the output voltage change caused by the change in measured field.

The magnetic field produced by the compensation coil is in the opposite direction to the measured field, so when it is added to the measured field, it compensates exactly for the change in the output signal, regardless of its actual, temperature-dependent value. This principle is called current compensation and because the sensor is always used at its 'zero' point, compensation current is independent of the actual sensitivity of the sensor or sensitivity drift with temperature.

Information on the measured magnetic signal is effectively given by the current fed to the compensating coil. If the field factor of the compensation coil is known, this simplifies calculation of the compensating field from the compensating current and therefore the calculation of the measured magnetic field. If this field factor is not precisely known, then the resistor performing the current/voltage conversion must be trimmed. Figure 24 shows a block diagram of a compensated sensor set-up including the flipping circuit.

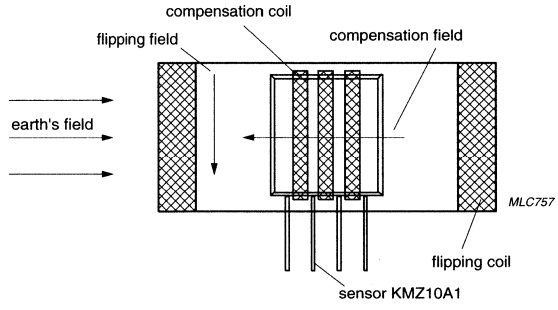

Fig.23 Magnetic field directions and the flipping and compensation coils.

The influence of other disturbing fields can also be eliminated provided they are well known, by adding a second current source to the compensating coil. Such fields might be those arising from the set-up housing, ferromagnetic components placed close to the sensor or magnetic fields from electrical motors.

The brief summary in Table 3 compares the types of compensation and their effects, so they can be assessed for their suitability in a given application. Because these options encompass a range of costs, the individual requirements of an application should be carefully analysed in terms of the performance gains versus relative costs.

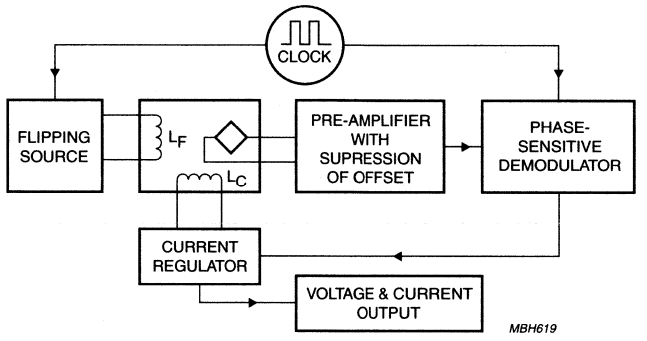

Fig.24 Block diagram of compensation circuit.

Table 3 Summery of compensation techniques

TECHNIQUE	EFFECT
Setting	avoids reduction in sensitivity due to constant stabilization field
Flipping	avoids reduction in sensitivity due to constant stabilization field, as well as compensating for sensor offset and offset drift due to temperature
Current supply	reduction of sensitivity drift with temperature by a factor of two
Electro-magnetic feedback	accurate compensation of sensitivity drift with temperature

Philips sensors for weak field measurement

Philips Semiconductors has at present four different sensors suitable for weak field applications, with the primary device being the KMZ51, an extremely sensitive sensor with integrated compensation and set/reset coils.(see Fig.25)

This sensor is ideal for many weak field detection applications such as compasses, navigation, current measurement, earth magnetic field compensation, traffic detection and so on. The integrated set/reset coils provide for both the flipping required in weak field sensors and also allow setting/resetting the orientation of the sensitivity after proximity to large disturbing magnetic fields. Philips also has the KMZ10A and KMZ10A1, similar sensors which do not have integrated coils and therefore require external coils. Table 4 provides a summary of the main single sensors in Philips' portfolio for weak field measurement.

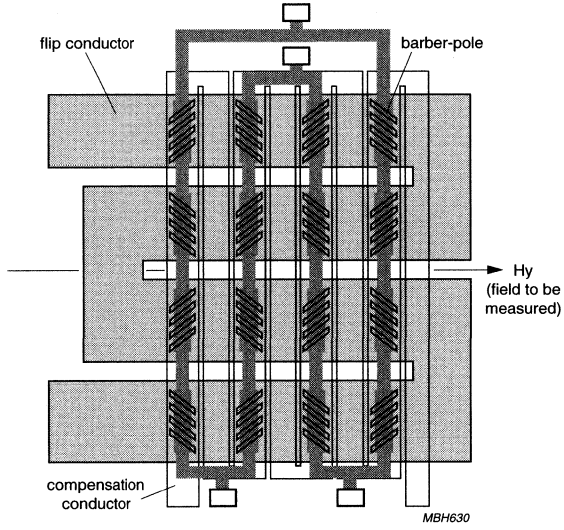

Fig.25 Layout of Philips' KMZ51 magnetoresistive sensor.

Table 4 Properties of Philips Semiconductors single sensors for a weak field applications

	KMZ10A	KMZ10A1	KMZ50	KMZ51	UNIT
Package	SOT195	SOT195	SO8	SO8	–
Supply voltage	5	5	5	5	V
Sensitivity	16(1)	22	16	16	(mV/V)/ (kA/m)
Offset voltage	±1.5	±1.5	±1	±1	mV/V
Offset voltage temperature drift	±6	±6	±3	±3	μV/V/K
Applicable field range (y-direction)	±0.5	±0.5	±0.2	±0.2	kA/m
Set/reset coil on-board	no	no	yes	yes	–
Compensation coil on-board	no	no	no	yes	–

Note

1. H_x = 0.5 kA/m.

Typical drive circuit

The principles of an application circuit required to achieve the performance mentioned, using the KMZ51, are described below (based on the simplified circuit in Fig.26). The fully compensated circuit is described; various elements which can be omitted are also indicated, if the application dictates that a given functional block is not needed. All figures quoted and the oscillograph (see Fig.27) were obtained using the circuit shown in Fig.35.

A. FLIPPING CIRCUIT WITH COMPENSATION

Although the circuit described here uses a KMZ51 sensor with its integrated coils, circuits for the KMZ10A or the KMZ10A1 would essentially be similar. However, in these cases the drive circuitry for the flipping and compensation coils would probably have to be adapted to provide a different drive capability, as the coil field factor can vary for these sensors due to the differing current density of external wire-wound coils. (The field factor for the KMZ51 is 22 A/m.mA^{-1}).
This depends on the number of windings and the naturally larger chip-coil distance for external coils.

The energy that needs to be expended to generate the same physical effect using discrete coils is much higher than with the KMZ51 integrated solution, to the point where applications with a 5 V supply may become unfeasible. Also, there are competitive products that also have integrated coils, but which have a worse field factor than that produced by the patented design of the KMZ51. These may require expensive DC-DC converters to drive the necessary current through the coils.

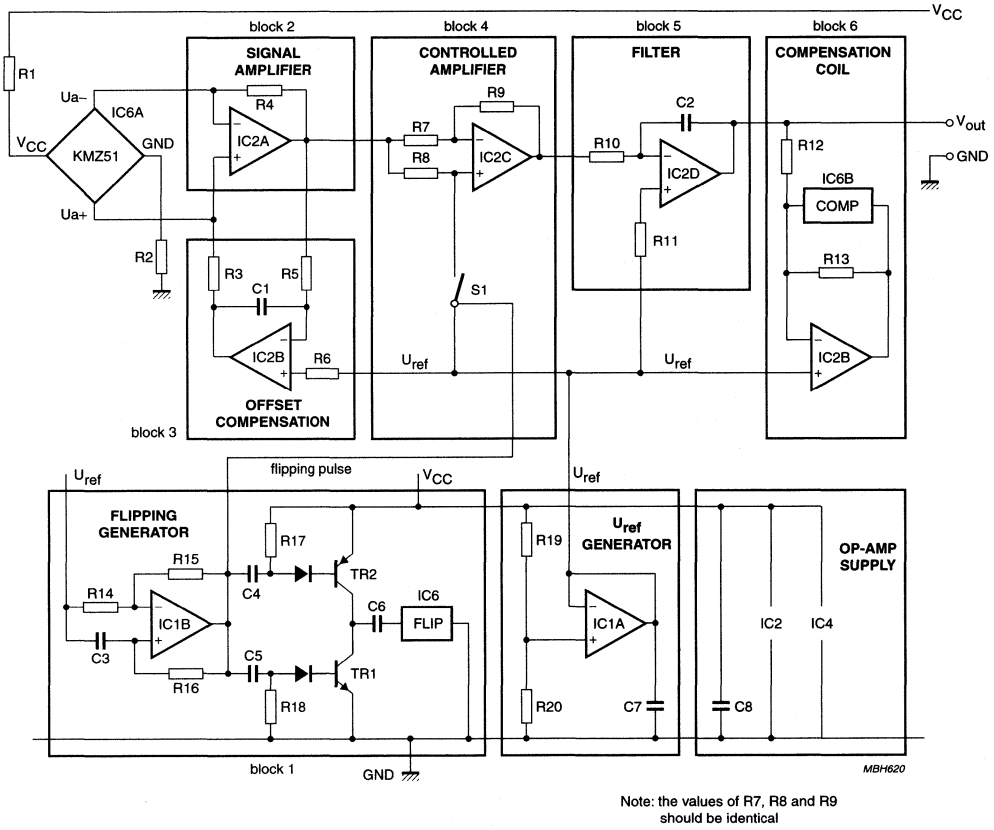

Fig.26 Application circuit using the KMZ51 sensor.

The 'flipper' circuit (Block 1) generates the flipping current, with a flipping frequency determined by R16 and C3, about 1 kHz in this case. As previously stated, the frequency is not critical and can be selected to minimize the need for post filtering and/or to provide the required response time.

The flipping frequency drives the synchronous rectifier as well as the flipping coil. As the signal passes from high to low, C4/R17 together produce a pulse that switches TR2 on. This charges C6 and a short positive pulse is passed to the flipping coil. For a low-to-high signal transition, C5/R18 forces TR1 to conduct, making C6 discharge and providing a negative pulse through to coil. An oscillograph of the current through the flipping coil is shown in Fig.27c, with a duration of about 10 µs and maximum current amplitude of around 0.7 A. The other diagrams show the responses of offset compensation (Fig.27b), and measuring magnetic pulses (Fig.27a).

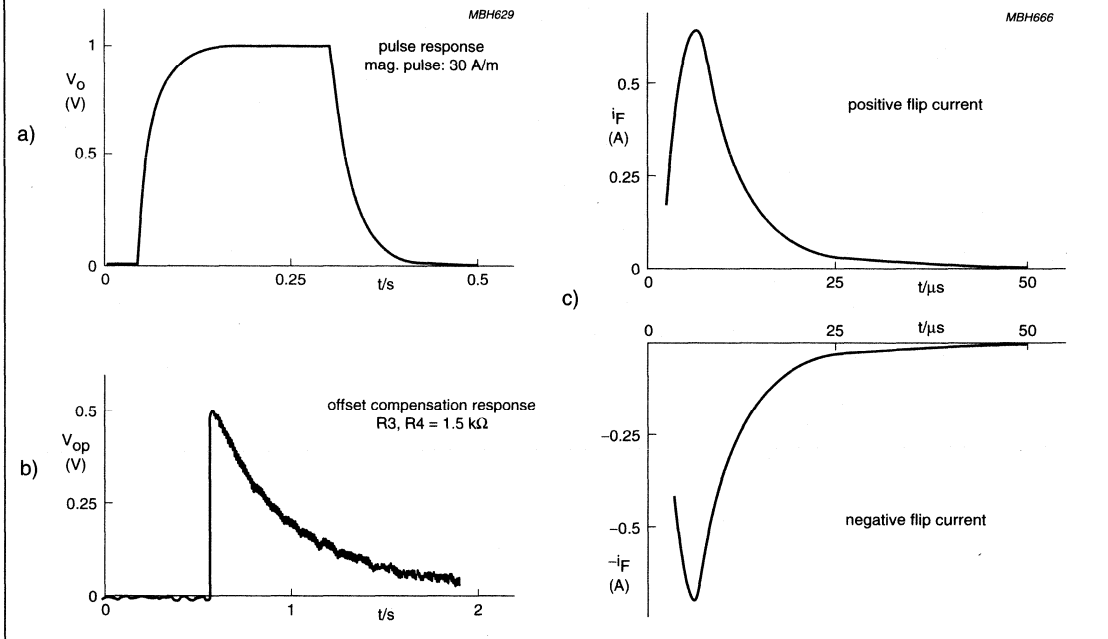

Fig.27 Oscillograph of flipping current in a MR sensor.

This circuit actually produces the necessary supply to drive two flipping coils, which may be needed in some applications such as an electronic compass (see Section "Application examples"). Another separate clock or clock generated by a µP in the system could also be used to drive TR1 and TR2.

The two resistors, R1 and R2, reduce the supply voltage of the set-up down to the level required for the sensor bridge, in this case reducing VCC = 10 V down to about 5 V. The flipped output signal of the sensor bridge is amplified by the pre-amplification circuit (Block 2) by a factor of 100, providing a signal up to about 300 mV_{PP} (given a field of about 15 A/m in the sensor plane). Of course, this voltage would only be visible in un-compensated mode; when the circuit is being used in compensated mode, this voltage will be approximately 0 mV_{PP}.

Referring to the block diagram, Fig.26, the integrator around IC2B in Block 3 provides the filtering to remove the offset. In fact, in this set-up it is performed with a low pass filter rather than high pass filtering. The low-pass filter extracts the offset and uses it as negative feedback at IC2A. It does not use the measured signal which, because of the flipping, is now a signal modulated at the flipping frequency. This has two main advantages:

- The op-amp in Block 2 is only amplifying the wanted signal, allowing the gain to be higher with no overload (or clipping) due to DC components.
- The offset of the op-amp in Block 2 will also be compensated, eliminating the need for special low offset amplifiers, reducing overall system costs.

The design of this filter affects system performance significantly. In this example, the flipping frequency is 1 kHz with a filter roll off of 4 Hz.

Block 4 (rectification) performs synchronous rectification of the flipped signal, to recover measured field information. If R7 = R8 = R9 this block performs alternate +1 and −1 amplification, depending whether the sensor is operating with a normal or inverted characteristic. When the flipping signal is LOW, switch S1 is closed and the op-amp acts as an inverting amplifier (−1 amplification); if the flipping signal is HIGH, then S1 is open and the amplification is +1 and no modifications are made to the input signal. With this rectification, the offset-compensated measured signal is recovered from the original sensor signal.

Block 5 smoothes the rectified signal so that a single continuous output signal is generated. As long as a compensation coil is used, it is recommended that this filter is also used, to ensure stable operation. If compensation is not used, then it is possible to use less expensive components. This block, as well as the rectifier Block 4 can even be omitted entirely if, for example, the output signal is then passed to a microcontroller which can easily perform the rectification and smoothing, especially if it is also being used to generate the flipping frequency.

The components in Block 6 drive the compensation coil and ensure that V_{out} is proportional to the compensation current. If the application does not need the highest accuracy, reduced circuit complexity can be used.

B. FLIPPING CIRCUIT WITH NO OFFSET COMPENSATION

In this case, Block 3 should be removed.

C. CIRCUIT WITH NO FLIPPING COMPENSATION

If a stabilization magnet or periodic re-setting is used instead of flipping, then Block 3 (flipping filter), Block 4 (rectifier) and Block 5 (smoothing) can be omitted. The flipping generation circuitry can also be simplified (by leaving out C5, R18, and TR1) or omitted if a stabilization magnet is used.

D. GENERAL REMARKS

The circuitry described above operates with inexpensive op-amps such as the LM324 and LM532, keeping costs low. However, this represents just one possible system solution and, depending on the required functions, further reductions in cost can be achieved by replacing the op-amps with transistor solutions. In designs that do not utilize some blocks in the circuit, such as offset compensation, this should certainly be considered. A very simple set-up can be used if a microprocessor is already available within the system (Fig.28).

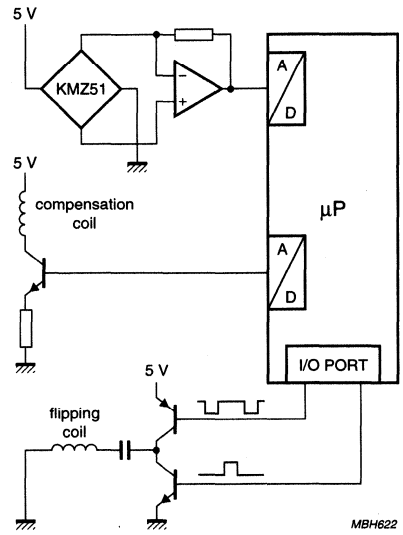

Fig.28 Set-up for weak field measurement using a microprocessor.

Application examples

In this section, we look at three weak field measurement applications:

1. Electronic compass
2. Earth geomagnetic field compensation in CRTs
3. Traffic detection.

Note: topics related to the measurement of weak currents are described in detail in Chapter "Current measurement".

ELECTRONIC COMPASS

A typical application of weak field measurement is that of the electronic compass. Here, two sensors are aligned in the same plane but at 90 degrees to one another. This provides a two dimensional compass, with the sensors measuring the x- and y-components of the measured (earth) field.

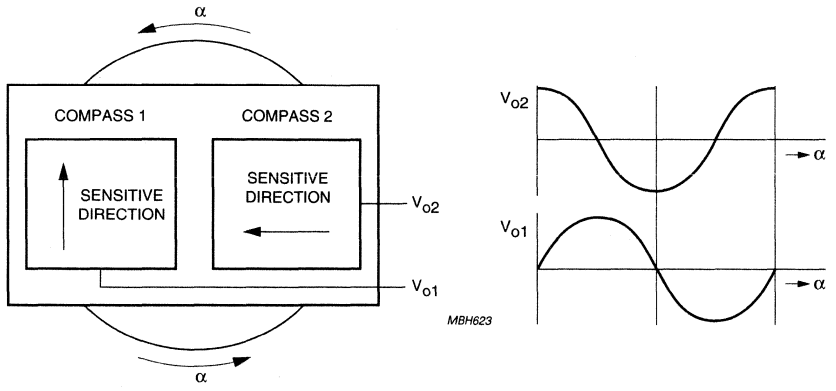

Fig.29 Simplified block diagram of an electronic compass.

Both of the sensors deliver a single sinewave when rotated in the Earth's geomagnetic field (see Fig.29). This two dimensional compass is sensitive to the angle α between the Earth's surface and the measurement plane of the sensors: a change in this angle will change the alignment between the sensitivity axis of the sensor and the Earth's field, and therefore affect sensor output. This effect, similar to that seen in conventional compasses, can be clearly observed in automotive applications, when a car is going up- or downhill. High precision systems eliminate this problem using a three dimensional compass and a gravity sensor.

Table 5 Typical disturbances in compass systems for different angles α

	ANGLE α		
LOCATION	**5°**	**10°**	**15°**
Zürich	9.7°	18.8°	26.9°
Hamburg	12.5°	23.8°	33.3°
Anchorage	17°	31.2°	42.1°
Singapore	1.5°	2.9°	4.3°
Tokyo	5.7°	11.2°	16.5°

Various levels of complexity can be incorporated in the drive circuit, to include the various compensation techniques described earlier in this chapter, depending on the level of accuracy required and expected environmental influences. A basic and a high-end compass example are described below.

A. Simple 8-segment compass

The main function of a simple compass application is to purely indicate direction (N, NE, E, etc.). This basic functionality is typically found in simple navigation aids where, for example, car drivers may require only an indication of their orientation and not an accurate indication of their direction. For such simple application set-ups, the accuracy produced by the sensor electronics need only be of the order of 3°.

In such a simple compass application, the compass may be required only to display the eight major compass directions. In this case, the two output signals can be compared with each other to achieve three digital signals (Fig.31). These provide the basic N, S, E, W information while a third, inverted sensor signal determines whether the sensor signal is changing positively or negatively and this is included in the comparison, to distinguish between the eight positions on the compass. Simple comparators can be used to obtain three digital signals, which drive a display unit via a multiplexer.

Note: Figure 30 shows the principles of a typical compass sensor set-up and for maximum clarity, compensation and flipping coils are shown separately. Of course the KMZ51, which has compensation and flipping coils incorporated into the sensor housing, would be used in a real-life application.

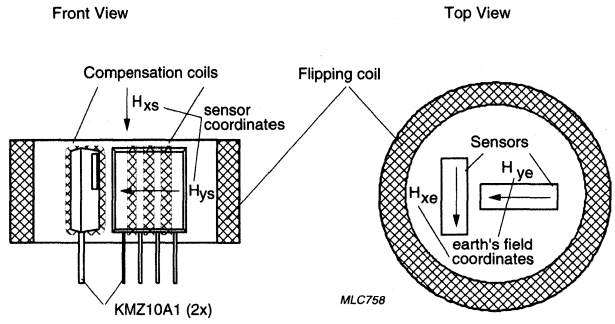

Fig.30 Compass sensor system.

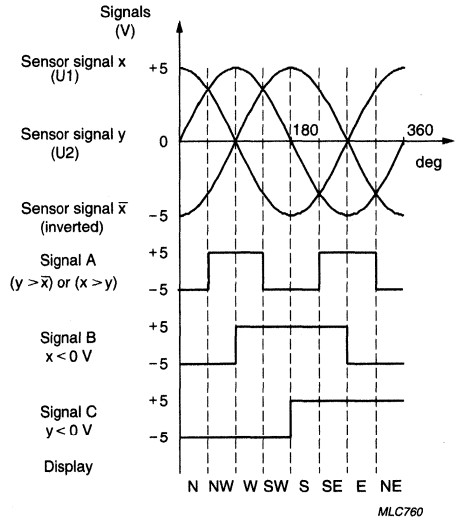

Fig.31 Evaluated signals.

B. High-end compass

Compass resolution can be increased from the basic eight by adapting the evaluation circuit and using a microcontroller to calculate the arctan function of the ratio of the two signals to determine the angle. The resolution of the compass then depends on the microcontroller and the A/D converters used. The use of a microcontroller also enables additional functionality, such as storing a reference direction or eliminating magnetic influences from encapsulation or other magnetic components.

Simple alignment using opposite directions

Electronic compasses need calibrating to eliminate the effects of these extraneous fields produced, for example, by the compass casing. The simplest method is known as Bi-directional Calibration. Requiring no external calibration devices, in this technique the output is measured twice with each measurement shifted by 180°. From this, the x- and y- components of the extraneous field can be determined and simply compensated for by applying the appropriate current to the coils, synthesizing a compensation field.

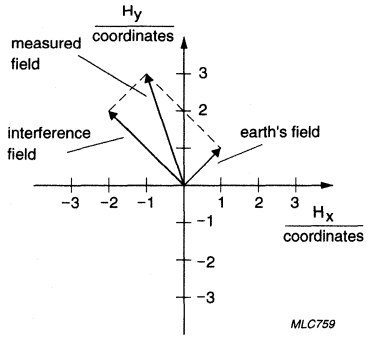

Fig.32 Two-dimensional vector space.

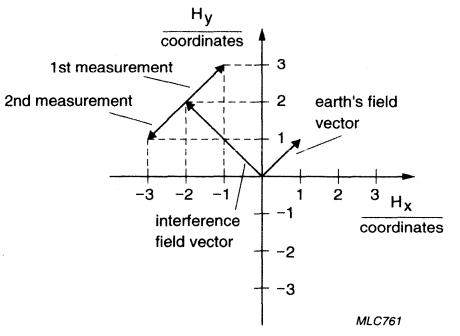

Fig.33 Measured fields in vector space.

Continuous alignment

With high-end compass applications, the microcontroller can also be used to adjust the calibration of the compass continually. This is especially useful in automotive compasses, eliminating the need for manual re-adjustment according to variable vehicle load.

Compass test units

For test purposes, Philips designed an SMD board (Figs 34 and 35) with the following parameters:

- Supply: 10 V
- Current: 25 mA (typ.)
- $V_{O\ (x,y)}$: 30 mV per A/m (V_x, $V_y \leftrightarrow V_{ref}$)
- Load: >10 kΩ
- $I_{O\ (x,y)}$: 62.5 μA per A/m (5 mA/Gauss) (I_x, $I_y \leftrightarrow V_{ref}$)
- Noise: 0.05 A/m
- Range: 100 A/m
- Load: <70 Ω (<500 Ω at V_{CC} = 16 V)
- Bandwidth: ≈ 10 Hz.

An SMD compass sensor test unit was rotated in an Earth field rotational unit, resulting in the test-diagram shown in Fig.36.

Note: U_{ref} is internally generated on the board, it does not need to be provided externally.

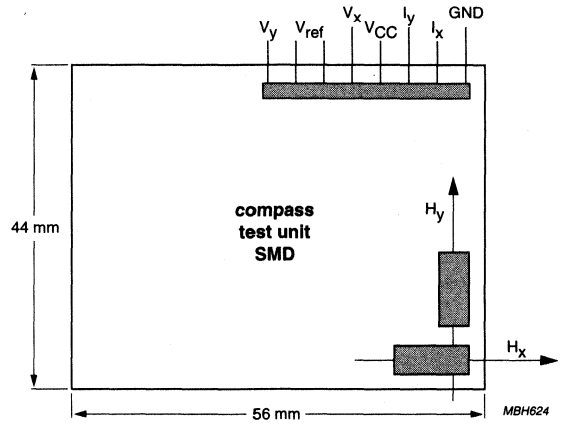

Fig.34 SMD test unit.

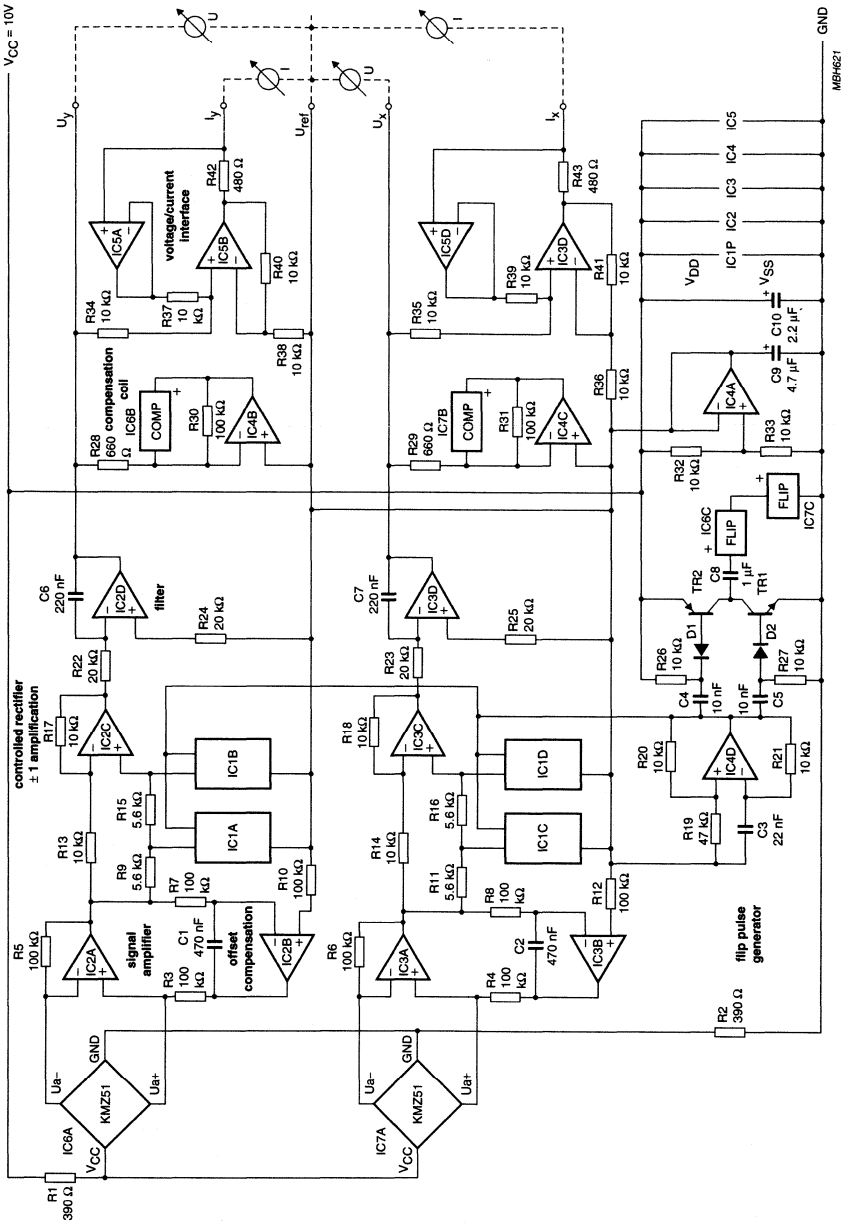

Fig.35 Circuit diagram for an electronic compass.

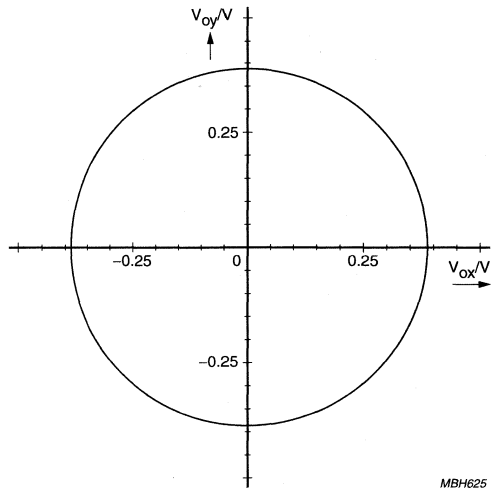

Fig.36 Typical test-diagram.

EARTH GEOMAGNETIC FIELD COMPENSATION IN CRTS

The Earth's geomagnetic field has always caused problems for TV and monitor manufacturers, as it influences the trajectory of electrons in a CRT tube producing a horizontal tilt in the geometry and convergence error shifts. With the introduction of wide screen picture tubes, this problem has become unacceptable, especially with geometric test patterns and 16:9 aspect ratios. With the continuing goal of improving picture quality and allowing for varying magnetic fields in every part of the world, a compensation circuit was required to reduce this effect.

A simple one-dimensional solution is to wrap a DC-current carrying coil around the neck of the CRT to generate a magnetic field opposite to the Earth's field, cancelling the twist in the electrons path and reducing by approximately 50% the number of convergence errors.

This coil also has the additional advantage of compensating for any other extraneous electromagnetic field sources emanating from the TV such as the loudspeakers. By including a magnetoresistive sensor to detect the Earth field, the output from the sensor can be used to drive the compensation field, making adjustment automatic.

Although residual picture twist and North/South trapezoid errors can still be seen, a simple DC-shift in the compensation current will eliminate the picture twist and the addition of a vertical sawtooth (ramp) current, derived from the vertical deflection, will remove the N/S trapezoid.

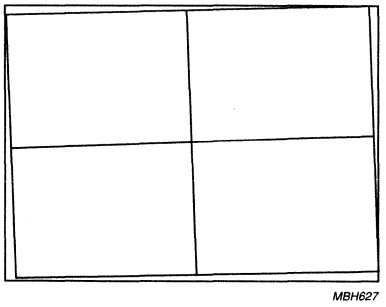

Fig.37 Geometry error - horizontal picture tilt.

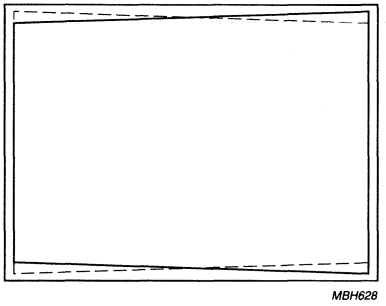

Fig.38 Geometry error - North/South trapezoid.

TRAFFIC DETECTION

As the number of vehicles using already congested roads steadily increases, traffic control systems are becoming necessary to avoid time consuming traffic jams. These systems monitor traffic flow, average speed and traffic density, allowing electronic road signs to control the flow and speed of traffic at known trouble spots. They also have the advantage of indicating possible incidents, where traffic speeds fall significantly below average on certain sections of road. Simple modifications to these systems allows them to be used to improve safety, and also to monitor ground traffic at airports.

Although highly sophisticated computer systems are used to analyse the various inputs in traffic systems, currently this input information is gained from inductive systems which have a number of disadvantages. The low sensitivity offered by inductive measuring systems requires large areas of road to be lifted and re-surfaced during installation. With their high power consumption, and the fact they produce very little information regarding the type of traffic passing over them, makes them both costly and inefficient. They are also rather unreliable due to road thermal stress.

As practically every vehicle manufactured contains a high number of ferromagnetic components, a measurable magnetic field specific to an individual model from every manufacturer can be detected, using weak field measurement techniques with magnetoresistive sensors. Even with the greater use of aluminium in manufacture and if the vehicle has been demagnetized, it will still create a measurable change in geomagnetic field strength and flux density.

In comparison with inductive methods, with its high sensitivity magnetoresistive measuring can provide information on the passing vehicle type. Also, due to the sensor size and placement, systems can be easily and quickly installed in any stretch of road, or even by the side of the road, if necessary. Combined with almost negligible power consumption, this makes magnetoresistive control systems an inexpensive and highly efficient method of monitoring traffic levels.

A. Measurements on roads

A field test with three-dimensional sensor modules was set-up, firstly to measure the signals of different vehicles; and secondly, the relative occurrence of signal values of three vehicle categories (car, van and truck). For the first test, one module was placed in the road, under the vehicle and for comparison, a second module was placed at the side of the road. For the second test, which was performed 'live' on a street in Hamburg, Germany, the module could only be positioned at the side of the road.

The local geomagnetic field was calibrated to zero, so that only the disturbance in the field caused by the passing vehicle would be recorded. Figure 39 shows the spectra produced by an Opel Kadett.

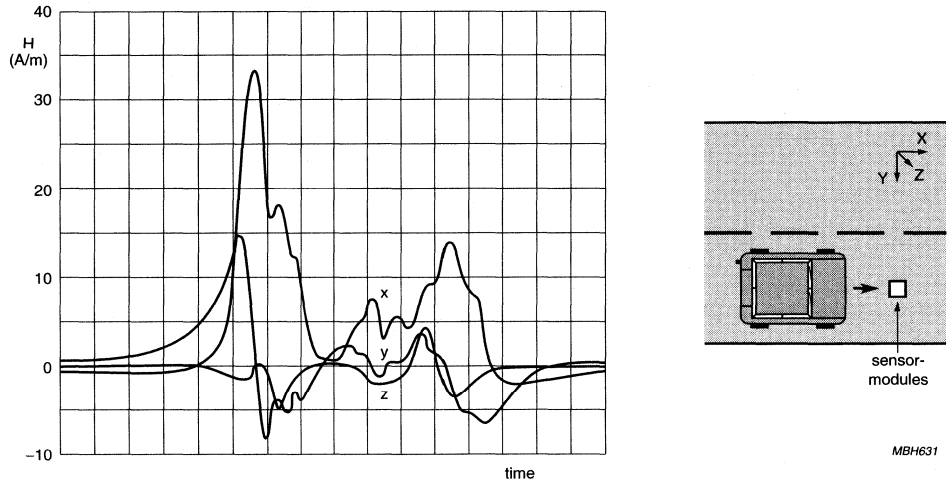

Fig.39 Spectra for an Opel Kadett from ground sensor.

The sensor modules also proved sensitive enough to detect and distinguish motorbikes (even with engine, frame and wheels being made of aluminium), which produced the following roadside spectra.

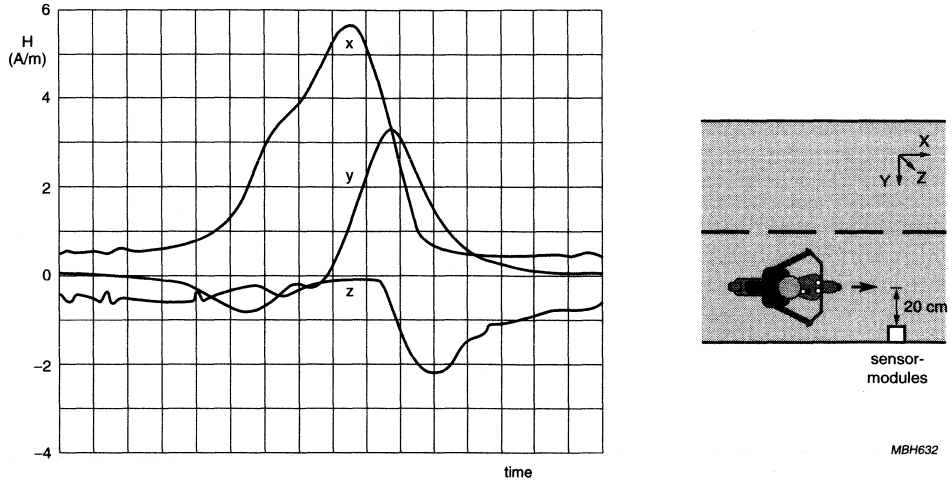

Fig.40 Spectra for a motorbike.

For the roadside test in Hamburg, the road was chosen at random and the maximum signal value was recorded for different vehicles, being grouped into cars, vans and trucks. The relative occurrence of signal values are shown in the following diagram.

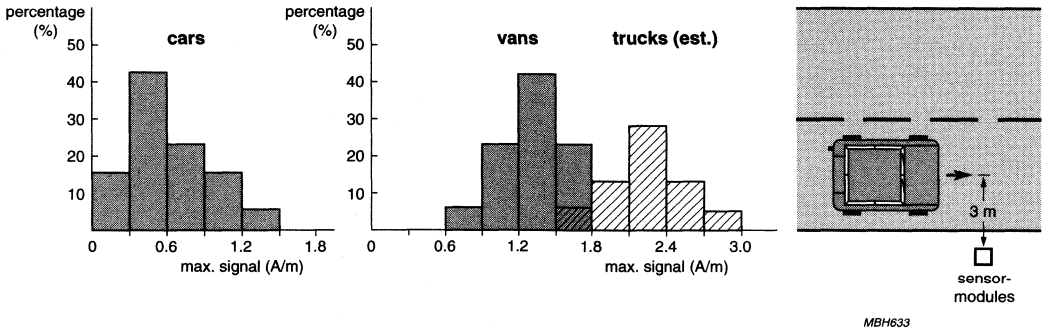

Fig.41 Distribution graphs of maximum signal versus occurrence.

The signals in each group seem to have a Gaussian distribution with a characteristic maximum (although in fact there were only three trucks, so the values for this group are an estimate).

B. Airport ground traffic control

With the constant growth in air traffic around the world, one serious consideration in the improvement of safety and the ability to improve the handling capacity of airports, is the control of traffic on and around runways. Using a traffic control system, it is possible to introduce automatic guidance systems and prevent runway incursions even at heavily congested airports or under low visibility conditions, in accordance with regulations set-down by the internationally recognized authorities.

Although there are a number of possible sensor solutions, traffic systems using magnetoresistive technology have none of the drawbacks of existing radar, microwave, I/R, pressure, acoustic or inductive systems (see Table 6). They meet all of the functional and environmental restraints, such as large temperature ranges, insensitivity to climatic changes, low power consumption and, most of all, low cost, high reliability and ruggedness. They can also perform a range of signalling functions including detection of presence, recognition, classification, estimation of speed and deviation from path.

Table 6 Disadvantages of various sensors for airport ground traffic control units

Radar	Microwave barriers	Inductive sensors
• High costs • Reduced efficiency with large number of targets • Line of sight only • Complex target identification • Low resolution • Slow response times	• Cannot be installed flush with the ground • Creates new obstacles in surveyed area • Produce EM interference	• Low sensitivity and short range • Poor target information • High power consumption • Unreliable in harsh environments • Repairs require traffic to be stopped or diverted
Pressure sensors	**Acoustic sensors**	**I/R signalling**
• Frequent mechanical breakdowns when used in harsh environments • Associated ageing problems • Poor target identification	• Signal interference when used outdoor and due to weather conditions • Trade-off between sensitivity and range • Large power consumption	• Greatly affected by weather conditions • Complex target identification

CURRENT MEASUREMENT

Contents:

- Principles
- Some practical sensing set-ups
- Measurement examples using Philips' sensors.

Principles

The principle of measuring current with a magnetoresistive sensor is straightforward. As a current, i, flows through a wire, it generates a magnetic field around it which is directly proportional to the current. By measuring the strength of this magnetic field with a magnetoresistive sensor, the current can thus be accurately determined.

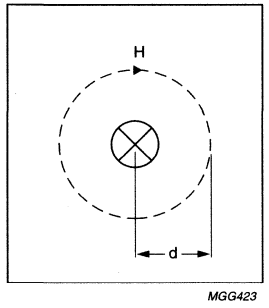

Fig.42 Diagram showing field direction in a current carrying wire.

The relationship between magnetic field strength H, current i and distance d is given by:

$$H = \frac{i}{2\pi d} \qquad (14)$$

Some calculated values of H for typical conditions are given in Table 7.

Table 7 Values for the magnetic field generated by a current carrying wire at various distances and currents

EXAMPLE	CURRENT (i)	DISTANCE (d)	MAGNETIC FIELD (H)
1	10 mA	0.5 mm	3.18 A/m
2	1 A	0.5 mm	318 A/m
3	1000 A	10 mm	15.9 kA/m

Table 7 clearly indicates that current measurement can involve measurement of weak or strong magnetic fields. As the sensitivity of magnetoresistive sensors can easily be adjusted, using different set-ups and different electronics (refer to the selection guide in the General section), an individual sensor can be optimized for a specific current measurement application, a clear advantage over Hall effect sensors.

The accuracy achievable in current measurement using magnetoresistive sensors is highly dependent on the specific application set-up. Factors which affect accuracy are mechanical tolerances (such as the distance between the sensor and the wire), temperature drift and the sensitivity of the conditioning electronics. However, with Philips magnetoresistive sensors accuracies to within about 1% are possible.

There is a general difference in the set-up used when using MR sensors for AC or DC current measurement, due to the effects of disturbance fields such as the Earth's geomagnetic field. For AC currents, disturbing fields can be eliminating using filtering techniques (similar to those described in the Chapter "Weak field measurements"), while for DC currents, compensation techniques must be used (for example by using two sensors).

Some practical sensing set-ups

DIRECT MEASUREMENT WITH A SINGLE SENSOR

Philips' sensors can be used in a number of standard set-ups for current measurement. The simplest places a single sensor close to the current carrying wire, to measure directly the field generated by the current (see Fig.43). Figure 44 shows how the sensitivity of the sensor varies with distance from the wire.

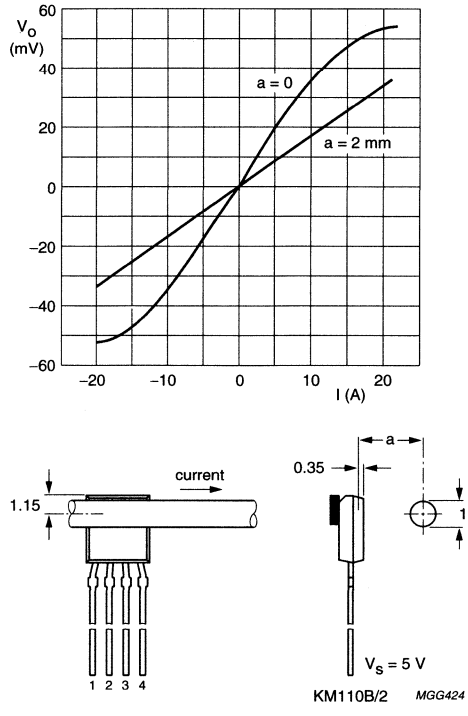

Fig.43 Simple set-up for measuring current using a KM110B/2 sensor with an external magnet.

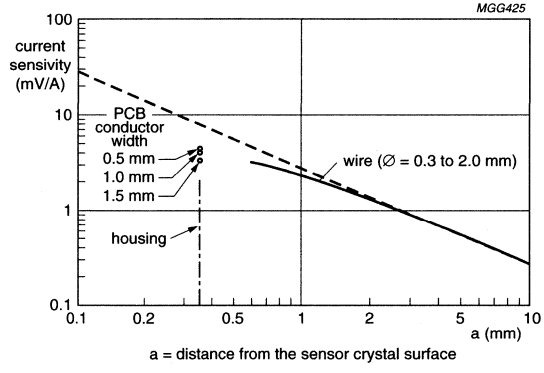

Fig.44 Sensor sensitivity versus distance for wires with diameters ranging from 0.3 to 2.0 mm.

Not surprisingly, sensor sensitivity rises as distance 'a' decreases. For relatively large values of 'a' (say 5 mm), the increase in sensitivity is substantially linear, but at closer spacings, when the magnetic field generated by the current is no longer uniform over the sensor, the rate of increase drops off. For higher currents, a similar drop off from linearity would be observed at quite large distances, but this is due to the magnetic field generated by the current saturating the sensor. In this case, an optimal linear relationship can be simply restored by using a less sensitive sensor (refer to Table 2 in the 'General introduction' for a summary of Philips sensors and their main characteristics).

The sensor can also be laid directly onto the conductor in a PCB and Fig.44 also shows the sensitivity of the sensor for three widths of PCB conductor.

IMPROVING ACCURACY WITH A FERRITE CORE

A second set-up, shown in Fig.45, is a more sophisticated arrangement in which the magnetic field generated by the current-carrying wire is compensated by a secondary circuit wrapped around a ferrite core. At the 'null-field' point, detected by the sensor located in the air gap between the ends of the core, the magnitude of the current in the secondary circuit is a measure of the current in the main circuit. This arrangement provides a more accurate means of measuring current, reducing any inaccuracies as a result of tolerances, temperature drift and slight non-linearities in the sensor characteristics, lending itself more to precision applications.

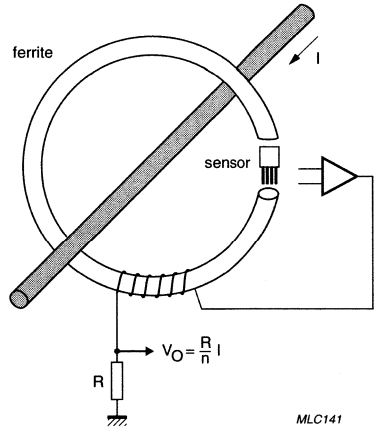

Fig.45 Current measurement using a compensating coil.

Both these first two set-ups allow current measurement without breaking the conductor or interfering with the circuit in any way, providing a distinct advantage over resistor based systems. They can be used, for example, for measuring the current in a headlamp-failure detection system in motor vehicles or in clamp-on (non-contacting) meters, as used in the power industry.

For applications where an analog signal is measured, such as in these two measurement set-ups, a good evaluation circuit should be used to allow for temperature drift compensation and for offset and sensitivity adjustment. This applies generally to measurement circuits using magnetoresistive sensors. This is discussed in more detail in Chapter "Weak field measurements".

Compensating for external magnetic fields

In any measurement set-up, there are always other magnetic fields present besides that generated by the current, such as the earth's magnetic field, and these interfere with the measurement. A more accurate measurement set-up uses two magnetic field sensors, to compensate for these external fields (see Fig.46).

The first sensor detects both the interference field and the current-field in the positive direction, and the second sensor detects the interference field in the negative direction and the current-field in the positive direction. These two signals are added, cancelling out the interference field, leaving a signal that is representative of only the current-field.

This set-up works with homogeneous interference fields like that from the earth. Inhomogeneous fields, which will produce different interference fields inside the two sensors, will still affect the current measurement. This error can be minimized by keeping the distance between the sensors small or integrating both sensors onto a single piece of silicon. Large magnetic fields which fall outside the range of the sensors can also produce errors, so the size of external fields must be limited.

Another advantage of using two sensors, at a fixed distance apart, is that measurement is less sensitive to sensor-conductor distance. If the conductor is moved closer to the first sensor, then its distance from the second sensor is correspondingly increased and the effect is compensated. For small differences in distance between the conductor and sensors, sensitivity is nearly constant and the conductor need not be fixed in place. This method lends itself to measurement of current in free cables.

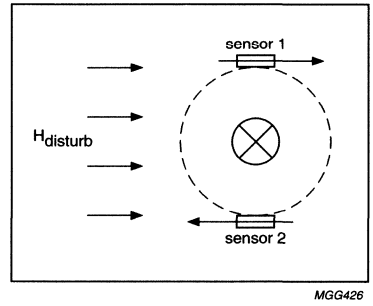

Fig.46 Diagram showing two sensors to measure current.

Table 8 summarizes the various advantages and disadvantages of one-sensor and two-sensor measurement set-ups as described above.

Table 8 Summary of advantages and disadvantages of typical measurement set-ups

CURRENT MEASUREMENT WITH TWO MAGNETIC FIELD SENSORS		CURRENT MEASUREMENT WITH ONE MAGNETIC FIELD SENSOR	
PROS	**CONS**	**PROS**	**CONS**
• no galvanic connection	• interference effects from inhomogeneous fields	• no galvanic connection	• effects of interference from external fields
• no breaking of the conductor	• errors generated from large external fields	• no breaking of the conductor	• sensitive to the sensor-conductor distance
• small physical dimensions		• small physical dimensions	
• reduced sensitivity to sensor-conductor distance			
• reduced interference effects from homogeneous fields			

Measurement examples using Philips' sensors

For measurement, Philips' KMZ10A/B/C and KMZ51 sensor types can be used. The KMZ10A/B/C have to be stabilized with auxiliary magnets, for example as in the KM110B/2. KMZ51 sensors contain internal conductors ('coils') to compensate for offset and temperature drift and do not need an auxiliary magnet, allowing for simple circuitry with reduced need for adjustments. As these sensors do not measure fields above about ±230 A/m (approx. ten times the earth's magnetic field), they must be used in a measurement set-up that reduces the effects of interference fields, as described above.

The following examples demonstrate Philips' magnetoresistive sensors being used in real-life situations.

AC CURRENT MEASUREMENT USING DUAL KM110B/2 SENSORS

Two KM110B/2 sensors, placed as outlined above, are in-phase for current measurement and antiphase for external field compensation, eliminating the effects from stray fields and improving sensitivity (see figs 47 and 48).

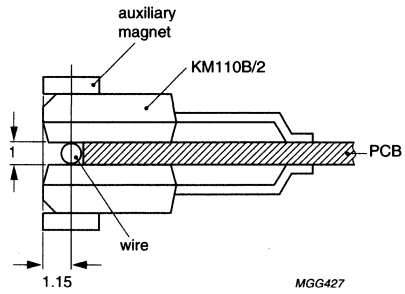

Fig.47 Diagram showing set-up for AC current measurement.

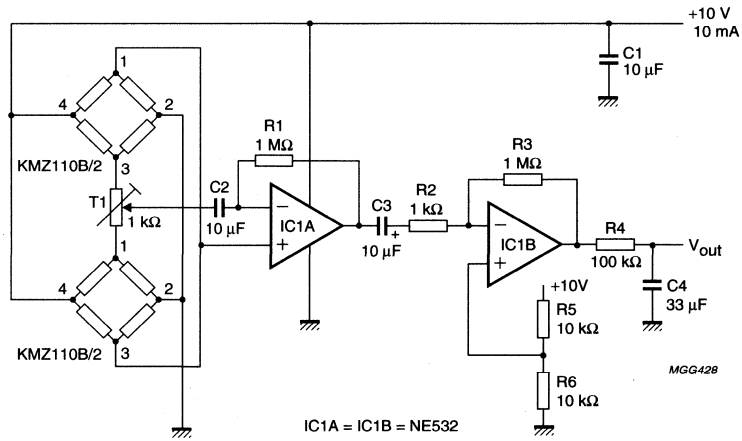

Fig.48 Circuit diagram.

This circuit shown in Fig.48 is a pre-tested design for 50 Hz currents, delivering very high sensitivity. Two KM110B/2 sensors are connected in parallel, with T1 aligned such that the signals produced by external disturbing fields is minimized. The output signal is then amplified and DC signal components are considerably reduced with filtering, through R1-C2 and R2-C3. This circuit gives the following characteristics:

Amplification: 120 dB (50 Hz)
Sensitivity: 5 V/mA
Noise level: 0.37 V
Max. output: 2.1 V (@ 0.4 mA measured current)

If R1 is adjusted to about 39 kΩ, this changes the data to:

Amplification: 92 dB
Sensitivity: 0.2 V/mA
Noise level: 0.015 V
Max. output: 2.1 V (@ 10 mA measured current)

SENSITIVE MEASUREMENT USING WEAK FIELDS WITH DUAL KMZ51 SENSORS

This section describes a practical set-up that can be used for measuring currents in the metal tracks of a PC-board. Using the paired sensor approach again, the following set-up can also be used to measure currents producing only weak magnetic fields. In this case, the conductor is also locked mechanically to the sensors, eliminating variations due to the movement of the conductor and allowing small currents to be measured to an accuracy of approximately 1%, with no galvanic connection.

Note: since this involves the measurement of weak magnetic fields, techniques must be used to suppress the influence of sensor offset and temperature drift. For more detailed information on these techniques, refer to the sections on Flipping and Compensation in Chapter "Weak field measurements".

Generally there are several sensor set-ups which can be used to compensate for the external field. If there are components on both sides of the PCB, the set-up in Fig.49 can be used.

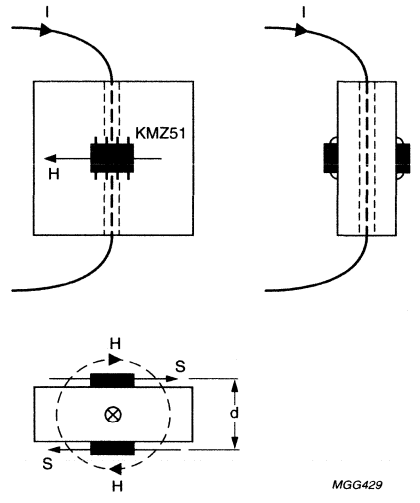

Fig.49 Sensor positioning for current measurement with double-sided PC-boards.

The current carrying track is in the centre of the board with the sensors' sensitive direction marked with an 'S'. This set-up clearly follows the conditions described in Section "Compensating for external magnetic fields" earlier (see also Fig.46).

If components are only placed on one side of the PCB, then the track carrying the current to be measured must be laid in such a way that the conditions described in Section "Compensating for external magnetic fields" are adhered to. Figure 50 illustrates three possible set-ups of sensor and current-carrier, used in Philips Semiconductors' demonstration board.

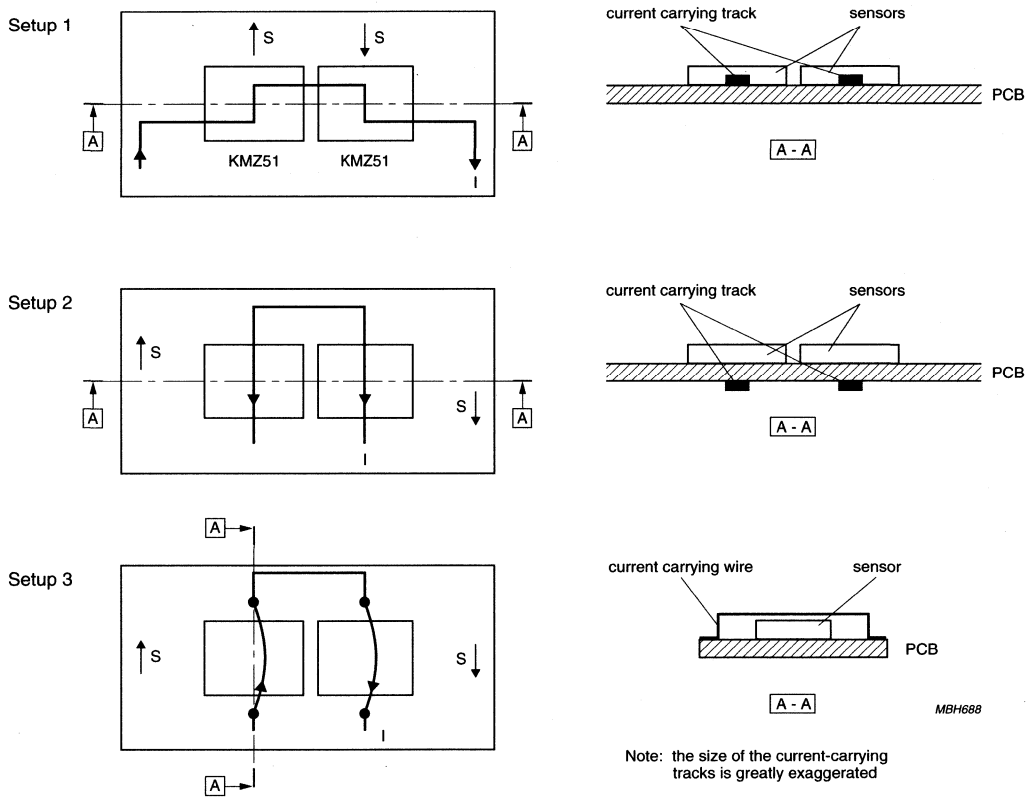

Fig.50 Sensor positioning for single-sided PCBs: (a) track directly under the sensor, same side of the PCB; (b) track on opposite side of PCB; and (c) wire on top of sensor.

The circuitry used to condition the sensor output to a usable signal (see Fig.51) can be the same for all three set-ups. The basic principle is to have the sensors electrically parallel, effectively merging the output signals. This gives the following advantages that

- Only one conditioning circuit is required for both sensors
- The sensors themselves automatically compensate for any disturbing fields.

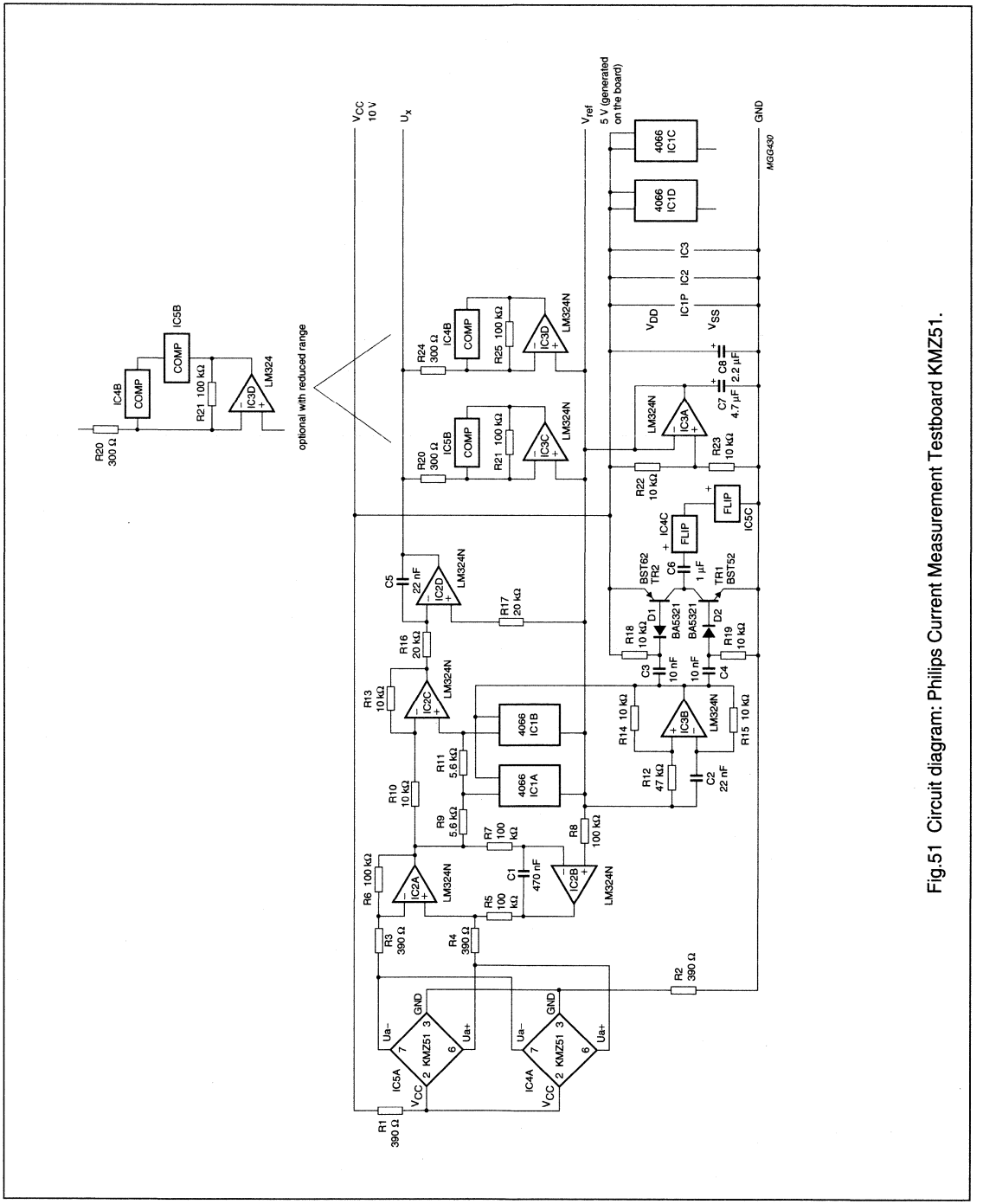

Fig.51 Circuit diagram: Philips Current Measurement Testboard KMZ51.

After the output signals of the two sensors have been merged, the basic conditioning circuitry is similar to that used for weak field measurement. The basic principles of the electronics are described in more detail in Chapter "Weak field measurements"; however, the figures quoted in that example are for a compass application and this circuit is optimized for current measurement, with the following characteristics:

Table 9

Maximum level of compensation for current and disturbing fields	±230 A/m
$I_{comp(max.)}$	±10 mA
Time constant	200 Hz

The sensitivities and ranges of the three different sensor set-ups shown in Fig.50 are:

Set-up 1: 1.8 V/A; range: ±1.1 A
Set-up 2: 1.1 V/A; range: ±1.8 A
Set-up 3: 5.7 V/A; range: ±0.35 A

Note: this example uses an analog circuit, to clarify the principles of current measurement including flipping and magnetic compensation. A large part of the functionality of the circuitry could easily be handled by a microprocessor (see Fig.52 for a typical circuit diagram).

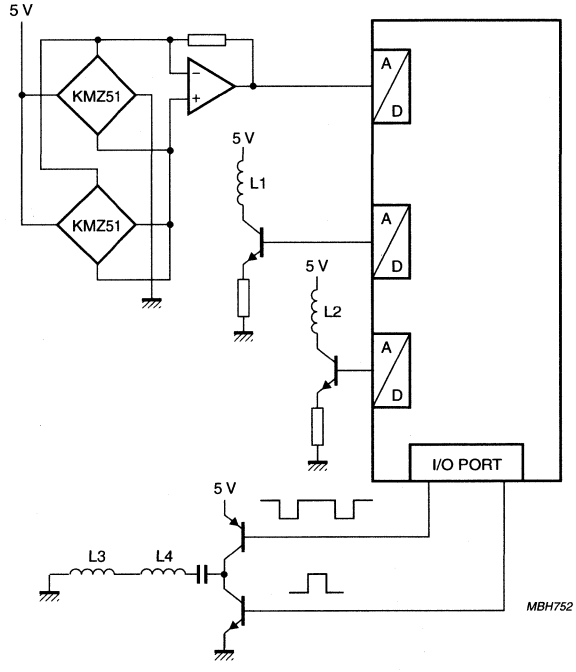

Fig.52 Circuit diagram using two sensors and a microprocessor.

HIGH DC CURRENT MEASUREMENTS

Interest in sensors for contactless measurement of high currents has been steadily increasing and to help customers apply this technology, Philips has prepared a module for testing, based on our KM110B/2 magnetoresistive sensor (equipped with a stabilization magnet). It consists of the KM110B/2 sensor, conditioning electronics and a U-core.

The wire carrying the current to be measured should be fed through the U-core, but a short distance should be maintained between the wire and the sensor. Figure 53 shows the influence of wire position on sensitivity. If wires are thin, a spacer above the sensor can prevent errors in the measurement. Cables or conductors with large diameters are less sensitive to this effect. Ring cores with an air gap are generally less sensitive to wire position but are more difficult to obtain and mount, so a U-core was used for these test modules.

Figure 54 shows the conditioning electronics for this set-up. In principle, it is similar to the basic conditioning circuit in the 'General introduction' (see Fig.11), although it has been optimized for this particular application and has the following characteristics:

Supply voltage V_B: 5 V
Current range: 16 A
Frequency range: 0 to 1000 Hz
Temperature range: −40 to +80 °C
Sensitivity: 135 mV/A
Sensitivity temperature drift (temperature range −20/+85 °C): < 0.8%
Quiescent output voltage (I = 0 A): 2.5 V
Quiescent output voltage temperature drift (temperature range −20/+85 °C): < 25 mV
Equivalent current drift: < 0.2 A.

The typical response of this sensor and circuit set-up is shown in Fig.55 and shows the excellent linearity, even for large currents.

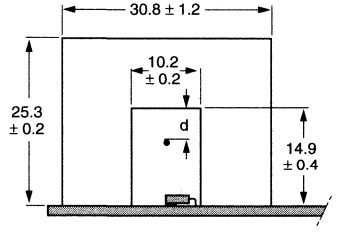

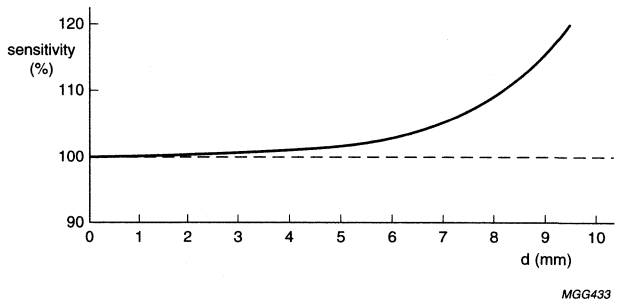

Fig.53 Influence of wire position.

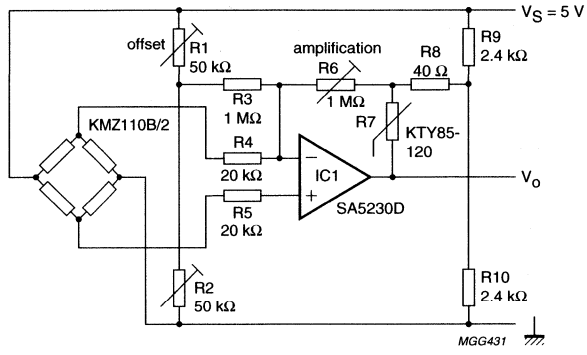

Fig.54 Circuit diagram for a current sensor based on this module.

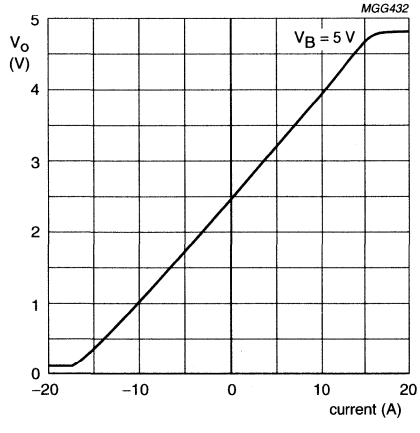

Fig.55 Typical response of a current sensor based on this module.

Other current ranges can be obtained by varying the following:

- Sensor (KMZ10C with auxiliary magnet, delivering a current range of about ±50 A)
- Core type
- Sensor position relative to the core.

Varying these parameters as described in general produces higher current ranges. Sensitivity can also be increased by winding the wire repeatedly through the core or by applying a higher amplification range. Modules have also been prepared with higher current ranges (up to ±300 A), using stronger auxiliary magnets. More information is available on request.

These are just a few of the possibilities offered by magnetoresistive sensors for current measurement. With their inherent simplicity of application and ability to compensate easily for disturbing fields, MR sensors are easily the most flexible choice.

LINEAR POSITION AND PROXIMITY MEASUREMENT

Contents:

- Principles and standard set-ups
- Position measurement applications
- Reference set-ups.

Principles and standard set-ups

The sensitivity of magnetoresistive sensors lends itself to linear position measurement systems, with a number of possible applications. Simple basic set-ups can be used for one-point position measurement and a linear position measurement set-up and can be easily modified to produce a proximity switch sensor.

The underlying principle is very similar to that used for angular measurement, in that as a magnet on the target is moved, the internal magnetization vectors of the permalloy strips on the sensor change, aligning themselves with the external magnetic field and thus changing their resistance.

When a magnetoresistive sensor is placed in a permanent magnetic field, generally it is exposed to fields in both the x- and y-direction. If the magnet is oriented is such a way that the axis of the auxiliary field in the x-direction is parallel to the permalloy strips in the sensor, then any movement in the y-direction can be seen as fluctuations in the transverse field, which can be equated to the position of the magnet with respect to the sensor.

The linear region of the sensor's sinusoidal output is defined roughly by the length of the magnet. Outside this area, the axial field produced by the magnet is becomes weaker and near the poles, it also changes direction, both of which can cause sensor flipping. (For further information on sensor flipping, please refer to Appendix 2 and the Chapter on "Weak field measurements").

Figure 56 shows one of the simplest arrangements for using a sensor/magnet combination to measure linear displacement.

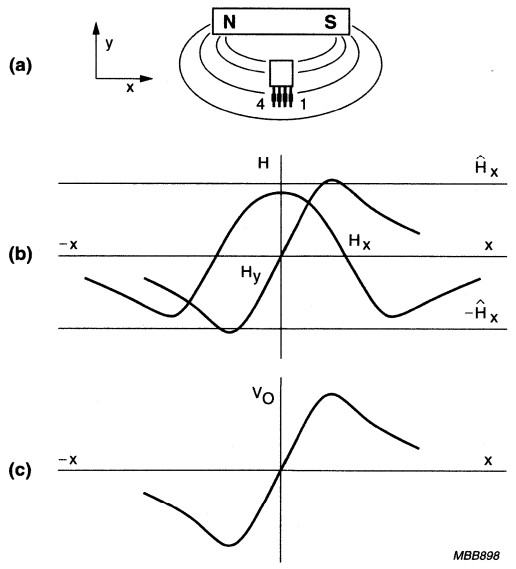

Fig.56 Sensor output in the field of a permanent magnet.

If a strong magnetic field is used or the sensor is placed very close to the magnet, there is a danger that the auxiliary field will exceed field required to flip the sensor characteristic, producing a hysteresis in sensor output (shown by the hysteresis loop ABCD in Fig.57

This can actually be used to positive effect under certain circumstances, where temporary or fluctuating external fields may interfere with the measured signal. In this case, as long as the sensor is used in the region between D and D', the strength of the magnetic field from the permanent magnet will block out any extraneous fields.

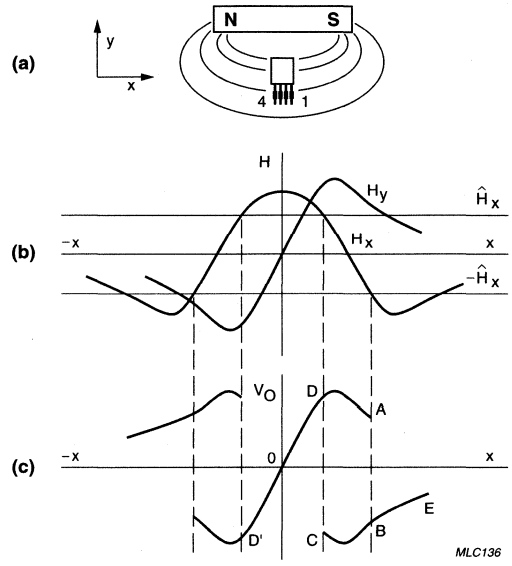

Fig.57 Sensor output in a strong magnetic field.

By orienting a sensor's axis to 45° with respect to the axis of the permanent magnet, as shown in Fig.58, it is possible to use the sensor along with a comparator, as a proximity switch. In this arrangement the sensor has a negative output, for both axial arrangements of the magnet, which can then be passed onto the inverting input of a comparator.

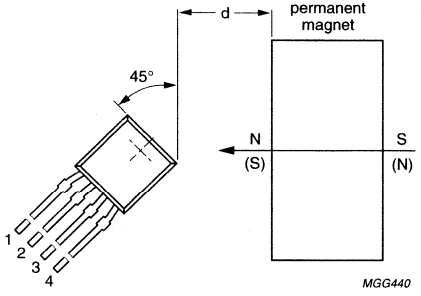

Fig.58 Proximity sensing using a magnetoresistive sensor.

The resulting output is clearly indicative of the distance 'd' between the magnet and the sensor (see Fig.59). Sensor switching levels are very important in this application; below a certain level, strong external magnetic fields may disturb the sensor sufficiently to produce ambiguous results.

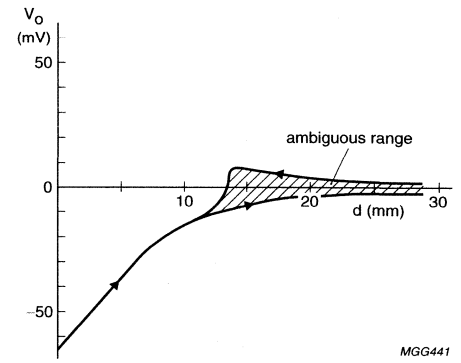

Fig.59 Sensor output as a function of distance.

Besides being used for general position sensing and measurement, by incorporating a back biasing magnet, single-point measurements are possible using any non-symmetrical region of material within the target such as a hole, pin, or region of non-magnetic material integrated into a metal plate's structure. The resulting disturbance in the magnetic field produces a variation in sensor output. Figure 60 shows the basic set-up and at the crossover point, where the hole and sensor match precisely, the sensor output is clearly independent of separation distance.

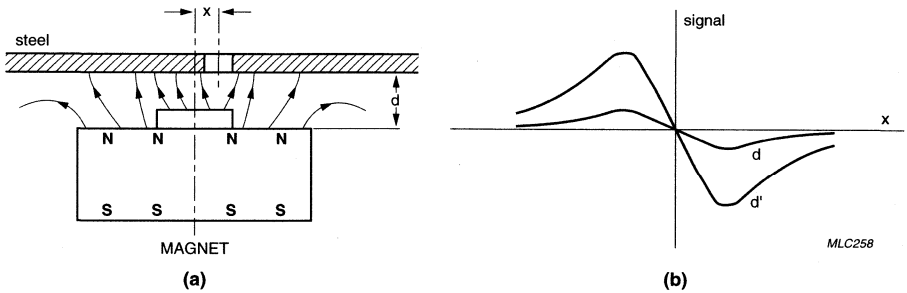

Fig.60 One-point measurement with a KM110B/1.

The obvious advantage of this technique is that the precise location of the sensor/magnet combination is irrelevant and as the sensor is basically acting as a 'null-field' detector at this point, the set-up is also independent of temperature effects. This makes the system very simple to design in.

Position measurement applications

The output from a KMZ10B and a KMZ10C sensor was measured as a function of sensor displacement, parallel to the magnetic axis. This was done using varying magnet/sensor separation distances and three different sized FXD330 magnets: a $\phi 10 \times 15$ mm, a single $\phi 4 \times 5$ mm, and two $\phi 4 \times 5$ mm placed end-to-end to make a single 10 mm long magnet. Two different set-ups were used, first with the magnetic field parallel to the sensor and second with the magnetic field perpendicular to the sensor.

MAGNETIC FIELD PARALLEL TO THE PLANE OF THE SENSOR

In this set-up the magnet is oriented with the sensor so that it is broadside-on, with its poles lying in the plane containing the sensor chip. With this arrangement, the auxiliary field is supplied by the axial field (H_x) of the magnet, which remains reasonably constant over the region of interest.

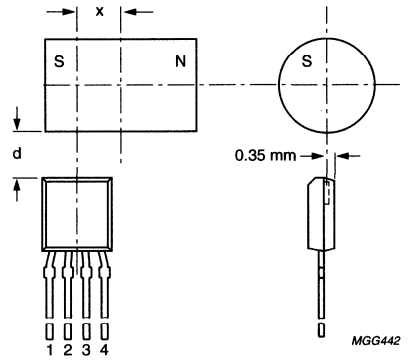

Fig.61 Position measurement with sensor broadside-on to an FXD330 magnet.

The following plots show the sensor output as a function of distance for all three magnet set-ups, with both the KMZ10B and KMZ10C.

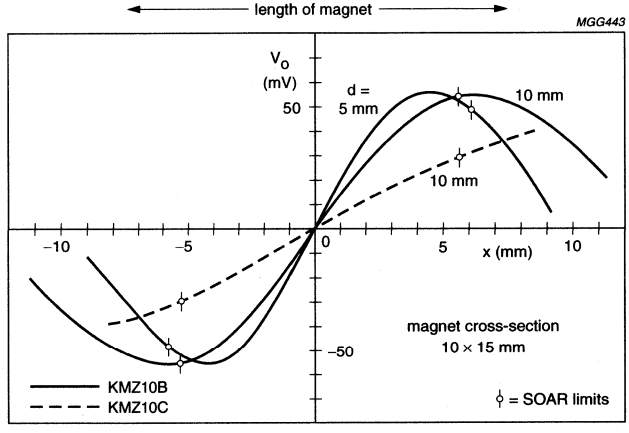

(a)

Fig.62 Sensor output as a function of displacement.

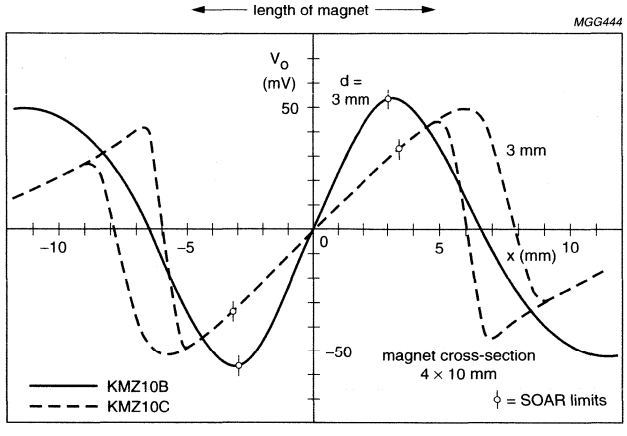

(b)

Fig.63 Sensor output as a function of displacement.

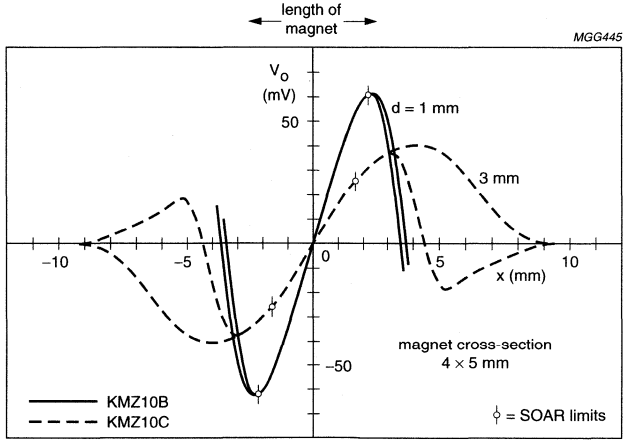

(c)

Fig.64 Sensor output as a function of displacement.

The first graph shows that as the separation distance increases, the curve flattens out. This is because as the sensor is moved closer to the magnet, the transverse field H_y of the magnet has a greater effect on the sensor, giving rise to increased rotation of the internal magnetization. As the gradient of the curve is a direct indication of the sensitivity of the sensor, then in practical application designs, sensor/magnet separation is an important factor.

From these curves it is also clear that for the KMZ10C sensor, with shorter magnets at close separation distances, switching hysteresis becomes a major factor at the limits of the sensors linear region.

MAGNETIC FIELD PERPENDICULAR TO THE SENSOR

When the sensor is oriented so that its plane is perpendicular to the magnetic axis, it is impossible for the magnet to provide the auxiliary field. In this case an additional auxiliary magnet is required, placed on the sensor as shown in Fig.65.

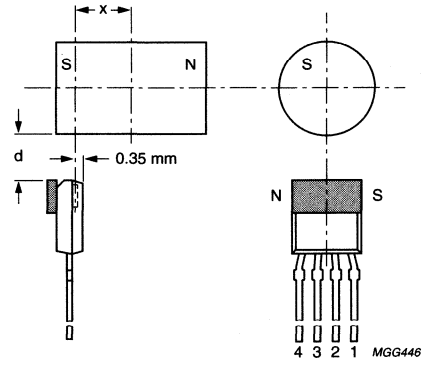

Fig.65 Sensor perpendicular to magnetic field using an FXD330 magnet.

With this set-up, the following plots were obtained using the same FXD330 magnets as with the parallel arrangement.

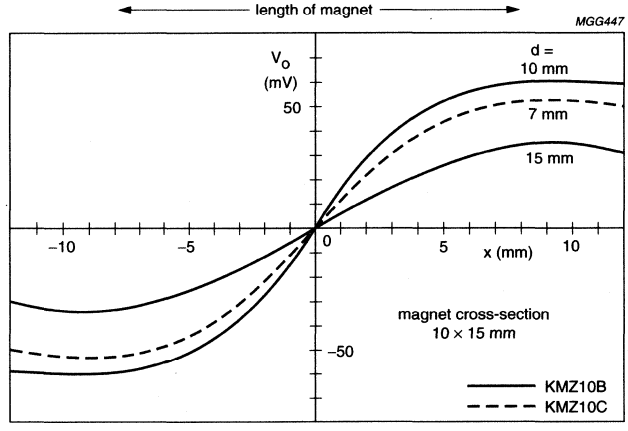

(a)

Fig.66 Sensor output as a function of displacement.

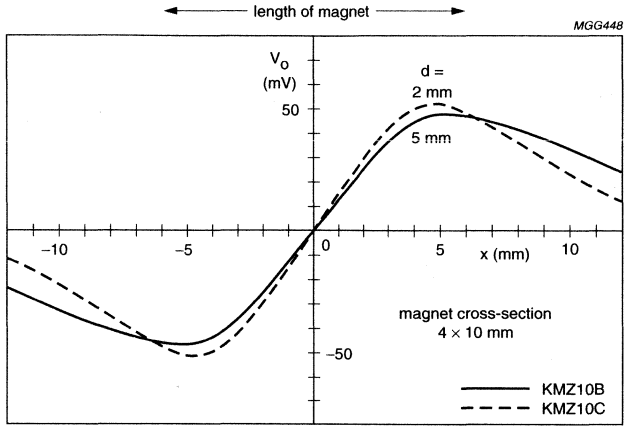

(b)

Fig.67 Sensor output as a function of displacement.

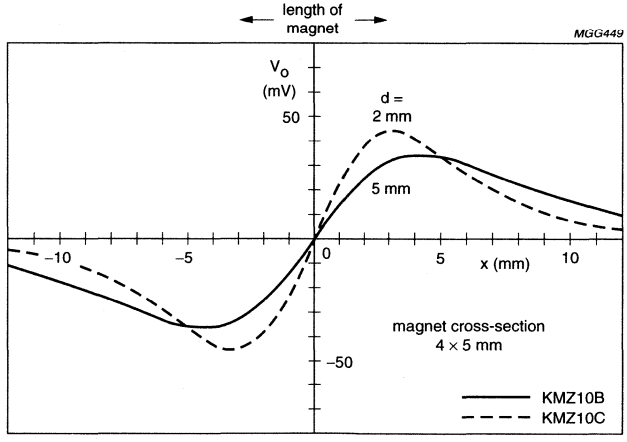

(c)

Fig.68 Sensor output as a function of displacement.

The most noticeable difference in these curves, compared to the parallel results, is the lack of hysteresis switching. This is due partly to the auxiliary magnet stabilizing the sensor and the fact that the orientation of the target magnet means it does not produce a magnetic field in the x-direction and cannot therefore adversely affect the sensor.

An interesting feature of these curves is the way the curvature changes near the ends of the magnet. This slight flattening and possible reversal of the curve can be seen more clearly when a single $\phi 4 \times 5$ mm FXD330 magnet is used with the KMZ10B sensor at very small separation distances (d = 1 mm).

The reason for the change in curvature is that at small distances from the target magnet, the radial field H_y at the ends of the magnet is stronger than the field required to induce a maximum response in the sensor. This effectively saturates the sensor and the output can fall even as H_y increases.

A slightly different approach can be used for very high resolution measurements. Using a compact RES190 magnet with dimensions of $3 \times 2 \times 1$ mm, placed at the back of the sensor rather than directly above it (see Fig.70), the output of the sensor was plotted for separation distances of 1 mm, 0.5 mm and 0.1 mm.

Figure 71 clearly shows that this set-up is very well suited for high resolution or high sensitivity measurement of position at very short distances, using the linear part of the response curve.

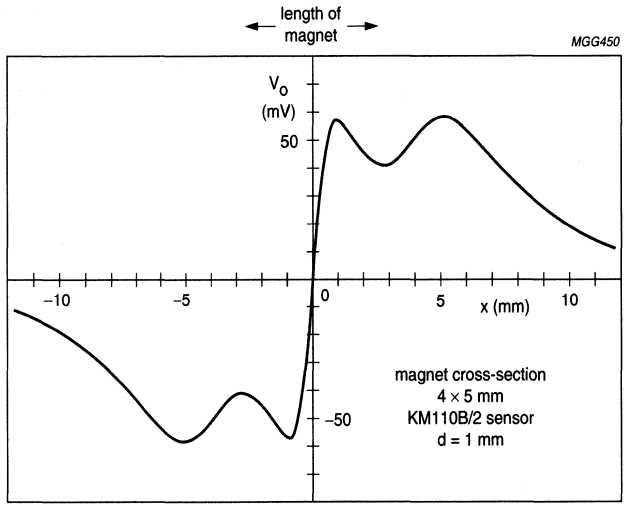

Fig.69 Sensor output as a function of x for a single FXD330 magnet.

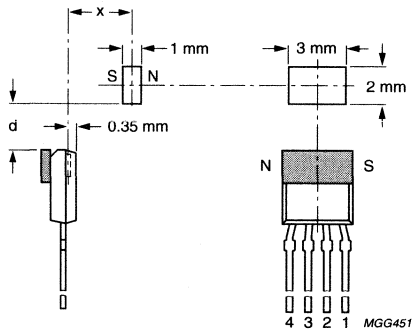

Fig.70 Sensor KM110B/2 perpendicular to magnet field using RES190 magnet.

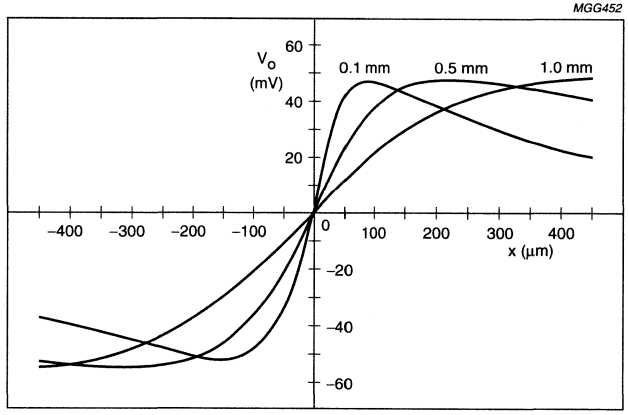

Fig.71 Sensor output as a function of displacement using RES190 magnet.

Reference set-ups

The following are two common set-ups (Fig.72 and Fig.73) that could be used for linear position measurement in real-life applications, together with typical response curves.

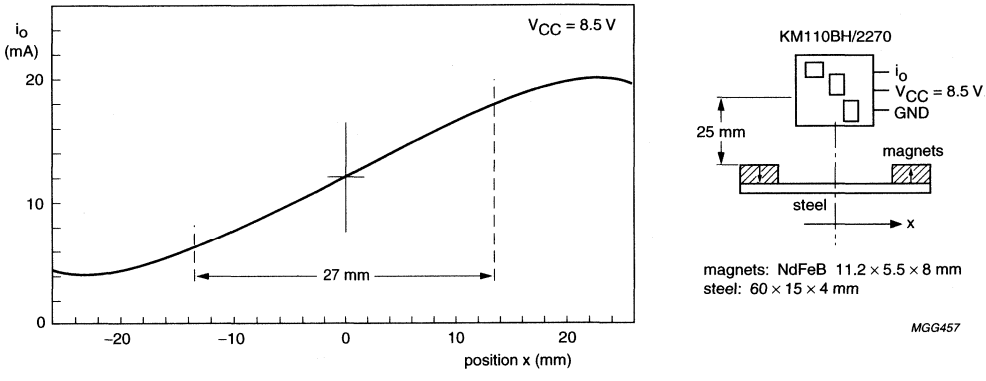

Fig.72 Angle sensor hybrid KM110BH/22/70 in linear position measurement set-up using two magnets and typical response curve.

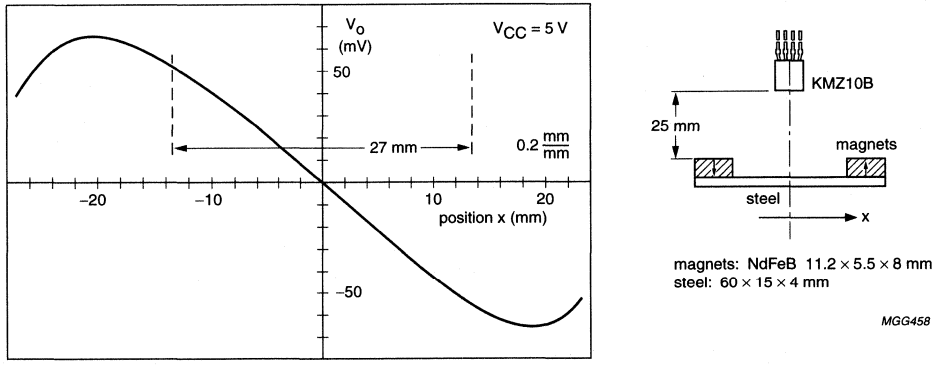

Fig.73 KMZ10B linear position measurement set-up using two magnets and typical response curve.

THE MAGNETORESISTIVE EFFECT

Magnetoresistive sensors make use of the fact that the electrical resistance ρ of certain ferromagnetic alloys is influenced by external fields. This solid-state magnetoresistive effect, or anisotropic magnetoresistance, can be easily realized using thin film technology, so lends itself to sensor applications.

Resistance- field relation

The specific resistance ρ of anisotropic ferromagnetic metals depends on the angle Θ between the internal magnetization M and the current I, according to:

$$\rho(\Theta) = \rho_{\perp} + (\rho_{\perp} - \rho_{\parallel}) \cos^2 \Theta \quad (1)$$

where $\rho_{\perp}$ and $\rho_{\parallel}$ are the resistivities perpendicular and parallel to M. The quotient $(\rho_{\perp} - \rho_{\parallel})/\rho_{\perp} = \Delta\rho/\rho$ is called the magnetoresistive effect and may amount to several percent.

Sensors are always made from ferromagnetic thin films as this has two major advantages over bulk material: the resistance is high and the anisotropy can be made uniaxial. The ferromagnetic layer behaves like a single domain and has one distinguished direction of magnetization in its plane called the easy axis (e.a.), which is the direction of magnetization without external field influence.

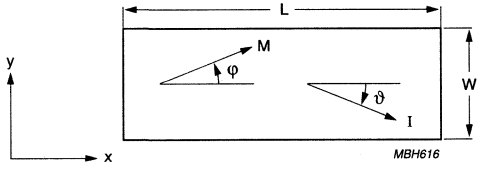

Fig.1 Geometry of a simple sensor.

Figure 1 shows the geometry of a simple sensor where the thickness (t) is much smaller than the width (w) which is in turn, less than the length (l) (i.e. $t \ll w < l$). With the current (I) flowing in the x-direction (i.e. $\theta = 0$ or $\Theta = \phi$) then the following equation can be obtained from equation 1:

$$R = R_0 + \Delta R \cos^2\phi \quad (2)$$

and with a constant current I, the voltage drop in the x-direction U_x becomes:

$$U_x = \rho_{\perp} I \left(\frac{L}{wt}\right)\left(1 + \left(\frac{\Delta\rho}{\rho}\right)\cos^2\phi\right) \quad (3)$$

Besides this voltage, which is directly allied to the resistance variation, there is a voltage in the y-direction, U_y, given by:

$$U_y = \rho_{\perp} I \left(\frac{1}{t}\right)\left(\frac{\Delta\rho}{\rho}\right)\sin\phi\cos\phi \quad (4)$$

This is called the planar or pseudo Hall effect; it resembles the normal or transverse Hall effect but has a physically different origin.

All sensor signals are determined by the angle φ between the magnetization M and the 'length' axis and, as M rotates under the influence of external fields, these external fields thus directly determine sensor signals. We can assume that the sensor is manufactured such that the e.a. is in the x-direction so that without the influence of external fields, M only has an x-component ($\phi = 0°$ or $180°$).

Two energies have to be introduced when M is rotated by external magnetic fields: the anisotropy energy and the demagnetizing energy. The anisotropy energy E_k, is given by the crystal anisotropy field H_k, which depends on the material and processes used in manufacture. The demagnetizing energy E_d or form anisotropy depends on the geometry and this is generally a rather complex relationship, apart from ellipsoids where a uniform demagnetizing field H_d may be introduced. In this case, for the sensor set-up in Fig.1.

$$H_d \approx \frac{t}{w}\left(\frac{M_s}{\mu_0}\right) \quad (5)$$

where the demagnetizing factor N – t/w, the saturation magnetization $M_s \approx 1$ T and the induction constant $\mu 0 = 4\pi^{-7}$ Vs/Am.

The field $H_0 - H_k + t/w(M_0/m_0)$ determines the measuring range of a magnetoresistive sensor, as f is given by:

$$\sin\phi = \frac{H_y}{H_o + \frac{H_x}{\cos\phi}} \quad (6)$$

where $|H_y| \leq |H_0 + H_x|$ and H_x and H_y are the components of the external field. In the simplest case $H_x = 0$, the voltages U_x and U_y become:

$$U_x = \rho_\perp I \left(\frac{L}{wt}\right)\left(1 + \left(\frac{\Delta\rho}{\rho}\right)\left(1 - \left(\frac{H_y}{H_0}\right)^2\right)\right) \quad (7)$$

$$U_y = \rho_\perp I \left(\frac{1}{t}\right)\left(\frac{\Delta\rho}{\rho}\right)\left(\frac{H_y}{H_0}\right)\sqrt{1 - (H_y/H_0)^2} \quad (8)$$

(Note: if $H_x = 0$, then H_0 must be replaced by $H_0 + H_x/\cos\phi$).

Neglecting the constant part in U_x, there are two main differences between U_x and U_y:

1. The magnetoresistive signal U_x depends on the square of H_y/H_0, whereas the Hall voltage U_y is linear for $H_y \ll H_0$.
2. The ratio of their maximum values is L/w; the Hall voltage is much smaller as in most cases L » w.

Magnetization of the thin layer

The magnetic field is in reality slightly more complicated than given in equation (6). There are two solutions for angle ϕ:

$\phi 1 < 90^\circ$ and $\phi 2 > 90^\circ$ (with $\phi 1 + \phi 2 = 180^\circ$ for $H_x = 0$).

Replacing ϕ by $180^\circ - \phi$ has no influence on U_x except to change the sign of the Hall voltage and also that of most linearized magnetoresistive sensors.

Therefore, to avoid ambiguity either a short pulse of a proper field in the x-axis ($|H_x| > H_k$) with the correct sign must be applied, which will switch the magnetization into the desired state, or a stabilizing field Hst in the x-direction can be used. With the exception of $H_y \ll H_0$, it is advisable to use a stabilizing field as in this case, H_x values are not affected by the non-ideal behaviour of the layer or restricted by the so-called 'blocking curve'.

The minimum value of H_{st} depends on the structure of the sensitive layer and has to be of the order of H_k, as an insufficient value will produce an open characteristic (hysteresis) of the sensor. An easy axis in the y-direction leads to a sensor of higher sensitivity, as then $H_o = H_k - H_d$.

Linearization

As shown, the basic magnetoresistor has a square resistance-field (R-H) dependence, so a simple magnetoresistive element cannot be used directly for linear field measurements. A magnetic biasing field can be used to solve this problem, but a better solution is linearization using barber-poles (described later). Nevertheless plain elements are useful for applications using strong magnetic fields which saturate the sensor, where the actual value of the field is not being measured, such as for angle measurement. In this case, the direction of the magnetization is parallel to the field and the sensor signal can be described by a $\cos^2\alpha$ function.

Sensors with inclined elements

Sensors can also be linearized by rotating the current path, by using resistive elements inclined at an angle θ, as shown in Fig.2. An actual device uses four inclined resistive elements, two pairs each with opposite inclinations, in a bridge.

The magnetic behaviour of such is pattern is more complicated as M_0 is determined by the angle of inclination θ, anisotropy, demagnetization and bias field (if present). Linearity is at its maximum for $\phi + \theta \approx 45^\circ$, which can be achieved through proper selection of θ.

A stabilization field (H_{st}) in the x-direction may be necessary for some applications, as this arrangement only works properly in one magnetization state.

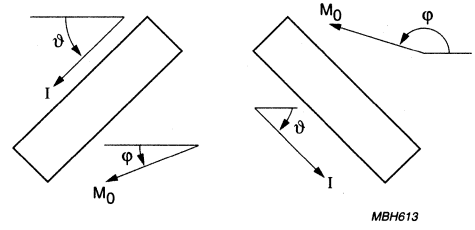

Fig.2 Current rotation by inclined elements (current and magnetization shown in quiescent state).

BARBER-POLE SENSORS

A number of Philips' magnetoresistive sensors use a 'barber-pole' construction to linearize the R-H relationship, incorporating slanted strips of a good conductor to rotate the current. This type of sensor has the widest range of linearity, smaller resistance and the least associated distortion than any other form of linearization, and is well suited to medium and high fields.

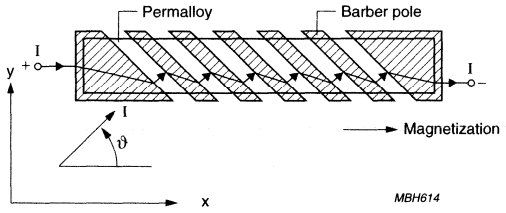

Fig.3 Linearization of the magnetoresistive effect with barber-poles (current and magnetization shown in quiescent state).

The current takes the shortest route in the high-resistivity gaps which, as shown in Fig.3, is perpendicular to the barber-poles. Barber-poles inclined in the opposite direction will result in the opposite sign for the R-H characteristic, making it extremely simple to realize a Wheatstone bridge set-up.

The signal voltage of a Barber-pole sensor may be calculated from the basic equation (1) with $\Theta = \phi + 45^\circ$ ($\theta = +45^\circ$):

$$U_{BP} = \rho_\perp I\left(\frac{L}{wt}\right)\alpha\left(1 + \frac{1}{2}\left(\frac{\Delta\rho}{\rho}\right) \pm \frac{\Delta\rho}{\rho}\frac{H_y}{H_0}\sqrt{1 - \left(\frac{H_y}{H_0}\right)^2}\right) \qquad (9)$$

where a is a constant arising from the partial shorting of the resistor, amounting to 0.25 if barber-poles and gaps have equal widths. The characteristic is plotted in Fig.4 and it can be seen that for small values of H_y relative to H_0, the R-H dependence is linear. In fact this equation gives the same linear R-H dependence as the planar Hall-effect sensor, but it has the magnitude of the magnetoresistive sensor.

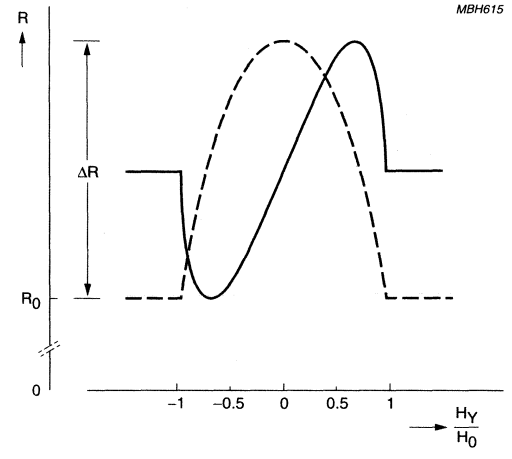

Fig.4 Calculated R-H characteristic of a barber-pole sensor.

Barber-pole sensors require a certain magnetization state. A bias field of several hundred A/m can be generated by the sensing current alone, but this is not sufficient for sensor stabilization, so can be neglected. In most applications, an external field is applied for this purpose.

Sensitivity

Due to the high demagnetization, in most applications field components in the z-direction (perpendicular to the layer plane) can be ignored. Nearly all sensors are most sensitive to fields in the y-direction, with H_x only having a limited or even negligible influence.

Definition of the sensitivity S contains the signal and field variations (DU and DH), as well as the operating voltage U_0 (as D_U is proportional to U_0):

$$S_o = \frac{\Delta U}{\Delta H}\left(\frac{1}{U_0}\right) = \left(\frac{\Delta U}{U_0 \Delta H}\right) \qquad (10)$$

This definition relates DU to a unit operating voltage.

The highest (H_G) and lowest (H_{min}) fields detectable by the sensor are also of significance. The measuring range H_G is restricted by non-linearity - if this is assumed at 5%, an approximate value for barber-pole sensors is given by:

$$H_G \approx 0.5\,(H_0 + H_x) \qquad (11)$$

From this and equation (9) for signal voltage (U_{BP}) for a barber-pole sensor, the following simple relationship can be obtained:

$$H_G S_0 \approx 0.5\left(\frac{\Delta\rho}{\rho}\right) \qquad (12)$$

Other sensor types have a narrower range of linearity and therefore a smaller useful signal.

The lowest detectable field H_{min} is limited by offset, drift and noise. The offset is nearly cancelled in a bridge circuit and the remaining imbalance is minimized by symmetrical design and offset trimming, with thermal noise negligible in most applications (see section on sensor layout). Proper film deposition and, if necessary, the introduction of a stabilization field will eliminate magnetization switching due to domain splitting and the introduction of 'Barkhausen noise'.

Sensitivity S_0 is essentially determined by the sum of the anisotropy (H_k), demagnetization (H_d) and bias (H_x) fields. The highest sensitivity is achievable with $H_x = 0$ and $H_d \ll H_k$, although in this case S_0 depends purely on H_k which is less stable than H_d. For a permalloy with a thickness greater than or equal to 20 µm, a width in excess of 60 µm is required which, although possible, has the drawback of producing a very low resistance per unit area.

The maximum theoretical S_0 with this permalloy (at H_k = 250 A/m and $\Delta\rho/\rho$ = 2.5%) is approximately:

$$S_0(\max) = 10^{-4}\left(\frac{A}{m}\right)^1 = 100\frac{\left(\frac{mV}{V}\right)}{\left(\frac{kA}{m}\right)} \qquad (13)$$

For the same reasons, sensors with reduced sensitivity should be realized with increased H_d, which can be estimated at a maximum for a barber-pole sensor at 40 kA/m. A further reduction in sensitivity and a corresponding growth in the linearity range is attained using a biasing field. A magnetic shunt parallel to the magnetoresistor or only having a small field component in the sensitive direction can also be employed with very high field strengths.

A high signal voltage U_x can only be produced with a sensor that can tolerate a high supply voltage U_o. This requires a high sensor resistance R with a large area A, since there are limits for power dissipation and current density. The current density in permalloy may be very high ($j > 10^6$ A/cm^2 in passivation layers), but there are weak points at the current reversal in the meander (see section on sensor layout) and in the barber-pole material, with five-fold increased current density.

A high resistance sensor with U_0 = 25 V and a maximum S_0 results in a value of 2.5 x 10^{-3} (A/m)$^{-1}$ for Su or, converted to flux density, S_T = 2000 V/T. This value is several orders of magnitude higher than for a normal Hall effect sensor, but is valid only for a much narrower measuring range.

Materials

There are five major criteria for a magnetoresistive material:

- Large magnetoresistive effect Dr/r (resulting in a high signal to operating voltage ratio)
- Large specific resistance r (to achieve high resistance value over a small area)
- Low anisotropy
- Zero magnetostriction (to avoid influence of mechanical stress)
- Long-term stability.

Appropriate materials are binary and ternary alloys of Ni, Fe and Co, of which NiFe (81/19) is probably the most common.

Table 1 gives a comparison between some of the more common materials, although the majority of the figures are only approximations as the exact values depend on a number of variables such as thickness, deposition and post-processing.

Table 1 Comparison of magnetoresistive sensor materials

Materials	ρ ($10^{-8}\Omega$m)	$\Delta\rho/\rho$(%)	H_k(A/m)
NiFe 81:19	22	2.2	250
NiFe 86:14	15	3	200
NiCo 50:50	24	2.2	2500
NiCo 70:30	26	3.7	2500
CoFeB 72:8:20	86	0.07	2000

$\Delta\rho$ is nearly independent of these factors, but r itself increases with thickness ($t \leq 40$ nm) and will decrease during annealing. Permalloys have a low H_k and zero magnetostriction; the addition of C_o will increase $\Delta\rho/\rho$, but

this also considerably enlarges H_k. If a small temperature coefficient of $\Delta\rho$ is required, NiCo alloys are preferable. The amorphous alloy CoFeB has a low $\Delta\rho/\rho$, high H_k and slightly worse thermal stability but due to the absence of grain boundaries within the amorphous structure, exhibits excellent magnetic behaviour.

APPENDIX 2: SENSOR FLIPPING

During deposition of the permalloy strip, a strong external magnetic field is applied parallel to the strip axis. This accentuates the inherent magnetic anisotropy of the strip and gives them a preferred magnetization direction, so that even in the absence of an external magnetic field, the magnetization will always tend to align with the strips.

Providing a high level of premagnetization within the crystal structure of the permalloy allows for two stable premagnetization directions. When the sensor is placed in a controlled external magnetic field opposing the internal aligning field, the polarity of the premagnetization of the strips can be switched or 'flipped' between positive and negative magnetization directions, resulting in two stable output characteristics.

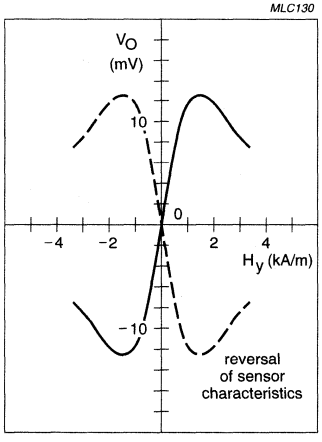

Fig.5 Sensor characteristics.

The field required to flip the sensor magnetization (and hence the output characteristic) depends on the magnitude of the transverse field H_y. The greater this field, the more the magnetization rotates towards 90° and therefore it becomes easier to flip the sensor into the corresponding stable position in the '-x' direction. This means that a smaller $-H_x$ field is sufficient to cause the flipping action

As can be seen in Fig.6, for low transverse field strengths (0.5 kA/m) the sensor characteristic is stable for all positive values of H_x, and a reverse field of approximately 1 kA/m is required to flip the sensor. However at higher values of H_y (2 kA/m), the sensor will also flip for smaller values of H_x (at 0.5 kA/m). Also illustrated in this figure is a noticeable hysteresis effect; it also shows that as the permalloy strips do not flip at the same rate, the flipping action is not instantaneous.

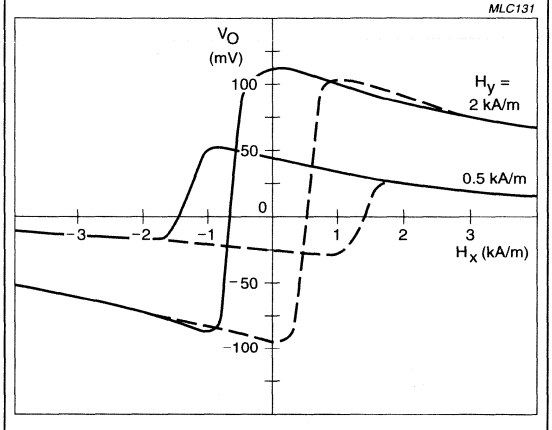

Fig.6 Sensor output 'V_o' as a function of the auxiliary field H_x.

The sensitivity of the sensor reduces as the auxiliary field H_x increases, which can be seen in Fig.6 and more clearly in Fig.7. This is because the moment imposed on the magnetization by H_x directly opposes that of H_y, resulting in a reduction in the degree of bridge imbalance and hence the output signal for a given value of H_y.

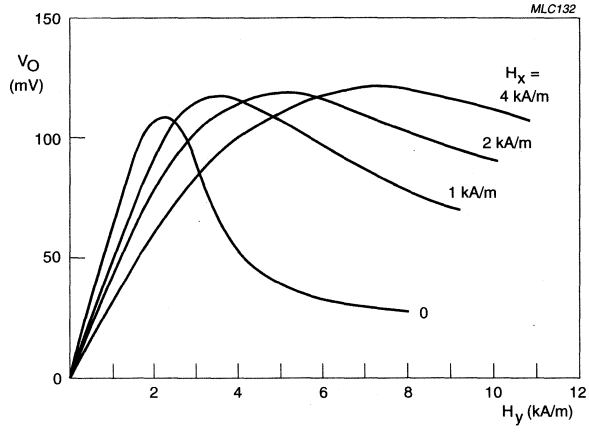

Fig.7 Sensor output 'V_o' as a function of the transverse field H_y.

A Safe Operating ARea (SOAR) can be determined for magnetoresistive sensors, within which the sensor will not flip, depending on a number of factors. The higher the auxiliary field, the more tolerant the sensor becomes to external disturbing fields (H_d) and with an H_x of 3 kA/m or greater, the sensor is stabilized for all disturbing fields as long as it does not irreversibly demagnetize the sensor. If Hd is negative and much larger than the stabilising field H_x, the sensor will flip. This effect is reversible, with the sensor returning to the normal operating mode if H_d again becomes negligible (see Fig.8). However the higher H_x, the greater the reduction in sensor sensitivity and so it is generally recommended to have a minimum auxiliary field that ensures stable operation, generally around 1 kA/m. The SOAR can also be extended for low values of H_x as long as the transverse field is less than 1 kA/m. It is also recommended to apply a large positive auxiliary field before first using the sensor, which erases any residual hysteresis

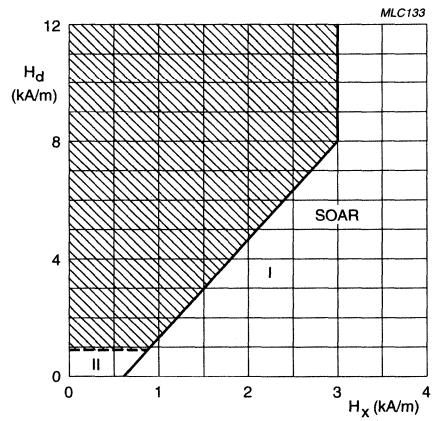

Fig.8 SOAR of a KMZ10B sensor as a function of auxiliary field 'H_x' (MLC133).

APPENDIX 3: SENSOR LAYOUT

In Philips' magnetoresistive sensors, the permalloy strips are formed into a meander pattern on the silicon substrate. With the KMZ10 (see Fig.9) and KMZ51 series, four barber-pole permalloy strips are used while the KMZ41 series has simple elements. The patterns used are different for these three families of sensors in every case, the elements are linked in the same fashion to form the four arms of a Wheatstone bridge. The meander pattern used in the KMZ51 is more sophisticated and also includes integrated compensation and flipping coils (see chapter on weak fields); the KMZ41 is described in more detail in the chapter on angle measurement.

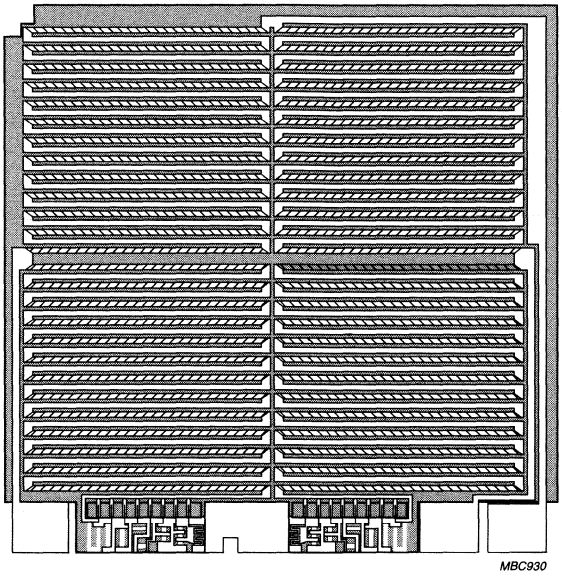

Fig.9 KMZ10 chip structure.

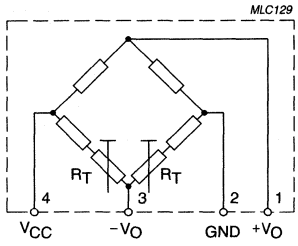

Fig.10 KMZ10 and KMZ11 bridge configuration.

In one pair of diagonally opposed elements the barber-poles are at +45° to the strip axis, with the second pair at –45°. A resistance increase in one pair of elements due to an external magnetic field is matched by an equal decrease in resistance of the second pair. The resulting bridge imbalance is then a linear function of the amplitude of the external magnetic field in the plane of the permalloy strips normal to the strip axis.

This layout largely eliminates the effects of ambient variations (e.g. temperature) on the individual elements and also magnifies the degree of bridge imbalance, increasing sensitivity.

Fig.10 indicates two further trimming resistors (R_T) which allow the sensors electrical offset to be trimmed down to zero during the production process.

DEVICE DATA

in alphanumeric sequence

Magnetic field sensor KMZ10A

DESCRIPTION

The KMZ10A is an extremely sensitive magnetic field sensor, employing the magnetoresistive effect of thin-film permalloy. Its properties enable this sensor to be used in a wide range of applications for navigation, current and field measurement, revolution counters, angular or linear position measurement and proximity detectors, etc.

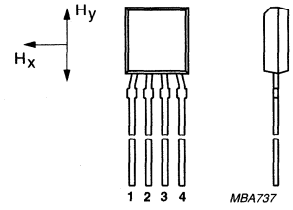

Fig.1 Simplified outline.

PINNING

PIN	SYMBOL	DESCRIPTION
1	$+V_O$	output voltage
2	GND	ground
3	$-V_O$	output voltage
4	V_{CC}	supply voltage

QUICK REFERENCE DATA

SYMBOL	PARAMETER	MIN.	TYP.	MAX.	UNIT
V_{CC}	bridge supply voltage	–	5	–	V
T_{bridge}	bridge operating temperature	−40	–	+150	°C
H_y	magnetic field strength	−0.5	–	+0.5	kA/m
H_x	auxiliary field	–	0.5	–	kA/m
S	sensitivity	–	16	–	$\frac{mV/V}{kA/m}$
R_{bridge}	bridge resistance	0.8	–	1.6	kΩ
V_{offset}	offset voltage	−1.5	–	+1.5	mV/V

CIRCUIT DIAGRAM

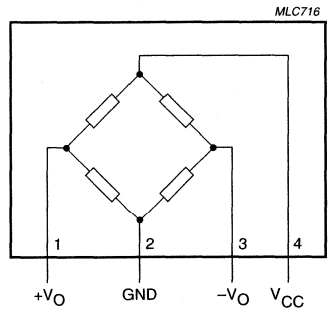

Fig.2 Simplified circuit diagram.

LIMITING VALUES

In accordance with the Absolute Maximum Rating System (IEC 134).

SYMBOL	PARAMETER	CONDITIONS	MIN.	MAX.	UNIT
V_{CC}	bridge supply voltage		–	9	V
P_{tot}	total power dissipation	up to T_{amb} = 134 °C	–	90	mW
T_{stg}	storage temperature	note 1	−65	+150	°C
T_{bridge}	bridge operating temperature		−40	+150	°C

Note

1. Maximum operating temperature of the thin-film permalloy.

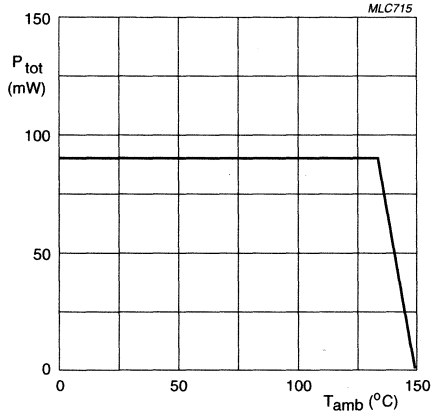

Fig.3 Power derating curve.

THERMAL CHARACTERISTICS

SYMBOL	PARAMETER	VALUE	UNIT
$R_{th\ j\text{-}a}$	thermal resistance from junction to ambient	180	K/W

CHARACTERISTICS

T_{amb} = 25 °C; H_x = 0.5 kA/m; notes 1 and 2; V_{CC} = 5 V unless otherwise specified.

SYMBOL	PARAMETER	CONDITIONS	MIN.	TYP.	MAX.	UNIT
H_y	magnetic field strength	note 2	−0.5	–	+0.5	kA/m
S	sensitivity	notes 2 and 3	13	–	19	$\frac{mV/V}{kA/m}$
TCV_O	temperature coefficient of output voltage	V_{CC} = 5 V; T_{amb} = −25 to +125 °C	–	−0.4	–	%/K
		I_{CC} = 3 mA; T_{amb} = −25 to +125 °C	–	−0.15	–	%/K
R_{bridge}	bridge resistance		0.8	–	1.6	kΩ
TCR_{bridge}	temperature coefficient of bridge resistance	T_{bridge} = −25 to +125 °C	–	0.25	–	%/K
V_{offset}	offset voltage		−1.5	–	+1.5	mV/V
TCV_{offset}	offset voltage drift	T_{bridge} = −25 to +125 °C	−6	–	+6	$\frac{\mu V/V}{K}$
FL	linearity deviation of output voltage	H_y = 0 to ±0.25 kA/m	–	–	0.8	%·FS
		H_y = 0 to ±0.4 kA/m	–	–	2.5	%·FS
		H_y = 0 to ±0.5 kA/m	–	–	4.0	%·FS
FH	hysteresis of output voltage		–	–	0.5	%·FS
f	operating frequency		0	–	1	MHz

Notes

1. Before first operation or after operation outside the SOAR (Fig.4) the sensor has to be reset by application of an auxiliary field H_x = 3 kA/m.
2. No disturbing field (H_d) allowed; for stable operation under disturbing conditions see Fig.4 (SOAR) and see Fig.5 for decrease of sensitivity.
3. $S = \frac{(V_O \text{ at } H_y = 0.4\ kA/m) - (V_O \text{ at } H_y = 0)}{0.4 \times V_{CC}}$.

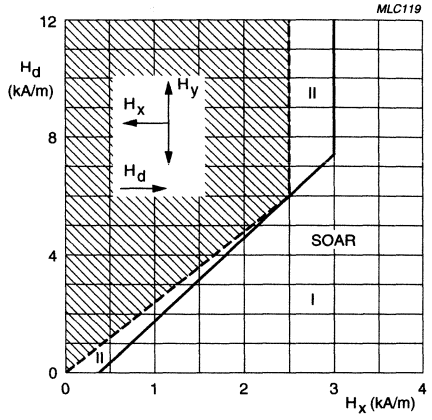

In applications with $H_x < 3$ kA/m, the sensor has to be reset, after leaving the SOAR, by an auxiliary field of $H_x = 3$ kA/m.

I = Region of permissible operation.

II = Permissible extension if $H_y < 0.15$ A/m.

Fig.4 Safe Operating Area (permissible disturbing field H_d as a component of auxiliary field H_x).

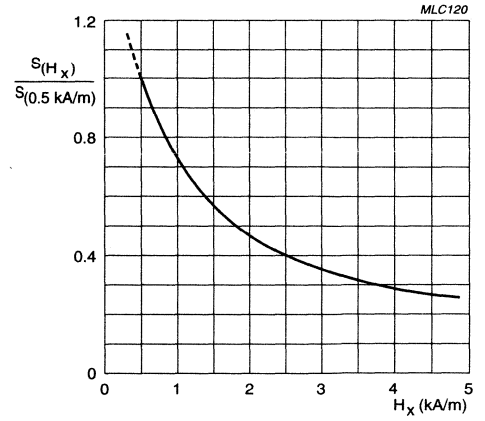

In applications with $H_x \leq 3$ kA/m, the sensor has to be reset by an auxiliary field of $H_x = 3$ kA/m before using.

Fig.5 Relative sensitivity (ratio of sensitivity at certain H_x and sensitivity at $H_x = 0.5$ kA/m).

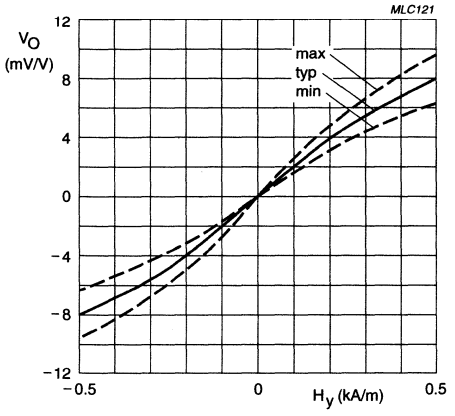

$H_x = 0.5$ kA/m; $T_{amb} = 25$ °C; $V_{offset} = 0$.

Fig.6 Sensor output characteristics.

PACKAGE OUTLINE

Plastic single-ended flat package; 4 in-line leads **SOT195**

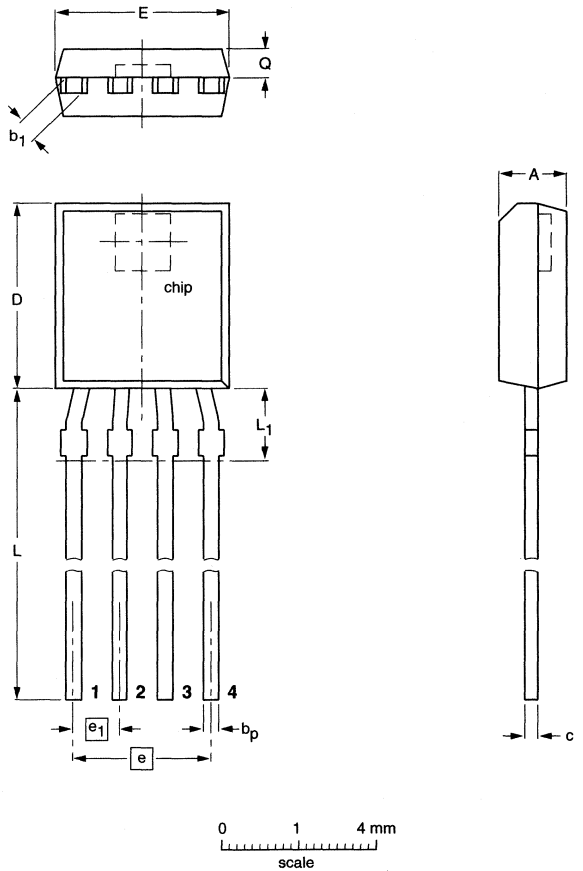

DIMENSIONS (mm are the original dimensions)

UNIT	A	b_p	b_1	c	D	E	e	e_1	L	L_1(1) max.	Q
mm	1.8 1.6	0.48 0.40	0.7 0.5	0.45 0.39	5.2 5.0	4.8 4.4	3.75	1.25	14.5 12.7	2	0.8 0.7

Notes

1. Terminal dimensions within this zone are uncontrolled to allow for flow of plastic and terminal irregularities.

OUTLINE VERSION	REFERENCES				EUROPEAN PROJECTION	ISSUE DATE
	IEC	JEDEC	EIAJ			
SOT195						97-06-02

Magnetic field sensor KMZ10A1

DESCRIPTION

The KMZ10A1 is an extremely sensitive magnetic field sensor, employing the magnetoresistive effect of thin-film permalloy. Its properties enable this sensor to be used in a wide range of applications such as navigation, current and earth magnetic field measurement etc. The special arrangement of the sensing chip allows the construction of coils for switching the auxiliary field (H_x) along the length axis of the sensor. The sensor can be operated at any frequency between DC and 1 MHz.

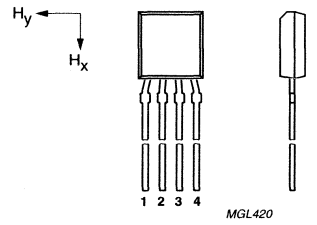

Fig.1 Simplified outline.

PINNING

PIN	SYMBOL	DESCRIPTION
1	$+V_O$	output voltage
2	GND	ground
3	$-V_O$	output voltage
4	V_{CC}	supply voltage

QUICK REFERENCE DATA

SYMBOL	PARAMETER	MIN.	TYP.	MAX.	UNIT
V_{CC}	DC supply voltage	–	5	–	V
H_y	magnetic field strength	−0.5	–	+0.5	kA/m
H_x	auxiliary field	–	0.5	–	kA/m
S	sensitivity	–	14	–	$\frac{mV/V}{kA/m}$
S_s	sensitivity (with switched H_x)	–	22	–	$\frac{mV/V}{kA/m}$
R_{bridge}	bridge resistance	0.85	–	1.75	kΩ
V_{offset}	offset voltage	−1.5	–	+1.5	mV/V

CIRCUIT DIAGRAM

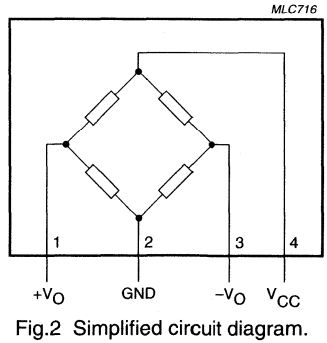

Fig.2 Simplified circuit diagram.

LIMITING VALUES

In accordance with the Absolute Maximum Rating System (IEC 134).

SYMBOL	PARAMETER	CONDITIONS	MIN.	MAX.	UNIT
V_{CC}	DC supply voltage		–	9	V
P_{tot}	total power dissipation	up to T_{amb} = 132 °C	–	100	mW
T_{stg}	storage temperature		–65	+150	°C
T_{bridge}	bridge operating temperature		–40	+150	°C

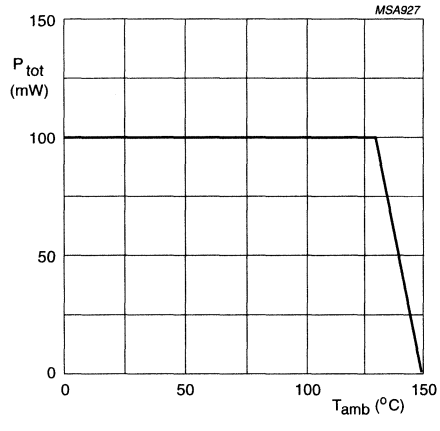

Fig.3 Power derating curve.

THERMAL CHARACTERISTICS

SYMBOL	PARAMETER	VALUE	UNIT
$R_{th\ j\text{-}a}$	thermal resistance from junction to ambient	180	K/W

CHARACTERISTICS

T_{amb} = 25 °C and H_x = 0.5 kA/m unless otherwise specified; see notes 1 and 2.

SYMBOL	PARAMETER	CONDITIONS	MIN.	TYP.	MAX.	UNIT
V_{CC}	DC supply voltage		–	5	–	V
H_y	operating range	note 2	−0.5	–	+0.5	kA/m
S	sensitivity	open circuit; notes 2 and 3	11	–	17	$\frac{mV/V}{kA/m}$
TCV_O	temperature coefficient of output voltage at constant supply voltage	V_{CC} = 5 V; T_{amb} = −25 to +125 °C	–	−0.4	–	%/K
VCV_O	temperature coefficient of output voltage at constant supply current	I_B = 3 mA; T_{amb} = −25 to +125 °C	–	−0.15	–	%/K
R_{bridge}	bridge resistance		0.85	–	1.75	kΩ
TCR_{bridge}	temperature coefficient of bridge resistance	T_j = −25 to +125 °C	–	0.25	–	%/K
V_{offset}	offset voltage		−1.5	–	+1.5	mV/V
TCV_{offset}	offset voltage drift	T_{bridge} = −25 to +125 °C	−6	–	+6	$\frac{\mu V/V}{K}$
FL	linearity deviation of output voltage	H_y = 0 to ±0.25 kA/m^{-1}	–	–	0.8	%·FS
		H_y = 0 to ±0.4 kA/m^{-1}	–	–	2.5	%·FS
		H_y = 0 to ±0.5 kA/m^{-1}	–	–	4.0	%·FS
FH	hysteresis of output voltage		–	–	0.5	%·FS
f	operating frequency		0	–	1	MHz
Characteristics with H_x = 0 (switched H_x, see note 4); V_{CC} = 5 V						
H_y	operating range	note 2	−0.05	–	+0.05	kA/m
S_s	sensitivity	slope between H_y = 0 and H_y = 40 A/m	14	–	27	$\frac{mV/V}{kA/m}$

Notes

1. Before first operation or after operation outside the SOAR (Fig.4) the sensor has to be reset by application of an auxiliary field H_x = 3 kA/m.
2. No disturbing field (H_d) allowed; for stable operation under disturbing conditions see Fig.4 (SOAR) and see Fig.5 for decrease of sensitivity.
3. Sensitivity measured as $\Delta V_O/\Delta H_y$ between H_y = 0 and H_y = 0.4 kA/m.
4. See application information.

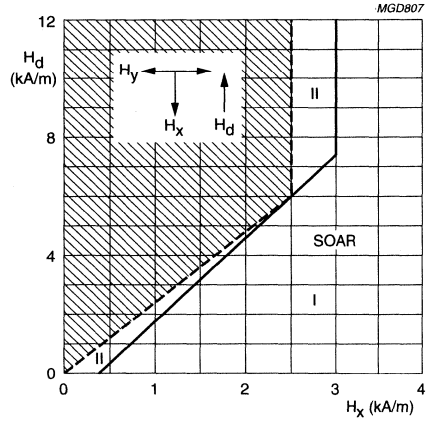

I = Region of permissible operation.

II = Permissible extension if H_y < 0.05 kA/m.

In applications with H_x < 3 kA/m, the sensor has to be reset, after leaving the SOAR, by an auxiliary field of H_x = 3 kA/m.

Fig.4 Safe Operating Area (permissible disturbing field H_d as a component of auxiliary field H_x).

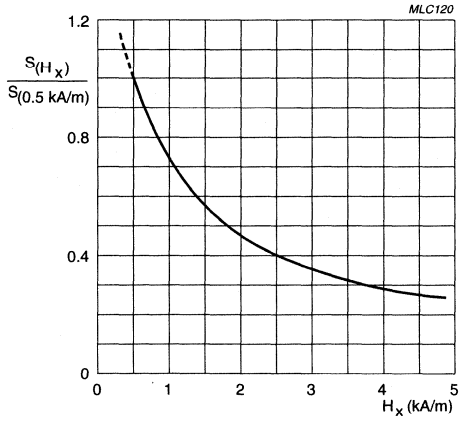

In applications with $H_x \leq 3$ kA/m, the sensor has to be reset by an auxiliary field of H_x = 3 kA/m before use.

Fig.5 Relative sensitivity (ratio of sensitivity at certain H_x and sensitivity at H_x = 0.5 kA/m).

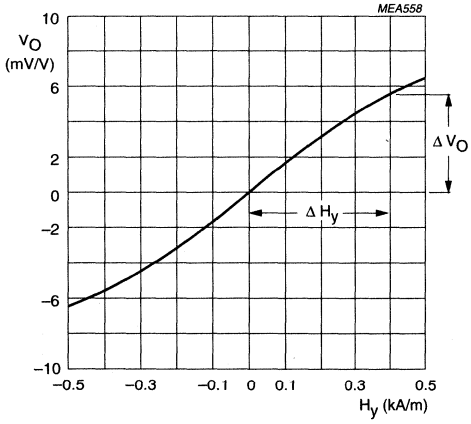

H_x = 0.5 kA/m; T_{amb} = 25 °C; V_{offset} = 0; $S = \Delta V_O / \Delta H_y$.

Fig.6 Sensor output characteristics.

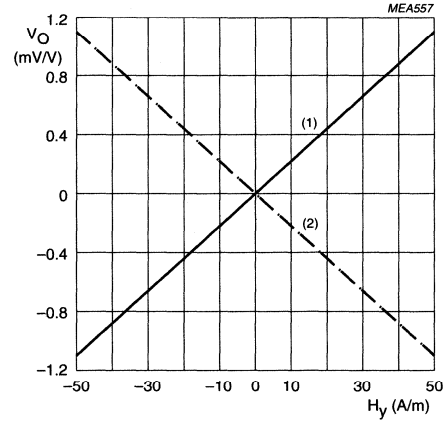

(1) Sensor reset with H_x = 3 kA/m.

(2) Sensor reset with H_x = −3 kA/m.

Fig.7 Output characteristic with H_x = 0 (switched H_x).

APPLICATION INFORMATION

A problem with measuring weak magnetic fields is that precision is limited by drift in both the sensor and amplifier offset. In these instances, it is possible to take advantage of the 'flipping' characteristics of the KMZ10 series to generate an output that is independent of offset. The sensor, located in a coil connected to a current pulse generator producing magnetic field pulses periodically reversed by alternate positive and negative going current pulses, is continually flipped from its normal to its reversed polarity and back again. The polarity of the offset however, remains unchanged, so the offset itself can be eliminated by passing the output signal through a filter circuit.

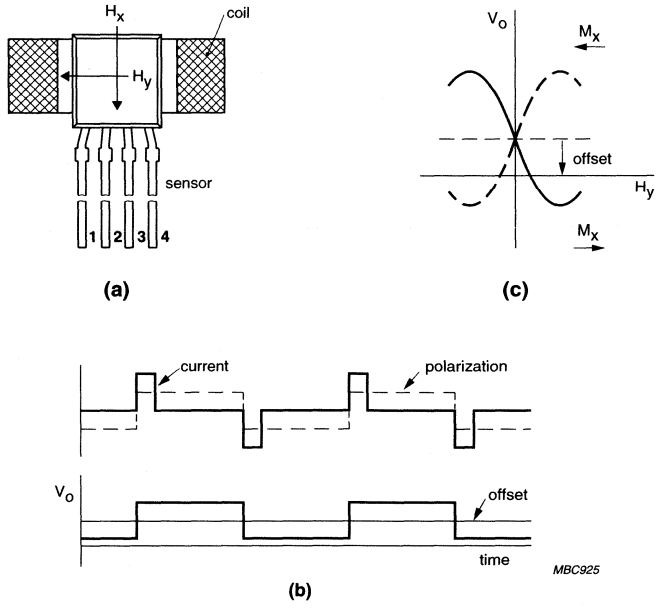

(a) Set-up.
(b) Pulse diagram.
(c) Sensor output characteristics.

Fig.8 Measuring weak magnetic fields with the KMZ10A1.

PACKAGE OUTLINE

Plastic single-ended flat package; 4 in-line leads **SOT195**

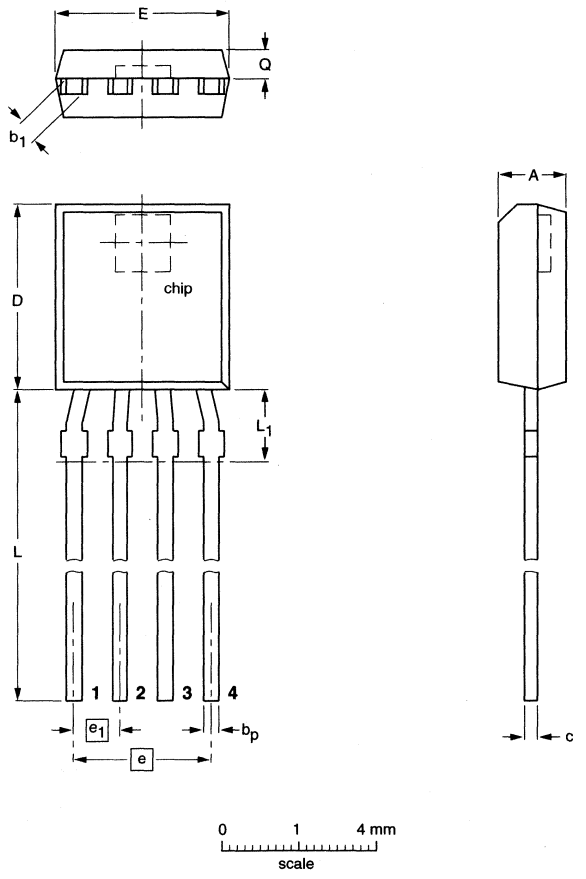

DIMENSIONS (mm are the original dimensions)

UNIT	A	b_p	b_1	c	D	E	e	e_1	L	L_1(1) max.	Q
mm	1.8 1.6	0.48 0.40	0.7 0.5	0.45 0.39	5.2 5.0	4.8 4.4	3.75	1.25	14.5 12.7	2	0.8 0.7

Notes

1. Terminal dimensions within this zone are uncontrolled to allow for flow of plastic and terminal irregularities.

OUTLINE VERSION	REFERENCES				EUROPEAN PROJECTION	ISSUE DATE
	IEC	JEDEC	EIAJ			
SOT195						97-06-02

Magnetic field sensor KMZ10B

DESCRIPTION

The KMZ10B is a sensitive magnetic field sensor, employing the magnetoresistive effect of thin-film permalloy. Its properties enable this sensor to be used in a wide range of applications for current and field measurement, revolution counters, angular or linear position measurement, proximity detectors, etc.

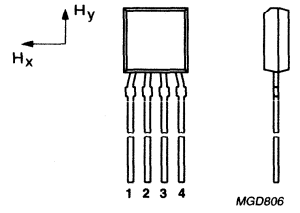

Fig.1 Simplified outline SOT195.

PINNING

PIN	SYMBOL	DESCRIPTION
1	$+V_O$	output voltage
2	GND	ground
3	$-V_O$	output voltage
4	V_{CC}	supply voltage

QUICK REFERENCE DATA

SYMBOL	PARAMETER	MIN.	TYP.	MAX.	UNIT
V_{CC}	bridge supply voltage	–	5	12	V
H_y	magnetic field strength	−2	–	+2	kA/m
H_x	auxiliary field	–	3	–	kA/m
S	sensitivity	–	4	–	$\frac{mV/V}{kA/m}$
R_{bridge}	bridge resistance	1.6	–	2.6	kΩ
V_{offset}	offset voltage	−1.5	–	+1.5	mV/V

CIRCUIT DIAGRAM

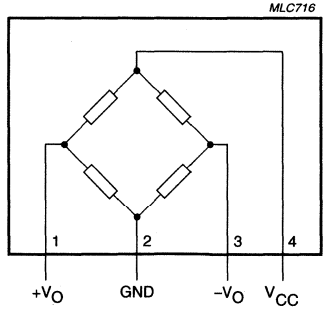

Fig.2 Simplified circuit diagram.

LIMITING VALUES

In accordance with the Absolute Maximum Rating System (IEC 134).

SYMBOL	PARAMETER	CONDITIONS	MIN.	MAX.	UNIT
V_{CC}	bridge supply voltage		–	12	V
P_{tot}	total power dissipation	up to T_{amb} = 130 °C	–	120	mW
T_{stg}	storage temperature		–65	+150	°C
T_{bridge}	bridge operating temperature		–40	+150	°C

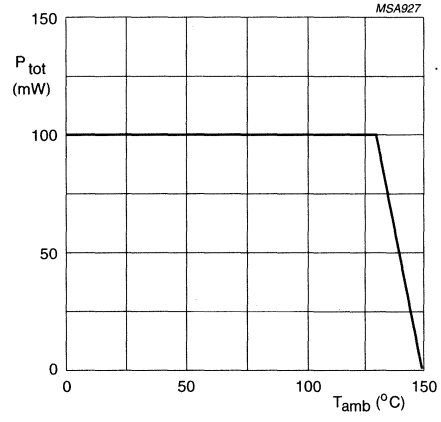

Fig.3 Power derating curve.

THERMAL CHARACTERISTICS

SYMBOL	PARAMETER	VALUE	UNIT
$R_{th\ j\text{-}a}$	thermal resistance from junction to ambient	180	K/W

CHARACTERISTICS

T_{amb} = 25 °C; H_x = 3 kA/m; note 1.

SYMBOL	PARAMETER	CONDITIONS	MIN.	TYP.	MAX.	UNIT
V_{CC}	bridge supply voltage		–	5	–	V
H_y	magnetic field strength		−2	–	+2	kA/m
S	sensitivity	open circuit, notes 2 and 3	3.2	–	4.8	$\frac{mV/V}{kA/m}$
TCV_O	temperature coefficient of output voltage	V_{CC} = 5 V; T_j = −25 to +125 °C	–	−0.4	–	%/K
		I_B = 3 mA; T_j = −25 to +125 °C	–	−0.1	–	%/K
R_{bridge}	bridge resistance		1.6	–	2.6	kΩ
TCR_{bridge}	temperature coefficient of bridge resistance	T_{bridge} = −25 to +125 °C	–	0.3	–	%/K
V_{offset}	offset voltage		−1.5	–	+1.5	mV/V
TCV_{offset}	offset voltage drift	T_j = −25 to +125 °C	−3	–	+3	$\frac{\mu V/V}{K}$
FL	linearity deviation of output voltage	H_y = 0 to ±1 kA/m	–	–	±0.5	%·FS
		H_y = 0 to ±1.6 kA/m	–	–	±1.7	%·FS
		H_y = 0 to ±2 kA/m	–	–	±2	%·FS
FH	hysteresis of output voltage		–	–	0.5	%·FS
f	operating frequency		0	–	1	MHz

Notes

1. In applications with H_x < 3 kA/m the sensor has to be reset before first operation by application of an auxiliary field H_x = 3 kA/m.
2. No disturbing field (H_d) allowed; for stable operation under disturbing conditions see Fig.4 (SOAR) and see Fig.5 for decrease of sensitivity.
3. $$S = \frac{(V_O \text{ at } H_y = 1.6 \text{ kA/m}) - (V_O \text{ at } H_y = 0)}{1.6 \times V_{CC}}.$$

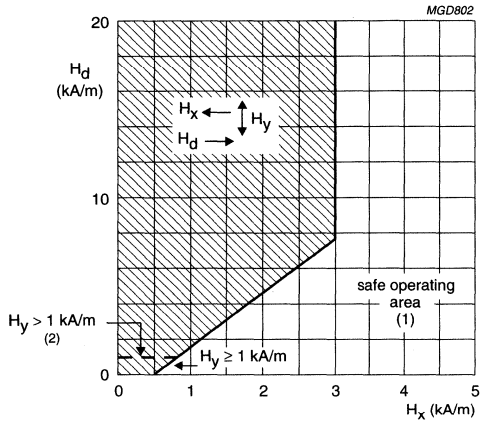

In applications with $H_x < 3$ kA/m, the sensor has to be reset, after leaving the SOAR, by an auxiliary field of $H_x = 3$ kA/m.

(1) Region of permissible operation.

(2) Permissible extension if $H_y < 1$ kA/m.

Fig.4 Safe Operating Area (permissible disturbing field H_d as a component of auxiliary field H_x).

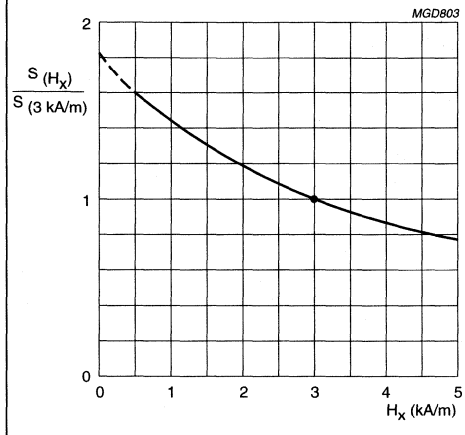

In applications with $H_x \leq 3$ kA/m, the sensor has to be reset by an auxiliary field of $H_x = 3$ kA/m before using.

Fig.5 Relative sensitivity (ratio of sensitivity at certain H_x and sensitivity at $H_x = 3$ kA/m).

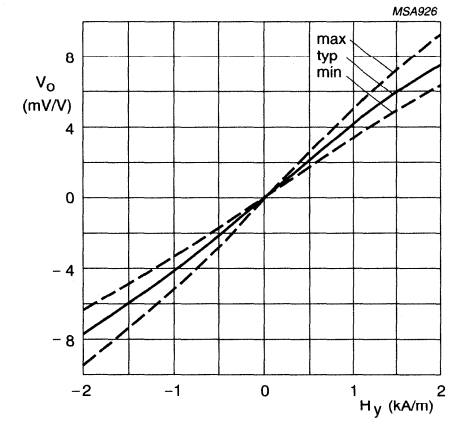

V_B = constant; $H_x = 3$ kA/m; $T_{amb} = 25$ °C; $V_{offset} = 0$.

Fig.6 Sensor output characteristics.

PACKAGE OUTLINE

Plastic single-ended flat package; 4 in-line leads **SOT195**

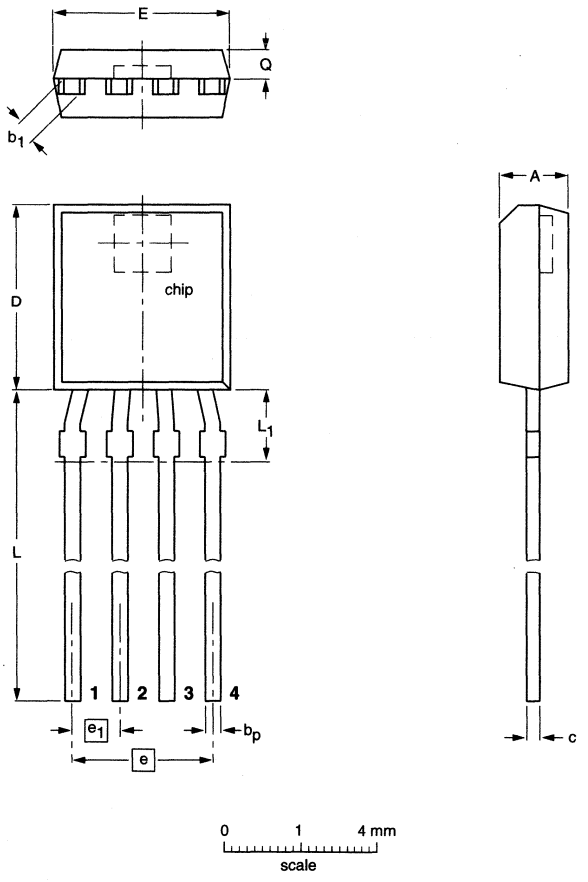

DIMENSIONS (mm are the original dimensions)

UNIT	A	b_p	b_1	c	D	E	e	e_1	L	L_1(1) max.	Q
mm	1.8 1.6	0.48 0.40	0.7 0.5	0.45 0.39	5.2 5.0	4.8 4.4	3.75	1.25	14.5 12.7	2	0.8 0.7

Notes

1. Terminal dimensions within this zone are uncontrolled to allow for flow of plastic and terminal irregularities.

OUTLINE VERSION	REFERENCES				EUROPEAN PROJECTION	ISSUE DATE
	IEC	JEDEC	EIAJ			
SOT195						97-06-02

Magnetic field sensor KMZ10C

DESCRIPTION

The KMZ10C is a magnetic field sensor, employing the magnetoresistive effect of thin-film permalloy. Its properties enable this sensor to be used in a wide range of applications for current and field measurement, revolution counters, angular or linear position measurement and proximity detectors, etc.

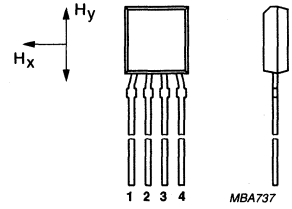

Fig.1 Simplified outline.

PINNING

PIN	SYMBOL	DESCRIPTION
1	$+V_O$	output voltage
2	GND	ground
3	$-V_O$	output voltage
4	V_{CC}	supply voltage

QUICK REFERENCE DATA

SYMBOL	PARAMETER	MIN.	TYP.	MAX.	UNIT
V_{CC}	DC supply voltage	–	5	–	V
T_{bridge}	bridge operating temperature	–40	–	+150	°C
H_y	magnetic field strength	–7.5	–	+7.5	kA/m
H_x	auxiliary field	–	3	–	kA/m
S	sensitivity	–	1.5	–	$\frac{mV/V}{kA/m}$
R_{bridge}	bridge resistance	1	–	1.8	kΩ
V_{offset}	offset voltage	–1.5	–	+1.5	mV/V

CIRCUIT DIAGRAM

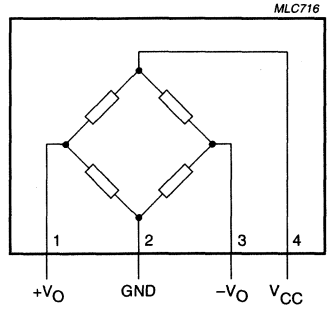

Fig.2 Simplified circuit diagram.

LIMITING VALUES

In accordance with the Absolute Maximum Rating System (IEC 134).

SYMBOL	PARAMETER	CONDITIONS	MIN.	MAX.	UNIT
V_{CC}	DC supply voltage		–	10	V
P_{tot}	total power dissipation	up to T_{amb} = 132 °C	–	100	mW
T_{stg}	storage temperature	note 1	−65	+150	°C
T_{bridge}	bridge operating temperature		−40	+150	°C

Note

1. Maximum operating temperature of the thin-film permalloy.

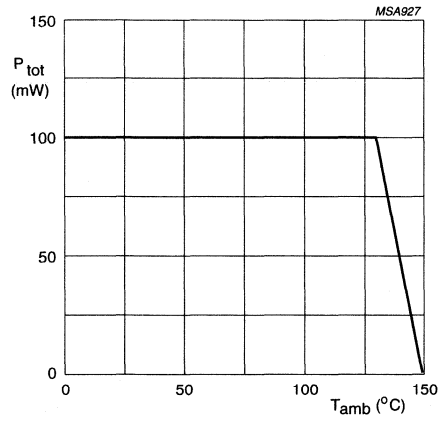

Fig.3 Power derating curve.

THERMAL CHARACTERISTICS

SYMBOL	PARAMETER	VALUE	UNIT
$R_{th\ j\text{-}a}$	thermal resistance from junction to ambient	180	K/W

CHARACTERISTICS

T_{amb} = 25 °C; H_x = 3 kA/m; note 1; V_{CC} = 5 V unless otherwise specified.

SYMBOL	PARAMETER	CONDITIONS	MIN.	TYP.	MAX.	UNIT
H_y	magnetic field strength		−7.5	–	+7.5	kA/m
S	sensitivity	notes 1 and 2	1	–	2	$\frac{mV/V}{kA/m}$
TCV_O	temperature coefficient of output voltage	V_{CC} = 5 V; T_{amb} = −25 to +125 °C	–	−0.5	–	%/K
		I_{CC} = 3 mA; T_{amb} = −25 to +125 °C	–	−0.15	–	%/K
R_{bridge}	bridge resistance		1	–	1.8	kΩ
TCR_{bridge}	temperature coefficient of bridge resistance	T_{bridge} = −25 to +125 °C	–	0.35	–	%/K
V_{offset}	offset voltage		−1.5	–	+1.5	mV/V
TCV_{offset}	temperature coefficient of offset voltage	T_{bridge} = −25 to +125 °C	−2	–	+2	(μV/V)/K
FL	linearity deviation of output voltage	H_y = 0 to ±3.75 kA/m	–	–	0.8	%·FS
		H_y = 0 to ±6.0 kA/m	–	–	2.4	%·FS
		H_y = 0 to ±7.5 kA/m	–	–	2.7	%·FS
FH	hysteresis of output voltage		–	–	0.5	%·FS
f	operating frequency		0	–	1	MHz

Notes

1. In applications with H_x < 3 kA/m the sensor has to be reset before first operation by application of an auxiliary field H_x = 3 kA/m.
2. $S = \frac{(V_O \text{ at } H_y = 6\ kA/m) - (V_O \text{ at } H_y = 0)}{6 \times V_{CC}}$.

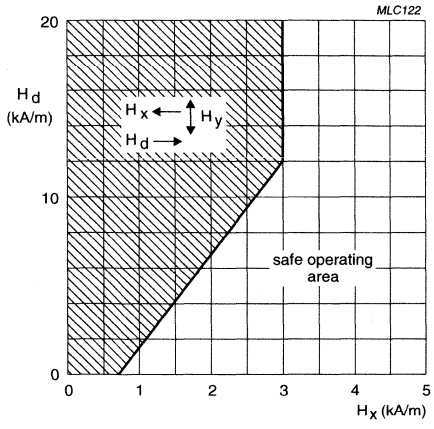

In applications with $H_x < 3$ kA/m, the sensor has to be reset, after leaving the SOAR, by an auxiliary field of $H_x = 3$ kA/m.

Fig.4 Safe Operating Area (permissible disturbing field H_d as a component of auxiliary field H_x).

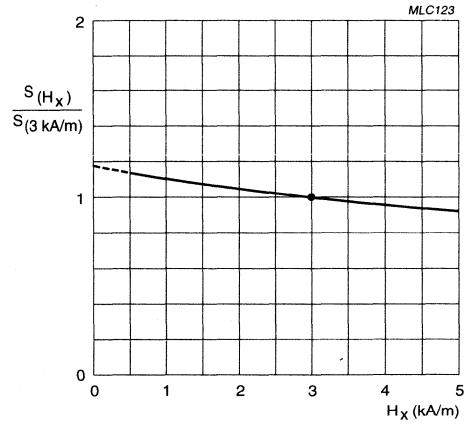

In applications with $H_x \leq 3$ kA/m, the sensor has to be reset by an auxiliary field of $H_x = 3$ kA/m before using.

Fig.5 Relative sensitivity (ratio of sensitivity at certain H_x and sensitivity at $H_x = 3$ kA/m).

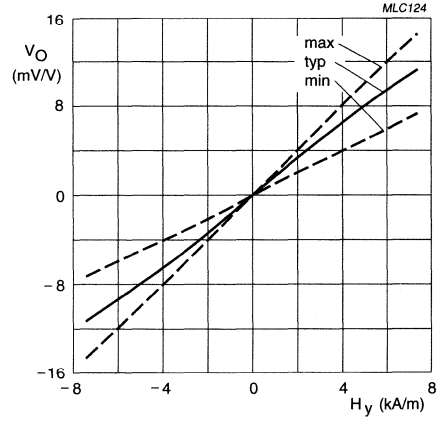

$H_x = 3$ kA/m; $T_{amb} = 25$ °C; $V_{offset} = 0$.

Fig.6 Sensor output characteristics.

PACKAGE OUTLINE

Plastic single-ended flat package; 4 in-line leads **SOT195**

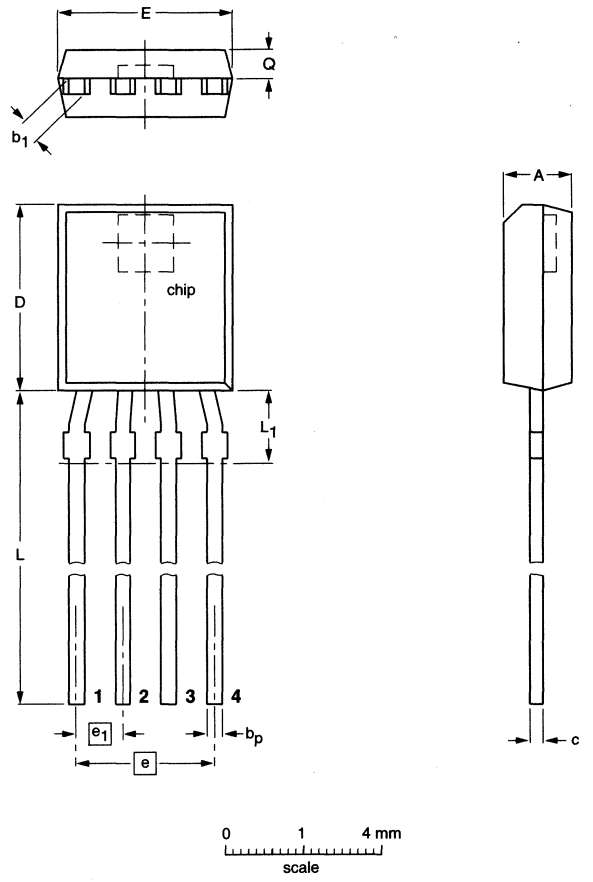

DIMENSIONS (mm are the original dimensions)

UNIT	A	b_p	b_1	c	D	E	e	e_1	L	L_1(1) max.	Q
mm	1.8 1.6	0.48 0.40	0.7 0.5	0.45 0.39	5.2 5.0	4.8 4.4	3.75	1.25	14.5 12.7	2	0.8 0.7

Notes

1. Terminal dimensions within this zone are uncontrolled to allow for flow of plastic and terminal irregularities.

OUTLINE VERSION	REFERENCES				EUROPEAN PROJECTION	ISSUE DATE
	IEC	JEDEC	EIAJ			
SOT195						97-06-02

Magnetic field sensor KMZ41

DESCRIPTION

The KMZ41 is a sensitive magnetic field sensor, employing the magnetoresistive effect of thin-film permalloy. The sensor contains two galvanic separated Wheatstone bridges. Its properties enable this sensor to be used in angle measurement applications under strong field conditions. A rotating magnetic field (strength > 100 kA/m) in the x-y plane will deliver a sinusoidal output signal. The sensor can be operated at any frequency between DC and 1 MHz.

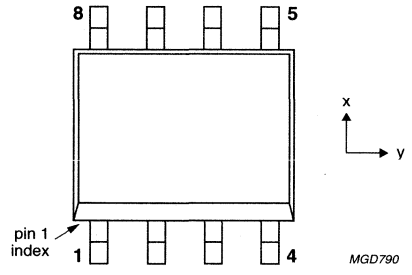

Fig.1 Simplified outline SOT96-1.

PINNING

PIN	SYMBOL	DESCRIPTION
1	$-V_{O1}$	output voltage bridge 1
2	$-V_{O2}$	output voltage bridge 2
3	V_{CC2}	supply voltage bridge 2
4	V_{CC1}	supply voltage bridge 1
5	$+V_{O1}$	output voltage bridge 1
6	$+V_{O2}$	output voltage bridge 2
7	GND2	ground 2
8	GND1	ground 1

QUICK REFERENCE DATA

SYMBOL	PARAMETER	MIN.	TYP.	MAX.	UNIT
V_{CC1}	bridge supply voltage	–	5	9	V
V_{CC2}	bridge supply voltage	–	5	9	V
S	sensitivity (α = 0°, 45°)	–	2.86	–	mV/°
R_{bridge}	bridge resistance	2	–	3	kΩ
$V_{offset1}$	offset voltage	–8	–	+8	mV/V
$V_{offset2}$	offset voltage	–8	–	+8	mV/V

CIRCUIT DIAGRAM

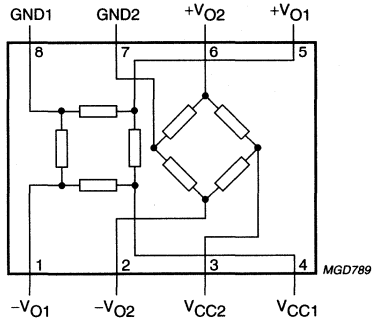

Fig.2 Simplified circuit diagram.

LIMITING VALUES

In accordance with the Absolute Maximum Rating System (IEC 134).

SYMBOL	PARAMETER	CONDITIONS	MIN.	MAX.	UNIT
V_{CC}	bridge supply voltage		–	12	V
P_{tot}	total power dissipation	up to T_{amb} = 130 °C	–	120	mW
T_{stg}	storage temperature		–65	+150	°C
T_{bridge}	bridge operating temperature		–40	+150	°C

THERMAL CHARACTERISTICS

SYMBOL	PARAMETER	VALUE	UNIT
$R_{th\ j\text{-}a}$	thermal resistance from junction to ambient	155	K/W

CHARACTERISTICS

T_{amb} = 25 °C; $H_{rotation}$ = 100 kA/m; V_{CC1} = 5 V; V_{CC2} = 5 V unless otherwise specified.

SYMBOL	PARAMETER	CONDITIONS	MIN.	TYP.	MAX.	UNIT
V_{CC1}	bridge supply voltage		–	5	9	V
V_{CC2}	bridge supply voltage		–	5	9	V
S	sensitivity	open circuit, note 1; α = 0° (bridge 2); α = 90° (bridge 1)	2.62	2.86	3.10	mV/°
$V_{peak\ 1}$	peak voltage		75	82	89	mV
$V_{peak\ 2}$	peak voltage		75	82	89	mV
TCV_O	temperature coefficient of output voltage	V_{CC} = 5 V; T_{amb} = –25 to +125 °C	–	–0.4	–	%/K
		I_{CC} = 3 mA; T_{amb} = –25 to +125 °C	–	–0.1	–	%/K
R_{bridge}	bridge resistance		2	–	3	kΩ
TCR_{bridge}	temperature coefficient of bridge resistance	T_{bridge} = –25 to +125 °C	–	0.3	–	%/K
V_{offset}	offset voltage		–8	–	+8	mV/V
TCV_{offset}	temperature coefficient of offset voltage	T_{bridge} = –25 to +125 °C	–3	–	+3	$\frac{\mu V/V}{K}$
FH	hysteresis of output voltage		–	–	0.5	%·FS
f	operating frequency		0	–	1	MHz

Note

1. Sensitivity changes with angle due to sinusoidal output.

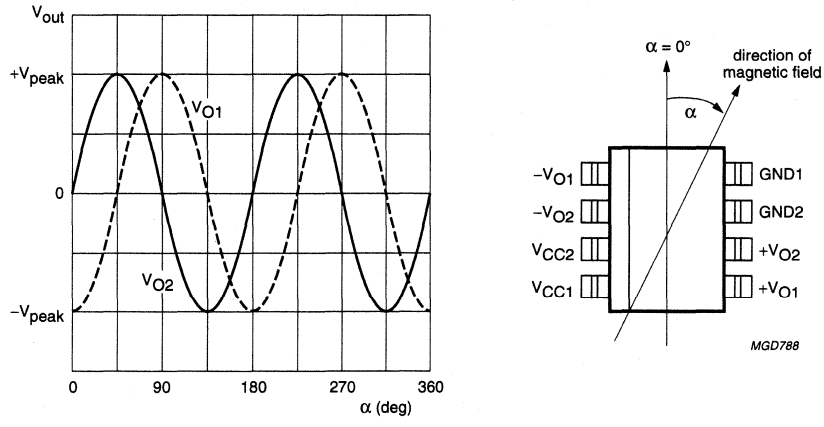

Fig.3 Output signals related to the direction of the magnetic field.

PACKAGE OUTLINE

SO8: plastic small outline package; 8 leads; body width 3.9 mm **SOT96-1**

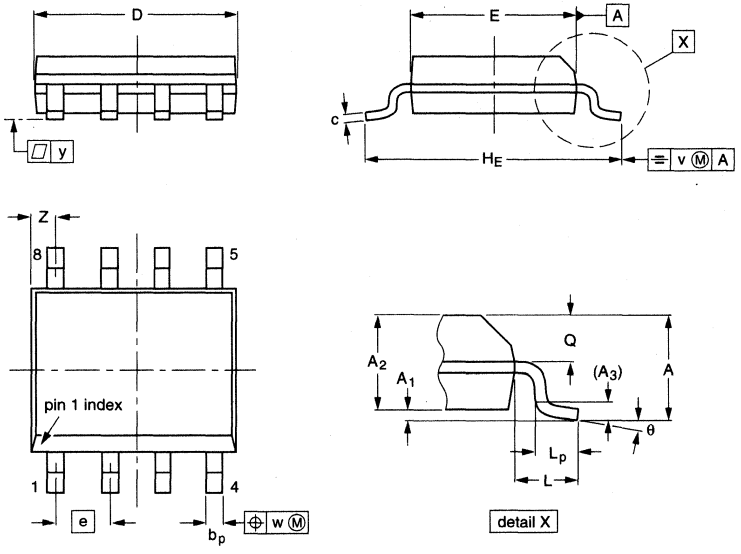

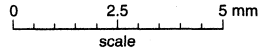

DIMENSIONS (inch dimensions are derived from the original mm dimensions)

UNIT	A max.	A_1	A_2	A_3	b_p	c	$D^{(1)}$	$E^{(2)}$	e	H_E	L	L_p	Q	v	w	y	$Z^{(1)}$	θ
mm	1.75	0.25 0.10	1.45 1.25	0.25	0.49 0.36	0.25 0.19	5.0 4.8	4.0 3.8	1.27	6.2 5.8	1.05	1.0 0.4	0.7 0.6	0.25	0.25	0.1	0.7 0.3	8° 0°
inches	0.069	0.010 0.004	0.057 0.049	0.01	0.019 0.014	0.0100 0.0075	0.20 0.19	0.16 0.15	0.050	0.244 0.228	0.041	0.039 0.016	0.028 0.024	0.01	0.01	0.004	0.028 0.012	

Notes

1. Plastic or metal protrusions of 0.15 mm maximum per side are not included.
2. Plastic or metal protrusions of 0.25 mm maximum per side are not included.

OUTLINE VERSION	REFERENCES				EUROPEAN PROJECTION	ISSUE DATE
	IEC	JEDEC	EIAJ			
SOT96-1	076E03S	MS-012AA				~~95-02-04~~ 97-05-22

Magnetic field sensor — KMZ50

FEATURES

- High sensitivity
- Integrated set/reset coil.

APPLICATIONS

- Navigation
- Current and earth magnetic field measurement
- Traffic detection.

DESCRIPTION

The KMZ50 is an extremely sensitive magnetic field sensor, employing the magnetoresistive effect of thin-film permalloy. The sensor contains one magnetoresistive Wheatstone bridge and integrated set/reset conductors. With the integrated set/reset conductor the orientation of sensitivity may be set or changed (flipped). A short current pulse on this conductor is needed to recover (set) the sensor after exposure to strong disturbing magnetic fields. A negative current pulse will reset the sensor to reversed sensitivity. By use of periodically alternated flipping pulses and a lock-in amplifier, output will become independent of sensor and amplifier offset.

PINNING

PIN	SYMBOL	DESCRIPTION
1	$+I_{flip}$	flip coil
2	V_{CC}	bridge supply voltage
3	GND	ground
4	n.c.	not connected
5	n.c.	not connected
6	$-V_O$	bridge output voltage
7	$+V_O$	bridge output voltage
8	$-I_{flip}$	flip coil

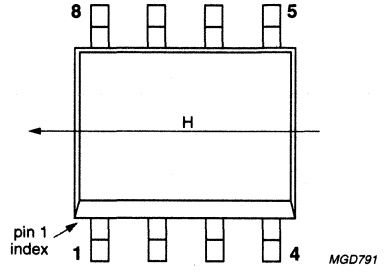

Fig.1 Simplified outline.

QUICK REFERENCE DATA

SYMBOL	PARAMETER	MIN.	TYP.	MAX.	UNIT
V_{CC}	bridge supply voltage	–	5	8	V
S	sensitivity (uncompensated)	12	16	–	$\frac{mV/V}{kA/m}$
V_{offset}	offset voltage	−1.5	–	+1.5	mV/V
R_{bridge}	bridge resistance	1	–	3	kΩ
R_{flip}	flip coil resistance	1	3	5	Ω
$I_{flip\ (min)}$	minimum recommended flipping current; note 1	800	1000	1200	mA
$t_{flip\ (min)}$	minimum flip pulse duration; note 1	1	3	100	μs

Note

1. Average power consumption in flip conductor, defined by current, pulse duration and pulse repetition rate may not exceed the specified limit, see "Limiting values".

CIRCUIT DIAGRAM

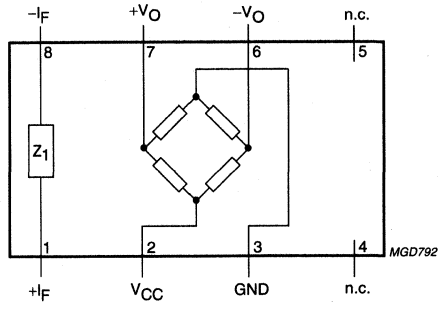

Fig.2 Simplified circuit diagram.

LIMITING VALUES

In accordance with the Absolute Maximum Rating System (IEC 134).

SYMBOL	PARAMETER	MIN.	MAX.	UNIT
V_{CC}	bridge supply voltage	–	9	V
P_{tot}	total power dissipation	–	130	mW
T_{stg}	storage temperature	−65	+150	°C
T_{bridge}	bridge operating temperature	−40	+125	°C
$I_{flip\ (max)}$	maximum flipping current	–	1500	mA
$P_{flip\ (max)}$	maximum flipping power dissipation	–	50	mW
V_{isol}	voltage between isolated systems: flip conductor - Wheatstone bridge	–	60	V

THERMAL CHARACTERISTICS

SYMBOL	PARAMETER	VALUE	UNIT
$R_{th\ j\text{-}a}$	thermal resistance from junction to ambient	155	K/W

CHARACTERISTICS

T_{amb} = 25 °C unless otherwise specified.

SYMBOL	PARAMETER	CONDITIONS	MIN.	TYP.	MAX.	UNIT
V_{CC}	bridge supply voltage		–	5	8	V
H_y	operating range in sensitive direction		−0.2	–	+0.2	kA/m
H_x	operating range perpendicular to sensitive direction		−0.2	–	+0.2	kA/m
S	sensitivity	open circuit	12	16	–	$\frac{mV/V}{kA/m}$
TCV_O	temperature coefficient of output voltage	V_{CC} = 5 V; T_{amb} = −25 to +125 °C	–	−0.4	–	%/K
		I_{CC} = 3 mA; T_{amb} = −25 to +125 °C	–	−0.1	–	%/K
R_{bridge}	bridge resistance	resistance pins 2 to 3	1	–	3	kΩ
TCR_{bridge}	temperature coefficient of bridge resistance	T_{bridge} = −25 to +125 °C	–	0.3	–	%/K
V_{offset}	offset voltage		−1.5	–	+1.5	mV/V
TCV_{offset}	temperature coefficient of offset voltage	T_{bridge} = −25 to +125 °C	−3	–	+3	$\frac{\mu V/V}{K}$
FH	hysteresis of output voltage		–	–	2	%FS
R_{flip}	resistance of set/reset conductor	resistance pins 1 to 8	1	3	5	Ω
I_{flip}	recommended flipping current for stable operation	current pins 1 to 8	±800	±1000	±1200	mA
t_{flip}	flip pulse duration		1	3	100	µs
R_{isol}	isolating resistance	resistance pins 1 to 2, 1 to 4, 2 to 4	1	–	–	MΩ
V_{isol}	voltage between isolated systems	voltage pins 1 to 2, 1 to 4, 2 to 4	–	–	50	V
f	operating frequency		0	–	1	MHz

PACKAGE OUTLINE

SO8: plastic small outline package; 8 leads; body width 3.9 mm **SOT96-1**

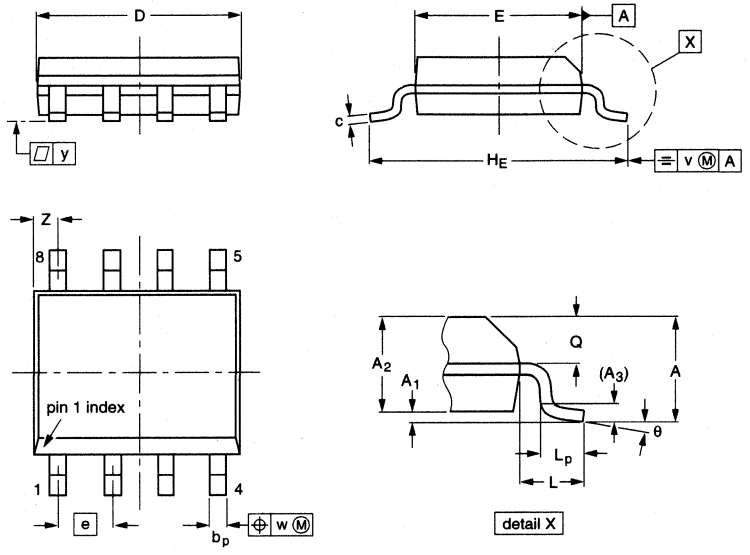

DIMENSIONS (inch dimensions are derived from the original mm dimensions)

UNIT	A max.	A_1	A_2	A_3	b_p	c	$D^{(1)}$	$E^{(2)}$	e	H_E	L	L_p	Q	v	w	y	$Z^{(1)}$	θ
mm	1.75	0.25 0.10	1.45 1.25	0.25	0.49 0.36	0.25 0.19	5.0 4.8	4.0 3.8	1.27	6.2 5.8	1.05	1.0 0.4	0.7 0.6	0.25	0.25	0.1	0.7 0.3	8° 0°
inches	0.069	0.010 0.004	0.057 0.049	0.01	0.019 0.014	0.0100 0.0075	0.20 0.19	0.16 0.15	0.050	0.244 0.228	0.041	0.039 0.016	0.028 0.024	0.01	0.01	0.004	0.028 0.012	

Notes

1. Plastic or metal protrusions of 0.15 mm maximum per side are not included.
2. Plastic or metal protrusions of 0.25 mm maximum per side are not included.

OUTLINE VERSION	REFERENCES				EUROPEAN PROJECTION	ISSUE DATE
	IEC	JEDEC	EIAJ			
SOT96-1	076E03S	MS-012AA				~~95-02-04~~ 97-05-22

Magnetic field sensor KMZ51

FEATURES

- High sensitivity
- Integrated compensation coil
- Integrated set/reset coil.

APPLICATIONS

- Navigation
- Current and earth magnetic field measurement
- Traffic detection.

DESCRIPTION

The KMZ51 is an extremely sensitive magnetic field sensor, employing the magnetoresistive effect of thin-film permalloy. The sensor contains one magnetoresistive Wheatstone bridge and integrated compensation and set/reset conductors. The integrated compensation conductor allows magnetic field measurement with current feedback loops to generate an output that is independent of drift in sensitivity. With the integrated set/reset conductor the orientation of sensitivity may be set or changed (flipped). A short current pulse on this conductor is needed to recover (set) the sensor after exposure to strong disturbing magnetic fields. A negative current pulse will reset the sensor to reversed sensitivity. By use of periodically alternated flipping pulses and a lock-in amplifier, output will become independent of sensor and amplifier offset.

PINNING

PIN	SYMBOL	DESCRIPTION
1	$+I_{flip}$	flip coil
2	V_{CC}	bridge supply voltage
3	GND	ground
4	$+I_{comp}$	compensation coil
5	$-I_{comp}$	compensation coil
6	$-V_O$	bridge output voltage
7	$+V_O$	bridge output voltage
8	$-I_{flip}$	flip coil

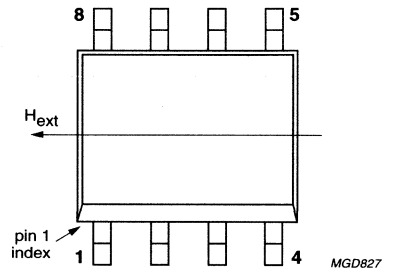

Fig.1 Simplified outline.

QUICK REFERENCE DATA

SYMBOL	PARAMETER	MIN.	TYP.	MAX.	UNIT
V_{CC}	bridge supply voltage	–	5	8	V
S	sensitivity (uncompensated)	12	16	–	$\frac{mV/V}{kA/m}$
V_{offset}	offset voltage	−1.5	–	+1.5	mV/V
R_{bridge}	bridge resistance	1	–	3	kΩ
R_{comp}	compensation coil resistance	100	170	300	Ω
A_{comp}	compensation coil field factor; note 1	19	22	25	A/m/mA
R_{flip}	flip coil resistance	1	3	5	Ω
$I_{flip\ (min)}$	minimum recommended flipping current; note 2	800	1000	1200	mA
$t_{flip\ (min)}$	minimum flip pulse duration; note 2	1	3	100	µs

Notes

1. Compensation conductor will generate a field $H_{comp} = A_{comp} \cdot I_{comp}$ additional to the external field H_{ext}. Sensor output will become zero if $H_{ext} = -H_{comp}$.
2. Average power consumption in flip conductor, defined by current, pulse duration and pulse repetition rate may not exceed the specified limit, see "Limiting values".

CIRCUIT DIAGRAM

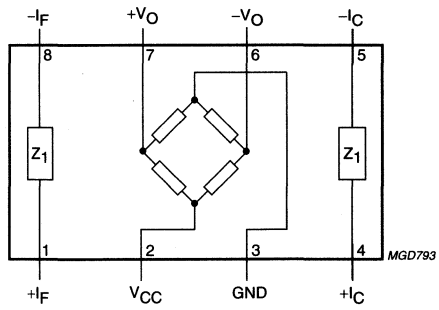

Fig.2 Simplified circuit diagram.

LIMITING VALUES

In accordance with the Absolute Maximum Rating System (IEC 134).

SYMBOL	PARAMETER	MIN.	MAX.	UNIT
V_{CC}	bridge supply voltage	–	9	V
P_{tot}	total power dissipation	–	130	mW
T_{stg}	storage temperature	−65	+150	°C
T_{bridge}	bridge operating temperature	−40	+125	°C
I_{comp}	maximum compensation current	–	15	mA
$I_{flip\ (max)}$	maximum flipping current	–	1500	mA
$P_{flip\ (max)}$	maximum flipping power dissipation	–	50	mW
V_{isol}	voltage between isolated systems: flip conductor - Wheatstone bridge; compensation conductor - bridge; flip conductor - compensation conductor	–	60	V

THERMAL CHARACTERISTICS

SYMBOL	PARAMETER	VALUE	UNIT
$R_{th\ j\text{-}a}$	thermal resistance from junction to ambient	155	K/W

CHARACTERISTICS

T_{amb} = 25 °C unless otherwise specified.

SYMBOL	PARAMETER	CONDITIONS	MIN.	TYP.	MAX.	UNIT
V_{CC}	bridge supply voltage		–	5	8	V
H_y	operating range in sensitive direction		−0.2	–	+0.2	kA/m
H_x	operating range perpendicular to sensitive direction		−0.2	–	+0.2	kA/m
S	sensitivity	open circuit	12	16	–	$\frac{mV/V}{kA/m}$
TCV_O	temperature coefficient of output voltage	V_{CC} = 5 V; T_{amb} = −25 to +125 °C	–	−0.4	–	%/K
		I_{CC} = 3 mA; T_{amb} = −25 to +125 °C	–	−0.1	–	%/K
R_{bridge}	bridge resistance	resistance pins 2 to 3	1	–	3	kΩ
TCR_{bridge}	temperature coefficient of bridge resistance	T_{bridge} = −25 to +125 °C	–	0.3	–	%/K
V_{offset}	offset voltage		−1.5	–	+1.5	mV/V
TCV_{offset}	temperature coefficient of offset voltage	T_{bridge} = −25 to +125 °C	−3	–	+3	$\frac{\mu V/V}{K}$
FH	hysteresis of output voltage		–	–	2	%FS
R_{comp}	resistance of compensation conductor	resistance pins 4 to 5	100	170	300	Ω
A_{comp}	field factor of compensation conductor		19	22	25	A/m/mA
R_{flip}	resistance of set/reset conductor	resistance pins 1 to 8	1	3	5	Ω
I_{flip}	recommended flipping current for stable operation		±800	±1000	±1200	mA
t_{flip}	flip pulse duration;		1	3	100	µs
R_{isol}	isolating resistance	resistance pins 1 to 2, 1 to 4, 2 to 4	1	–	–	MΩ
V_{isol}	voltage between isolated systems	voltage pins 1 to 2, 1 to 4, 2 to 4	–	–	50	V
f	operating frequency		0	–	1	MHz

PACKAGE OUTLINE

SO8: plastic small outline package; 8 leads; body width 3.9 mm **SOT96-1**

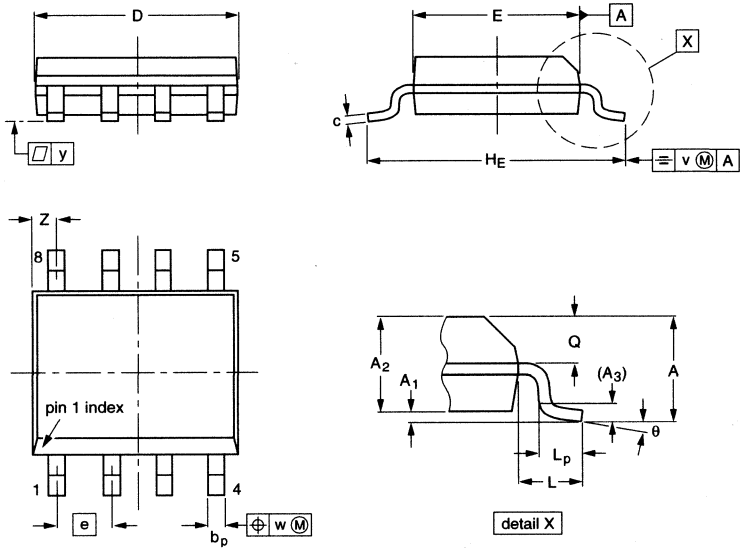

DIMENSIONS (inch dimensions are derived from the original mm dimensions)

UNIT	A max.	A_1	A_2	A_3	b_p	c	$D^{(1)}$	$E^{(2)}$	e	H_E	L	L_p	Q	v	w	y	$Z^{(1)}$	θ
mm	1.75	0.25 0.10	1.45 1.25	0.25	0.49 0.36	0.25 0.19	5.0 4.8	4.0 3.8	1.27	6.2 5.8	1.05	1.0 0.4	0.7 0.6	0.25	0.25	0.1	0.7 0.3	8° 0°
inches	0.069	0.010 0.004	0.057 0.049	0.01	0.019 0.014	0.0100 0.0075	0.20 0.19	0.16 0.15	0.050	0.244 0.228	0.041	0.039 0.016	0.028 0.024	0.01	0.01	0.004	0.028 0.012	

Notes

1. Plastic or metal protrusions of 0.15 mm maximum per side are not included.
2. Plastic or metal protrusions of 0.25 mm maximum per side are not included.

OUTLINE VERSION	REFERENCES				EUROPEAN PROJECTION	ISSUE DATE
	IEC	JEDEC	EIAJ			
SOT96-1	076E03S	MS-012AA				~~95-02-04~~ 97-05-22

GENERAL
ROTATIONAL SPEED MEASUREMENT

ROTATIONAL SPEED MEASUREMENT

Contents

Principles and standard set-ups

The basic properties of the magnetoresistive technique make it highly suitable for measuring the rotational or angular speed of an object:

- It offers high sensitivity (about 10 to 100 times stronger than the Hall effect), which allows large air gaps (>2.5 mm) to be used between the target and sensor, and produces strong primary signals, making the sensing set-up largely insensitive to disturbances.
- It has a very wide operating frequency range (DC up to >1 MHz), with the sensor still producing a signal down to 0 Hz, allowing its use in very low speed applications (e.g. in car navigation systems).
- As the sensors are metal-based, they can operate up to 190 °C, making them extremely well suited to high temperature situations. These are commonly found in automotive applications such as in braking systems and under the car bonnet, near the engine (cam and crankshaft speed measurement, for example).
- Magnetoresistive sensors are highly insensitive to mechanical stress in comparison to Hall effect sensors, due to the relatively small piezoresistive effect in the permalloy material, so they can be encapsulated simply and cost-effectively.

Since the magnetoresistive effect cannot measure rotational speed directly, a practical set-up uses a magnetic field applied to the sensor from a permanent magnet. Typically, this 'back-biasing' magnet is simply glued to the back of the sensor, so that the sensor sees a uniform parallel field with no component in the sensitive direction and sensor output is zero. Then, if a ferromagnetic target with teeth is brought close to the sensor, the field of the back-biasing magnet is affected by the target and the influence depends on the position of the target in front of the sensor (see Fig.1).

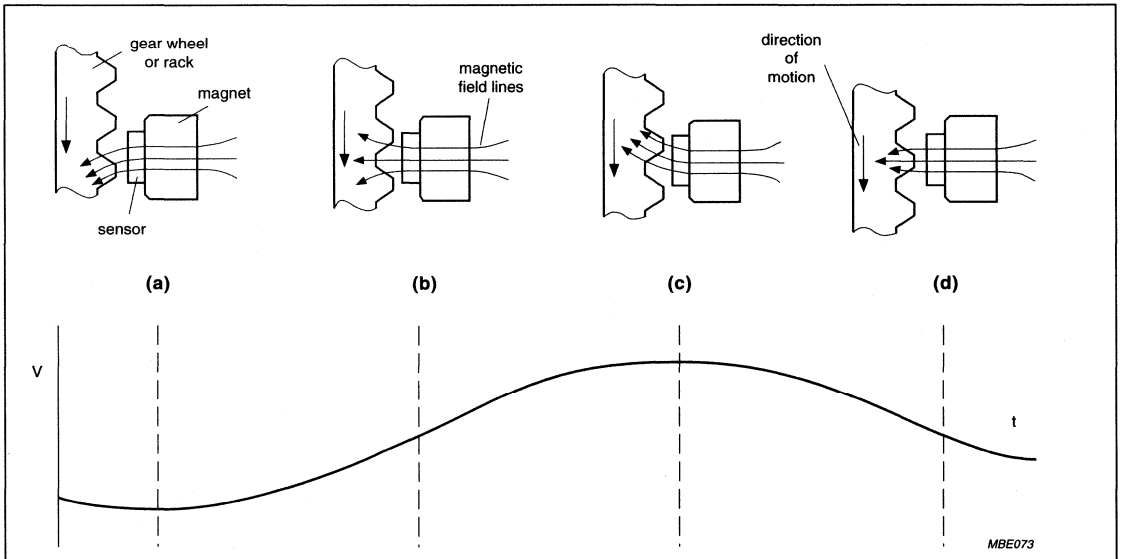

Fig.1 Speed detection using a magnetoresistive sensor.

At a 'symmetric' position, where a tooth or valley is exactly in front of the sensor, the target has no effect on the field seen by the sensor, so the sensor still gives a zero output. For a 'non-symmetric' position, as the target rotates in front of the target, the effect and thus the amplitude of the sensor output varies according to the actual wheel position.

The peak value of the output, V_{peak}, depends on the magnetic field strength of the biasing magnet, the distance between the sensor and the target and, obviously, the structure of the target. Large, solid targets will give stronger signals at larger distances from the sensor than small targets. In general, the 'size' of the structure in this application can be described as a relationship between wheel diameter and the number of teeth, described in Table 1.

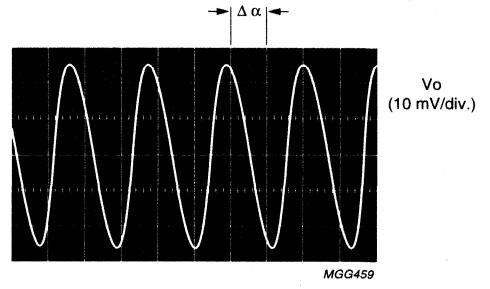

Fig.2 Typical oscilloscope trace for rotational speed measurement.

Table 1 Gear wheel dimensions (see Fig.3)

SYMBOL	DESCRIPTION	UNIT
German DIN		
z	number of teeth	
d	diameter	mm
m	module m = d/z	mm
p	pitch p = π • m	mm
ASA(1)		
PD	pitch diameter (d in inches)	inch
DP	diametric pitch DP = z/PD	$inch^{-1}$
CP	circular pitch CP = π /DP	inch

Note

1. For conversion from ASA to DIN: m = 25.4 mm/DP; p = 25.4 × CP.

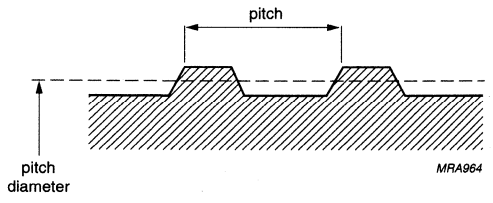

Fig.3 Gear wheel dimensions.

Figure 4 shows a typical relationship between the primary output signal (i.e. with no signal conditioning electronics) of a KMZ10B sensor (with a back biasing magnet) and various target structures, with module 'm'.

This principle is for so-called 'passive' ferrous targets, where the target is not itself magnetized (see Fig.5).

MR sensors are naturally bi-stable devices, with two stable but opposite operating characteristics, so they also need an external magnetic field for stabilization. With a suitably magnetized magnet positioned correctly, a single magnet can perform both stabilization and back-biasing. (For more details on sensor stabilization, please refer to the General Introduction to this handbook and Appendix 2.)

'Active' targets can also be used, where the target has alternating magnetic poles. In this case, the target itself provides the 'working' field, so no back-biasing magnet is required, only a stabilization magnet, which can be smaller than the ones used for both stabilization and back-biasing with passive targets. Also, it should be noted that an active target need not have teeth. An 'active' set-up is shown in Fig.6.

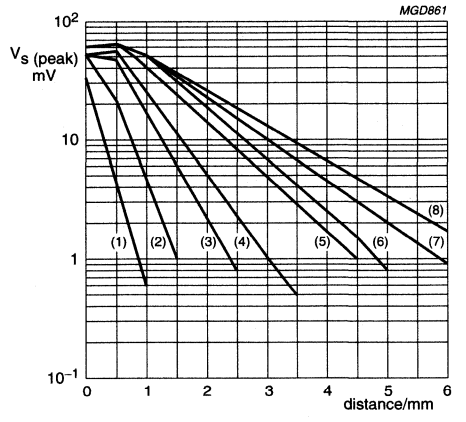

(1) m = 0.5; (2) m = 0.75; (3) m = 1; (4) m = 1.25; (5) m = 2; (6) m = 2.5; (7) m = 3; (8) m = 4.

Fig.4 Typical relationship between the airgap of a KMZ10B sensor, with a back biasing magnet (8 mm x 8 mm x 4.35 m, used eg for KMI15/1), and target module, 'm'.

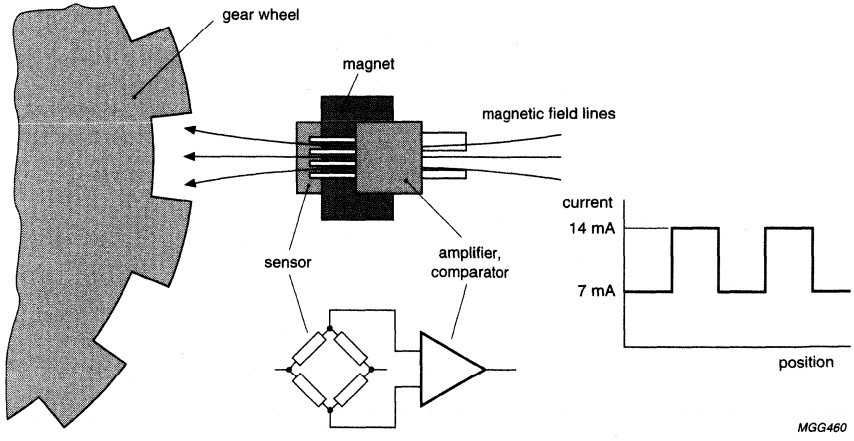

Fig.5 Simple set-up using a passive target.

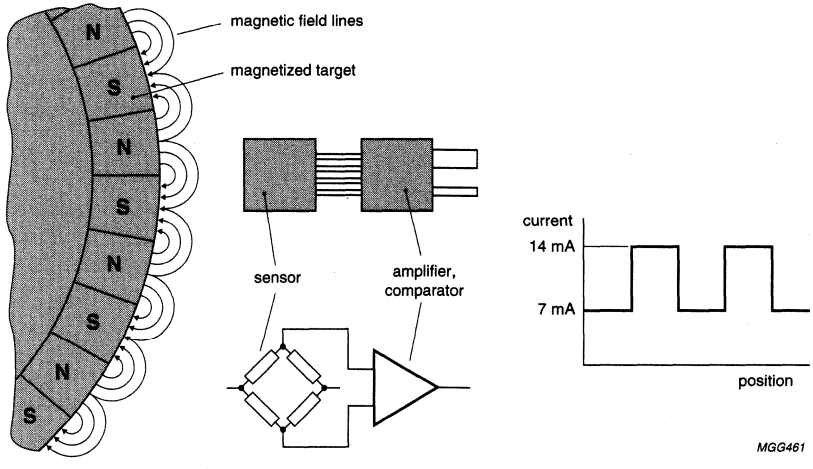

Fig.6 Simple set-up using an active target.

Rotational speed measurement

General

The structure of an active target can be expressed similarly to that for passive targets (Table 1). In this case, a tooth/valley pair is represented by a North-South magnetic pole pair. Figure 7 shows a typical relationship between the primary output signal (i.e. with no signal conditioning electronics) of a KM110B/2 sensor and various active target structures, with module 'm'.

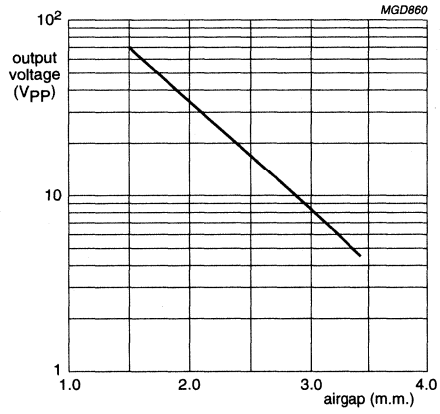

Fig.7 Typical relationship between the airgap of a KM110B/2 sensor and active target module, 'm'.

Both measurement techniques are inherently accurate, as the frequency of the output is directly proportional to the rotational speed. Although in principle, for a basic application requiring minimal accuracy, the output from the sensor can be used directly, in practice the use of signal conditioning circuitry stabilizes the output from the sensor and ensures accurate speed measurement under varying environmental conditions. Typical conditioning includes EMC filtering, amplification, temperature compensation and switching hysteresis.

Philips' sensors for rotational speed measurement

Practical rotational speed sensors are always delivered complete with a back biasing magnet, with the signal conditioning circuitry contained in a separate IC, for both active and passive set-ups. To simplify system design, Philips has developed a series of ready to use sensors, the KMI15/X family, which comprises a magnetoresistive sensor (an adapted version of the KMZ10B), a ferrite back-biasing magnet and an advanced bipolar signal conditioning IC, mounted on a single lead frame. The three sensors in the family are the KMI15/1 and KMI15/4 for passive targets, and the KMI15/2 for active targets.

For passive set-ups, the magnets are specially designed to apply a symmetrical magnetic field in the y-z plane of the sensor and a field at 30° relative to the z-axis in the x-z plane. The symmetrical field in the y-z plane (Figs 9 and 10) provides the back-biasing and the component in the x-direction of the sensor plane stabilizes the magnetoresistive element, as described earlier.

For active set-ups, the KMI15/2 comes with a small stabilization magnet (see Fig.11) and needs no back-biasing (the operational field being supplied by the target itself).

These sensors provide a compact design and cost-effective customization possibilities and, as they are simple to design-in, time-to-market is significantly reduced. In addition to the advantages described earlier, these sensors are almost immune to vibration effects (an inherent property of the magnetoresistive effect), can be used with a large variety of gear-tooth structures, are EMC resistant and offer a digital current output signal. The two-wire digital current signal has the advantages of considerably reduced wiring and connections, which can actually be a more significant cost than that of the sensor itself. The IC and sensor are separated physically within the encapsulation, to optimize the KMI15's high temperature performance (so that the sensor can then be exposed to higher temperatures than the IC and the power dissipation of the IC will not cause inhomogeneous heating of the sensor element).

In the signal conditioning circuit, the sensor output signal is passed through an EMC filter, amplified and then digitized by a comparator which has built-in switching hysteresis, performed by a Schmitt trigger (for more details, refer to the section on switching hysteresis). The voltage control block provides a stabilized 5 V power supply for the sensor, amplifier and comparator and is itself stabilized by a bandgap reference diode.

KMI sensors were developed as magnetoresistive devices with a current output, which has the advantage of using low cost two-wire technology. They use two current sources, integrated into the signal conditioning IC: one supplies a base current output of 7 mA (partly used for the 5 V supply) and a second, switchable 7 mA current source is added when triggered by the amplified and digitized sensor output signal. Thus, during operation the output current, I_{CC}, switches between 7 mA and 14 mA (see Fig.8). A set-up providing a three-wire voltage output is described later and an integrated sensor with three-wire open collector output is under development.

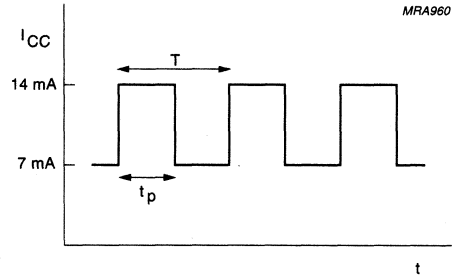

Fig.8 Current output signal.

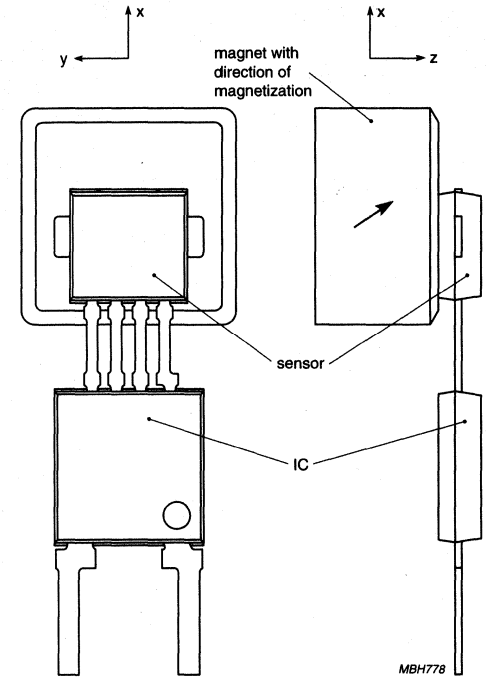

Fig.9 Typical outline of a KMI15/1 rotational sensor module for passive targets.

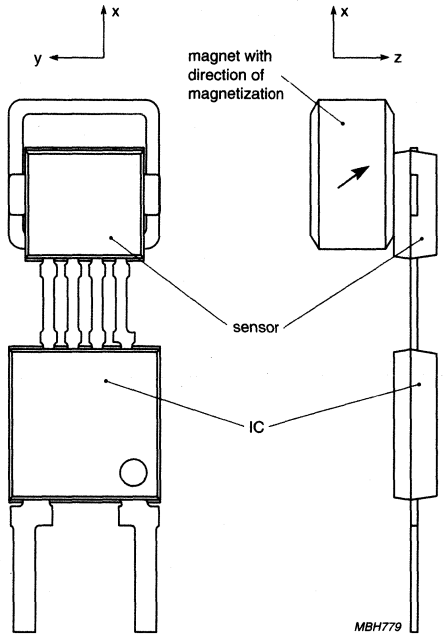

Fig.10 Typical outline of a KMI15/4 rotational sensor module for passive targets.

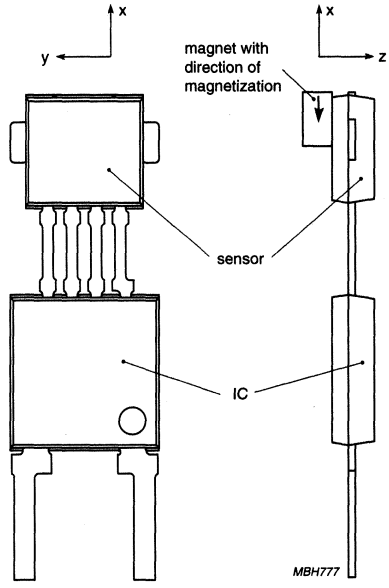

Fig.11 Typical outline of a KMI15/2 rotational sensor module for active targets.

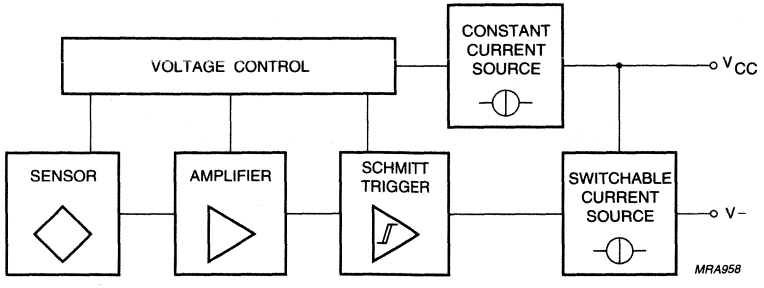

Fig.12 Block diagram of sensor and signal conditioning circuitry.

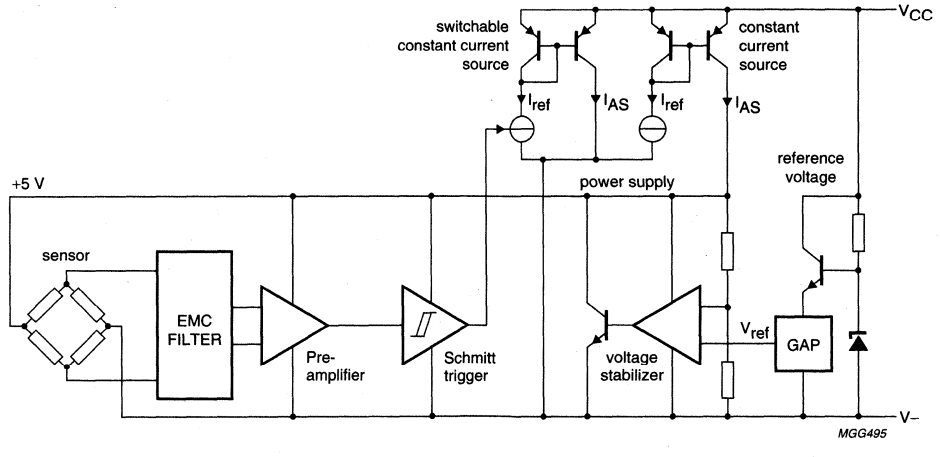

Fig.13 Sensor signal conditioning circuit diagram.

SENSING DISTANCE AND MOUNTING

Sensing distance 'd' is defined as the distance between the front of the sensor and the tips of the teeth, measured on the central axis of the magnet (see Fig.14). Above a certain value of 'd', I_{CC} ceases to vary between 7 mA and 14 mA and becomes a constant 7 mA. The KMI15 sensors are optimized to deliver a stable digital output signal for a large range of 'd' values and have a large switching hysteresis, to avoid unwanted signals arising through vibrations. Variations due to temperature are compensated by the signal conditioning IC; the residual temperature effect is shown in Fig.15.

Movements of the ferromagnetic target wheel in the magnetic field of the sensor system will induce eddy currents in the wheel, generating an offset voltage in the sensor's output which increases linearly with rotational speed. This reduces the maximum sensing distance slightly at higher frequencies, since this offset is in addition to the static offset, so the available voltage from the switching hysteresis (set to ±3 mV) is reduced, decreasing the maximum airgap at which the sensor operates (switching hysteresis is described in more detail later in this chapter). (Eddy currents can also be used to positive effect in some applications: see the Section on "Information for advanced users and applications" later in this chapter.) Finally, the structure of the wheel itself will affect maximum sensing distance, according to how large and well-defined the teeth are. Figure 16 shows the variation of the maximum distance of 'd' with tooth module for a KMI15/1.

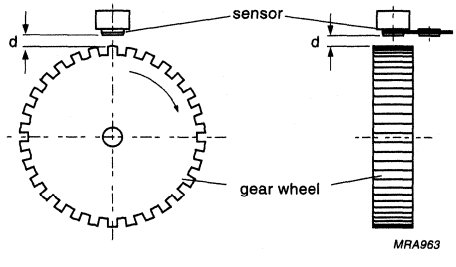

Fig.14 Sensor positioning.

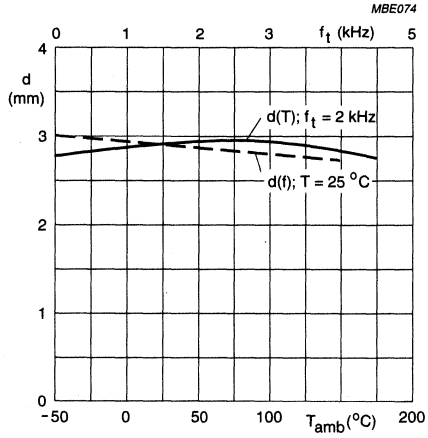

Fig.15 Maximum sensing distance of the KMI15/1 as a function of temperature and tooth frequency.

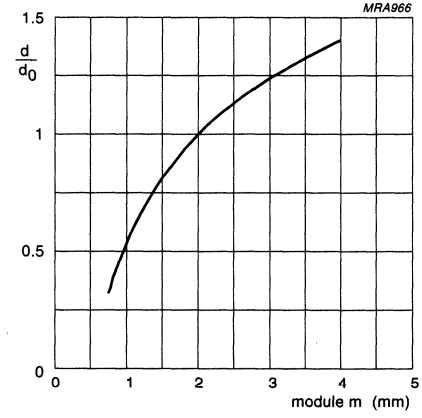

Fig.16 Normalized maximum sensing distance as a function of wheel module.

When mounting the KMI15, there are two important factors to take into consideration:

The angle between the symmetry axes of the sensor and wheel (in the y-z plane)

The horizontal shift 'y' relative to the optimum sensor position.

Both of these values should be minimized. Recommended tolerances for optimal operating conditions are $|\Theta| < 1°$ and $|y| < 0.5$ mm. Their effect is shown in Figs 17 and 18.

A shift in position in the x-direction is not very critical to the KMI15's performance, but the magnet's field component in the x-direction means that an x-shift produces non-symmetrical behaviour (see Fig.19). The optimum position is when x = 0; x should in any case be minimized, especially for small values of 'd'. A tilt in the x-z plane has negligible influence on the optimum sensing distance for angles <4°.

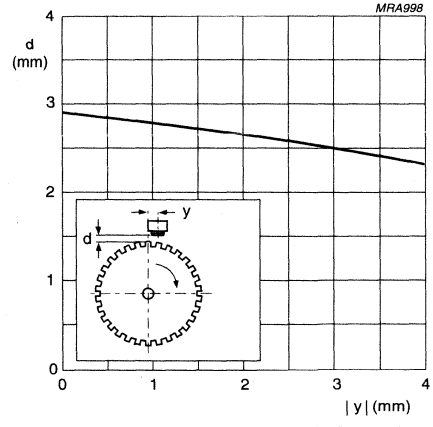

Fig.17 Influence of position tolerance '|y|' on maximum sensing distance 'd' for KMI15/1.

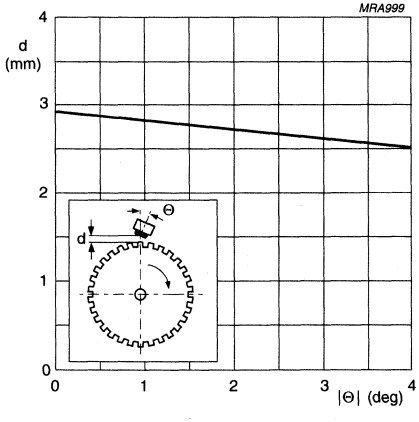

Fig.18 Influence of angular tolerance '|Θ|' on maximum sensing distance 'd' for KMI15/1.

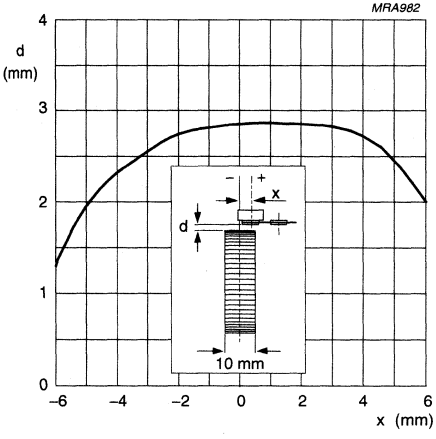

Fig.19 Influence of position tolerance '|x|' on maximum sensing distance 'd' for KMI15/1.

SWITCHING HYSTERESIS

Switching hysteresis is included in the signal conditioning circuitry, to prevent unwanted electrical switching of the KMI15 due to:

Mechanical vibration of the sensor or the gear wheel

Electrical interference (EMC)

Circuit oscillation at very low rotational speeds.

Larger hysteresis provides better immunity to disturbances but also reduces sensing distance 'd', so a compromise is required between hysteresis and sensing distance. The KMI15 sensors have a hysteresis set to ±3 mV and so the maximum attainable distance 'd' will be achieved with a sensor signal level of 6 mV peak-to-peak. Figure 4 shows typical KMZ10B sensor output signal values, with back-biasing magnet), with different target wheel modules and shows clearly that the hysteresis directly determines the usable airgap.

For the KMI15/1, the maximum distance 'd' is always >2.5 mm and is typically up to 2.9 mm; for the KMI15/4, the maximum distance 'd' is >2.0 mm and is typically 2.3 mm (m = 2 mm).

A hysteresis test set-up is shown in Fig.20, together with its test results as a function of distance. This set-up allows simple testing of products and there is a direct correlation between the test results obtained and the equivalent properties of the most commonly-used gear wheels. In the case of a gear wheel with m = 2 mm and a sensor with d = 1.5 mm, expressed in terms of linear movement of a gear tooth the hysteresis corresponds to 0.3 mm. If the gear wheel diameter is 100 mm, this hysteresis is equivalent to a 0.32° ∞rotation. Obviously, these figures will be different for different gear wheels.

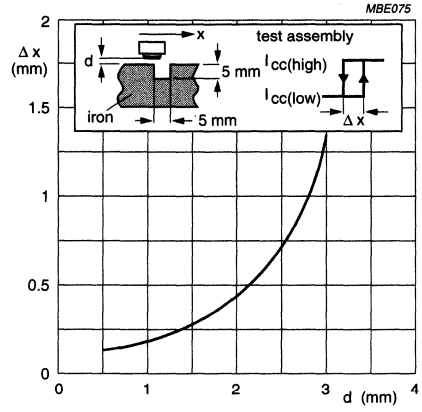

Fig.20 Mechanically measured hysteresis 'x' of the KMI15 as a function of sensing distance 'd' for the test assembly shown.

CHARACTERISTICS OF THE KMI15/X

To determine sensor characteristics in an actual application, the KMI15/4 was used to measure the rotation of a toothed wheel (m α 0.8).

Sensor output

For these measurements, the output signal of the sensor (KMZ10B with a back biasing magnet) was measured with the sensor placed at a distance of 0.5 mm from the wheel, with no signal conditioning. Figure 21 shows the oscilloscope trace obtained from one full revolution of the wheel and the points where the signal shows a peak correspond to missing teeth, due to an effective change in wheel module at these points. Such a well defined trace at the teeth 'holes' demonstrates the intrinsic high sensitivity of the sensor and shows that as well as being able to measure the speed of the wheel, it can also be used to indicate reference marks such as missing teeth (e.g. crankshaft applications) or irregular target structures (e.g. camshaft applications).

Maximum air gap

To be able to define the maximum air gap for a given sensor, it is first necessary to know how the behaviour of the sensor signal changes with measuring distance.

The peak voltage of the output signal, again with no signal conditioning, is shown in Fig.22.

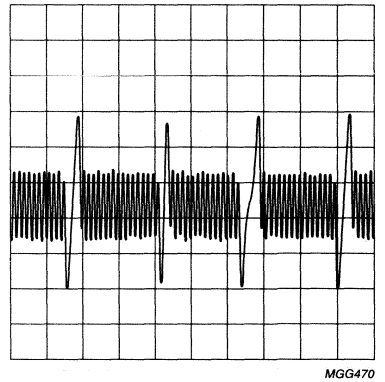

Fig.21 Sensor signal over one revolution.

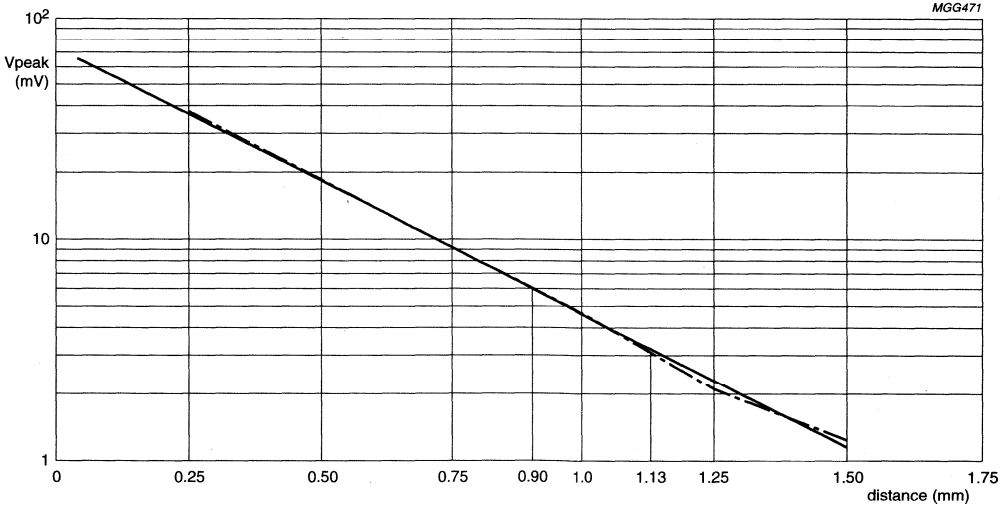

Fig.22 Output signal from a KMZ10B sensor with back-biasing magnet versus distance.

As the hysteresis voltage is set to 6 mV peak-to-peak (3 mV peak), the results show the theoretical maximum air gap is 1.13 mm. However, this does not take into account any eddy currents that may be induced as the wheel rotates, which produce an offset voltage proportional to the speed (for more details, see the section on eddy currents later in this chapter). Taking eddy currents into account, as well as other factors producing offsets such as non-optimal sensor positioning, the maximum permissible air gap is reduced to 0.9 mm.

Eddy currents

The influence of eddy currents was measured by increasing the wheel rotation speed from 500 Hz through to 3000 Hz, with the sensor placed at 0.5 mm from the wheel. From the graph below, the maximum additional speed-dependent offset voltage is determined as approximately ±2.8 mV, with the sign determined by the direction of measurement. If the application requires a large air gap, special attention should be given to the target material and structure to reduce any unwanted influences from eddy currents.

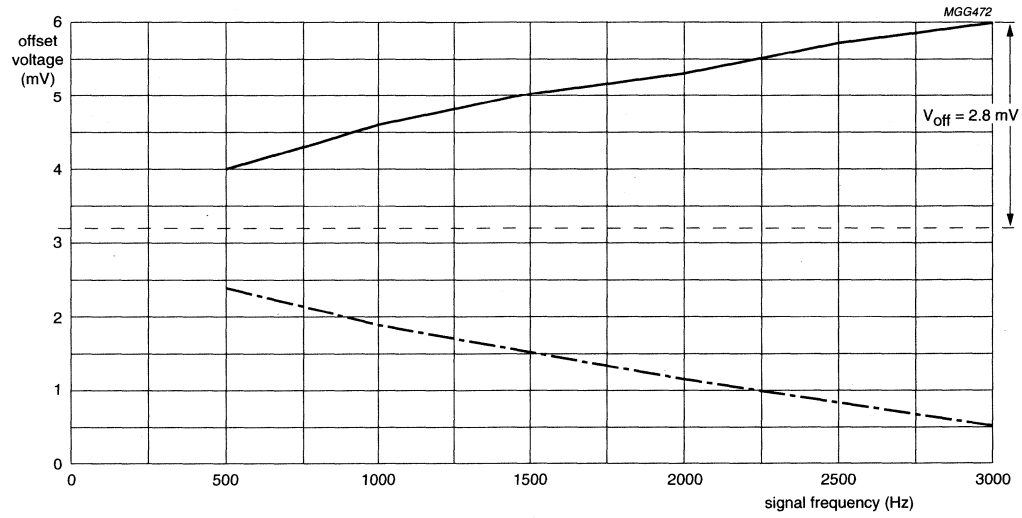

Fig.23 Offset voltage of the KMI15/4 versus frequency, in both directions.

Repeatability

In this test, the speed of the wheel was measured using two sensors: a KMI15/4 in front of the teeth and a reference sensor in front of a small reference (rare earth) magnet placed on the wheel. As it is essential that the measurements are taken on the same tooth, this second sensor is used to trigger the counter at the same moment in every revolution.

One problem in measuring the repeatability of a sensor is that over the length of time taken to make the measurements, the actual velocity of the wheel can vary. This is a basic error within the measurement technique, so the test in fact measures the relative repeatability achievable with the sensor.

Test conditions:

Target RPM (n) = 1000

Sensing distance (d) = 0.5 mm

10 measurements were taken every 4 seconds; the results are tabulated below. From this data an average t_m was calculated.

As shown in the table, during the measurements the motor changed its speed by approximately 0.35%. The result in the last column gives a comparison between the KMI15/4 values and the reference sensor values. The maximum difference between the two sensors is only 0.161‰. This result is also shown in Fig.25.

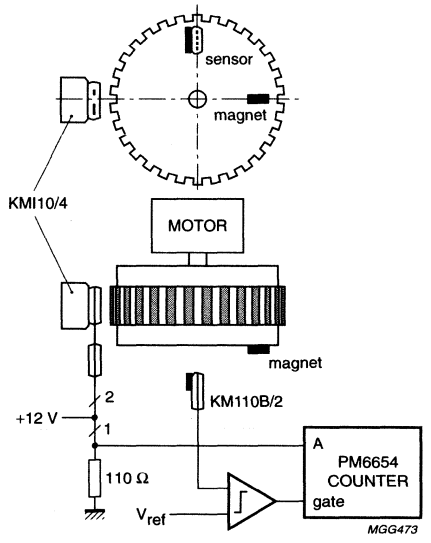

Fig.24 Repeatability measuring arrangement.

Table 2 Repeatability results

MEAS. NO.	KMI 15/4 t KMI (μs)	REFERENCE SENSOR t/t_m (‰)	t/t_m (KMZ) - t/t_m (KM) t KM (ms)
1	840.7	+2.349	60.4563
2	839.6	+0.918	60.3605
3	842.1	+3.898	60.4036
4	841.4	+3.064	60.4931
5	840.4	+1.872	60.4261
6	836.9	−2.301	60.1753
7	835.9	−3.493	60.1042
8	835.3	−4.208	60.0554
9	836.9	−2.301	60.1851
10	839.0	+0.203	60.3283
t_m	838.83		60.31419

Note: to convert tolerance to degrees, the formula was used:

0.01% 83.883 ns 83.883 ns/60.31419 ms × 360 0.0005.

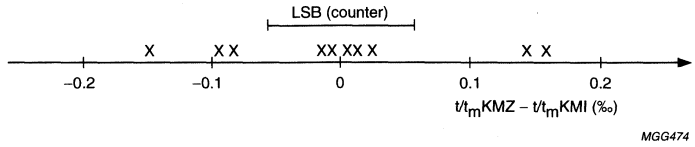

Fig.25 Repeatability of 10 measurements (X).

As shown in the calculation, a tolerance of 0.1‰ equates to 0.005 degrees. So the maximum tolerance and therefore the repeatability of the sensor is better than **0.0008 degrees**.

Due to the effect of the three independent parameters in the test (two sensors and the counter), exact repeatability figures for a single sensor cannot be derived, but what these results clearly show is that the repeatability of the KMI15/4 is much better than the worst result in this particular test.

FUNCTIONAL TESTING OF THE KMI15/1 ROTATIONAL SPEED SENSOR

This was carried out in two steps, testing switching behaviour and sensitivity by electromagnetic stimulation of the device in a Helmholtz coil. The set-up used for the tests, with the direction of the stimulating field parallel to the sensitive direction of the sensor, is shown in Fig.26.

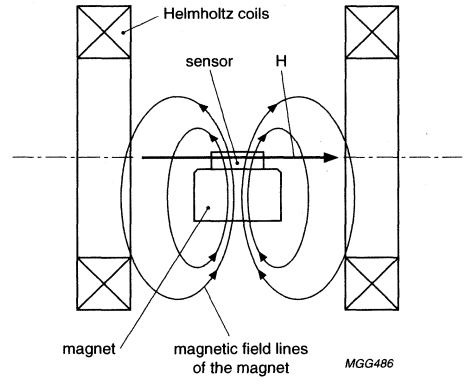

Fig.26 Electromagnetic stimulation of a KMI15/1 sensor.

Control of sensitivity

The measurement of sensitivity (calculating minimum sensing distance) of the KMI15/1 is a more complex operation. Based on the same coil arrangement as shown in Fig.26, the coil and the sensor are linked together as part of an electronic control loop, as shown in Fig.28.

Sensitivity is tested by measuring the minimum magnetic fields (in both the positive and negative rotational directions) required to switch the sensor from a low current state to high and back again. This is done by automatically ramping the magnetic field in the control loop.

The peak-to-peak difference in the minimum magnetic field strength (H_{min}) generates an output voltage when dropped across a magnetoresistive element. This voltage corresponds to the hysteresis voltage V_{hyst} of the Schmitt-trigger circuit in the signal conditioning IC. As the hysteresis voltage is a direct indicator of sensitivity, this test provides a very quick and accurate method for determining the maximum sensing distance (larger distances $H < H_{min}$, smaller distances $H > H_{min}$).

Using a number of gear wheels as test targets, it was found with the samples tested that the maximum sensing distance in rotational directions was d_{max} 2.5 mm (KMI15/1).

Switching behaviour

The magnetic field is switched between $H_{low} = -0.84$ kA/m and $H_{high} = +0.84$ kA/m, causing the KMI15/1 output status to switch low or high and by measuring the output current, it is possible to check the switching behaviour.

With the current switching hysteresis set at 7 mA and 14 mA, the final result showed the high and low current levels to be:

$I_{low} = 7.0 \pm 1.4$ mA

$I_{high} = 14.0 \pm 2.8$ mA,

showing that the switching behaviour is within acceptable parameters for most applications.

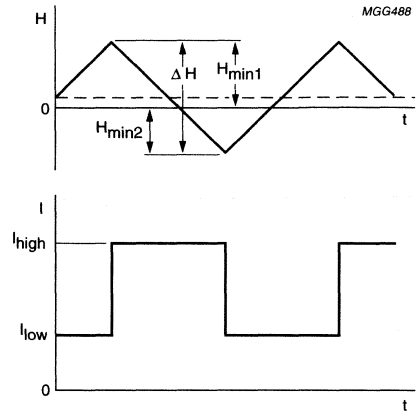

Fig.27 Magnetic field H and current output versus time.

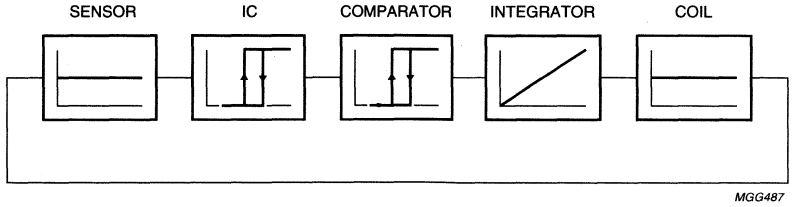

Fig.28 Simplified control loop for sensitivity measurement.

Information for advanced users and applications

DIRECTION DETECTION

All rotational set-ups can be used to measure rotational direction as well as speed, or improve the measurement sensitivity of the set-up, by using two sensors and comparing the phase difference (although the exact set-up will depend on the structure of the target). Three examples are described below:

1. Circuit using two half-bridges of a KMZ10B sensor
2. Dual KMI15/1 with a toothed wheel
3. Dual KMI15/1 with a slotted wheel.

1 "ONE SENSOR SOLUTION"

This concept uses the two magnetoresistive sensor half-bridges in a single KMZ encapsulation. There will be a very small phase difference between the outputs of the two half-bridges when the target wheel turns in front of the sensor and by using separate signal processing for each half, it is possible to indicate direction with only one sensor. As the bridge geometry is fixed within the sensor chip, there is an optimum wheel module but within this constraint, a wide range of wheel pitches is possible. If the target wheel does not have the optimum pitch, the phase difference is not at a maximum and the sensor electronics will have a relatively harder job to produce a clear, well-defined signal. In this case, additional filtering is required. AC coupling is useful, which means the sensor cannot measure down to 0 Hz (as with the dual sensor set-ups described below).

Without filtering, the circuit could indicate zero speed and would be capable of incremental counting, but the operating range would be limited.

2 DUAL KMI15/1 SENSORS WITH A TOOTHED WHEEL

As mentioned, dual sensor set-ups can be used to measure rotational direction as well as speed.

Using two KMI15/1 sensors separated by at least 20 mm and positioned at an angle (not equal to the angle between any two teeth), it is possible to measure the rotational speed and direction of a toothed wheel down to 0 Hz, which cannot be achieved by using two half-bridges. Ideally the phase difference between the outputs should be 90, and the resulting timing of the two output signals indicates direction. This means that the angle between the sensors should be proportional to the angle between two adjacent teeth according to the relationship:

$\alpha = (n + \frac{1}{4})\beta$.

If the distance between the sensors is less than 20 mm, the interaction between the magnets will cause an offset voltage in the sensor bridges, which has the effect of reducing the maximum tooth-to-sensor measuring distance.

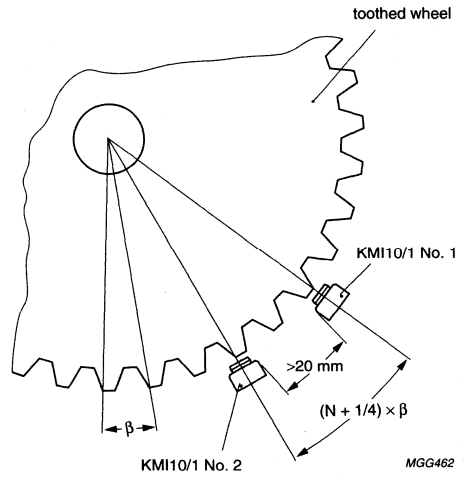

Fig.29 Measurement with toothed wheel.

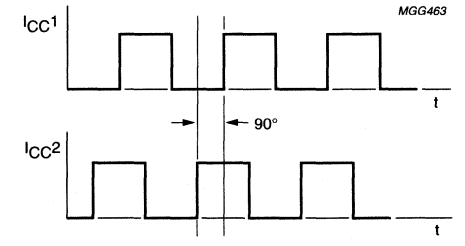

Fig.30 Optimum output signal for clockwise rotation.

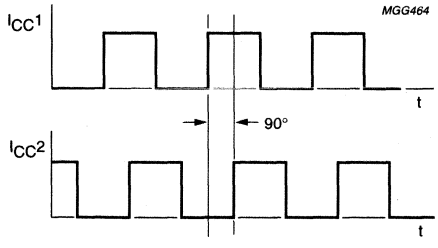

Fig.31 Optimum output signals for anti-clockwise rotation.

3 DUAL KMI15/1 SENSORS WITH A SLOTTED WHEEL

Instead of a toothed wheel, a slotted wheel can be used. In this case the sensors are not mounted in front of the wheel but radially above the surface.

The slotted wheel set-up can be further adapted to allow for sensor-to-sensor distances of less than 20 mm. The sensors are mounted next to each other but with opposite orientations, which reduces the effect of magnetic interaction. With this set-up, tolerances will limit the maximum measuring distance, but it does have the advantage that both sensors could be housed in the same encapsulation, with a single set of conditioning electronics for direction detection, resulting in a simple application design.

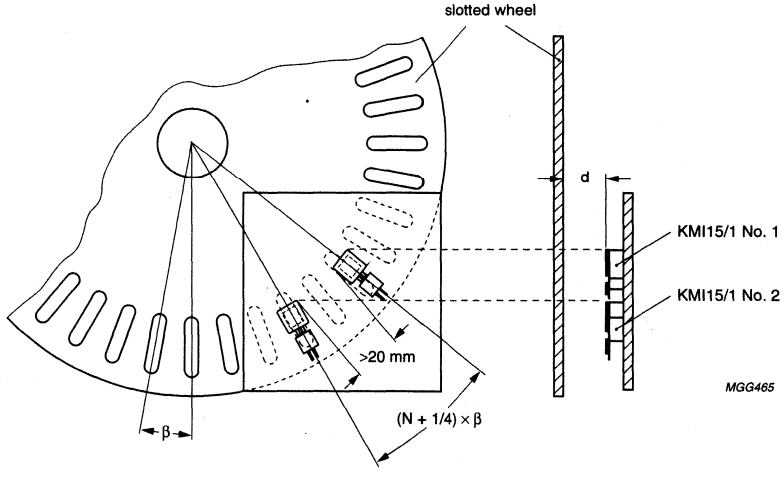

Fig.32 Measurement with slotted wheel.

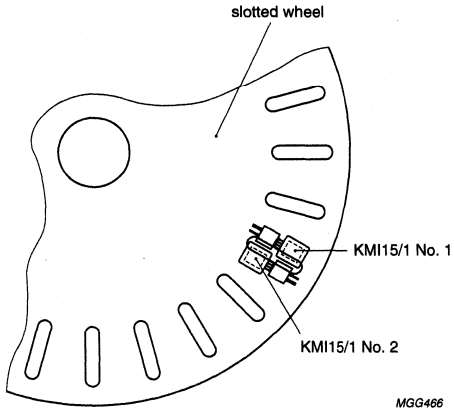

Fig.33 Alternative arrangement with short (<20 mm) sensor-to-sensor distance.

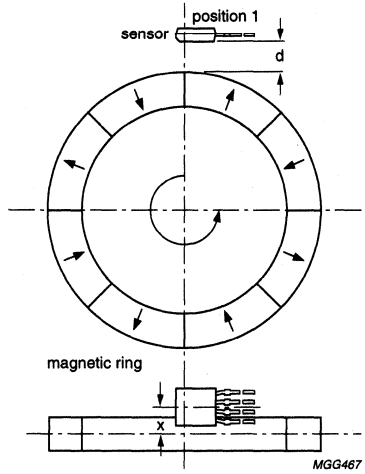

Fig.34 Frequency doubling arrangement using a KMZ10 B sensor.

FREQUENCY DOUBLING

For active targets, magnetic sensors normally output an electrical signal equivalent to the magnetic structure of the multipole rings, with the period of a sensor signal equating to a single magnetic pole pair (N, S). Driving a KMZ10B without an auxiliary magnet and with magnetic fields above about 3 kA/m, effectively doubles the frequency as the magnetic pole pairs deliver two signals in the same period. This is because outside the 'symmetrical' position ($x = 0$ in Fig.34), the magnetic field in the sensor plane describes one full rotation for each pole pair (N, S) passing in front of the sensor and as the sensor is saturated, due to the high magnetic field, the basic $\cos^2$ relationship holds true between the sensor output and the angle of the applied field (see Fig.35). For more details on this, please refer to Appendix 1 on the equations for the magnetoresistive effect and Appendix 2 on sensor flipping.

This improves the resolution of measurements and if the resolution is fixed, allows for magnets with reduced pole numbers.

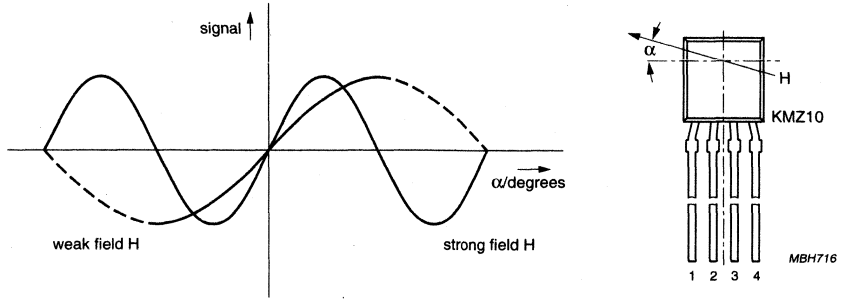

Fig.35 Sensor output with and without bias magnet.

EDDY CURRENTS

As the target rotates in the field of the magnet, eddy currents are induced in the target, according to the target material and rotational speed. These eddy currents themselves generate a magnetic field in addition to the field from the magnet, resulting in an additional offset in sensor output. For standard applications, there is therefore a need for increased hysteresis in the signal conditioning electronics (see Section on "Switching hysteresis" earlier in this chapter). This has an adverse effect on sensor performance in terms of its maximum sensing distance, leading to a reduced airgap, unless it is equipped with a filter.

However, these eddy currents themselves can be used to measure the speed of a metallic, non-ferrous wheel (e.g. copper). The sensor measures the magnetic field produced by the eddy currents induced in the wheel by the auxiliary magnet and increases in the rotational speed are matched by increases in the level of eddy currents. This type of arrangement is suitable for the permanent mounting of a simple tachometer.

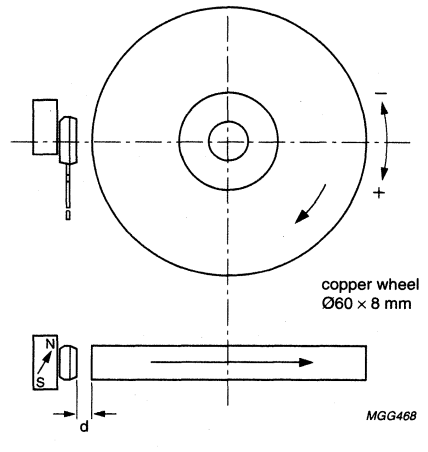

Fig.36 Set-up to measurement RPM using eddy currents.

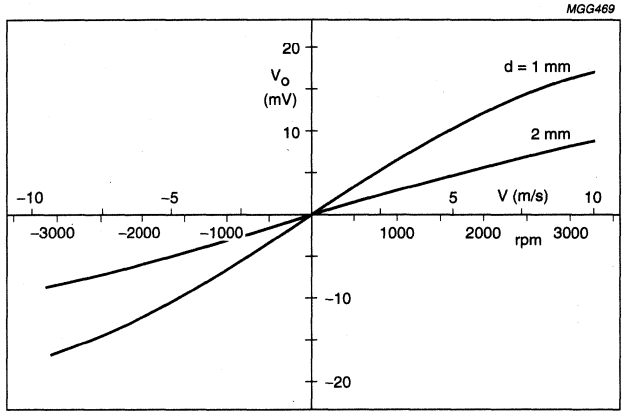

Fig.37 Sensor output versus RPM.

EMC CHARACTERISTICS

Any sensitive electronic system connected to other equipment by unshielded cables, is more susceptible to electromagnetic effects. To determine EM effects on rotational sensors in an ABS system using an unshielded wire 1.5 m in length, two tests were carried out: firstly to determine the influence of the field in a waveguide; and secondly, of a pulse along the cable.

Influence of an electrical field in a waveguide

The unshielded cable is subjected to an electrical field in a waveguide (wave resistance Z_L = 50 Ω). The sensor (EUT1) is located outside the waveguide and connected via the cable to a second electronic device (EUT2) which in turn, is connected to an oscilloscope to enable a functional check of the sensor. The waveguide is powered by a sweep generator connected to a 3 W amplifier and this test signal is checked and monitored at the waveguide input by the second oscilloscope. The quality of the signal from the first oscilloscope indicates any interference from the electrical field.

The following parameters were used in this test:

Unmodulated

frequency range - 10 MHz to 1 GHz

maximum electrical field intensity - E_{max} = 150 V/m.

Amplitude modulated (AM)

percentage modulation - m = 95%

modulation frequency - f_m = 1 kHz

frequency range - 10 MHz to 1 GHz

maximum electrical field intensity - E_{max} = 150 V/m.

Two set-ups had to be used (see Figs 38 and 39) as with frequencies over 200 MHz, the mismatch could no longer be considered negligible. Also, reflected waves between the waveguide and the amplifier were measured using a disconnected directional coupler and were included in the determination of the actual field intensity in the waveguide.

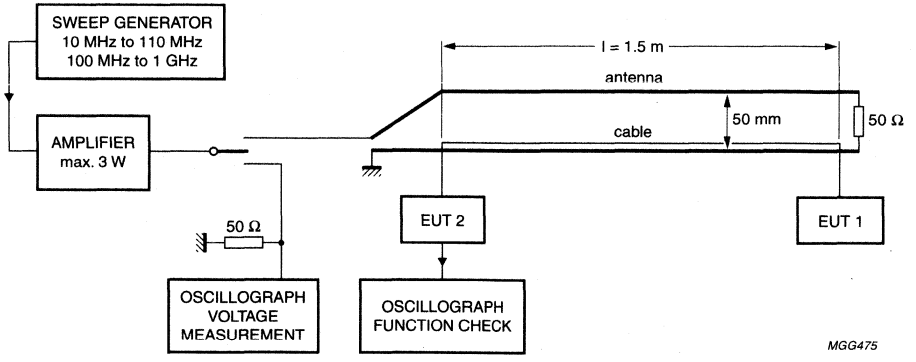

Fig.38 Test set-up with waveguide (antenna) for 10 MHz f 200 MHz.

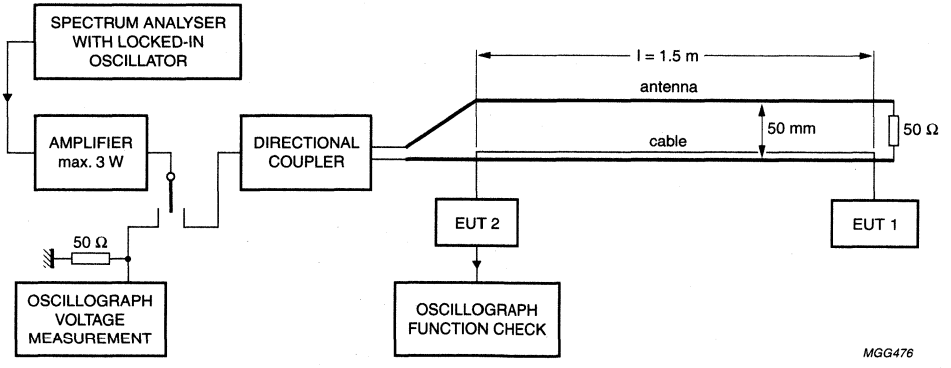

Fig.39 Test set-up with waveguide (antenna) for 200 MHz f 1 GHz.

No undesirable effects were observed on the sensor signal and therefore the system has the required resistance to electromagnetic interference. Also, a destructive test was carried out on the sensor and with field intensities up to E_{max} = 300 V/m throughout the frequency range, no destructive or irreversible changes in the sensor parameters occurred.

Influence of pulse along a cable

Using the following test circuit for the sensor, with the connection points for the test pulse and current measurement points as indicated, the currents i_2, i_3 and i_4 were measured using passive current sensors and a 400 MHz storage oscilloscope. Here the value $i_2(t)$ represents the time variation of the test pulse at the connection point.

The response behaviour to the input test pulse (i_2) is measured under least favourable conditions with low impedance grounding of the earth connection at the sensor output, resulting in higher values of i_{4max} than normally experienced. Figure 41a shows the test pulse $i_2(t)$ with a rise time of approximately 15 ns and a peak value of i_{2max} = 4000 mA.

The currents $i_3(t)$ and $i_4(t)$ clearly show an oscillation where the following peak values were obtained.

i_{3max} = 18 mA

i_{4max} = 2.2 mA

On the basis of i_{4max} = 2.2 mA and R = 115 Ω, then the voltage V_R (see Fig.41) is 253 mV. This voltage is at the input of the RC low-pass filter (R = 1.3 kΩ, C = 47 nF) which has a 3 dB cut-off frequency of f_g = 2.6 kHz. According to Fig.40, the period for i_4 to die away is approximately 16 ns, i.e. a frequency f = 62.5 MHz. This means that the distance between f and f_g is more than four decades and therefore, at 20 dB/decade (ideal low-pass), a distance of approximately 80 dB between V_R and V_T, where V_T represents the input voltage at the trigger unit (Z_T = 100 kΩ).

This clearly gives a value for V_T which is well below the required limit.

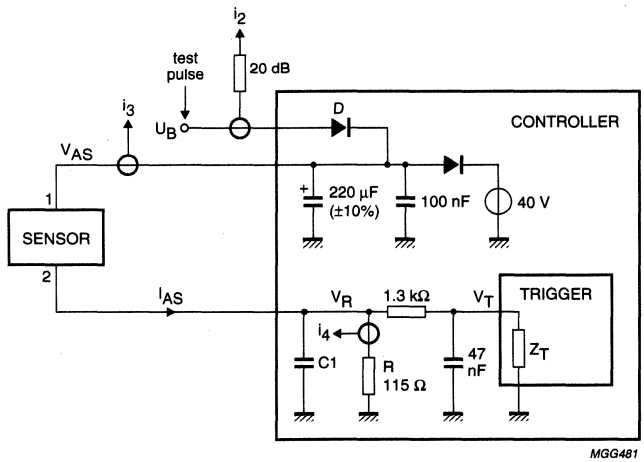

Fig.40 Pulse test circuit diagram for hybrid sensor.

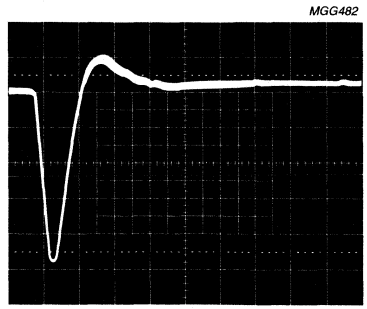

(a)

a. Test pulse I_2.

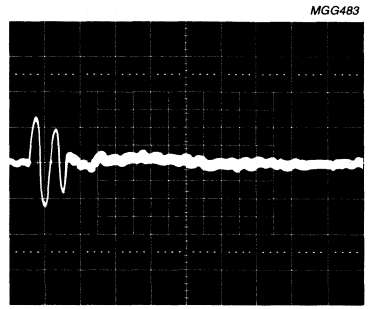

(b)

b. Test pulse I_3.

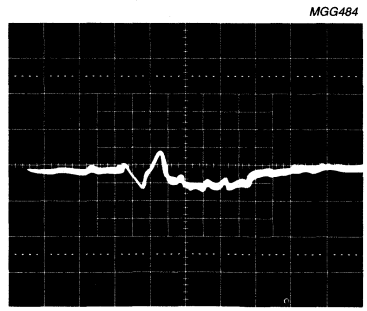

(c)

c. Test pulse I_4.

Fig.41 Oscilloscope traces showing.

DEVICE DATA

in alphanumeric sequence

Integrated rotational speed sensor KMI15/1

FEATURES

- Digital current output signal
- Zero speed capability
- Wide air gap
- Wide temperature range
- Insensitive to vibration
- EMC resistant.

DESCRIPTION

The KMI15/1 sensor detects rotational speed of ferrous gear wheels and reference marks(1).
The sensor consists of a magnetoresistive sensor element, a signal conditioning integrated circuit in bipolar technology and a magnetized ferrite magnet.
The frequency of the digital current output signal is proportional to the rotational speed of a gear wheel.

CAUTION
Do not press two or more products together against their magnetic forces.

(1) The sensor contains a customized integrated circuit. Usage in hydraulic brake systems and in systems with active brake control is forbidden.

PINNING

PIN	DESCRIPTION
1	V_{CC}
2	V–

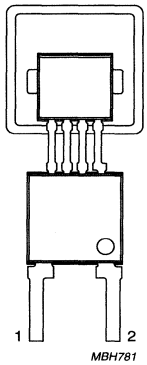

Fig.1 Simplified outline (SOT453B).

QUICK REFERENCE DATA

SYMBOL	PARAMETER	MIN.	TYP.	MAX.	UNIT
V_{CC}	DC supply voltage	–	12	–	V
$I_{CC\ (low)}$	current output signal low	–	7	–	mA
$I_{CC\ (high)}$	current output signal high	–	14	–	mA
d	sensing distance	0 to 2.5	0 to 2.9	–	mm
f_t	operating tooth frequency	0	–	25000	Hz
T_{amb}	ambient operating temperature	–40	–	+85	°C

LIMITING VALUES

In accordance with Absolute Maximum Rating System (IEC 134).

SYMBOL	PARAMETER	CONDITIONS	MIN.	MAX.	UNIT
V_{CC}	DC supply voltage	T_{amb} = –40 to +85 °C; R_L = 115 Ω	–0.5	+16	V
T_{stg}	storage temperature		–40	+150	°C
T_{amb}	ambient operating temperature		–40	+85	°C
T_{sld}	soldering temperature	t ≤ 10 s	–	260	°C
	output short-circuit duration to GND		continuous		

CHARACTERISTICS

T_{amb} = 25 °C; V_{CC} = 12 V; d = 2.1 mm; f_t = 2 kHz; test circuit: see Fig.7; R_L = 115 Ω; sensor positioning: see Fig.15; gear wheel: module 2 mm; material 1.0715; unless otherwise specified.

SYMBOL	PARAMETER	CONDITIONS	MIN.	TYP.	MAX.	UNIT
$I_{CC\ (low)}$	current output signal low	see Figs 6 and 8	5.6	7	8.4	mA
$I_{CC\ (high)}$	current output signal high	see Figs 6 and 8	11.2	14	16.8	mA
t_r	output signal rise time	C_L = 100 pF; see Fig.9; 10 to 90% value	–	0.5	–	µs
t_f	output signal fall time	C_L = 100 pF; see Fig.9; 10 to 90% value	–	0.7	–	µs
t_d	switching delay time	between stimulation pulse (generated by a coil) and output signal	–	1	–	µs
f_t	operating tooth frequency	for both rotation directions	0	–	25000	Hz
d	sensing distance	see Fig.15 and note 1	0 to 2.5	0 to 2.9	–	mm
δ	duty cycle	see Fig.6	30	50	70	%

Note

1. High rotational speeds of wheels reduce the sensing distance due to eddy current effects (see Fig.17).

FUNCTIONAL DESCRIPTION

The KMI15/1 sensor is sensitive to the motion of ferrous gear wheels or reference marks. The functional principle is shown in Fig.3. Due to the effect of flux bending, the different directions of magnetic field lines in the magnetoresistive sensor element will cause an electrical signal. Because of the chosen sensor orientation and the direction of ferrite magnetization, the KMI15/1 is sensitive to movement in the 'y' direction in front of the sensor only (see Fig.2).

The magnetoresistive sensor element signal is amplified, temperature compensated and passed to a Schmitt trigger in the conditioning integrated circuit (Figs 4 and 5).
The digital output signal level (see Fig.6) is independent of the sensing distance within the measuring range (Fig.14).
A (2-wire) output current enables safe transfer of the sensor signal to the detecting circuit (see Fig.7).
The integrated circuit housing is separated from the sensor element housing to optimize the sensor behaviour at high temperatures.

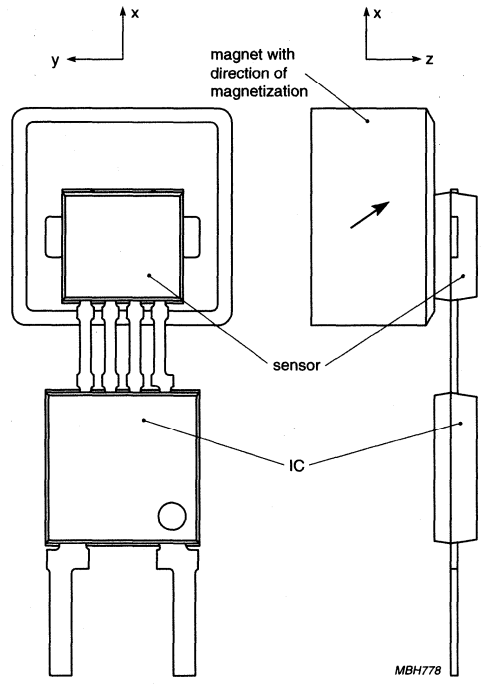

Fig.2 Component detail of the KMI15/1.

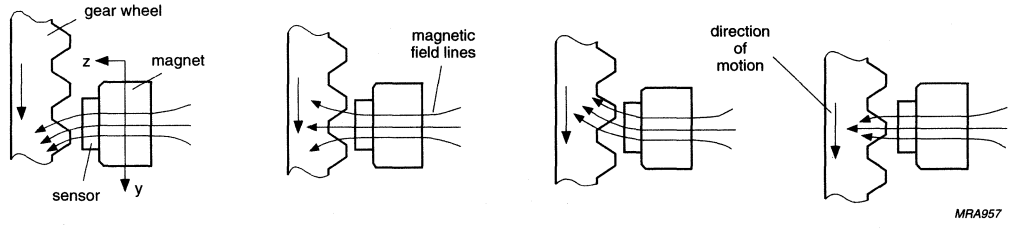

Fig.3 Functional principle.

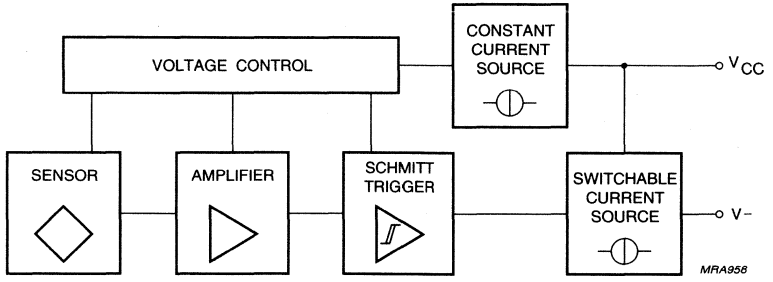

Fig.4 Block diagram.

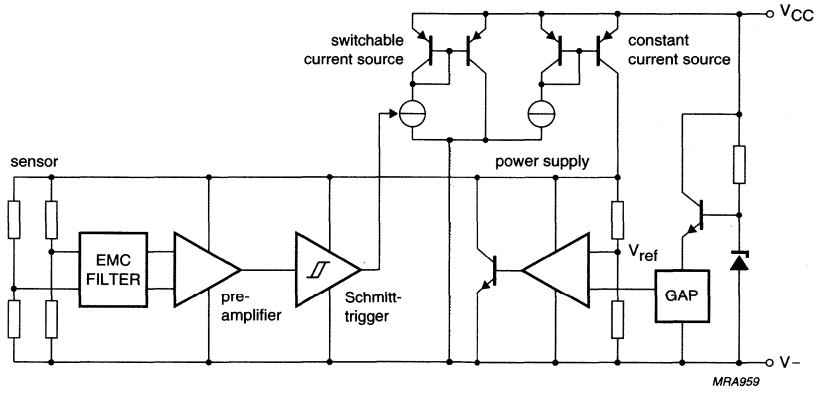

Fig.5 Simplified circuit diagram.

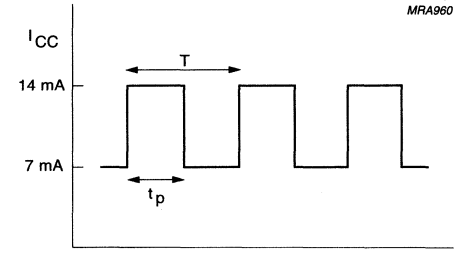

$$\delta = \frac{t_p}{T} \times 100\%$$

Fig.6 Output signal as a function of time.

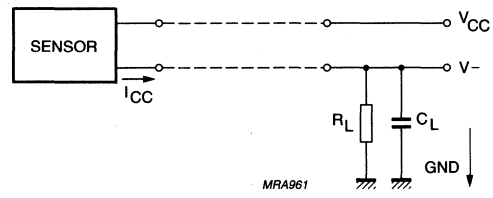

Fig.7 Test and application circuit.

APPLICATION INFORMATION

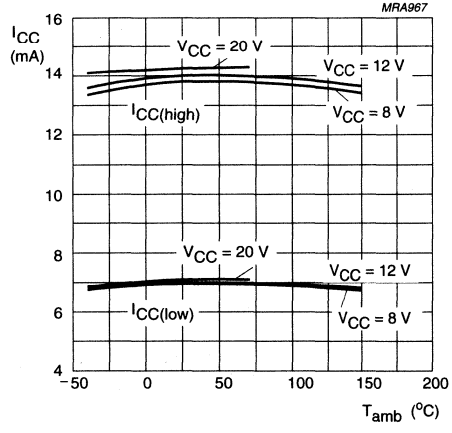

Fig.8 Output current levels as functions of ambient temperature; typical values.

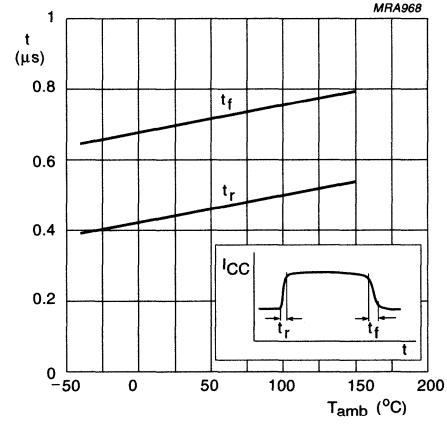

V_{CC} = 12 V; C_L = 100 pF; R_L = 115 Ω.

Fig.9 Output current switching times as functions of ambient temperature; typical values.

Mounting conditions

The recommended sensor position in front of a gear wheel is shown in Fig.15. The distance 'd' is measured between the sensor front and the tip of a gear wheel tooth.
The KMI15/1 senses ferrous indicators like gear wheels in the ± y direction only (no rotational symmetry of the sensor); see Fig.2. The effect of incorrect mounting positions on sensing distance is shown in Figs 11, 12 and 13. The symmetrical reference axis of the sensor corresponds to the axis of the ferrite magnet.

Environmental conditions

Due to eddy current effects the sensing distance depends on the tooth frequency (Fig.17). The influence of gear wheel module on the sensing distance is shown in Fig.16.

Gear Wheel Dimensions

SYMBOL	DESCRIPTION	UNIT
German DIN		
z	number of teeth	
d	diameter	mm
m	module m = d/z	mm
p	pitch p = π × m	mm
ASA; note1		
PD	pitch diameter (d in inch)	inch
DP	diametric pitch DP = z/PD	$inch^{-1}$
CP	circular pitch CP = π/DP	inch

Note

1. For conversion from ASA to DIN: m = 25.4 mm/DP; p = 25.4 mm × CP.

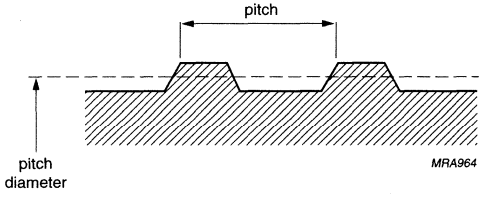

$$\text{module} = \frac{\text{pitch diameter}}{\text{number of teeth}}$$

$$\text{pitch} = \text{module} \times \pi$$

Fig.10 Gear wheel dimensions.

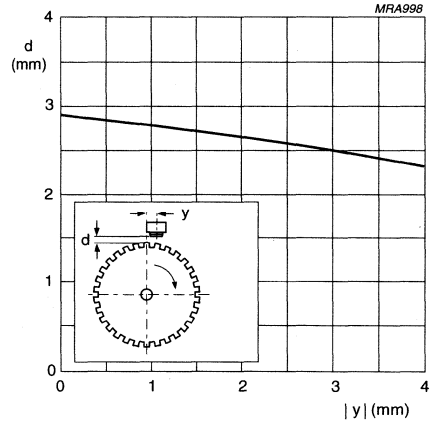

V_{CC} = 12 V; f_t = 2 kHz; module = 2 mm; pitch diameter = 100 mm.

Fig.11 Sensing distance as a function of positional tolerance in the y-axis; typical values.

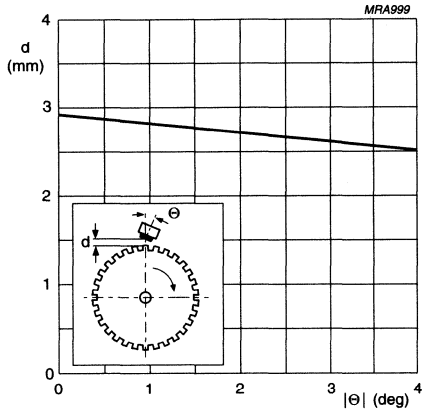

V_{CC} = 12 V; f_t = 2 kHz; module = 2 mm.

Fig.12 Sensing distance as a function of positional tolerance; typical values.

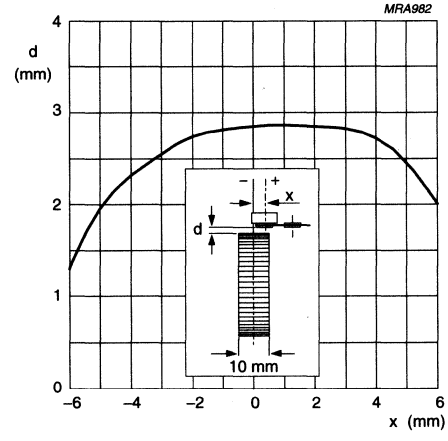

V_{CC} = 12 V; f_t = 2 kHz; module = 2 mm.

Fig.13 Sensing distance as a function of positional tolerance in the x-axis; typical values.

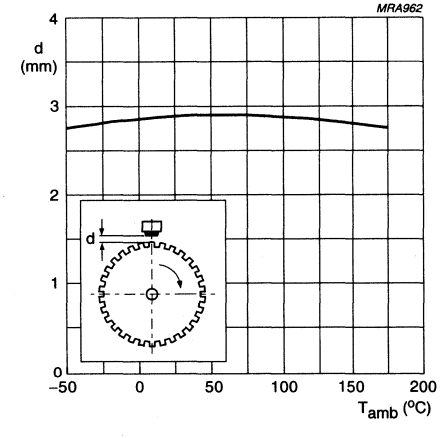

V_{CC} = 12 V; f_t = 2 kHz; module = 2 mm.

Fig.14 Sensing distance as a function of ambient temperature; typical values.

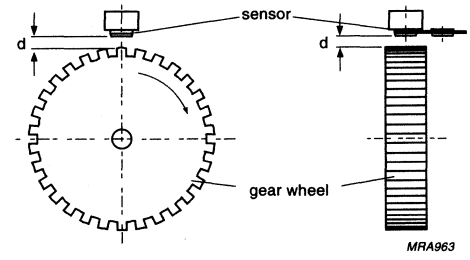

Fig.15 Sensor positioning.

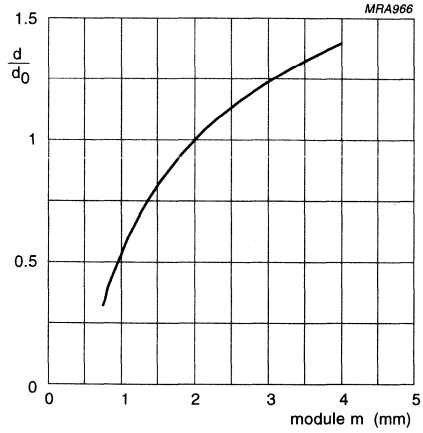

d_o = measuring distance for a gear wheel with module m = 2 mm.

Fig.16 Normalized maximum sensing distance as a function of gear wheel module; typical values.

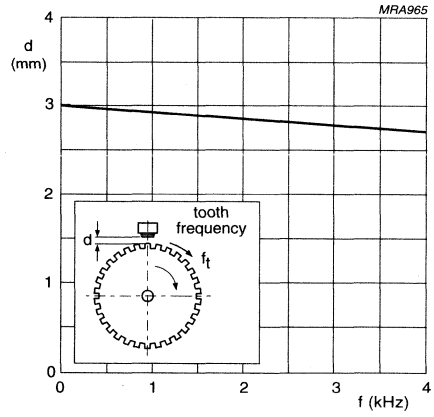

V_{CC} = 12 V; module = 2 mm.

Fig.17 Sensing distance as a function of tooth frequency; typical values.

EMC

Figure 18 shows a recommended application circuit for automotive applications (wheel sensing f_t < 5 kHz). It provides a protection interface to meet Electromagnetic Compatibility (EMC) standards and safeguard against voltage spikes. Table 1 lists the tests which are applicable to this circuit and the achieved class of functional status. Protection against 'load dump' (test pulse 5 according to *"DIN 40839"*) means a very high demand on the protection circuit and requires a suitable suppressor diode with sufficient energy absorption capability.

The board net often contains a central load dump protection that makes such a device in the protection circuit of the sensor module unnecessary.

Tests for electrostatic discharge (ESD) were conducted in line with *"IEC 801-2"* to demonstrate the KMI15/1's handling capabilities. The *"IEC 801-2"* test conditions were: C = 150 pF, R = 150 Ω, V = 2 kV.

Electromagnetic disturbances with fields up to 150 V/m and f = 1 GHz (ref. *"DIN 40839"*) have no influence on performance.

Table 1 EMC test results

EMC REF. DIN 40839	SYMBOL	MIN. (V)	MAX. (V)	REMARKS	CLASS
Test pulse 1	V_{LD}	−100	–	t_d = 2 ms	C
Test pulse 2	V_{LD}	–	100	t_d = 0.2 ms	A
Test pulse 3a	V_{LD}	−150	–	t_d = 0.1 µs	A
Test pulse 3b	V_{LD}	–	100	t_d = 0.1 µs	A
Test pulse 4	V_{LD}	−7	–	t_d = 130 ms	B
Test pulse 5	V_{LD}	–	120	t_d = 400 ms	B

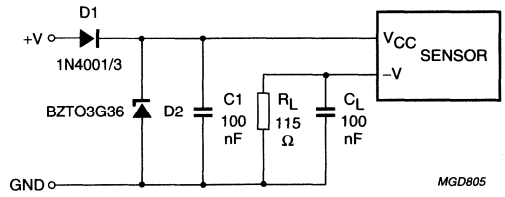

Fig.18 Test/application circuit for the KMI15/1.

PACKAGE OUTLINE

Plastic single-ended combined package; magnetoresistive sensor element; bipolar IC; magnetized ferrite magnet (8.0 x 8.0 x 4.5 mm); 2 in-line leads **SOT453B**

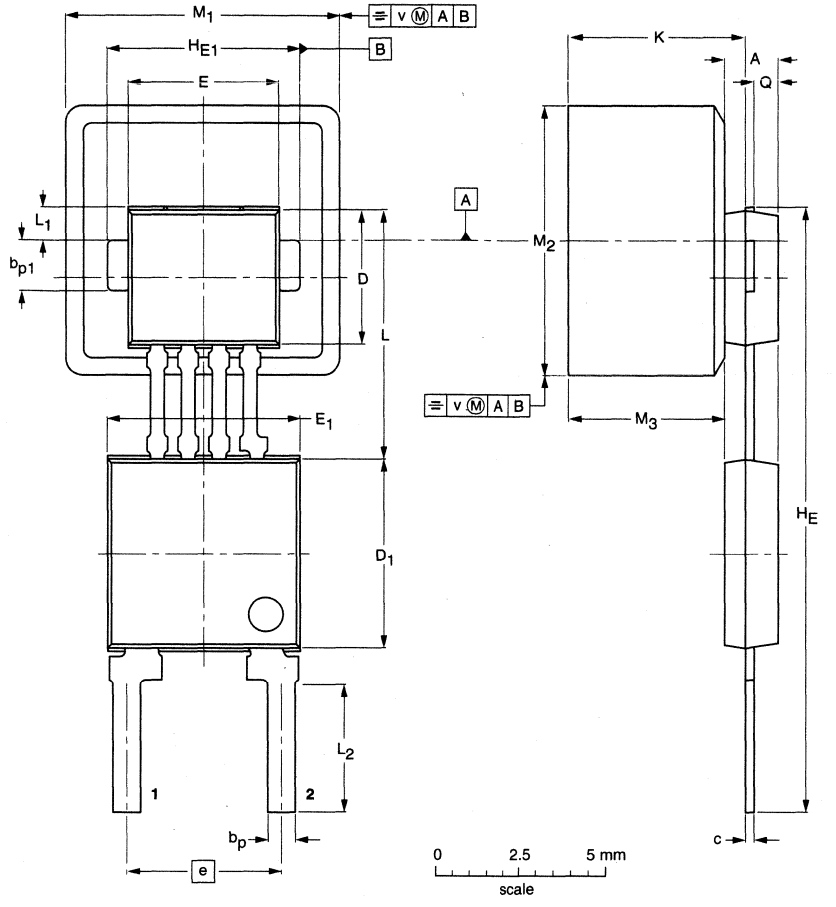

DIMENSIONS (mm are the original dimensions)

UNIT	A	b_p	b_{p1}	c	$D^{(1)}$	$D_1{}^{(1)}$	$E^{(1)}$	$E_1{}^{(1)}$	e	H_E	H_{E1}	K max.	L	L_1	L_2	M_1	M_2	M_3	Q	v
mm	1.7 1.4	0.8 0.7	1.5 1.4	0.3 0.24	4.1 3.9	5.7 5.5	4.5 4.3	5.7 5.5	4.6 4.4	18.2 17.8	5.6 5.5	5.37	7.55 7.25	1.2 0.9	3.9 3.5	8.15 7.85	8.15 7.85	4.7 4.3	0.75 0.65	0.25

Note

1. Plastic or metal protrusions of 0.15 mm maximum per side are not included.

OUTLINE VERSION	REFERENCES				EUROPEAN PROJECTION	ISSUE DATE
	IEC	JEDEC	EIAJ			
SOT453B						~~97-02-28~~ 98-03-26

Integrated rotational speed sensor KMI15/2

FEATURES

- Digital current output signal
- Zero speed capability
- Wide air gap
- Wide temperature range
- Insensitive to vibration
- EMC resistant.

DESCRIPTION

The KMI15/2 sensor detects (rotational) speed and reference mark detection of magnetized targets(1). The sensor consists of a magnetoresistive sensor element, a signal conditioning integrated circuit in bipolar technology and a magnetized ferrite magnet. The frequency of the digital current output signal is proportional to the rotational speed of a gear wheel.

CAUTION
Do not press two or more products together against their magnetic forces.

(1) The sensor contains a customized integrated circuit. Usage in hydraulic brake systems and in systems with active brake control is forbidden.

PINNING

PIN	DESCRIPTION
1	V_{CC}
2	V–

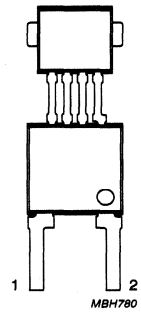

Fig.1 Simplified outline; (SOT453A).

QUICK REFERENCE DATA

SYMBOL	PARAMETER	MIN.	TYP.	MAX.	UNIT
V_{CC}	DC supply voltage	0.5	12	16	V
$I_{CC\ (low)}$	current output signal low	–	7	–	mA
$I_{CC\ (high)}$	current output signal high	–	14	–	mA
f_t	operating frequency	0	–	25000	Hz
T_{amb}	ambient operating temperature	–40	–	+85	°C

LIMITING VALUES

In accordance with Absolute Maximum Rating System (IEC 134).

SYMBOL	PARAMETER	CONDITIONS	MIN.	MAX.	UNIT
V_{CC}	DC supply voltage	T_{amb} = −40 to +85 °C; R_L = 115 Ω	0.5	16	V
T_{stg}	storage temperature		−40	+150	°C
T_{amb}	operating ambient temperature		−40	+85	°C
T_{sld}	soldering temperature	t ≤ 10 s	–	260	°C
	output short-circuit duration to GND		continuous		

CHARACTERISTICS

T_{amb} = 25 °C; V_{CC} = 12 V; f_t = 2 kHz; test circuit: see Fig.7; R_L = 115 Ω.

SYMBOL	PARAMETER	CONDITIONS	MIN.	TYP.	MAX.	UNIT
$I_{CC\ (low)}$	current output signal low	see Fig.6	5.6	7.0	8.4	mA
$I_{CC\ (high)}$	current output signal high	see Fig.6	11.2	14.0	16.8	mA
t_r	output signal rise time	C_L = 100 pF; 10 to 90% value	–	0.5	–	µs
t_f	output signal fall time	C_L = 100 pF; 10 to 90% value	–	0.7	–	µs
t_d	switching delay time	between stimulation pulse (generated by a coil) and output signal	–	1	–	µs
f_t	operating frequency	for both rotation directions	0	–	25000	Hz
Hs_{LH}	magnetic switching field strength		0.05	0.3	0.8	kA/m
Hs_{HL}	magnetic switching field strength		0.05	0.3	0.8	kA/m
Hs	magnetic switching hysteresis		0.15	–	1.6	kA/m

FUNCTIONAL DESCRIPTION

The KMI15/2 sensor is sensitive to magnetic fields. The functional principle is shown in Fig.3. The field lines of a magnetized target are shown in Fig.3 as a straight target (it could also be circular e.g. for rotational speed measurement). If a sensor KMI15/2 is moved as shown in this field, either of the magnetic field components Hs_{HL} or Hs_{LH} is dominant, and forces the sensor to switch to either the high current (14 mA) or to the low current (7 mA). Oscillation of the sensor output signal is avoided by the implementation of a hysteresis into the signal conditioning electronic.

The MR sensor is stabilized by a permanent magnet applying a continuous magnetic field of ≥6 kA/m to the sensor. If the magnetic field given by the magnetized target errors like frequency doubling might occur. The magnetoresistive sensor element signal is amplified, temperature compensated and forwarded to a Schmitt-trigger in the conditioning integrated circuit (Figs 4 and 5). The digital output signal levels (Fig.6) are independent of the magnetic field condition. A (2-wire) output current enables safe transfer of the sensor signal to the detecting circuit (Fig.7). The integrated circuit housing is separated from the sensor element housing to optimize the sensor behaviour at high temperatures.

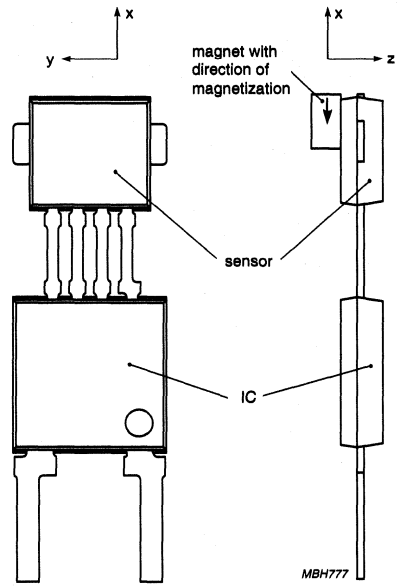

Fig.2 Component detail of the KMI15/2.

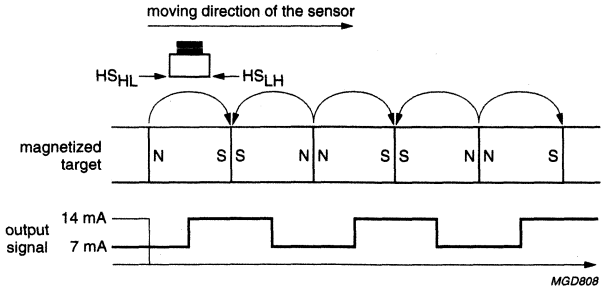

Fig.3 Functional principle of KMI15/2.

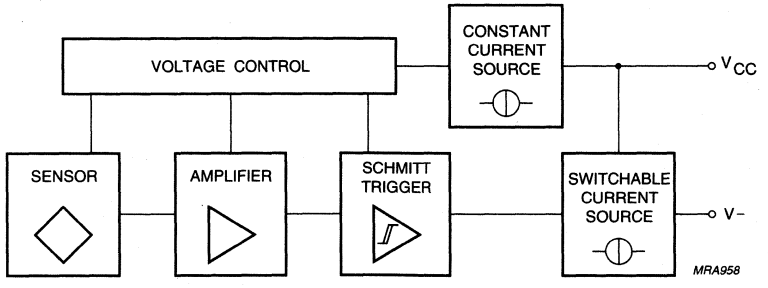

Fig.4 Block diagram.

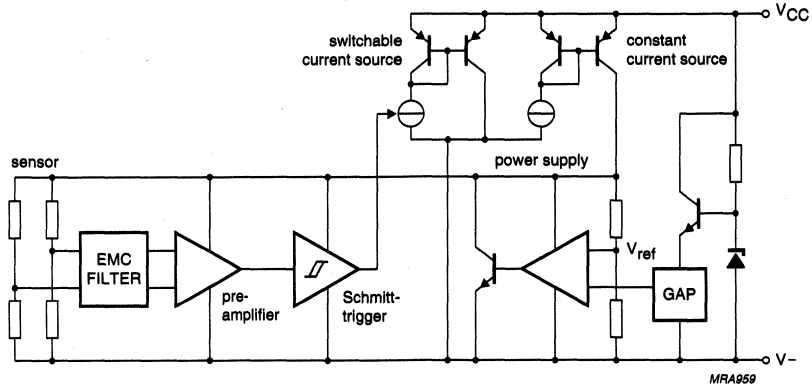

Fig.5 Simplified circuit diagram.

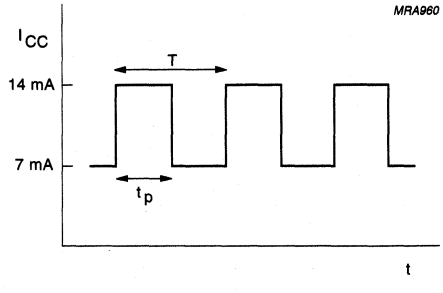

$$\delta = \frac{t_p}{T} \times 100\%$$

Fig.6 Output signal as a function of time.

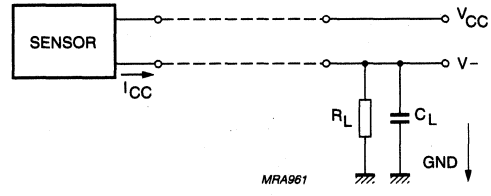

Fig.7 Test and application circuit.

PACKAGE OUTLINE

Plastic single-ended combined package; magnetoresistive sensor element; bipolar IC; magnetized ferrite magnet (3.8 x 2.0 x 0.8 mm); 2 in-line leads **SOT453A**

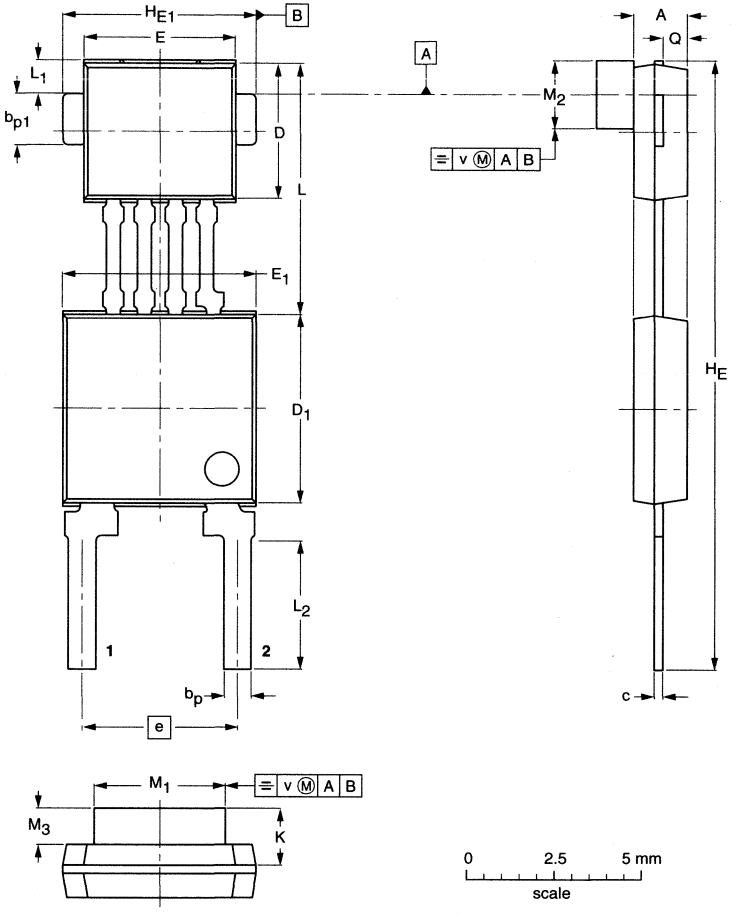

DIMENSIONS (mm are the original dimensions)

UNIT	A	b_p	b_{p1}	c	$D^{(1)}$	$D_1{}^{(1)}$	$E^{(1)}$	$E_1{}^{(1)}$	e	H_E	H_{E1}	K max.	L	L_1	L_2	M_1	M_2	M_3	Q	v
mm	1.7 1.4	0.8 0.7	1.5 1.4	0.3 0.24	4.1 3.9	5.7 5.5	4.5 4.3	5.7 5.5	4.6 4.4	18.2 17.8	5.6 5.5	1.67	7.55 7.25	1.2 0.9	3.9 3.5	3.9 3.7	2.1 1.9	0.9 0.75	0.75 0.65	0.25

Note

1. Plastic or metal protrusions of 0.15 mm maximum per side are not included.

OUTLINE VERSION	REFERENCES				EUROPEAN PROJECTION	ISSUE DATE
	IEC	JEDEC	EIAJ			
SOT453A						~~97-02-28~~ 98-03-26

Rotational speed sensor KMI15/4

FEATURES

- Digital current output signal
- Zero speed capability
- Wide air gap
- Wide temperature range
- Vibration insensitive
- EMC resistant.

DESCRIPTION

The KMI15/4 sensor detects rotational speed of ferrous gear wheels and reference marks(1).
The sensor consists of a magnetoresistive sensor element, a signal conditioning integrated circuit in bipolar technology and a ferrite magnet. The frequency of the digital current output signal is proportional to the rotational speed of a gear wheel.

CAUTION
Do not press two or more products together against their magnetic forces.

(1) The sensor contains a customized integrated circuit. Usage in hydraulic brake systems and in systems with active brake control is forbidden.

PINNING

PIN	DESCRIPTION
1	V_{CC}
2	V–

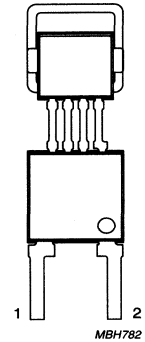

Fig.1 Simplified outline (SOT453C).

QUICK REFERENCE DATA

SYMBOL	PARAMETER	MIN.	TYP.	MAX.	UNIT
V_{CC}	DC supply voltage	–	12	–	V
T_{amb}	ambient operating temperature	–40	–	+85	°C
$I_{CC\ (low)}$	current output signal low	–	7	–	mA
$I_{CC\ (high)}$	current output signal high	–	14	–	mA
f_t	operating tooth frequency	0	–	25000	Hz
d	sensing distance	0 to 2.0	0 to 2.3	–	mm

LIMITING VALUES

In accordance with Absolute Maximum Rating System (IEC 134).

SYMBOL	PARAMETER	CONDITIONS	MIN.	MAX.	UNIT
V_{CC}	DC supply voltage	T_{amb} = −40 to +85 °C; R_L = 115 Ω	−0.5	+16	V
T_{stg}	storage temperature		−40	+150	°C
T_{amb}	operating ambient temperature		−40	+85	°C
T_{sld}	soldering temperature	t ≤ 10 s	–	260	°C
	output short-circuit duration to GND		continuous		

CHARACTERISTICS

T_{amb} = 25 °C; V_{CC} = 12 V; d = 1.5 mm; f_t = 2 kHz; test circuit: see Fig.7; R_L = 115 Ω; sensor positioning: see Fig.15; gear wheel: module 2 mm; material 1.0715; unless otherwise specified.

SYMBOL	PARAMETER	CONDITIONS	MIN.	TYP.	MAX.	UNIT
$I_{CC\ (low)}$	current output signal low	see Figs 6 and 8	5.6	7	8.4	mA
$I_{CC\ (high)}$	current output signal high	see Figs 6 and 8	11.2	14	16.8	mA
t_r	output signal rise time	C_L = 100 pF; see Fig.9; 10 to 90% value	–	0.5	–	µs
t_f	output signal fall time	C_L = 100 pF; see Fig.9; 10 to 90% value	–	0.7	–	µs
t_d	switching delay time	between stimulation pulse (generated by a coil) and output signal	–	1	–	µs
f_t	operating tooth frequency	for both rotation directions	0	–	25000	Hz
d	sensing distance	see Fig.15 and note 1	0 to 2.0	0 to 2.3	–	mm
δ	duty cycle	see Fig.6	20	50	80	%

Note

1. High rotational speeds of wheels reduce the sensing distance due to eddy current effects (see Fig.17).

FUNCTIONAL DESCRIPTION

The KMI15/4 sensor is sensitive to the motion of ferrous gear wheels or reference marks. The functional principle is shown in Fig.3. Due to the effect of flux bending, the different directions of magnetic field lines in the magnetoresistive sensor element will cause an electrical signal. Because of the chosen sensor orientation and the direction of ferrite magnetization, the KMI15/4 is sensitive to movement in the 'y' direction in front of the sensor only (see Fig.2).

The magnetoresistive sensor element signal is amplified, temperature compensated and passed to a Schmitt-trigger in the conditioning integrated circuit (Figs 4 and 5). The digital output signal level (see Fig.6) is at a fixed level independent of the sensing distance. A (2-wire) output current enables safe sensor signal transport to the detecting circuit (see Fig.7). The integrated circuit housing is separated from the sensor element housing to optimize the sensor behaviour at high temperatures.

The strength of the magnetic field caused by the Ferroxdure 100 magnet in the different sensor directions, measured at the centre of the magnetoresistive bridge, is typically: H_x = 7 kA/m (auxiliary field) and H_z = 17 kA/m (perpendicular to the sensor surface). H_y is zero due to the trimming process.

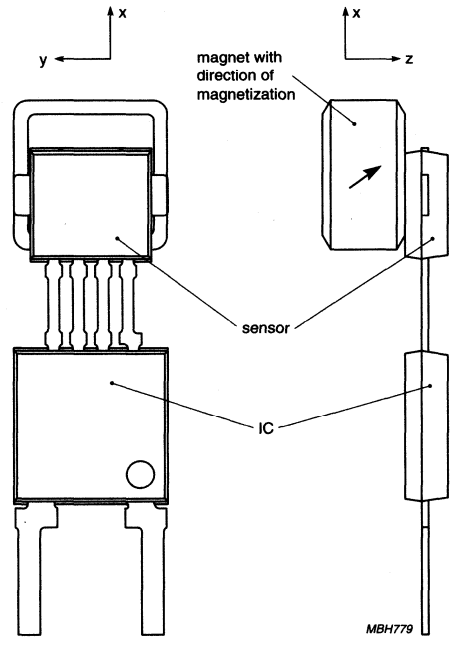

Fig.2 Component detail of the KMI15/4.

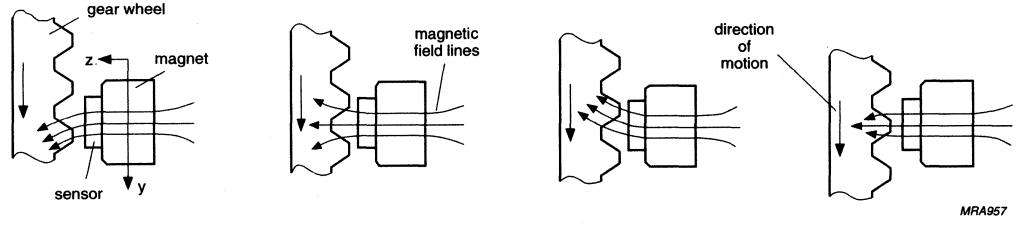

Fig.3 Functional principle.

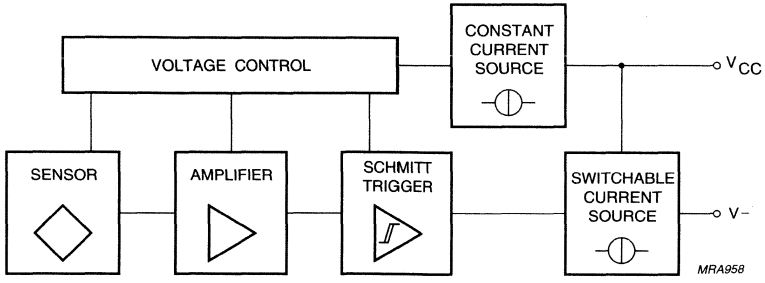

Fig.4 Block diagram.

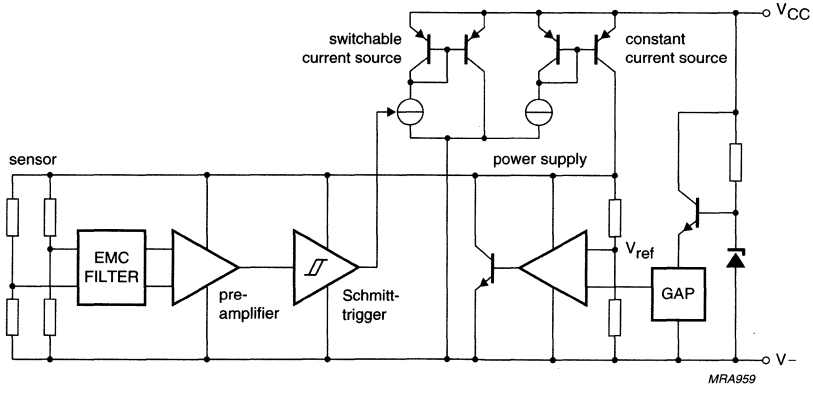

Fig.5 Simplified circuit diagram.

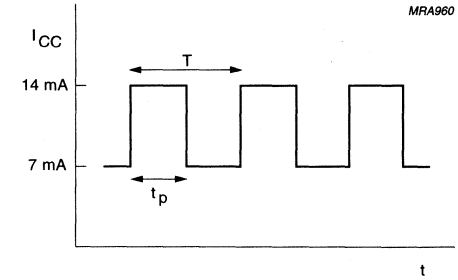

$$\delta = \frac{t_p}{T} \times 100\%$$

Fig.6 Output signal as a function of time.

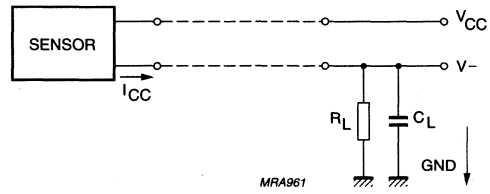

Fig.7 Test and application circuit.

APPLICATION INFORMATION

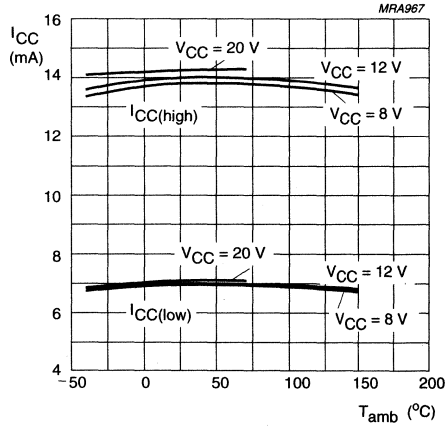

Fig.8 Output current levels as functions of ambient temperature; typical values.

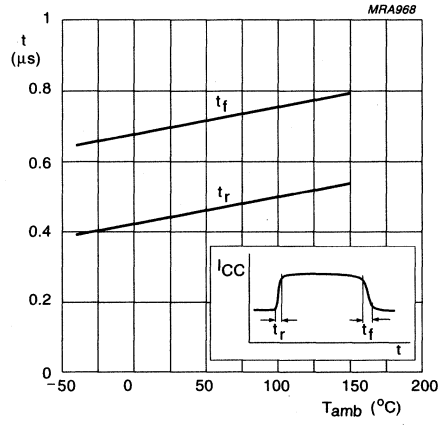

Fig.9 Output current switching times as functions of ambient temperature; typical values.

Mounting conditions

The recommended sensor position in front of a gear wheel is shown in Fig.15. Distance 'd' is measured between the sensor front and the tip of a gear wheel tooth. The KMI15/4 senses ferrous indicators like gear wheels in the ± y direction only (no rotational symmetry of the sensor); see Fig.2. The effect of incorrect mounting positions on sensing distance is shown in Figs 11, 12 and 13.
The symmetrical reference axis of the sensor corresponds to the axis of the ferrite magnet.

Environmental conditions

Due to eddy current effects the sensing distance depends on the tooth frequency (see Fig.17). The influence of gear wheel module on the sensing distance is shown in Fig.16.

Gear Wheel Dimensions

SYMBOL	DESCRIPTION	UNIT
German DIN		
z	number of teeth	
d	diameter	mm
m	module m = d/z	mm
p	pitch p = π × m	mm
ASA; note1		
PD	pitch diameter (d in inch)	inch
DP	diametric pitch DP = z/PD	$inch^{-1}$
CP	circular pitch CP = π/DP	inch

Note

1. For conversion from ASA to DIN: m = 25.4 mm/DP; p = 25.4 mm × CP.

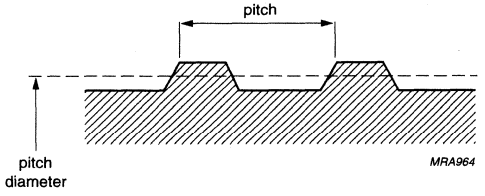

$$\text{module} = \frac{\text{pitch diameter}}{\text{number of teeth}}$$

pitch = module × π

Fig.10 Gear wheel dimensions.

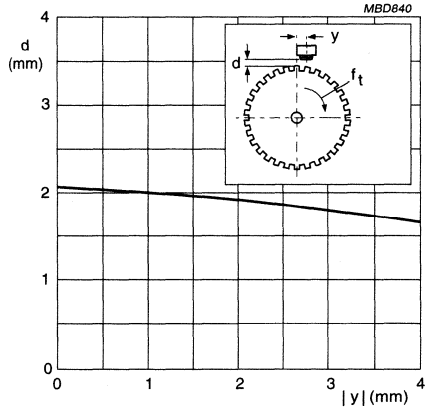

V_{CC} = 12 V; f_t = 2 kHz; module = 2 mm; pitch diameter = 100 mm.

Fig.11 Sensing distance as a function of positional tolerance in the y-axis; typical values.

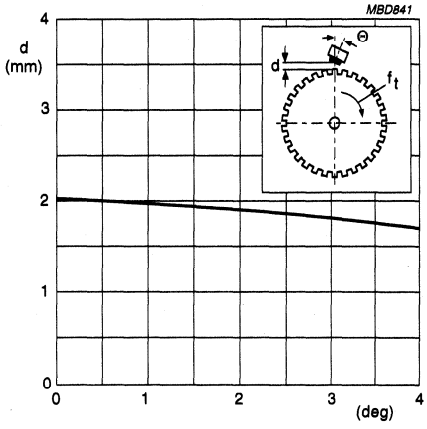

V_{CC} = 12 V; f_t = 2 kHz; module = 2 mm.

Fig.12 Sensing distance as a function of positional tolerance; typical values.

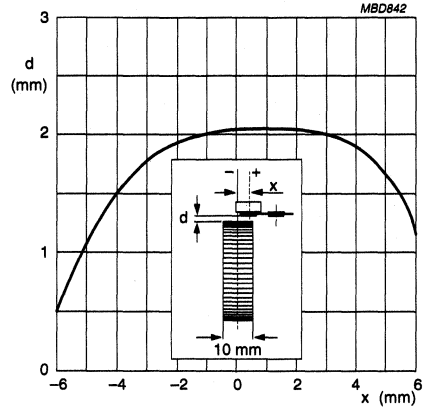

V_{CC} = 12 V; f_t = 2 kHz; module = 2 mm.

Fig.13 Sensing distance as a function of positional tolerance in the x-axis; typical values.

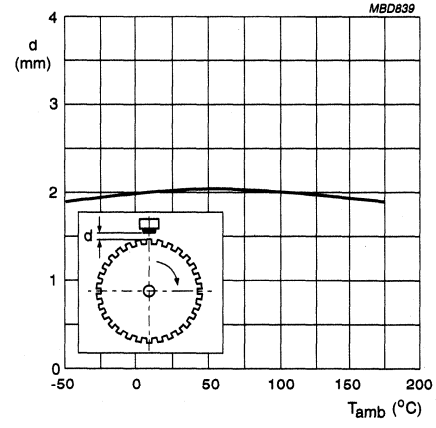

Fig.14 Typical sensing distance as a function of ambient temperature; typical values.

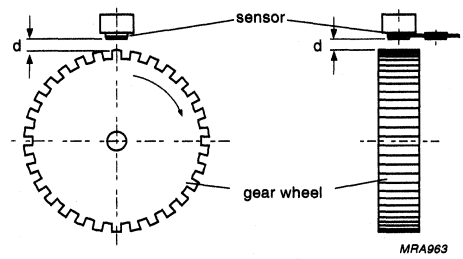

Fig.15 Sensor positioning.

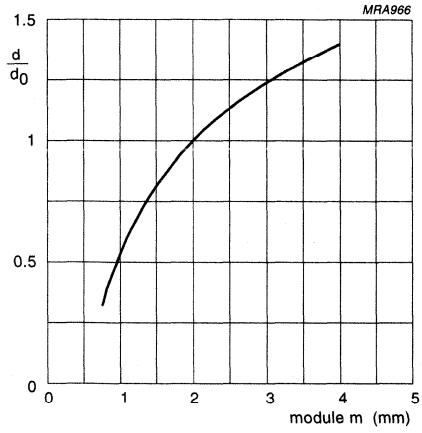

d_0 = sensing distance for gear wheel with module = 2 mm.

Fig.16 Normalized maximum sensing distance as a function of a gear wheel module; typical values.

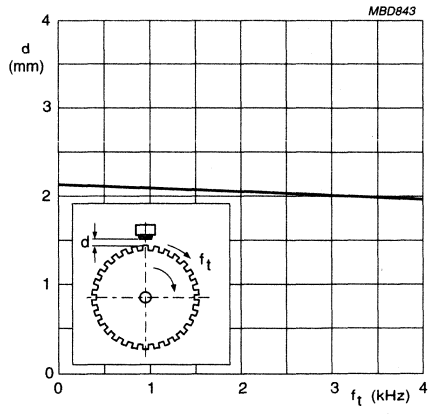

V_{CC} = 12 V; module = 2 mm.

Fig.17 Sensing distance as a function of tooth frequency; typical values.

EMC

Figure 18 shows a recommended application circuit for automotive applications (wheel sensing f_t < 5 kHz). It provides a protection interface to meet Electromagnetic Compatibility (EMC) standards and safeguard against voltage spikes Table 1 lists the tests which are applicable to this circuit and the achieved class of functional status. Protection against 'load dump' (test pulse 5 according to *"DIN 40839"*) means a very high demand on the protection circuit and requires a suitable suppressor diode with sufficient energy absorption capability.

The board net often contains a central load dump protection that makes such a device in the protection circuit of the sensor module unnecessary.

Tests for electrostatic discharge (ESD) were conducted in line with *"IEC 801-2"* to demonstrate the KMI15/4's handling capabilities. The *"IEC 801-2"* test conditions were: C = 150 pF, R = 150 Ω, V = 2 kV.

Electromagnetic disturbances with fields up to 150 V/m and f = 1 GHz (ref. *"DIN 40839"*) have no influence on performance.

Table 1 EMC test results

EMC REF. DIN 40839	SYMBOL	MIN. (V)	MAX. (V)	REMARKS	CLASS
Test pulse 1	V_{LD}	−100	−	t_d = 2 ms	C
Test pulse 2	V_{LD}	−	100	t_d = 0.2 ms	A
Test pulse 3a	V_{LD}	−150	−	t_d = 0.1 µs	A
Test pulse 3b	V_{LD}	−	100	t_d = 0.1 µs	A
Test pulse 4	V_{LD}	−7	−	t_d = 130 ms	B
Test pulse 5	V_{LD}	−	120	t_d = 400 ms	B

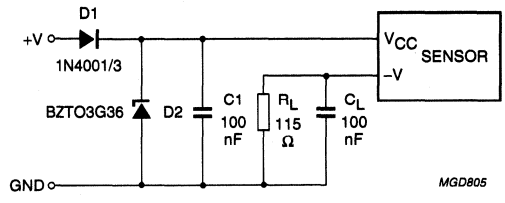

Fig.18 Test/application circuit for the KMI15/4.

PACKAGE OUTLINE

Plastic single-ended combined package; magnetoresistive sensor element; bipolar IC; magnetized ferrite magnet (5.5 x 5.5 x 3.0 mm); 2 in-line leads **SOT453C**

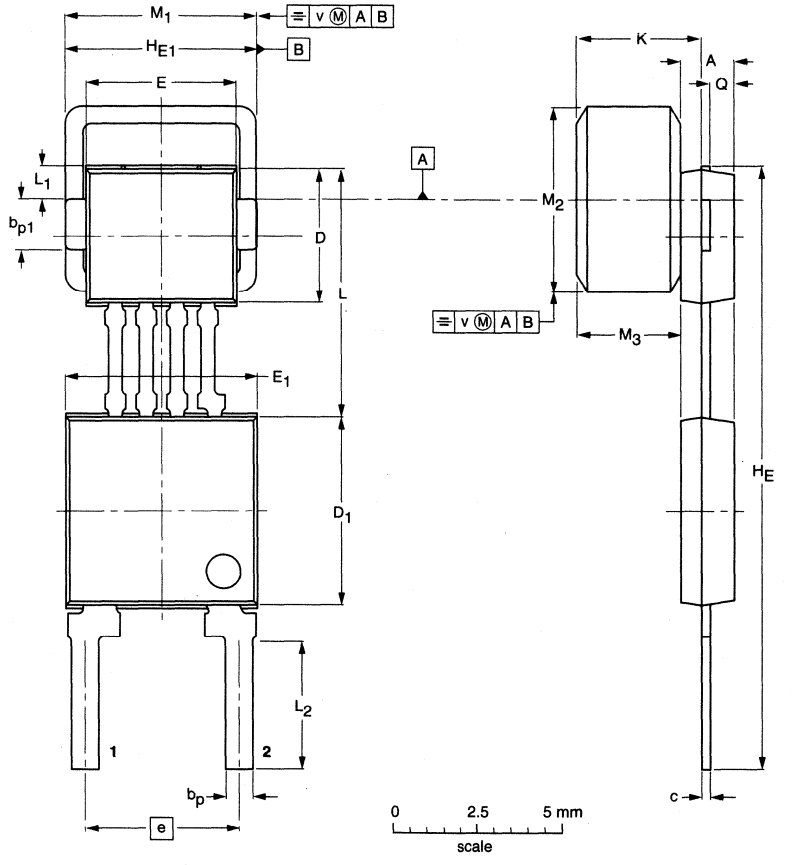

DIMENSIONS (mm are the original dimensions)

UNIT	A	b_p	b_{p1}	c	$D^{(1)}$	$D_1{}^{(1)}$	$E^{(1)}$	$E_1{}^{(1)}$	e	H_E	H_{E1}	K max.	L	L_1	L_2	M_1	M_2	M_3	Q	v
mm	1.7 1.4	0.8 0.7	1.5 1.4	0.3 0.24	4.1 3.9	5.7 5.5	4.5 4.3	5.7 5.5	4.6 4.4	18.2 17.8	5.6 5.5	3.87	7.55 7.25	1.2 0.9	3.9 3.5	5.65 5.35	5.65 5.35	3.15 2.85	0.75 0.65	0.25

Note

1. Plastic or metal protrusions of 0.15 mm maximum per side are not included.

OUTLINE VERSION	REFERENCES				EUROPEAN PROJECTION	ISSUE DATE
	IEC	JEDEC	EIAJ			
SOT453C						~~97-02-28~~ 98-03-26

Integrated rotational speed sensor KMI16/1

FEATURES

- Open collector output signal
- Zero speed capability
- Wide air gap
- Wide temperature range
- Insensitive to vibration
- EMC resistant.

DESCRIPTION

The KMI16/1 sensor detects rotational speed of ferrous gear wheels and reference marks.
The sensor consists of a magnetoresistive sensor element, a signal conditioning integrated circuit in bipolar technology and a magnetized ferrite magnet.
The frequency of the digital current output signal is proportional to the rotational speed of a gear wheel.

CAUTION
Do not press two or more products together against their magnetic forces.

PINNING

PIN	DESCRIPTION
1	V_{CC}
2	V_{out}
3	GND

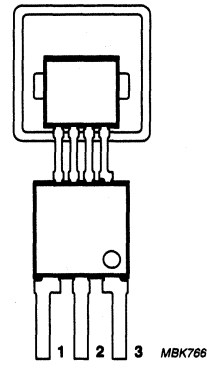

Fig.1 Simplified outline (SOT477B).

QUICK REFERENCE DATA

SYMBOL	PARAMETER	CONDITIONS	MIN.	TYP.	MAX.	UNIT
V_{CC}	DC supply voltage		4.5	12	16.5	V
$V_{out\ (low)}$	remaining open collector voltage		–	–	0.5	V
I_{CC}	DC supply current		6.5	10	12	mA
d_{max}	maximum sensing distance	target wheel m = 2 mm	–	2	–	mm
f_t	operating tooth frequency		0	–	25000	Hz
T_{amb}	ambient operating temperature		–40	–	+150	°C

LIMITING VALUES

In accordance with Absolute Maximum Rating System (IEC 134).

SYMBOL	PARAMETER	CONDITIONS	MIN.	MAX.	UNIT
V_{CC}	DC supply voltage	T_{amb} = −40 to +150 °C; $I_{out\ (low)}$ = 20 mA	–	16	V
V_{out}	output voltage		−0.5	+10	V
T_{stg}	storage temperature		−40	+150	°C
T_{amb}	ambient operating temperature		−40	+150	°C
T_{sld}	soldering temperature	t ≤ 10 s	–	260	°C

CHARACTERISTICS

T_{amb} = 25 °C; V_{CC} = 12 V; d = 1.9 mm; f_t = 2 kHz; test circuit: see Fig.5; sensor positioning: see Fig.11; gear wheel: module 2 mm; material 1.0715; see Fig.6; unless otherwise specified.

SYMBOL	PARAMETER	CONDITIONS	MIN.	TYP.	MAX.	UNIT
$V_{out\ (low)}$	remaining open collector voltage	$I_{out\ (low)}$ = 10 mA	–	–	0.5	V
		$I_{out\ (low)}$ = 20 mA	–	–	1	V
t_r	output signal rise time	10 to 90% value	–	11.5	–	µs
t_f	output signal fall time	10 to 90% value	–	0.3	–	µs
t_d	switching delay time	between stimulation pulse (generated by a coil) and output signal	–	1	–	µs
f_t	operating tooth frequency	for both rotation directions	0	–	25000	Hz
d_{min}	minimum sensing distance	target wheel m = 2 mm; see Fig.11; and note 1	–	0.3	–	mm
d_{max}	maximum sensing distance	target wheel m = 2 mm; see Fig.11; and note 1	–	2	–	mm
δ	duty cycle		30	50	70	%

Note

1. High rotational speeds of wheels reduce the sensing distance due to eddy current effects (see Fig.13).

FUNCTIONAL DESCRIPTION

The KMI16/1 sensor is sensitive to the motion of ferrous gear wheels or reference marks. The functional principle is shown in Fig.3. Due to the effect of flux bending, the different directions of magnetic field lines in the magnetoresistive sensor element will cause an electrical signal. Because of the chosen sensor orientation and the direction of ferrite magnetization, the KMI16/1 is sensitive to movement in the 'y' direction in front of the sensor only (see Fig.2).

The magnetoresistive sensor element signal is amplified, temperature compensated and passed to a Schmitt trigger in the conditioning integrated circuit (Fig 4).
The digital output signal level is independent of the sensing distance within the measuring range (Fig.10).
A (3-wire) output current enables safe transfer of the sensor signal to the detecting circuit (see Fig.5).
The integrated circuit housing is separated from the sensor element housing to optimize the sensor behaviour at high temperatures.

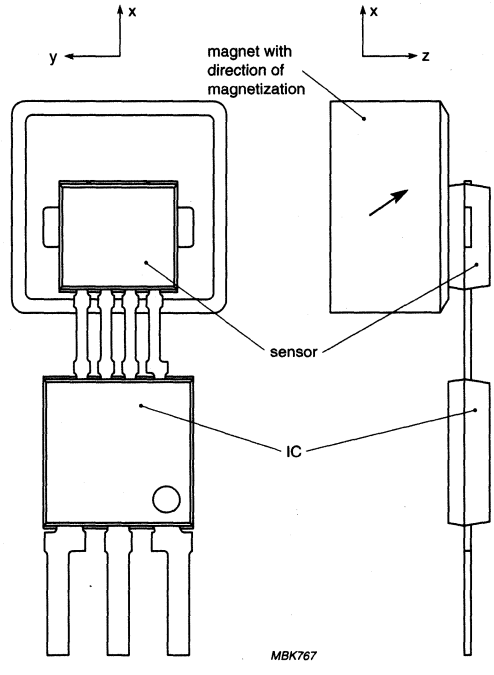

Fig.2 Component detail of the KMI16/1.

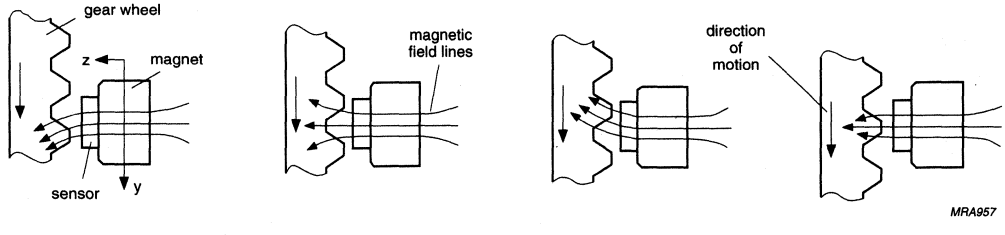

Fig.3 Functional principle.

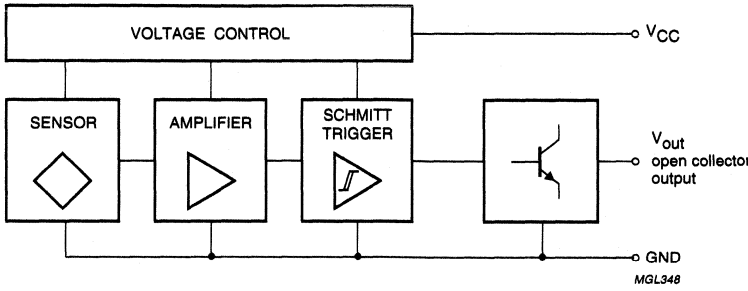

Fig.4 Block diagram.

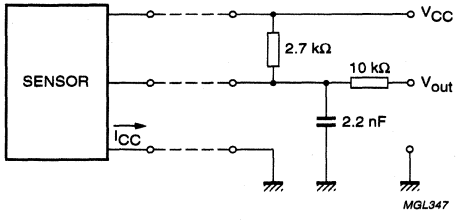

Fig.5 Test and application circuit.

APPLICATION INFORMATION

Mounting conditions

The recommended sensor position in front of a gear wheel is shown in Fig.11. The distance 'd' is measured between the sensor front and the tip of a gear wheel tooth.
The KMI16/1 senses ferrous indicators like gear wheels in the ± y direction only (no rotational symmetry of the sensor); see Fig.2. The effect of incorrect mounting positions on sensing distance is shown in Figs 7, 8 and 9. The symmetrical reference axis of the sensor corresponds to the axis of the ferrite magnet.

Environmental conditions

Due to eddy current effects the sensing distance depends on the tooth frequency (Fig.13). The influence of gear wheel module on the sensing distance is shown in Fig.12.

Gear Wheel Dimensions

SYMBOL	DESCRIPTION	UNIT
German DIN		
z	number of teeth	
d	diameter	mm
m	module m = d/z	mm
p	pitch $p = \pi \times m$	mm
ASA; note 1		
PD	pitch diameter (d in inch)	inch
DP	diametric pitch DP = z/PD	$inch^{-1}$
CP	circular pitch $CP = \pi/DP$	inch

Note

1. For conversion from ASA to DIN: m = 25.4 mm/DP; p = 25.4 mm × CP.

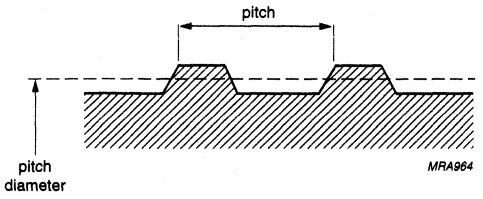

$$\text{module} = \frac{\text{pitch diameter}}{\text{number of teeth}}$$

$$\text{pitch} = \text{module} \times \pi$$

Fig.6 Gear wheel dimensions.

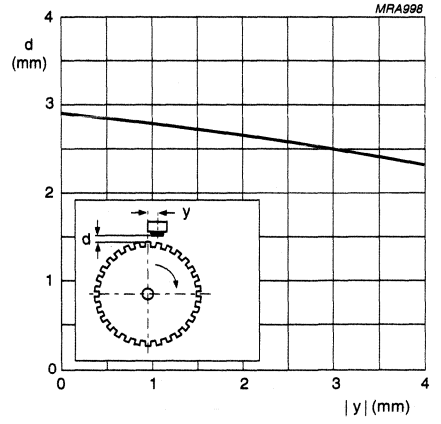

V_{CC} = 12 V; f_t = 2 kHz; module = 2 mm; pitch diameter = 100 mm.

Fig.7 Sensing distance as a function of positional tolerance in the y-axis; typical values.

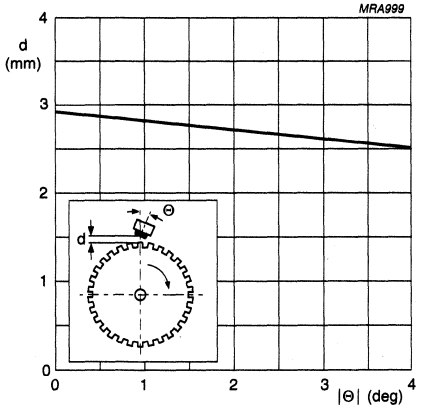

V_{CC} = 12 V; f_t = 2 kHz; module = 2 mm.

Fig.8 Sensing distance as a function of positional tolerance; typical values.

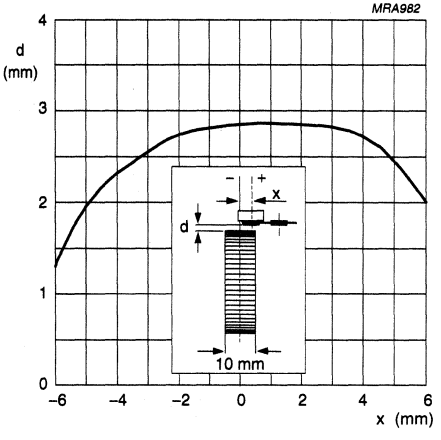

V_{CC} = 12 V; f_t = 2 kHz; module = 2 mm.

Fig.9 Sensing distance as a function of positional tolerance in the x-axis; typical values.

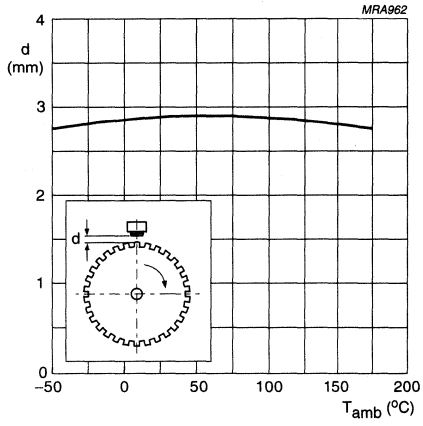

V_{CC} = 12 V; f_t = 2 kHz; module = 2 mm.

Fig.10 Sensing distance as a function of ambient temperature; typical values.

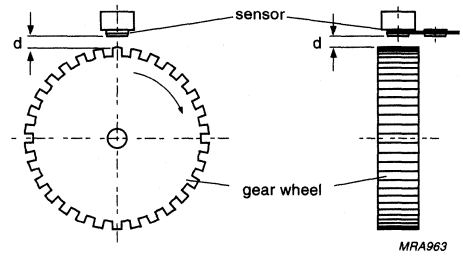

Fig.11 Sensor positioning.

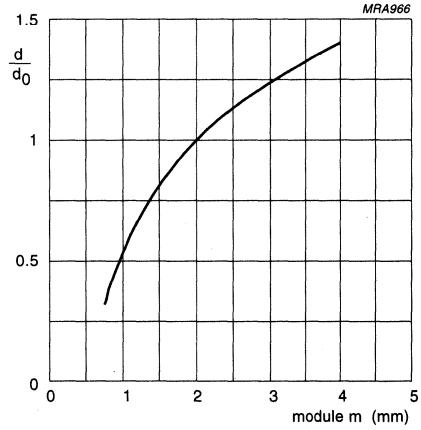

d_o = measuring distance for a gear wheel with module m = 2 mm.

Fig.12 Normalized maximum sensing distance as a function of gear wheel module; typical values.

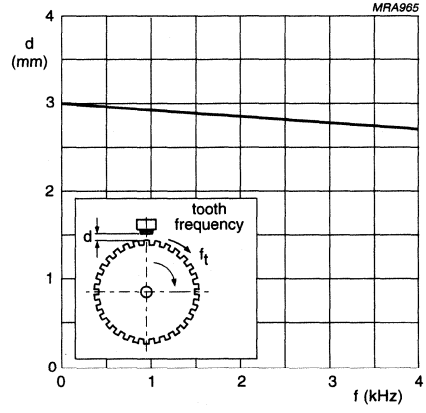

V_{CC} = 12 V; module = 2 mm.

Fig.13 Sensing distance as a function of tooth frequency; typical values.

PACKAGE OUTLINE

Plastic single-ended combined package; magnetoresistive sensor element; bipolar IC; magnetized ferrite magnet (5.5 x 5.5 x 3.0 mm); 3 in-line leads **SOT477B**

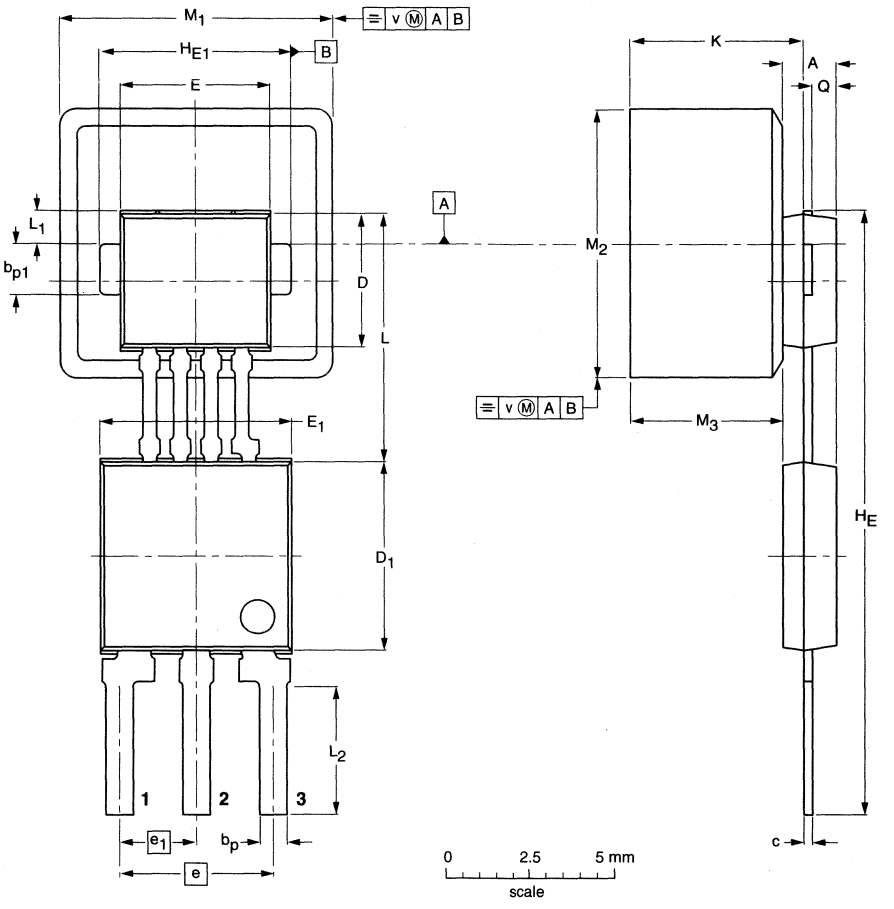

DIMENSIONS (mm are the original dimensions)

UNIT	A	b_p	b_{p1}	c	D(1)	D_1(1)	E(1)	E_1(1)	e	e_1	H_E	H_{E1}	K max.	L	L_1	L_2	M_1	M_2	M_3	Q	v
mm	1.7 1.4	0.8 0.7	1.57 1.47	0.3 0.24	4.1 3.9	5.7 5.5	4.5 4.3	5.7 5.5	4.6 4.4	2.35 2.15	18.2 17.8	5.6 5.5	5.37	7.55 7.25	1.2 0.9	3.9 3.5	8.15 7.85	8.15 7.85	4.7 4.3	0.75 0.65	0.25

Note

1. Plastic or metal protrusions of 0.15 mm maximum per side are not included.

OUTLINE VERSION	REFERENCES				EUROPEAN PROJECTION	ISSUE DATE
	IEC	JEDEC	EIAJ			
SOT477B						98-05-12

GENERAL
ANGULAR MEASUREMENT

ANGLE MEASUREMENT

Contents

- Principles and standard set-ups
- Philips sensors for angle measurement
- Real-life measurement applications
- Information for advanced users and applications
  - Additional measurement set-ups
  - Magnets
  - Angle sensor eccentricity.

Principles and standard set-ups

The principle behind magnetoresistive angular measurement is essentially simple: as explained in the general section, the MR effect is naturally an angular effect. The resistance of the permalloy strip depends on the angle α between the internal magnetization vector of the permalloy strip and the direction of the current through it.

When using the MR effect in sensors for measuring angles, no linearization using a barber-pole sensor layout Is required and the original direct relationship between the resistance R and angle α ($R = R_o + \Delta R_o \cos^2\alpha$) is valid.

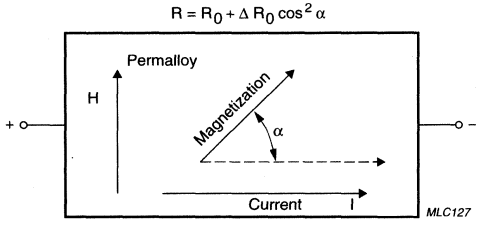

Fig.1 The magnetization effect in permalloy.

To achieve accurate measurement, the only condition is that the internal magnetization vector of the permalloy directly follows the external field. This is done by applying an external field very much greater than the internal field so the sensor is 'saturated'; with today's sensors, this is normally achieved by having a magnetic field strength of approximately 100 kA/m in the sensor plane. In this set-up, (Fig.3) angle is measured directly by detecting the field-direction and the set-up is independent of:

- Magnet field strength
- Magnetic drift with time
- Magnetic drift with temperature
- Ageing, and
- Mechanical tolerances.

which allows for reduced system tolerances and pre-trimming of the sensor. This is the solution adopted by Philips in its KM110B modules. The only precaution that need be taken with this technique is ensuring the field directions during trimming match the field directions after assembly.

There is ongoing development of sensors that can be placed in this 'saturated' condition using steadily smaller field strengths and this significantly reduces system costs, because relatively inexpensive normal ferrite magnets can be used rather than other, more costly permanent magnets.

Note: all Philips sensors and modules have in general been designed to be used with this 'direct' method. However, there are other techniques that can be used: for information on other methods, refer to 'Information for advanced users and applications' later in this chapter

The aim in angle measurement is to influence, as fully as possible, the internal magnetization of the sensor by the application of an external magnetic field, so the magnetization follows as closely as possible the external magnetic vector. If, as recommended, a typical 'saturation' field of 100 kA/m is applied, due to the vector addition of this external field with the internal magnetization of 2 kA/m, the result is a systematic error of about 2%. This error is eliminated during the production of Philips modules by trimming.

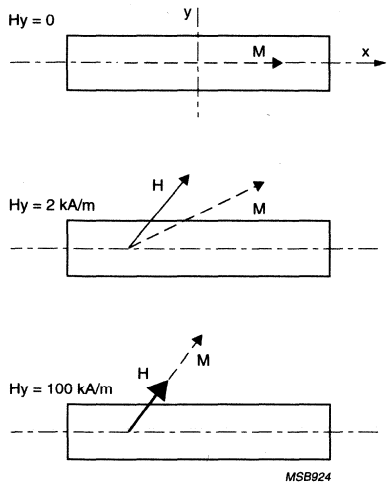

Fig.2 Internal field vectors align with a stronger external field.

When using a sensor/magnet combination in angular measurement applications, the magnet is placed on the target, in front of the sensor (which is positioned so that its internal magnetization vector is parallel to that of the magnet at the reference point).

When the target turns, the magnet is rotated in front of the sensor and the angle of the external field changes relative to the internal field of the permalloy strips. This causes the internal magnetization vector of the sensor to rotate by an angle α, aligning itself with the external field (see Fig.2).

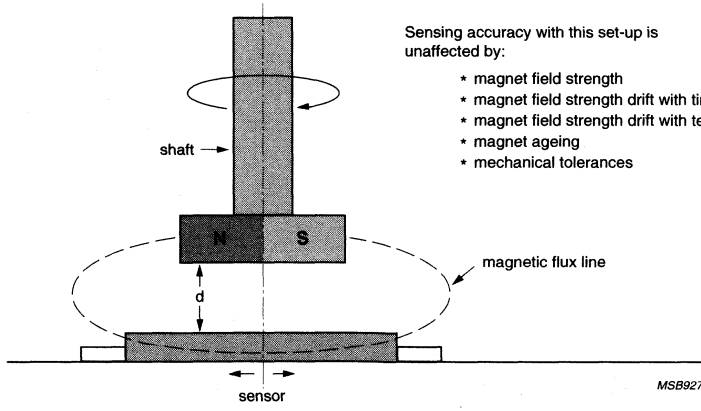

Fig.3 Arrangement of sensor and magnet.

EXTENDING ANGLE RANGE

From the basic relationship (see Appendix 1 on the magnetoresistive effect):

$(R = R_o + \Delta R_o \cos^2\alpha)$

it can easily be shown that:

$R \approx \sin 2\alpha$

If a sensor is used in non-linearized mode, then it translates a single rotation of the target (360°) into a 720° output signal (2 complete sine waves). This means that the output signal of the magnetoresistive sensor offers good linearity only within the angle range of ±15° (where $\sin\alpha \approx \alpha$). If a sine wave output is acceptable in the application (for example if there is a microprocessor in the system which can convert the output sine curve to a linear relationship), the angle range can to be extended to ±35° (see Fig.4). Resolution is reduced at the ends of the range, but behaviour is unaffected in the middle of the range.

To obtain a solution for angles in the range ±90°, two MR sensors are used (see Fig.5). If they are accurately positioned at 45° to one another mechanically, then electronically their output signals are 90° out of phase. Therefore the output signals from the two sensors represent $\sin 2\alpha$ and $\cos 2\alpha$ respectively, and as $\sin 2\alpha / \cos 2\alpha = \tan 2\alpha$, 2α and therefore a can be easily calculated.

Note: if the sensors are arranged in parallel, (positioned at 0° degree to one another) this set-up is excellent as a redundant set-up (although of course the angle measurement range will be limited). With this set-up, both sensors are influenced equally by the external magnet, so redundancy is achieved with only one external magnet and the need for signal conditioning is reduced.

Although in principle the set-up in Fig.5 is simple, two factors have to be addressed before this solution for the measurement of angles up to 90° is economically viable.

Firstly, there has to be an economic way of combining the $\sin 2\alpha$ and $\cos 2\alpha$ signals into a single signal representing the angle α. To answer this need, Philips is developing an ASIC (Fig.6) with the required signal conditioning on one chip and offering digital interfacing (solutions for PWM, serial bit stream and CAN.bus are now possible).

Secondly, the sensors have to be aligned mechanically at exactly 45°. This is achieved using advances in magnetoresistive manufacturing technology, where two overlapping sensor bridges are etched on the same substrate, using a photo-mask process. This process has extremely high accuracy, more than sufficient for this application

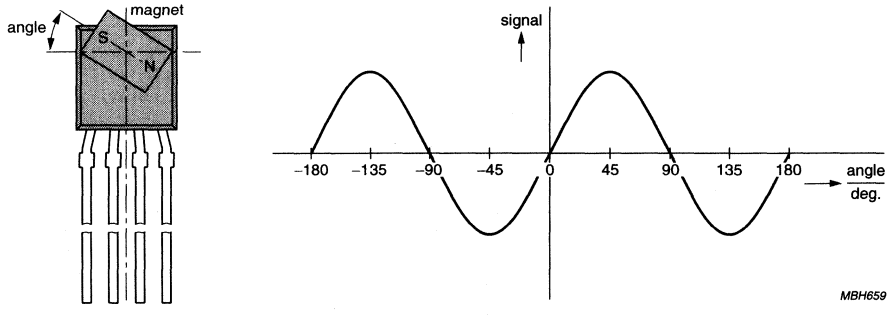

Fig.4 Angle measurement with a KMZ10B.

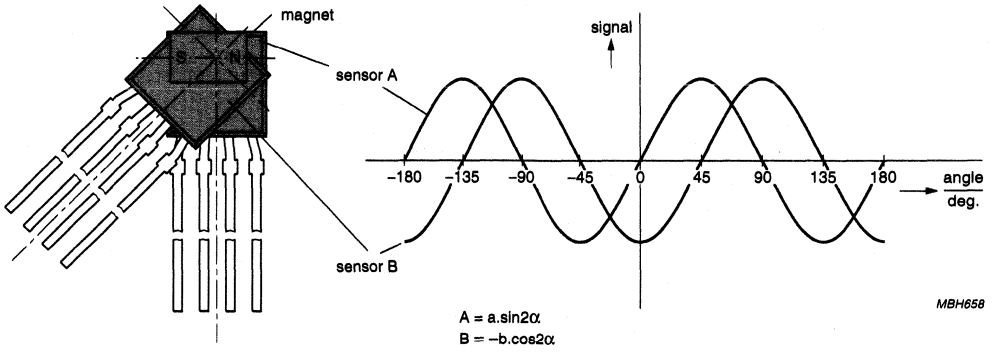

Fig.5 Angle measurement with two sensors.

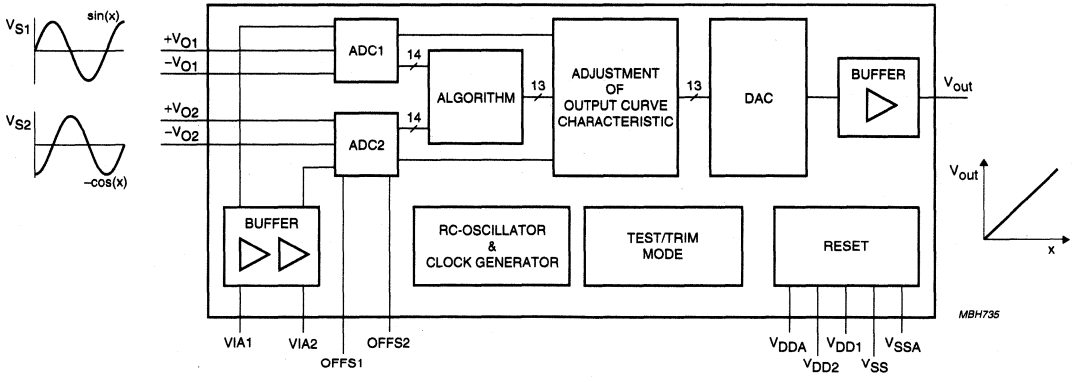

Fig.6 Block diagram of a 'one-chip' ASIC solution, UZZ9000.

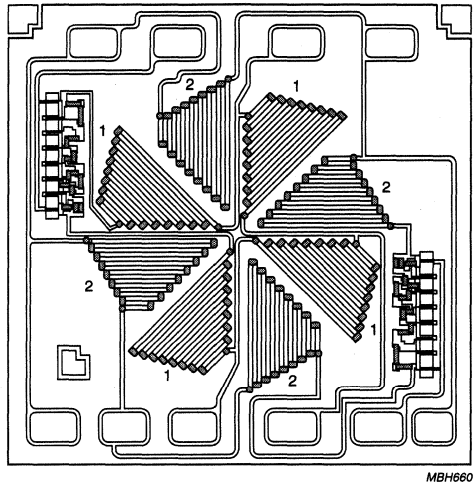

Fig.7 Layout KMZ41 chip.

Figure 7 shows the actual layout of Philips KMZ41. It has provides 8 MR resistor networks, connected as two individual Wheatstone bridges, aligned with a 45° shift in their sensitive magnetic directions, producing the required 90° electrical shift.

Of course, it is also possible align both bridges magnetically parallel to each other so they produce the same output signal. In that case, redundancy is achieved using a single sensor device. By increasing the number of bridges, a combination of both principles can be achieved to make, for example, a three-times redundant sensor or a fully redundant sensor that can measure over the full 90°, or any combination.

Philips sensor modules for angle measurement

Based on magnetoresistive sensors, Philips Semiconductors has developed a range of ready-to-use magnetoresistive sensor modules for contactless angle measurement offering the following features:

- Offset, zero point and sensitivity are pre-trimmed (so assembly of the final encapsulated sensor is simple and calibration after assembly is unnecessary)
- Integrated temperature compensation; and
- EMC protection.

These ready-to-use modules with built in signal conditioning electronics have several advantages:

- Output is independent of magnet tolerances, temperature coefficients, mechanical set-up and other tolerances
- A single linear output signal can be provided for angles up to 180°
- A variety of output signals can be provided: analog (voltage or current), Pulse Width Modulation (PWM) and bus interfaces (e.g. I^2C, CAN).

Philips' KM110BH/2xxx family is a range of modules using hybrid thick-film technology. The circuits and magnetic parameters of these modules have been designed so they can be used directly in many applications, with no further trimming or adjustment, as the basis for customized solutions.

To reduce system costs and simplify application even further, a family of ASIC solutions is in development, some of which
contain both sensor and conditioning electronics. By combining both elements in a single encapsulation, pre-aligned systems can be offered which can be simply mounted on a normal PCB.

In addition to the ready-made modules, Philips Semiconductors is willing to undertake customised designs for high volume applications (in excess of 50,000 units), either as specific hybrid or integrated solutions.

KMB110BH/21 MODULE SERIES

Figure 8 shows the construction of the KM110BH/21 module, which is based on the KMZ10B sensor and is available in two types: the KM110BH/2130 and KM110BH2190. They are both based on the same circuit, but are trimmed differently: the KM110BH/2130 is trimmed to a higher amplification and measures angles between –15° and +15°, generating a linear output signal; while the KM110BH/2190 measures angles from approximately –45° to +45° and produces a sinusoidal output. Both produce an analog voltage signal. Figure 9 shows the output V_o of the two modules, as a function of the measured angle α. For further details, refer to Table 1.

KM110BH/2270 MODULE

The KM110BH/2270 module, which is based on the KMZ11B1 sensor, is trimmed to measure angles ranging from –35° to +35° and has integrated input voltage stabilization. In contrast to the other modules in the KM110BH/2 range, the KM110BH/2270 has an analog current output signal (4 to 20 mA), which can be converted to a voltage signal using a simple resistor. The output is sinusoidal. This module has extremely good resolution and reproducibility (better than 0.001° at α = 0°) and hysteresis, which is typically 0.02° at a = 0°, is very low.

When designing an encapsulation for the KM110BH/2270, it may be necessary to have the pins of the hybrid bent into an 'S' shape, to avoid excessive force on the solder joints. In this case, please order the KM110BH/2270G. For further details, refer to Table 1.

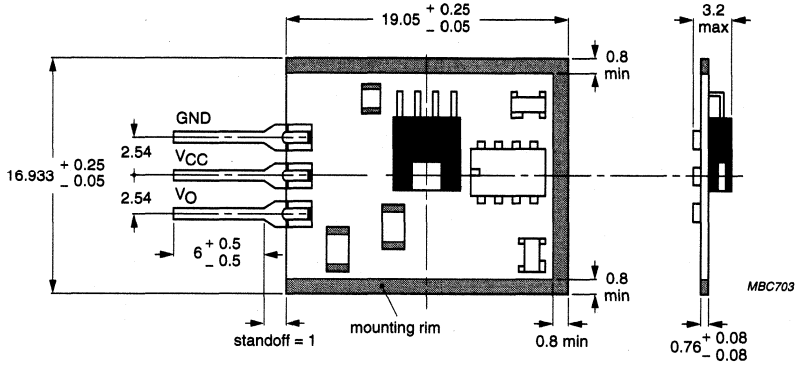

Fig.8 Construction of a KM110BH/21.

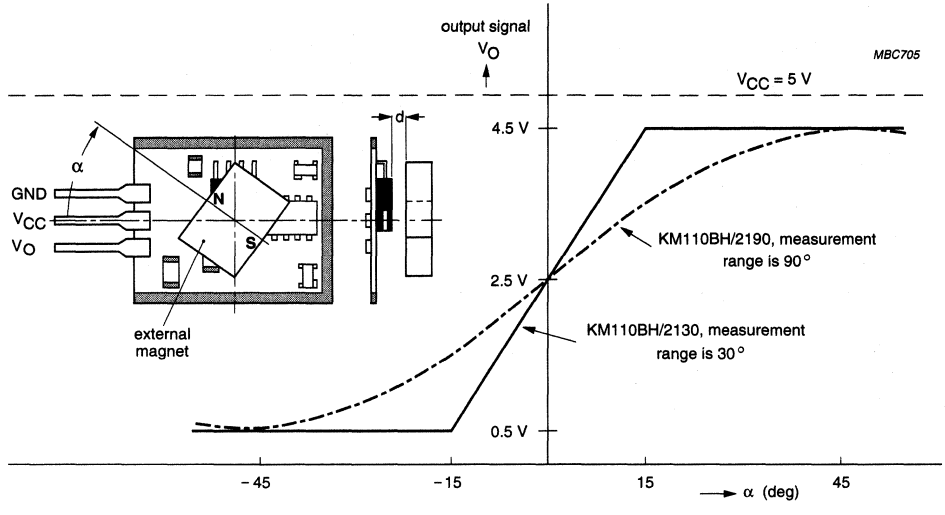

Fig.9 Output characteristics of the KM110BH/2130 and KM10BH/2190 modules.

Table 1 An overview of the main characteristics of Philips modules for angle measurement

PARAMETER	KM110BH					UNIT
	2130[1]	**2190**[2]	**2270**	**2430**	**2470**	
Angle range	30	90	70	30	70	deg
Output voltage[3]	0.5 to 4.5	0.5 to 4.5	–	0.5 to 4.5	0.5 to 4.5	V
Output current	–	–	4 to 20	–	–	mA
Output characteristic	linear	sinusoidal	sinusoidal	linear	sinusoidal	–
Supply voltage	5	5	5	5	5	V
Substrate dimensions	9.1 × 16.9	9.1 × 16.9	23.6 × 20.3	23.6 × 20.3	23.6 × 20.3	mm
Resolution	0.001	0.001	0.001	0.001	0.001	deg
Temperature range	–40 to +125	–40 to +125	–40 to +125	–40 to +125	–40 to +125	°C

KM110BH/24 MODULE

The KM110BH/24 is available in two versions based on the KMZ41: the KM110BH/2430 is trimmed to measure angles between –15° and +15°, generating a linear output signal (non-linearity is ≈1%); while the KM110BH/2490 measures angles from approximately –35° to +35° and produces a sinusoidal output. On-board protection circuitry makes these modules EMC tolerant.

Real-life angular measurement applications

With angular measurement using magnetoresistive sensors, the number of possible applications is very broad, replacing
and outperforming other types of sensors in a variety of applications, some of which are listed in Table 2:

Amongst these numerous applications, undoubtedly the most common is in the automotive industry, where they are used to measure pedal and throttle position.

REDUNDANT SYSTEMS

As multiple sensors with identical behaviour can be implemented on a single piece of silicon, a magnetoresistive set-up is an ideal solution for the construction of redundant systems, in safety critical applications, for example, such as a car accelerator pedal.

The essential functional blocks of a typical redundant sensor system are shown in Fig.10. For each sensor, the signal is first amplified. This stage also includes offset compensation and determines the characteristic of the output signal (sinusoidal or linear). After temperature compensation, the third stage provides additional trimming of the output signal and allows for the inclusion of diagnostic functions (for example, wire not connected or short circuit conditions). The final stage provides additional protection, against short circuits (between the supply voltage and the output signal, for example) or overvoltage (for example, if the 5 V module supply is accidentally connected to a 14 V battery supply).

Table 2 Typical applications for angle sensors

Automotive and agricultural	Industrial
• Pedal position • Active suspension units • Self-levelling systems • Automatic headlight adjustment	• Valve control • Material thickness • Feedback systems for belt control • Wear detection
Medical	**Consumer**
• Body and brain scanners where accurate angle information is vital to build up cross-sectional images • Control joysticks for tilting tables	• Games joysticks • Spirit levels

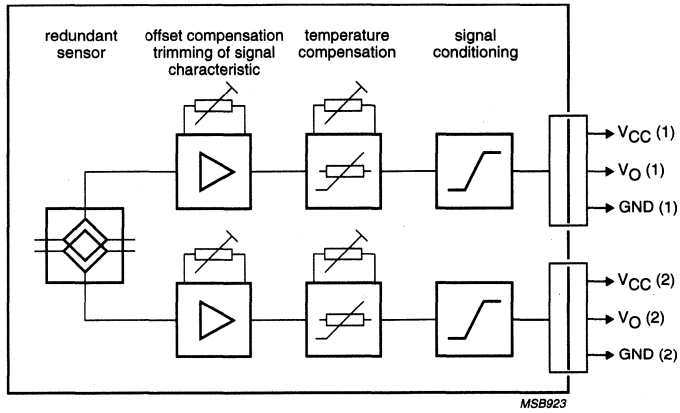

Fig.10 Functional block diagram of module with redundancy.

Information for advanced users and applications

ADDITIONAL MEASUREMENT SET-UPS

Linear

In linear angle measurement, the strength of the external magnetic field used is within normal sensitivity levels and the sensor measures the resulting field strength of the rotating magnet. As can be seen from Fig.11, the signal linearity of a weak field method allows for angles up to ±90° to be measured without correction for the sinusoidal shape of the wave. This is the technique used in most competing angle measurement set-ups. However, since the magnet's properties directly influence sensor output, the measurement equipment must be carefully calibrated after it is assembled and calibration for material ageing is not possible at all. Only with a very well defined magnetic system can a pre-calibrated circuit be used and defining such a system is difficult and expensive, due to the tolerances caused by the thermal sensitivity of the magnet and the mechanical set-up.

By using a set-up with two magnets placed on a rotatable frame, angular rotations of around ±85° can be measured and through the symmetrical positioning of the magnets, the effect of the magnet position is eliminated. Figure 12 shows a practical arrangement, which basically acts as a contactless potentiometer. However, the response is not a perfectly sinusoidal due to magnetic influences on the 'x' and 'y' axis.

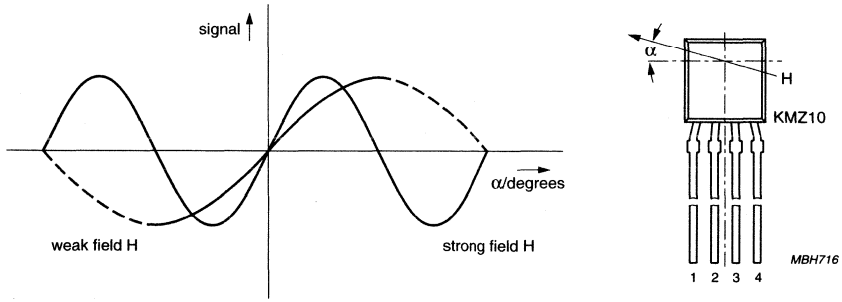

Fig.11 Sensor response for different magnetic fields.

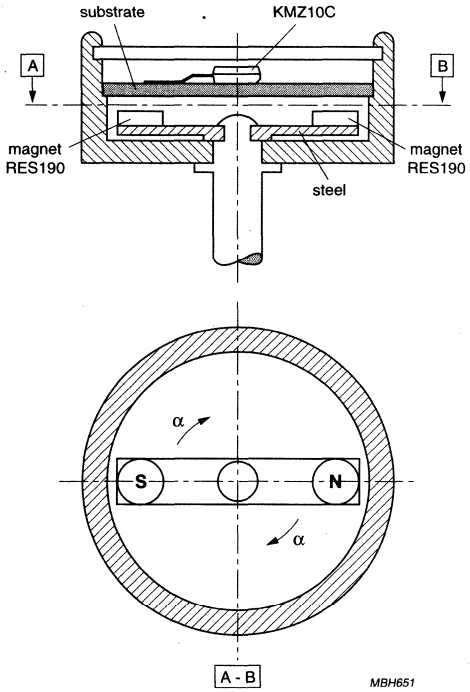

Fig.12 Contactless potentiometer for angle measurement.

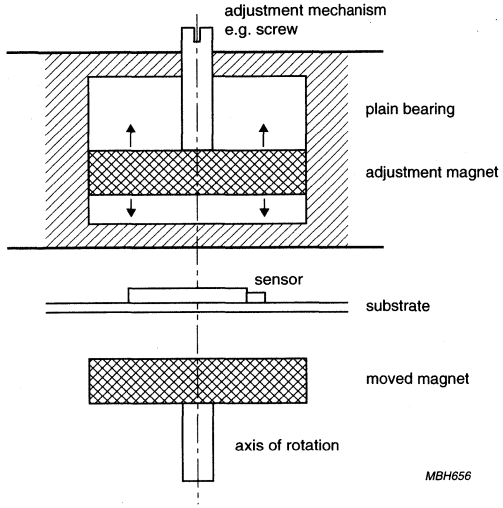

Fig.13 Angle sensor with adjustable measuring range.

Extending measurement angle to greater than 90°

With a second fixed magnet, it is possible to adjust the sensing distance and the angle range can be further extended, to cope with angles greater than ±90°. This can lead to increased mechanical tolerances although by using magnets of the same material, temperature variations can be disregarded. Figure 13 shows a typical set-up.

MAGNETS

The main requirement for the magnet is that it should be strong, to ensure all tolerances are negligible, but obviously cost and space must also be considered, according to individual application requirements. Table 3 compares three commercially available Samarium-Cobalt (SmCo) magnets suitable for angle measurement applications.

These magnets have a tolerance in their magnetization direction which affects angle measurement. This tolerance, which can be up to 2%, should be taken into account if no mechanical calibration is possible at $\alpha = 0°$.

The symmetry axis of the module and the rotation axis of the magnet should be identical, although if one of the axes is shifted slightly, the affect on sensing accuracy can be neglected because the field lines of the magnet are parallel. Measurements with magnets with a face of 11.2×8 mm oriented towards the sensor allow for eccentric tolerances of up to 0.5 mm, assuming an acceptable tolerance in V_o of 1%; and up to 0.25 mm, for an acceptable tolerance in V_o of 0.5%. Evidently, if the magnet is smaller, these values should be proportionately reduced.

Table 3 Typical values for various dimensions of Sm_2Co_{17} magnets

MATERIAL	DIMENSIONS[1] (mm)	d[2] (mm)	TOLERANCE d[3] (mm)	ECCENTRICITY[4] (mm)	T_{amb} (°C)
Sm_2Co_{17}	11.2 × 5.5 × 8	2.1	±0.30	±0.25	−55 to + 125
	6 × 3 × 5	0.7	±0.15	±0.15	
	8 × 3 × 5	0.5	±0.30	±0.20	

Notes

1. Magnetization is always parallel to the latter dimension.
2. d' is the distance between the magnet and the front of the sensor.
3. Tolerance' is the maximum deviation in 'd' for which the change in sensor output signal is <0.5% of full scale output.
4. Eccentricity' is the maximum deviation of the magnet rotational axis from the sensor rotational axis for which the change in sensor output signal is <0.5% of full scale output.

ANGLE SENSOR ECCENTRICITY

In angle measurement using the direct measurement technique, the ideal arrangement is with a homogeneous parallel field. Although large magnets fulfil this requirement, there is usually a compromise between magnet size and the corresponding tolerances of the sensor due to cost considerations.

If the sensor and the magnet rotation axes are in line, the sensor output characteristics follow approximately the following
signal voltage relationship:

$V_o = V_o(0) \times \sin 2\alpha$

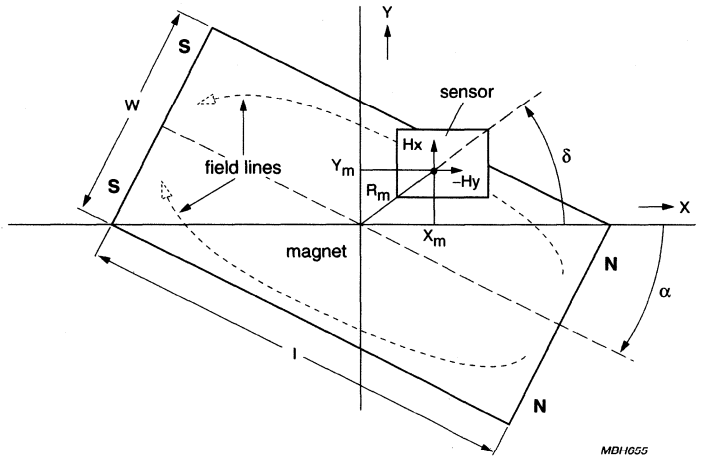

Fig.14 Angle sensor with eccentric sensor position.

However, depending on the sensor position in relation to the magnet and the angle to be measured (see Fig.14), offsets or sensitivity changes can occur. These conditions alter the ideal relationship as described by the equation above.Angle tolerance values can be calculated using the following relationship:

$$\Delta\alpha = C \times R_m^2 \times \sin 2(\alpha + \delta)$$

C is a magnetic constant and, provided the width and length of the magnet are approximately equal, can be calculated from the following equation:

$$C = \frac{320}{(w + l)^2}$$

Table 4 Typical values of C for Sm_2Co_{17} magnets

MAGNET DIMENSIONS (w × h × l, mm)	C (degree/mm²)
6 × 3 × 5	2.6
8 × 3 × 7.5	1.35
11.2 × 5 × 8	0.74

For positions on the x- and y-axis, there is a sensitivity change with a maximum tolerance level at $\alpha = \pm 45°$ and $\pm 135°$ (see Fig.15); for diagonal positions, an offset tolerance occurs with a maximum at $\alpha = \pm 90°$ and $\pm 180°$ (see Fig.16).

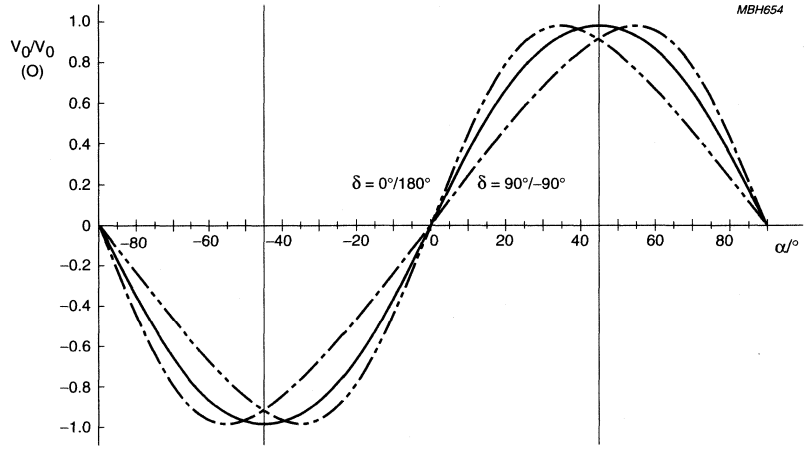

Fig.15 Response tolerances for sensor position on x- and y-axes.

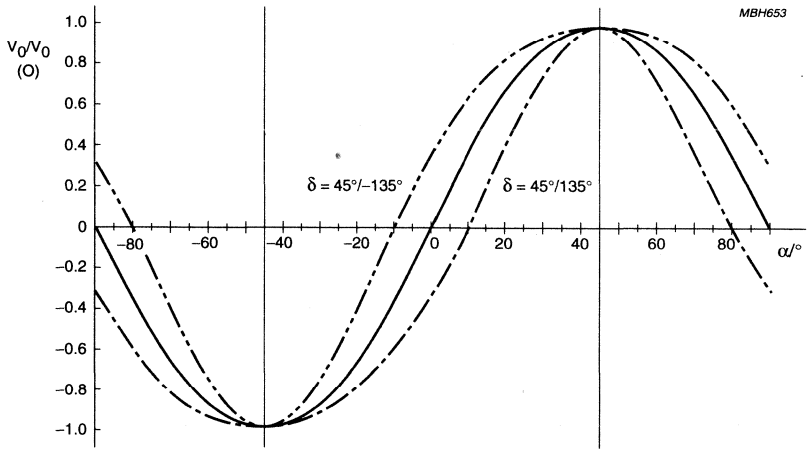

Fig.16 Response tolerances for sensor position diagonals.

Table 5 Typical tolerance values of $|\Delta\alpha|$ for $C \times R_m^2 = 1$

	$\|\Delta\alpha\|$ **(DEGREES)**			
Δ (DEGREES)	**0**	**15**	**30**	**45**
0/90/...	0	0.5	0.87	1
45/135/...	0	0.134	0.25	1

Single sensor system

If we assume that a single, encapsulated angle sensor with eccentricity will be adjusted mechanically to the specified output voltage $V_o(\alpha = 0)$, then the tolerances at $\alpha = 0$ are set to zero. Then over the useful angle range of ±45°, the original offset tolerances can be transformed into a resultant $|\Delta\alpha|$ tolerance:

$|\Delta\alpha| = 2C \times R_m^2 \sin^2\alpha$

Some typical values when $C \times R_m^2 = 1$ are shown in Table 5.

An adjusted 30° angle sensor has a maximum tolerance of:

$|\Delta\alpha| = \frac{1}{2}CR_m^2$ at ±15°

and in the range between 0° and 15°, the tolerance increases approximately linearly from zero to this value. Above ±15° the sinusoidal function given above is effective and has to be taken into account for the 70° and 90° sensors.

Figure 17 gives the maximum tolerances at $\alpha = \pm 15°$ for different magnets as a function of the eccentricity radius R_m.

In general, the tolerance is about 0.3° or 1% FS, provided R_m corresponds to about 10% of the magnetic dimensions l and w.

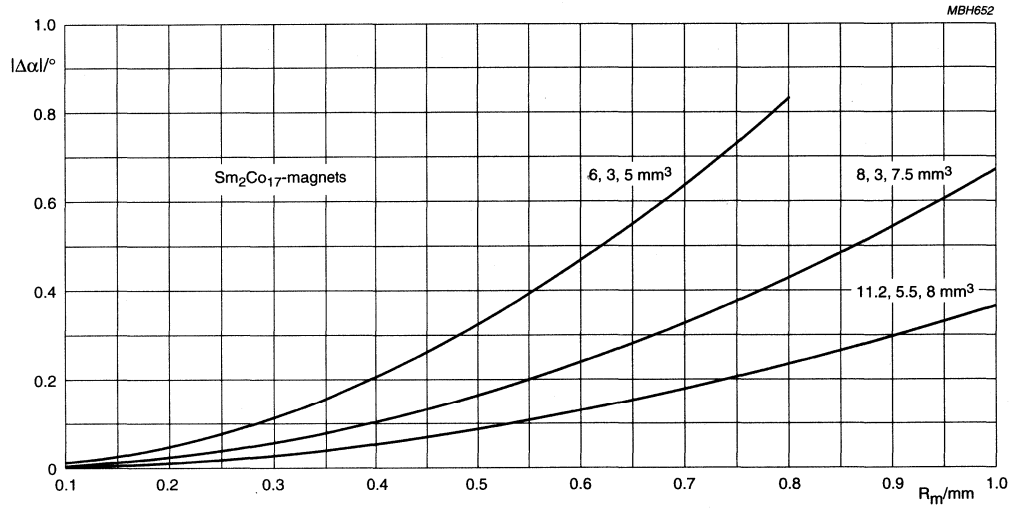

Fig.17 Maximum angle tolerances $\Delta\alpha$.

Double sensor system (KMZ41)

In this case, both sensors are influenced differently and the resulting tolerance $\Delta\alpha$ has to be calculated from the deviations of the two response curves. If C.Rm2 is sufficiently small, and the angle a is calculated from the relation of the two output signals via the arc-tan function, then the resulting measuring tolerance can be described by:

$$|\Delta\alpha| = C \times R_m^2 \times \cos 4\alpha \times \sin 2(\alpha + \delta)$$

This leads to the worst case tolerance of $|\Delta\alpha| = C \times R_m^2$ occurring at $\alpha = 0°$, 45° and 90° and a tolerance of zero at $\alpha = 22.5°$, 67.5° and 112.5°. These zero positions can be used to adjust the sensor for the highest precision measurements.

If the sensors are adjusted in this way, the maximum tolerance is limited to $C \times R_m^2$.

DEVICE DATA

in alphanumeric sequence

Angle sensor hybrid — KM110BH/2130; KM110BH/2190

DESCRIPTION

Sensor module for contactless measurement of angular displacements of strong magnetic fields. The module is a ready-trimmed (sensitivity and zero point) combination of the magnetoresistive sensor KMZ10B and a signal conditioning circuit in hybrid technology. The KM110BH/2130 delivers a linear output signal that is proportional to the direction of the magnetic field. The KM110BH/2190 delivers a sinusoidal signal.

For new design-ins the KM110BH/23 and KM110BH/24 modules are recommended.

PINNING

PIN	DESCRIPTION
1	ground
2	V_{CC}
3	V_O

PIN CONFIGURATION

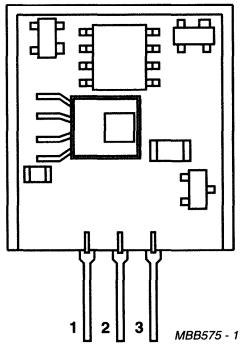

Fig.1 Simplified outline.

QUICK REFERENCE DATA

SYMBOL	PARAMETER	MIN.	TYP.	MAX.	UNIT
V_{CC}	DC supply voltage	–	5	–	V
V_O	output voltage range	0.5	–	4.5	V
α	angle range				
	KM110BH/2130	–15	–	+15	deg
	KM110BH/2190	–45	–	+45	deg
T_{op}	operating temperature	–40	–	+125	°C

LIMITING VALUES

In accordance with the Absolute Maximum Rating System (IEC 134).

SYMBOL	PARAMETER	MIN.	MAX.	UNIT
V_{CC}	supply voltage	4.5	5.5	V
I_{CC}	supply current	–	20	mA
T_{stg}	storage temperature	–40	+125	°C
T_{op}	operating temperature	–40	+125	°C
	output short-circuit duration	permanent (see note 1)		

Note

1. If pin 3 is shorted to either pin 1 or pin 2, current may flow permanently, without damage to the device.

CHARACTERISTICS

T_{amb} = 25 °C; V_{CC} = 5 V and a homogeneous magnetic field H_{ext} = 100 kA/m in the sensitive layer of the KMZ sensor; unless otherwise specified.

SYMBOL	PARAMETER	CONDITIONS	MIN.	TYP.	MAX.	UNIT
α	angle range (note 1)					
	KM110BH/2130		−15	–	+15	deg
	KM110BH/2190	note 2	−45	–	+45	deg
V_O	output voltage range					
	KM110BH/2130	linear; see Fig.4	0.5	–	4.5	V
	KM110BH/2190	sinusoidal; see Fig.5	0.5	–	4.5	V
V_{zero}	zero point voltage	α = 0 deg	–	2.5	–	V
V_{off}	zero point offset voltage					
	KM110BH/2130		−45	–	+45	mV
	KM110BH/2190		–	±35	–	mV
S	sensitivity (note 3)	α = 0 deg				
	KM110BH/2130		–	139	–	mV/deg
	KM110BH/2190		–	70	–	mV/deg
FL	deviation of linearity (note 4)					
	KM110BH/2130		–	–	±1	%/FS
	KM110BH/2190		–	–	–	%/FS
SP_{max}	maximum angular speed					
	KM110BH/2130		–	10	–	deg/ms
	KM110BH/2190		–	30	–	deg/ms
R_L	load resistance		10	–	–	kΩ
Temperature coefficients (−40 to +85 °C)						
TCV_{zero}	temperature coefficient of zero point voltage					
	KM110BH/2130		–	0.6	–	mV/K
	KM110BH/2190		–	0.3	–	mV/K
TCS	temperature coefficient of sensitivity		–	±200	–	ppm/K

Notes

1. Refer to Fig.3. The magnetic field can be produced by using the first magnet listed in Table 1. Other magnets, along with their required distances from the front of the KMZ sensor, are also given.
2. Valid for $H_{ext} = \infty$. The real field strength of 100 kA/m gives a slightly higher operating angle range of ±46.5 deg.
3. The sensitivity will change slightly with +0.33% per 10% magnetic field increase if H_{ext} deviates from 100 kA/m.
4. Deviation from best straight line in angle range.

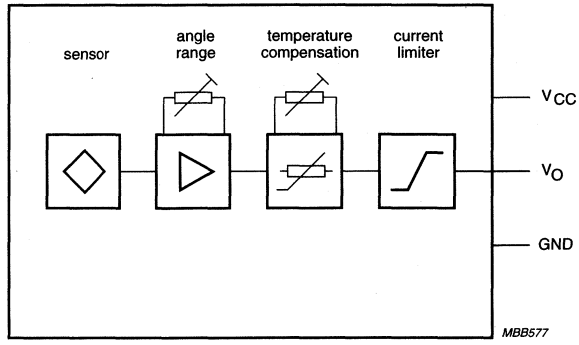

Fig.2 Circuit diagram.

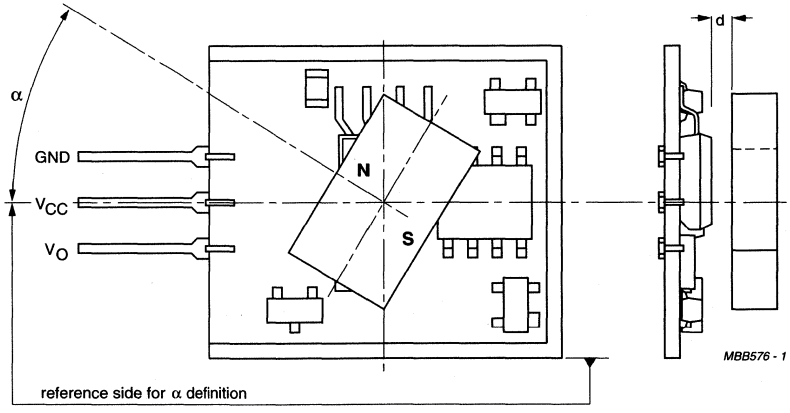

Fig.3 Optimum magnet position relative to the sensor module.

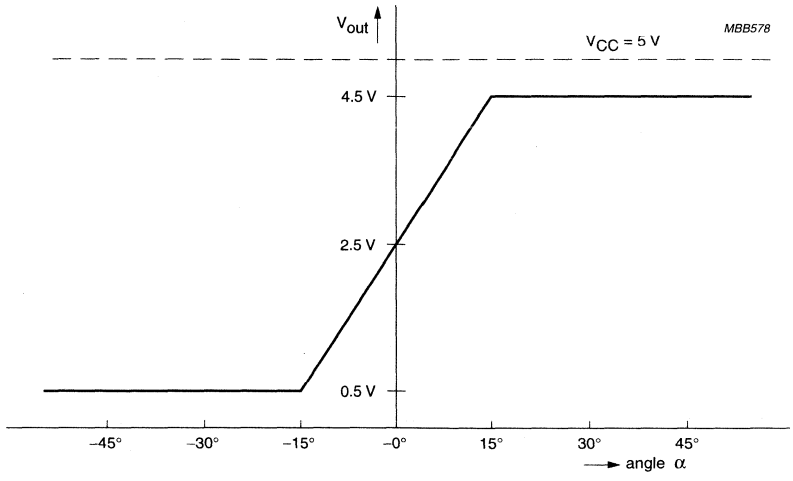

Fig.4 Output signal of KM110BH/2130.

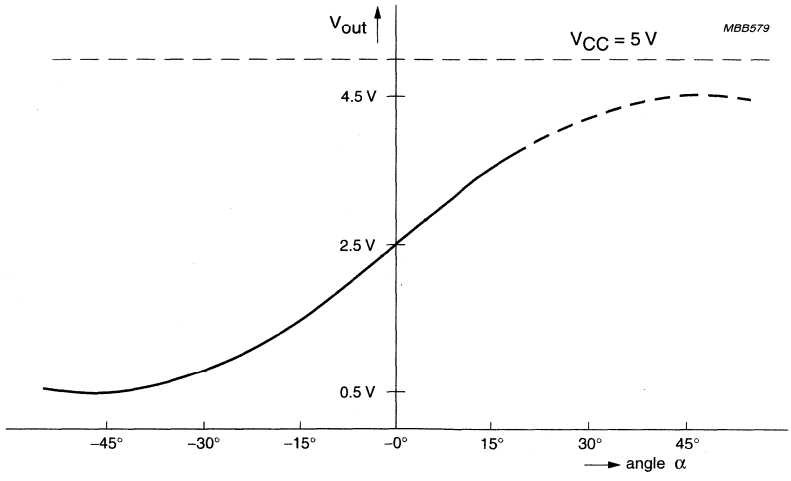

Fig.5 Output signal of KM110BH/2190.

Table 1 Magnets for angle sensor hybrids

MAGNETS			HYBRID ANGLE SENSORS			
MATERIAL	DIMENSIONS[1] (mm)	TEMP. RANGE (°C)	DISTANCE d[2] (mm)	ANGLE RANGE CORRESPONDING TO V_O = 0.5 to 4.5 V		TEMP. RANGE (°C)
				/2130	/2190	
NdFeB (note 3)	11.2 × 5.5 × 8	−55 to +110	2.5	30	93	−40 to +125
NdFeB (note 3)	6 × 3 × 5		0.8			
SmCo	11.2 × 5.5 × 8	−55 to +125	2.0	30	93	
SmCo	6 × 3 × 5		0.6			
FXD 330	10 × 7 × 8	−55 to +125	0.5	30.5	94.5	
FXD 330	7 × 5 × 4		0.2	30	93	

Notes

1. The magnetization is always parallel to the last dimension given for each magnet type.
2. Between magnet and KMZ sensor front as shown in Fig.3.
3. Special care must be taken to avoid exposure of NdFeB magnets to moisture or vapour.

APPLICATION

In life-support systems, the behaviour of electronic components throughout their working life can be unpredictable. The use of these devices in support systems can only be permitted when there is no danger to life caused by devices failing unexpectedly.

PACKAGE OUTLINE

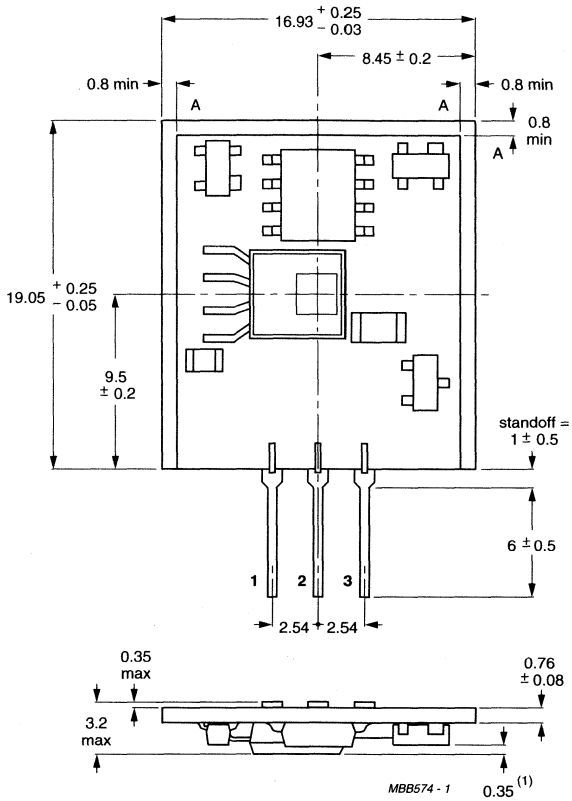

Dimensions in mm.

Area 'A' free of SMD devices.

(1) Sensitive layer below KMZ front.

Fig.6 KM110BH/2130; KM110BH/2190.

Angle sensor hybrid circuit KM110BH/2270

FEATURES

- Angle measuring range 70°
- Contactless, therefore wear-free and no micro-linearity problems
- Easy to mount, ready for use
- Analog current output signal
- Operating temperatures up to 100 °C
- EMC resistant
- Sample kit with magnet available.

DESCRIPTION

Sensor module for contactless measurement of angular displacements of strong magnetic fields between −35° and +35°. The module is a ready-trimmed (sensitivity and zero point) combination of the magnetoresistive sensor KMZ10B and a signal conditioning circuit in hybrid technology. The KMZ110BH/2270 delivers a sinusoidal current output signal which is a function of the direction of the magnetic field. The module can be used for contactless angle measurement.

PIN OPTIONS

The KMZ110BH/2270 sensor hybrid is available with different electrical contacts.

- Stretched pins (see Fig.8) with a pitch of 2.54 mm. These pins are recommended for connector and/or cable connections.
- Double 's' bent pins (see Fig.6) with a pitch of 5.71 mm. Bent pins are recommended for rigid soldered connections to compensate for mechanical stress. This hybrid circuit is available under type number KM110BH/2270G.

PINNING

PIN	DESCRIPTION
1	ground
2	V_{CC}
3	I_O

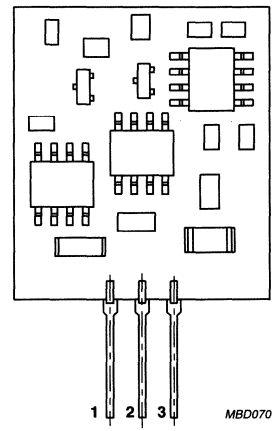

Fig.1 Simplified outline.

QUICK REFERENCE DATA

SYMBOL	PARAMETER	MIN.	TYP.	MAX.	UNIT
V_{CC}	DC supply voltage	–	8.5	–	V
I_O	output current range	–	4 to 20	–	mA
α	angle range	–	−35 to +35	–	deg
T_{op}	operating temperature	−40	–	+100	°C

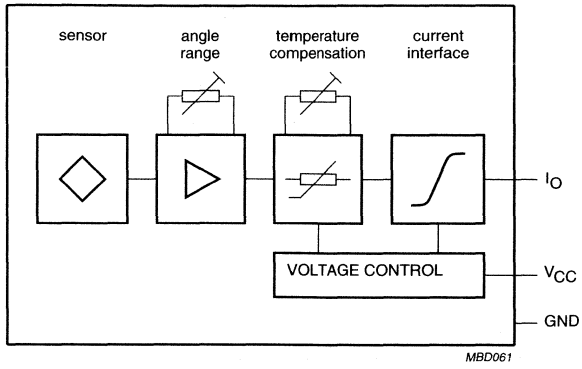

Fig.2 Circuit diagram.

LIMITING VALUES

In accordance with the Absolute Maximum Rating System (IEC 134).

SYMBOL	PARAMETER	MIN.	MAX.	UNIT
V_{CC}	DC supply voltage	8.1	11	V
I_{CC}	supply current	–	40	mA
T_{stg}	storage temperature	−40	+125	°C
T_{op}	operating temperature	−40	+100	°C
	output short-circuit duration	permanent; note 1		

Note

1. If pin 3 is shorted to either pin 1 or pin 2, current may flow permanently, without damage to the device.

CHARACTERISTICS

T_{amb} = 25 °C; V_{CC} = 8.5 V and a homogeneous magnetic field H_{ext} = 100 kA/m in the sensitive layer of the KMZ10B sensor; unless otherwise specified.

SYMBOL	PARAMETER	CONDITIONS	MIN.	TYP.	MAX.	UNIT
α	angle range	note 1	–	–35 to +35	–46.5 to +46.5	deg
I_O	output current range	note 2; sinusoidal; see Fig.4	–	4 to 20	3.2 to 20.8	mA
I_{zero}	zero point current	α = 0°	–	12	–	mA
I_{offset}	zero point offset current		–	±120	–	µA
S	sensitivity	α = 0°; note 3	0.289	0.292	0.295	mA/deg
Rp	reproducibility	α = 0°; note 4	–	<0.001	–	deg
Rs	resolution	α = 0°; note 5	–	<0.001	–	deg
Rhy	hysteresis	α = 0°; note 6	–	<0.05	–	deg
SP_{max}	maximum angular speed		–	20	–	deg/ms
R_L	load resistance		–	200	220	Ω
Temperature coefficients (–40 to +85 °C)						
TCI_{zero}	temperature coefficient of zero point current		–	±1.5	–	µA/K
TCS	temperature coefficient of sensitivity		–	±100	–	ppm/K

Notes

1. Refer to Fig.3. The magnetic field H_{ext} = 100 kA/m can be produced by using the magnets listed in Table 1.
2. Maximum values refer to ±46.5° including offset and sensitivity tolerances.
3. The sensitivity will change slightly with +0.33% per 10% magnetic field increase if H_{ext} deviates from 100 kA/m.
4. Difference in output signal (expressed in degrees) between two zero point (α = 0) measurements, in which the zerc point is approached from the same side of the measuring range (e.g. cycle: +35° → 0° → +35° → 0°).
5. The smallest detectable change of angle $\Delta\alpha$ for α = 0° (cycle: 0° → $\Delta\alpha$).
6. As note 4, but with the zero point being approached from the upper end and lower end of the measuring range respectively (cycle: +35° → 0° → –35° → 0°).

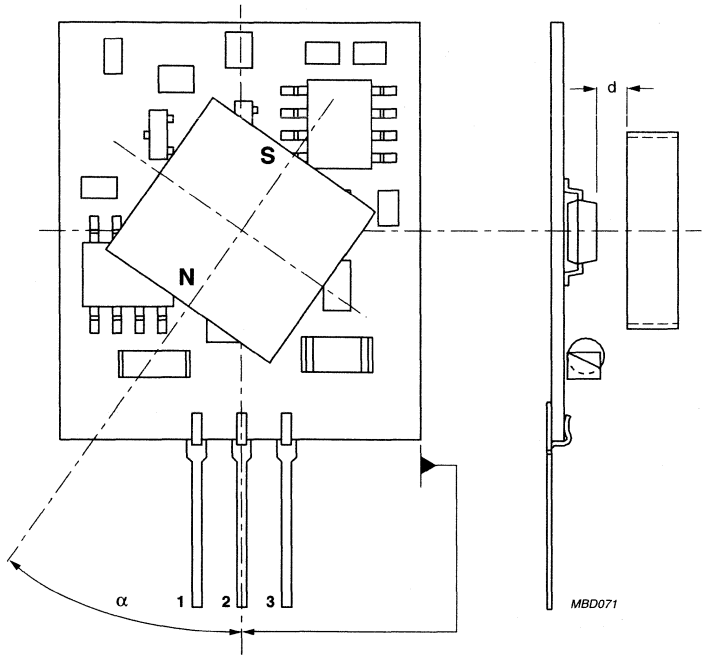

Fig.3 Optimum magnet position relative to the sensor module.

Table 1 Magnets for angle sensor hybrid

MATERIAL	DIMENSIONS[1] (mm)	DISTANCE 'd'[2] (mm)	TOLERANCE OF 'd'[3] (mm)	ECCENTRICITY[4] (mm)	TEMPERATURE RANGE (°C)
Sm_2Co_{17}	11.2 × 5.5 × 8	2.1	±0.30	±0.25	−55 to +125
	6 × 3 × 5	0.7	±0.15	±0.15	
	8 × 3 × 7.5	0.5	±0.30	±0.20	

Notes

1. The magnetization is always parallel to last dimension given in each of the cells in this column.
2. Between magnet and KMZ11B1 sensor front as shown in Fig.3.
3. Maximum deviation of distance 'd' for which the change in sensor output signal is smaller than 0.5% of full scale sensor signal.
4. Maximum deviation of magnet rotational axis to sensor rotational axis for which the change in sensor output signal is smaller than 0.5% of full scale sensor signal.

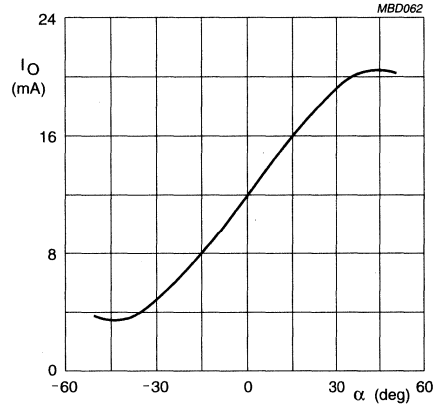

$I_{o(nom)} = 12 + 8.644 \times \sin(1.935 \times \alpha)$ in the range $-46.5° \leq \alpha \leq +46.5°$.
T_{amb} = 25 °C; V_{CC} = 8.5 V; H_{ext} = 100 kA/m.

Fig.4 Output current as a function of angular displacement.

APPLICATION INFORMATION

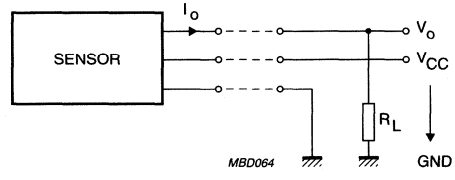

Fig.5 Application example.

PACKAGE OUTLINE - BENT PIN OPTION

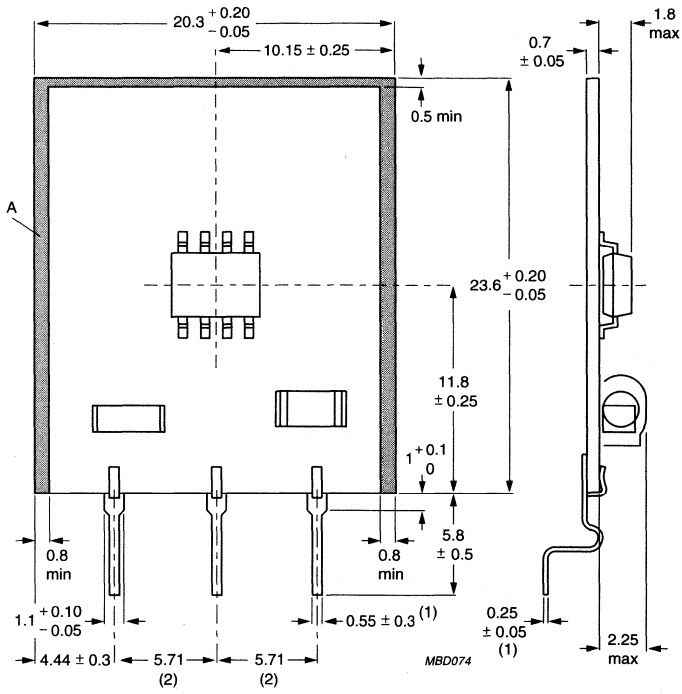

Dimensions in mm.

Area 'A' (shaded) free of SMD devices.

(1) Dimension before bath soldering; maximum dimension after bath soldering: 0.7 mm.

(2) Pitch tolerance: 0.2 mm.

Fig.6 KM110BH/2270G.

REFERENCE DATA FOR THE ASSEMBLY AND MAGNET POSITIONING - BENT PIN OPTION

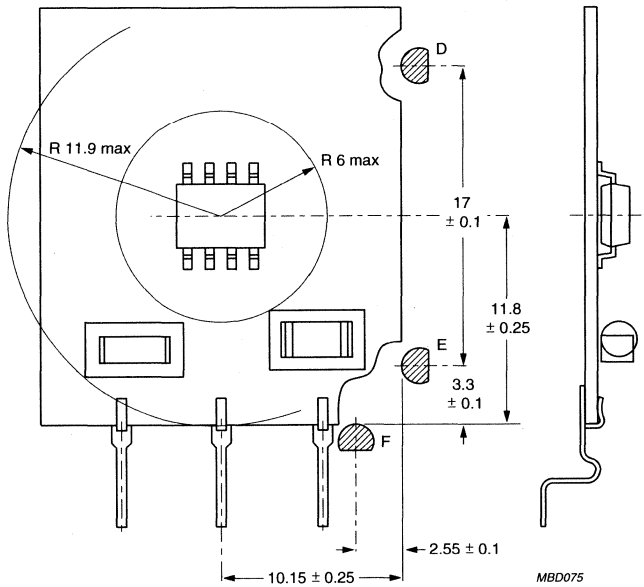

Dimensions in mm.

D, E: Definition of reference side for angle α.

D, E, F: Reference points for sensor assembly.

Radii for free rotation of magnets due to height of the components on the hybrid circuit.

Fig.7 KM110BH/2270G.

PACKAGE OUTLINE - STRETCHED PIN OPTION

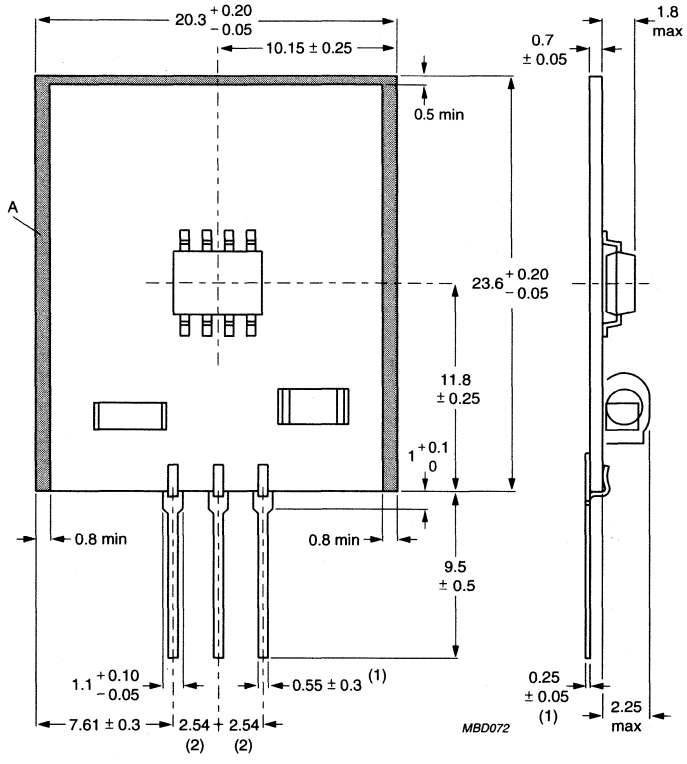

Dimensions in mm.

Area 'A' (shaded) free of SMD devices.

(1) Dimension before bath soldering; maximum dimension after bath soldering: 0.7 mm.

(2) Pitch tolerance: 0.2 mm.

Fig.8 KM110BH/2270.

REFERENCE DATA FOR THE ASSEMBLY AND MAGNET POSITIONING - STRETCHED PIN OPTION

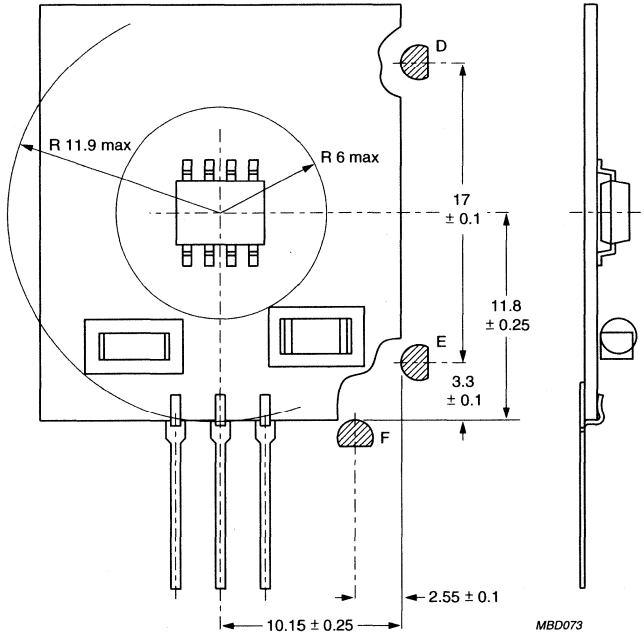

Dimensions in mm.

D, E: Definition of reference side for angle α.

D, E, F: Reference points for sensor assembly.

Radii for free rotation of magnets due to height of the components on the hybrid circuit.

Fig.9 KM110BH/2270.

30° and 70° angle sensor hybrids

KM110BH/2430; KM110BH/2470

FEATURES

- Angle measuring range 30° or 70°
- Contactless, therefore wear-free and no microlinearity problems
- Easy to mount, ready for use
- Analog voltage output signal
- Operating temperatures up to 125 °C
- Precision of ± 0.5° in the temperature range ($-15° \leq \alpha \leq +15°$)
- EMC resistant
- Sample kit with magnet available.

DESCRIPTION

The KM110BH/2430 and the KM110BH/2470 are sensor modules for contactless measurement of angular displacements of strong magnetic fields. The modules are a ready-trimmed (sensitivity and zero point) combination of a magnetoresistive KMZ sensor and a signal conditioning circuit in hybrid technology.

The KM110BH/2430 delivers a voltage output signal which is a linear function of the direction of the magnetic field. The KM110BH/2470 delivers a sinusoidal voltage output signal. The modules can be used for contactless angle measurement.

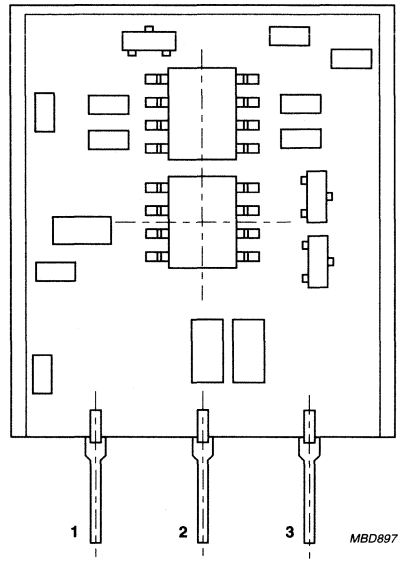

Fig.1 Simplified outline.

PINNING

PIN	SYMBOL	DESCRIPTION
1	GND	ground
2	V_{CC}	DC supply voltage
3	V_O	output voltage

QUICK REFERENCE DATA

SYMBOL	PARAMETER	MIN.	TYP.	MAX.	UNIT
V_{CC}	DC supply voltage	4.5	5	16	V
T_{oper}	operating temperature	−40	−	+125	°C
α	angle range:				
	KM110BH/2430	−	−15 to +15	−	deg
	KM110BH/2470	−	−35 to +35	−	deg
V_O	output voltage range	−	0.5 to 4.5	−	V

EMC RESISTIVITY

The EMC compatibility is dependent on the assembly of the sensors. The EMC resistivity has to be tested in the final application.

BLOCK DIAGRAM

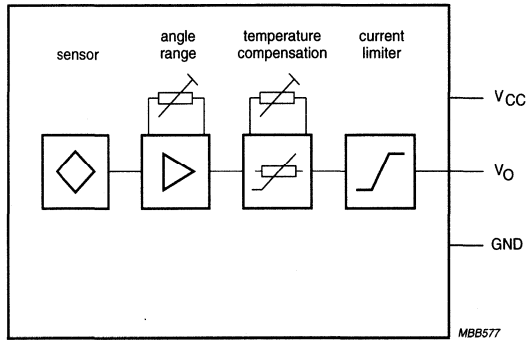

Fig.2 Block diagram.

LIMITING VALUES

In accordance with the Absolute Maximum Rating System (IEC 134).

SYMBOL	PARAMETER	MIN.	MAX.	UNIT
V_{CC}	DC supply voltage	4.5	16	V
I_{CC}	supply current	–	15	mA
T_{stg}	storage temperature	−40	+125	°C
T_{oper}	operating temperature; note 1	−40	+125	°C
	output short-circuit duration	permanent; see note 2		

Notes

1. For operations above T_{oper} = 100 °C, maximum V_{CC} derates linearly from 16 V to 5 V at T_{oper} = 125 °C.
2. If pin 3 is shorted to either pin 1 or pin 2, a current may flow permanently, without damaging the device.

CHARACTERISTICS

T_{amb} = 25 °C; V_{CC} = 5 V; R_L = 1.7 kΩ and a homogeneous magnetic field H_{ext} = 100 kA/m in the sensitive layer of the KMZ sensor, unless otherwise specified.

SYMBOL	PARAMETER	CONDITIONS	MIN.	TYP.	MAX.	UNIT
α	angle range:	note 1				
	KM110BH/2430		–	–15 to +15	–	deg
	KM110BH/2470		–	–35 to +35	–	deg
V_O	output voltage range:					
	KM110BH/2430	linear; see Fig.4	–	0.5 to 4.5	–	V
	KM110BH/2470	sinusoidal; see Fig.5	–	0.5 to 4.5	–	V
V_{zero}	zero point voltage	α = 0°	–	2.5	–	V
V_{off}	zero point offset voltage:	related to sinusoidal sensor characteristic; see Fig.5				
	KM110BH/2430		–	±25	–	mV
	KM110BH/2470		–	±15	–	mV
α_{off}	zero point offset angle	related to hybrid edges; see Fig.7	–	1	3	deg
S	sensitivity:	α = 0°; note 2				
	KM110BH/2430		137	140	143	mV/deg
	KM110BH/2470		73	74.5	76	mV/deg
P	precision:	–20 to +100 °C	–			
	KM110BH/2430			0.2	0.5	deg
	KM110BH/2470			0.5	1.2	deg
FL	deviation of linearity:	note 3				
	KM110BH/2430		–	±1	–	%·FS
	KM110BH/2470		–	–	–	%·FS
R_p	reproducibility	α = 0°; note 4	–	<0.001	–	deg
R_s	resolution	α = 0°; note 5	–	<0.001	–	deg
FH	hysteresis	α = 0°; note 6	–	<0.05	–	deg
SP_{max}	maximum angular speed:					
	KM110BH/2430		–	60	–	deg/ms
	KM110BH/2470		–	150	–	deg/ms
R_L	load resistance		1.7	–	–	kΩ
C_L	load capacitance		–	–	10	nF
Temperature coefficients (–40 to +100 °C)						
TCV_{zero}	temperature coefficient of zero point voltage:					
	KM110BH/2430		–	0.2	0.6	mV/K
	KM110BH/2470		–	0.1	0.3	mV/K
TCS	temperature coefficient of sensitivity	–20 to 100 °C	–	100×10^{-6}	–	K^{-1}

Notes to the characteristics

1. Refer to Fig.3. The magnetic field H_{ext} = 100 kA/m can be achieved using the magnets listed in Table 1.
2. The sensitivity will change slightly with +0.33% per 10% magnetic field increase if H_{ext} deviates from 100 kA/m.
3. Deviation from best straight line in angle range.
4. Difference in output signal (expressed in degrees) between two zero point (α = 0°) measurements, in which the zero point is approached from the same side of the measuring range (e.g. cycle: +15° ⇒ 0° ⇒ +15° ⇒ 0°).
5. The smallest detectable change of angle $\Delta\alpha$ for α = 0° (cycle: 0° ⇒ $\Delta\alpha$).
6. As note 4, but with the zero point being approached from the upper end and lower end of the measuring range respectively (cycle: +15° ⇒ 0° ⇒ −15° ⇒ 0°).

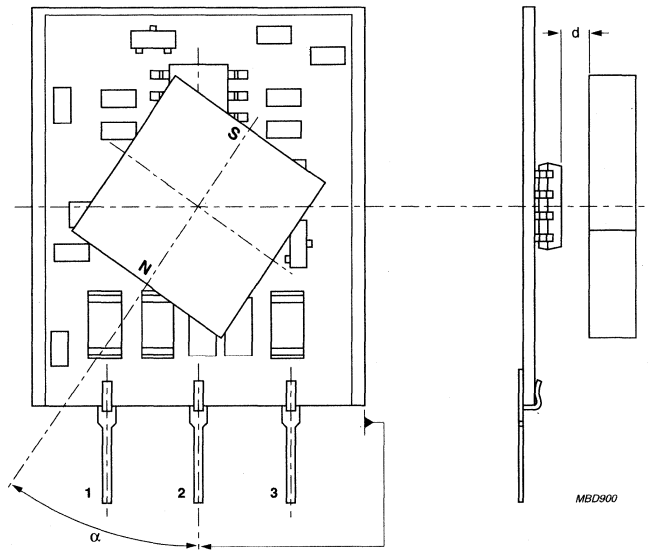

Fig.3 Optimum magnet position relative to the sensor module.

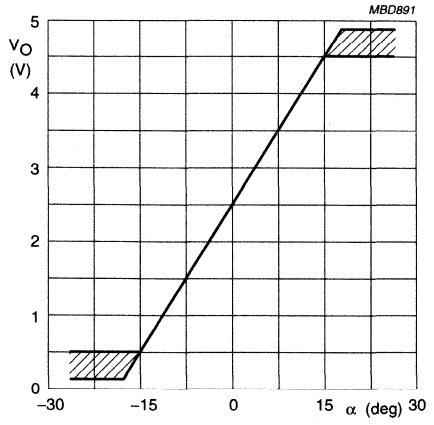

Fig.4 KM110BH/2430 output signal as a function of angle position.

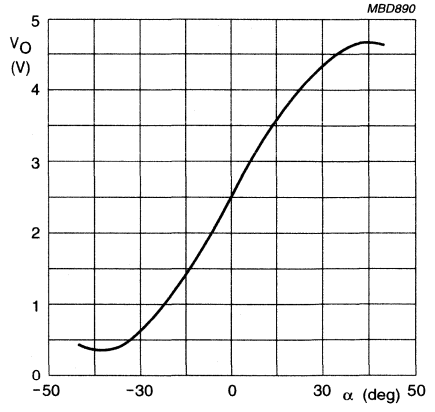

Fig.5 KM110BH/2470 output signal as a function of angle position.

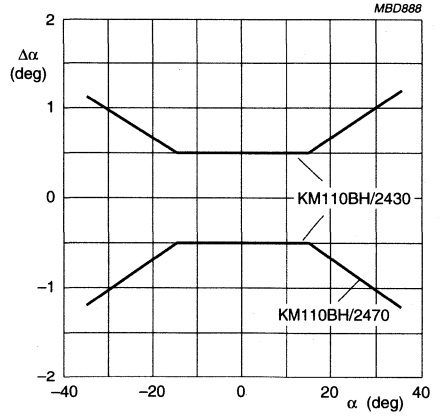

T_{amb} = −25 to +85 °C.
α = 0° for T_{amb} = 25 °C and V_O = 2.5 V.
Δα increases by a factor 2 in the temperature range:
$V_O = 2.5 + 2.128 \times \sin(2\alpha)$ for $-36.5° \leq \alpha \leq +36.5°$.
T_{amb} = 25 °C; V_{CC} = 5 V; H_{ext} = 100 kA/m.

Fig.6 Maximum angle error Δα as a function of the angle position.

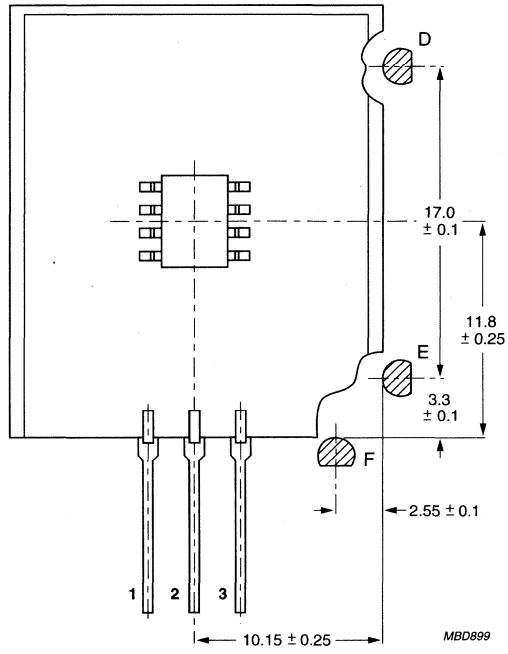

Dimensions in mm.
D, E, F : reference points for sensor assembly.
D, E : definition of reference side for angle α.

Fig.7 Reference data for hybrid assembly and magnet positioning.

Table 1 Magnets for angle sensor hybrid

MATERIAL	DIMENSIONS[1] (mm)	d[2] (mm)	TOLERANCE[3] d (mm)	ECCENTRICITY[4] (mm)	T_{amb} (°C)
Sm_2Co_{17}	11.2 × 5.5 × 8	2.1	±0.30	±0.25	−55 to +125
	6 × 3 × 5	0.7	±0.15	±0.15	
	8 × 3 × 7.5	0.5	±0.30	±0.20	

Notes

1. The magnetization is always parallel to the latter dimensions given.
2. Distance (d) between magnet and KMZ sensor front as shown in Fig.3.
3. Maximum deviation of distance (d) for which the change in sensor output signal is smaller than 0.5% of full scale sensor signal.
4. Maximum deviation of magnet rotational axis to sensor rotational axis for which the change in sensor output signal is smaller than 0.5% of full scale sensor signal.

APPLICATION INFORMATION

The sensor hybrids KM110BH/2430 and KM110BH/2470 are available with different electrical contacts:

1. Stretched pins with a pitch of 2.54 mm; these pins are recommended for connector and/or cable connections (see Fig.9).
2. Double 's' bent pins (see Fig.10) with a pitch of 5.71 mm; bent pins are recommended for rigid soldered connections to compensate for mechanical stress. Quote type numbers KM110BH/2430G and KM110BH/2470G respectively for these hybrids.

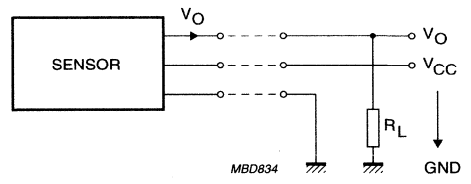

Fig.8 Application circuit.

PACKAGE OUTLINES

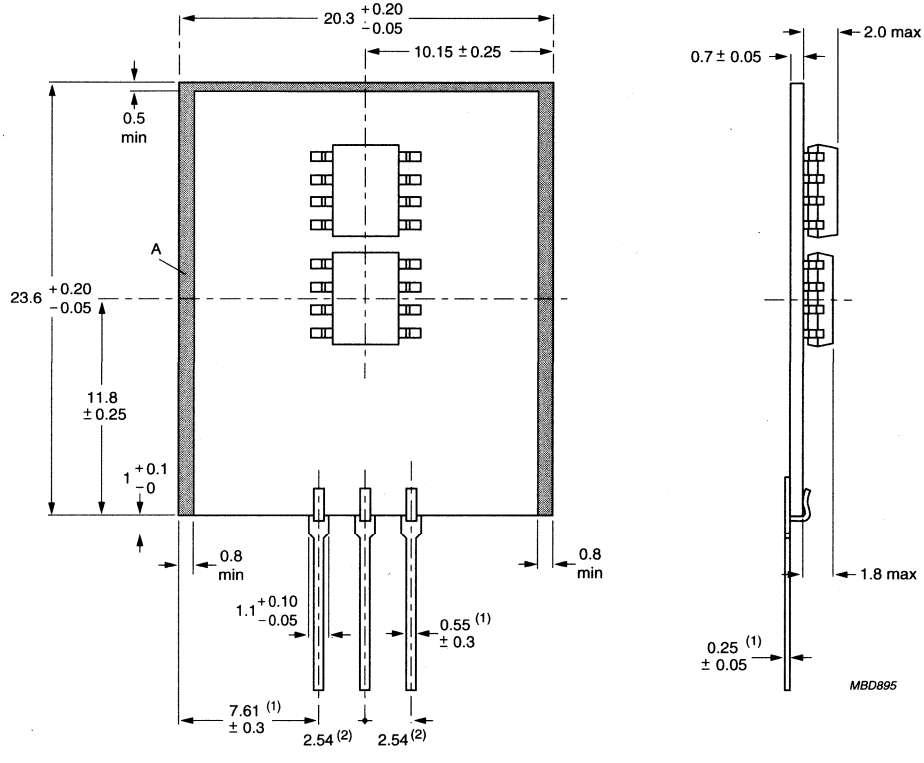

Dimensions in mm.

Area 'A' free of SMD devices.

(1) Dimension before bath soldering, maximum dimension after bath soldering: ∅ 0.7 mm.

(2) Pitch tolerance: ± 0.2 mm.

Fig.9 Outline of KM110BH/2430 and KM110BH/2470.

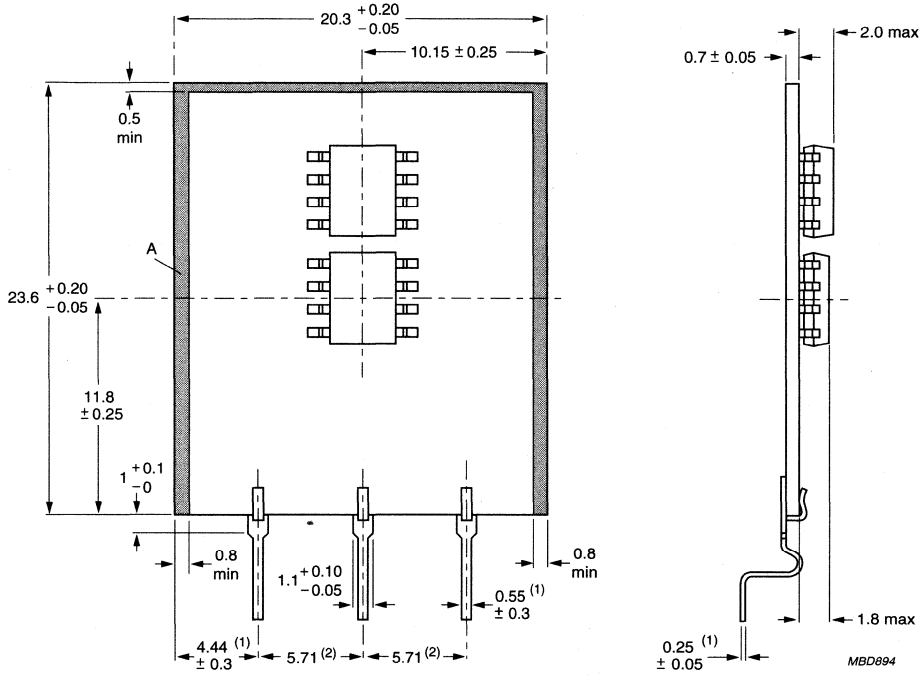

Dimensions in mm.

Area 'A' free of SMD devices.

(1) Dimension before bath soldering, maximum dimension after bath soldering: ∅ 0.7 mm.

(2) Pitch tolerance: ± 0.2 mm.

Fig.10 Outline of KM110BH/2430G and KM110BH/2470G.

Sensor Conditioning Electronics UZZ9000

FEATURES

- One chip angle sensor output signal conditioning
- Overall accuracy better than 1° for 100° angle range
- Temperature range from −40 to 150 °C
- Adjustable angle range
- Adjustable zero point.

DESCRIPTION

The UZZ9000 is an integrated circuit which is able to combine two sinusoidal signals (sin and cos) into one single linear output signal. These signals might come from magnetoresistive sensors. In that case this function can provide good results as the signal conditioning electronic for angle measurement forming from the output signal of two magnetoresistive sensors. This gives the sin (α) and the cos (α) of the angle to be measured a linear output characteristic for angles up to 360°. This integrated circuit can also be used for all other applications in which the sin and the cos of a signal have to be transferred in one output characteristic. A typical application would be any kind of resolver application. The two primary input signals are converted into the digital domain, with a CORDIC algorithm performing the arctan transformation. Since todays applications work typically with analog output signals (e.g. potentiometers), the resulting signal which is transferred back to the analog domain is a ratiometric one. This integrated circuit enables the user to set both the angle range to be measured (Fig.3, α_2 to α_1) and the zero point (Fig.3, α_1) in wide ranges. These ranges are determined by an external voltage divider.

PINNING

SYMBOL	PIN	DESCRIPTION
$+V_{O2}$	1	sensor 2 positive differential input
$+V_{O1}$	2	sensor 1 positive differential input
V_{DD2}	3	supply voltage (digital 2)
V_{SS}	4	ground (digital)
GND	5	ground
GND	6	ground
GND	7	ground
–	8	note 1
GND	9	ground
GND	10	ground
–	11	note 1
V_{OUT}	12	output voltage
VIA2	13	voltage input adjust 2
VIA1	14	voltage input adjust 1
OFFS2	15	voltage input adjust sensor offset 2
OFFS1	16	voltage input adjust sensor offset 1
V_{DDA}	17	supply voltage (analog)
V_{SSA}	18	ground (analog)
GND	19	ground
GND	20	ground
V_{DD1}	21	supply voltage (digital 1)
–	22	note 1
$-V_{O2}$	23	sensor 2 negative differential input
$-V_{O1}$	24	sensor 1 negative differential input

Note

1. Pin to be left unconnected.

QUICK REFERENCE DATA

SYMBOL	PARAMETER	MIN.	TYP.	MAX.	UNIT
V_{DDA}	supply voltage; note 1	4.5	5	5.5	V
V_{DD1}	supply voltage; note 1	4.5	5	5.5	V
V_{DD2}	supply voltage; note 1	4.5	5	5.5	V
$I_{CC\ (tot)}$	total supply current	–	12	–	mA
V_{S1}	differential input voltage (peak voltage)	−140	–	+140	mV
V_{S2}	differential input voltage (peak voltage)	−140	–	+140	mV
V_{S1}	common mode range	2.2	–	2.8	V
V_{S2}	common mode range	2.2	–	2.8	V
V_{out}	output voltage range (ratiometric)	5	–	95	$\%V_{DD}$
VIA1	programmable offset voltage	−2.5	–	+2.5	$\%V_{DD}$
VIA2	programmable gain factor	1	–	6	
A	accuracy (deviation from best straight line)	−0.5	–	+0.5	$\%V_{DD}$
R	resolution	–	0.05	0.1	$\%V_{DD}$
H	hysteresis	–	0.05	0.1	$\%V_{DD}$
T_{amb}	ambient temperature	−40	–	+150 (2)	°C

Notes

1. V_{DDA}, V_{DD1} and V_{DD2} must be connected to the same supply voltage.
2. 200 hours (125 °C continuous).

CIRCUIT BLOCK DIAGRAM

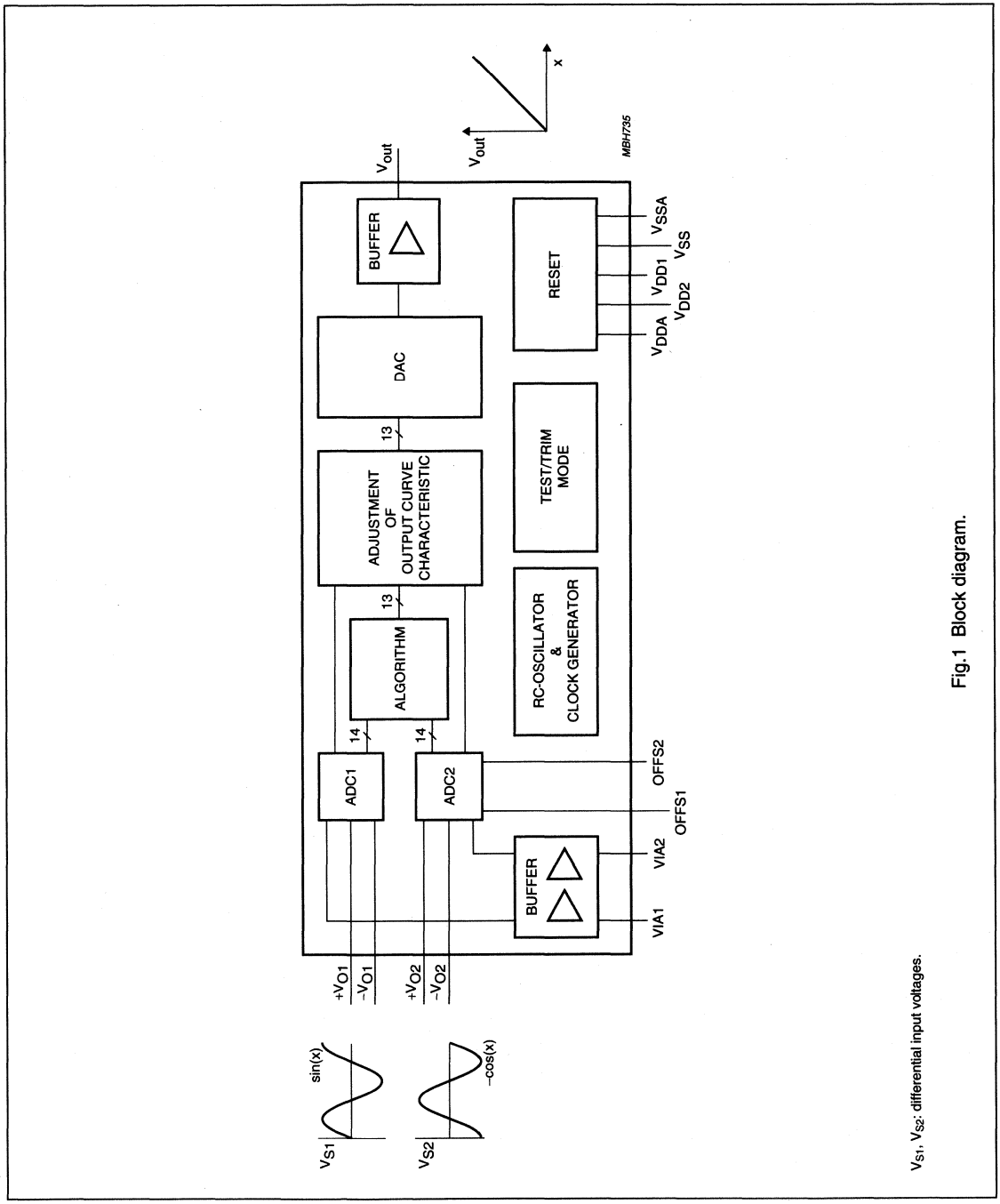

Fig.1 Block diagram.

V_{S1}, V_{S2}: differential input voltages.

APPLICATION INFORMATION

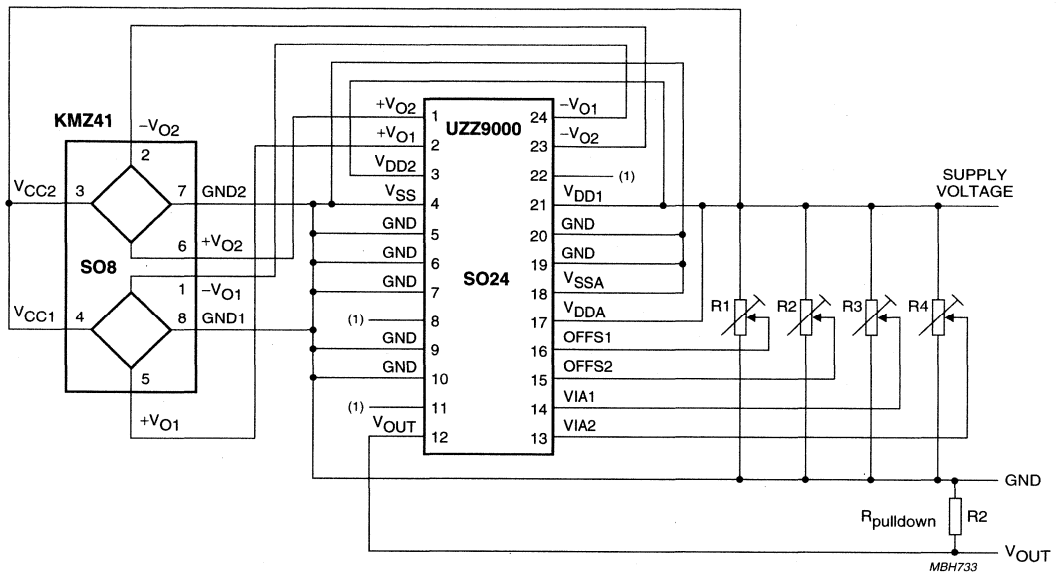

(1) Pin to be left unconnected.

Fig.2 Application circuit.

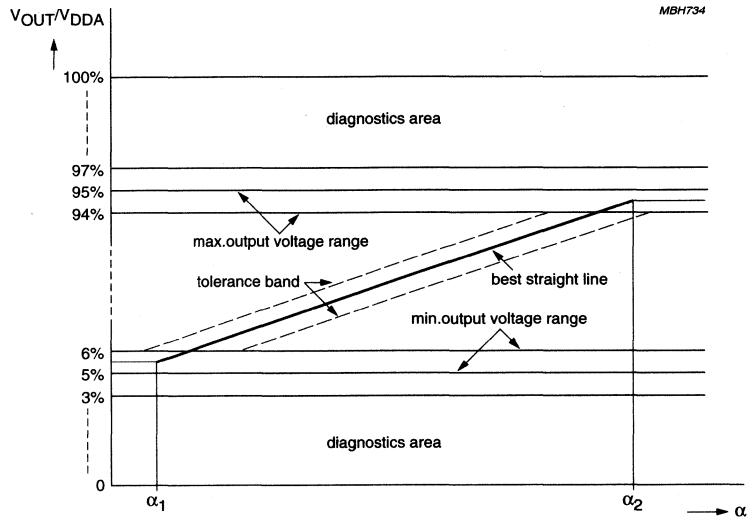

Fig.3 Output characteristic.

GENERAL
TEMPERATURE SENSORS

GENERAL

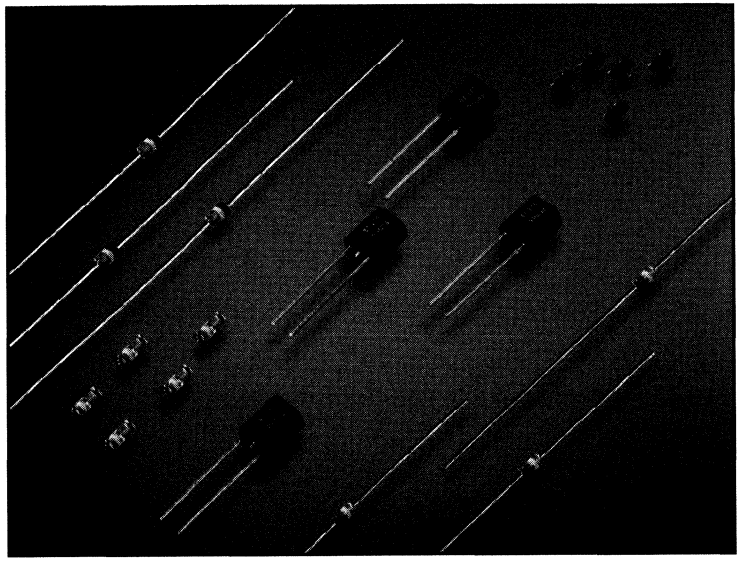

Fig.1 The KTY sensors.

With their high accuracy and excellent long term stability, the KTY series of silicon sensors in spreading resistor technology provide an attractive alternative to the more conventional sensors based on NTC or PTC technology. Their main advantages are:

- Long term stability
- Si batch process based technology
- Virtual linear characteristics.

Table 1 Drifts of Si Sensors

After 10000 hours permanent operation with nominal operating current at maximum operating temperature.

TYPE	TYPICAL DRIFT (K)	MAXIMUM DRIFT (K)
KTY81-1 KTY82-1	0.20	0.50
KTY81-2 KTY82-2	0.20	0.80
KTY83	0.15	0.40
KTY85	0.13	0.25

The properties of our temperature sensors are based on those of the chemical element silicon, and therefore sensor behaviour is as stable as this chemical element. This means that temperature drifts during the lifetime of the products are negligible. In recent tests this has been verified, when sensors operating at their maximum operating temperature for 10000 hours (equivalent to 1.14 years) have shown typical drifts of 0.2 K with a maximum of 0.4 K to 0.8 K.

Long term stability

Assuming that the sensor is typically used at half of the specified maximum temperature, our Si sensor will have a low drift as described in Table 1 for at least 450000 hours (equals 51 years). This calculation is based on the Arrenius equation (activation energy = 0.7 eV).

Si batch process products

Because our products are based on Si technology, we indirectly benefit from progress in this field, due to development of microprocessors and computer memory etc. Additionally, this indirect benefit also extends to encapsulation technology, where the trend is towards miniaturization and high volume manufacture.

Virtual linear characteristics

Si temperature sensors show a virtually linear characteristic compared to the exponential characteristic of NTCs (see Fig.2). This means that Si temperature sensors have a TK (temperature coefficient) which is nearly constant over the complete temperature range. This characteristic can be ideally exploited when the sensor is used to provide, for example, temperature compensation for a microprocessor with integrated A/D converter.

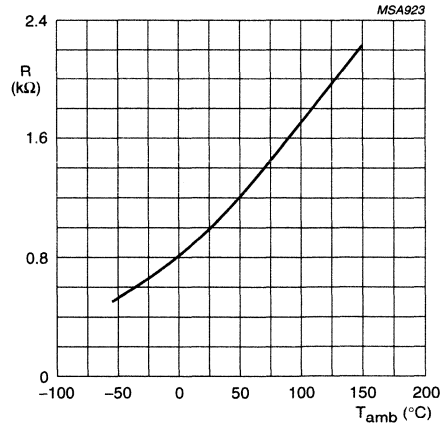

Fig.2 Characteristic of KTY81.

Construction of the sensor: spreading resistance principle

The construction of the basic sensor chip is shown in Fig.3. The chip size is ≈500 × 500 × 240 µm. The upper plane of the chip is covered by an SiO_2 insulation layer, in which a metallized hole with a diameter of ≈20 µm has been cut out. The entire bottom plane is metallized.

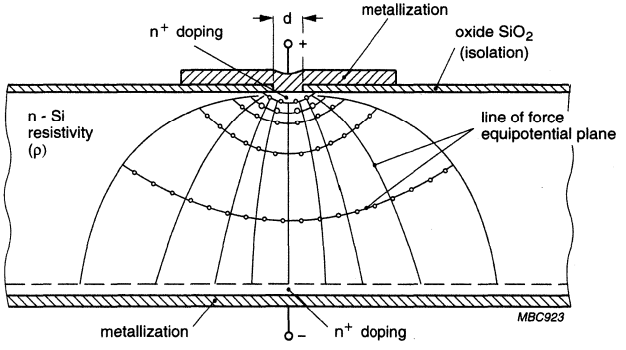

The top plane is provided with a circular metal contact; the entire bottom plane is metallized.

$$R \approx \frac{\rho}{\pi} \times \frac{1}{d}.$$

Fig.3 Section through the crystal showing the spreading resistance principle and the electrode arrangement.

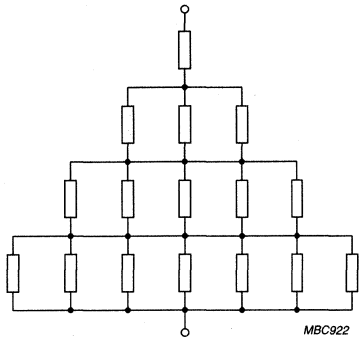

Fig.4 Equivalent circuit symbolically representing the spreading resistance principle shown in Fig.3.

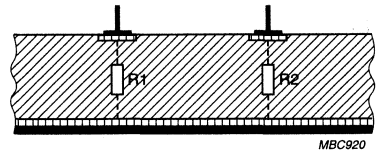

Fig.5 Setup consisting of two single sensors connected in series, but with opposite polarity.

This arrangement provides a conical current distribution through the crystal, hence the name 'spreading resistance' (see Fig.4). A major advantage of this arrangement is that the dependency of the sensor resistance on manufacturing tolerances is significantly reduced. The dominant part of the resistance is determined by the area close to the metallization hole which makes the setup independent of the Si crystal dimension tolerances. An n^+ region, diffused into the crystal beneath the metallization reduces barrier-layer effects at the metal-semiconductor junctions.

Figure 5 shows a second arrangement, effectively consisting of two single sensors connected in series, but with opposite polarity, which has the advantage of providing a resistance that is independent of current direction. This is in contrast to the single-sensor arrangement of Fig.3, which, for larger currents and temperatures above 100 °C, gives a resistance that varies slightly with the current direction.

Normally, silicon temperature sensors have a temperature limit of ≈150 °C, imposed by the intrinsic semiconductor properties of silicon. If, however, the single-sensor device is biased with its metal contact positive, the onset of intrinsic semiconductor behaviour is shifted to a higher temperature. This stems from the fact that a positive voltage on the gold contact severely depletes the hole concentration in the upper n^+ diffusion layer, and so effectively insulates holes spontaneously generated within the body of the crystal due to its intrinsic nature. As a result the holes are prevented from contributing to the total current, and hence from affecting the resistance.

The twin-sensor arrangement shown in Fig.5 has been applied in the KTY81 and KTY82 series. These sensors, in SOD70 (KTY81) and SOT23 (KTY82) packages (Figs 6 and 7), are therefore polarity independent.

The KTY83/84/85 series use the more basic single-sensor arrangement. The simplicity of this arrangement allows the sensors to be produced in the compact SOD68; DO-34 (KTY83/84) and SOD80 (KTY85) packages (Figs 8 and 9, respectively). In addition to simplicity, another important advantage of the single-sensor device is the potential for operation at temperatures up to 300 °C. The KTY84 makes use of this property, being specifically designed for operation at temperatures up to 300 °C. Table 2 provides an overview of product key characteristics.

Table 2 Overview of product - key characteristics

FAMILY TYPE	R_{25} (Ω)	AVAILABLE TOLERANCE (ΔR)	T_{oper} RANGE (°C)	PACKAGE
KTY81-1	1000	±1% up to ±5%	−55 to 150	SOD70
KTY81-2	2000	±1% up to ±5%	−55 to 150	SOD70
KTY82-1	1000	±1% up to ±5%	−55 to 150	SOT23
KTY82-2	2000	±1% up to ±5%	−55 to 150	SOT23
KTY83-1	1000	±1% up to ±5%	−55 to 175	SOD68 (DO-34)
KTY84-1	1000 (R_{100})	±3% up to ±5%	−40 to 300	SOD68 (DO-34)
KTY85-1	1000	±1% up to ±5%	−40 to 125	SOD80

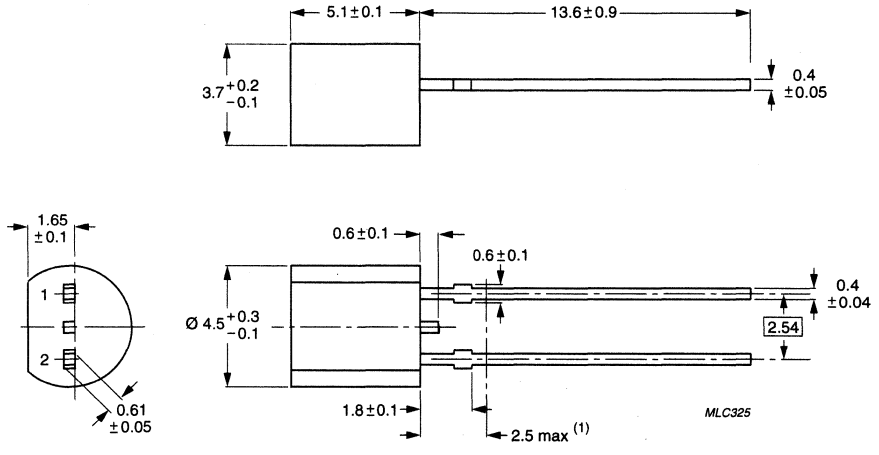

(1) Terminal dimensions within this zone are uncontrolled to allow for flow of plastic and terminal irregularities.

Fig.6 Outline of the KTY81 (SOD70).

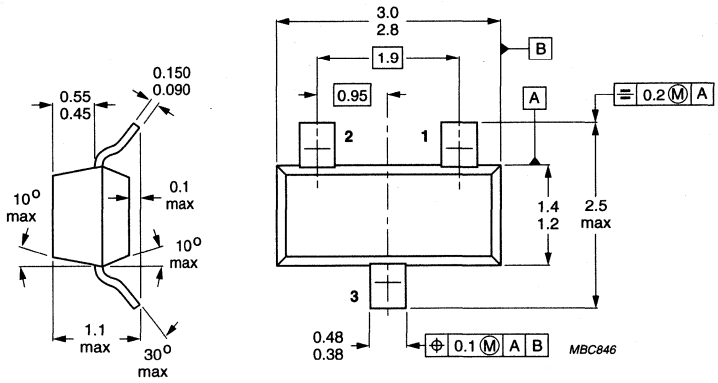

Fig.7 Outline of the KTY82 (SOT23).

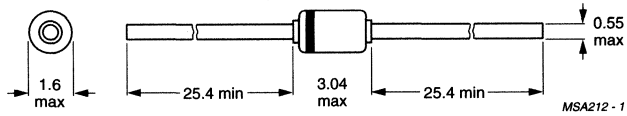

The marking band indicates the negative connector.

Fig.8 Outline of the KTY83/84 (SOD68; DO34).

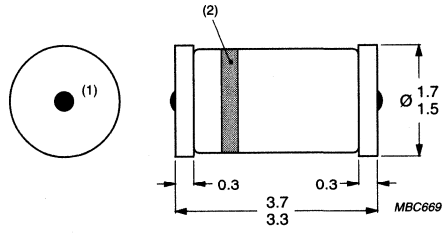

(1) Area not tinned; small elevations are possible.
(2) Indication of negative connection and product identity.

Fig.9 Outline of the KTY85 (SOD80).

TEMPERATURE DEPENDENCY

For the KTY83/85 series of temperature sensors, the mathematical expression for the sensor resistance 'R_T' as a function of temperature is given by:

$$R_T = R_{ref}\left[1 + A(T - T_{ref}) + B(T - T_{ref})^2\right] \quad (1)$$

where:

R_T is resistance at temperature T

R_{ref} is the nominal resistance at the reference temperature (T_{ref})

T_{ref} is reference temperature (100 °C for the KTY84, 25 °C for all other types)

A, B are type-dependent coefficients.

For the KTY81/82/84 series, the slope of the characteristic curve decreases slightly in the upper temperature range above a certain temperature T_I (point of inflection). Therefore, an additional term in equation (1) becomes necessary:

$$R_T = R_{ref}\left[1 + A(T - T_{ref}) + B(T - T_{ref})^2 - C(T - T_I)^D\right]$$

where:

T_I is temperature above which the slope of the characteristic curve starts to decrease (point of inflection).

C, D are type-dependent coefficients.

C is 0 for $T < T_I$.

For the types previously mentioned, the type-dependent constants 'A', 'B', 'C' and 'D', as well as 'T_I', are given in Table 3.

For high-precision applications, e.g. microcontroller-based control systems, the above expressions and the values in Table 3 can be used to generate a calibration table to store in a ROM for look-up and linear interpolation. Data for maximum expected temperature error is supplied separately in the related data sheets. The calculations are based on both specified resistance ratios (R_{25}/R_{100} and R_{25}/R_{-55}) and the basic resistance spread at 25 °C.

If a microcontroller is not used, the slight deviation from linearity can easily be compensated using a parallel resistor (if a constant current source is used), a series resistor (if a constant voltage source is used) or a suitable combination of both. This is discussed in the Section "Linearization".

Table 3 Type dependent constants

SENSOR TYPE	A (K^{-1})	B (K^{-2})	C[1] (K^{-D})	D	T_I (°C)
KTY81-1	7.874×10^{-3}	1.874×10^{-5}	3.42×10^{-8}	3.7	100
KTY81-2	7.874×10^{-3}	1.874×10^{-5}	1.096×10^{-6}	3.0	100
KTY82-1	7.874×10^{-3}	1.874×10^{-5}	3.42×10^{-8}	3.7	100
KTY82-2	7.874×10^{-3}	1.874×10^{-5}	1.096×10^{-6}	3.0	100
KTY83	7.635×10^{-3}	1.731×10^{-5}	–	–	–
KTY84	6.12×10^{-3}	1.1×10^{-5}	3.14×10^{-8}	3.6	250
KTY85	7.635×10^{-3}	1.731×10^{-5}	–	–	–

Note

1. For $T < T_I$: C = 0.

RESISTANCE/TEMPERATURE CHARACTERISTICS

Manufacturing tolerances

Silicon temperature sensors are normally produced to quite fine tolerances: 'ΔR' between ±0.5% and ±2%. Figure 10 illustrates how these tolerances are specified. The tolerance on resistance quoted in our data sheets is given by the resistance spread 'ΔR' measured at 25 °C.

Because of spread in the slope of the resistance characteristics, 'ΔR' will increase each side of the 25 °C point, to produce the butterfly curve shown in Fig.10. To give an indication of this spread in slope, we also quote the ratio of resistance at two other temperatures (–55 °C and 100 °C) to the nominal resistance at 25 °C, i.e. 'R_{-55}/R_{25}' and 'R_{100}/R_{25}'; for the KTY84, we quote 'R_{25}/R_{100}' and 'R_{250}/R_{100}'. A table giving the ΔR tolerances is included in each of the Temperature Sensor data sheets.

The user, however, is usually more interested in the maximum expected temperature error '$\pm\Delta T$'. We also provide this in the data sheets as a graph showing 'ΔT' as a function of 'T'. For the high temperature sensor KTY84, we specify the resistance spread at 100 °C.

The relation between the tolerance of the resistance of the sensor and the resulting accuracy of the temperature measurement is given by the temperature coefficient, Fig.10 shows a typical situation. In the range between –40 °C and +150 °C the temperature coefficient varies between about 1 (–40 °C) and about 0.35 (+150 °C). From this graph the relation between the expected resistance tolerance and the resulting temperature error can easily be derived. The calculated maximum temperature error is given in the form of a table in every data sheet.

Current dependency of sensor resistance

The resistance of silicon temperature sensors is dependent on the operating current. In applications with an operating current deviating from the nominal current, a deviation of sensor resistance from the nominal values has to be taken into account.

For any application, an operating current ≥0.1 mA is recommended. For lower operating currents, the current dependency is additionally influenced by temperature.

For any application with operating currents above the nominal values, it should be noted, that an additional error caused by self-heating effects will influence the measurement accuracy.

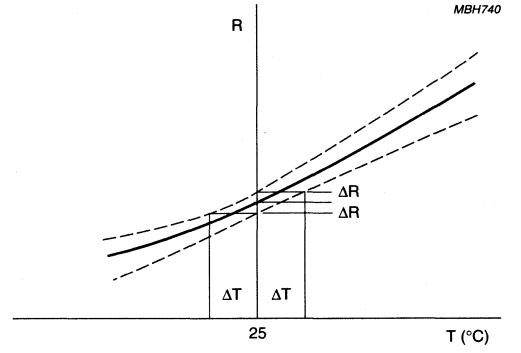

Fig.10 Butterfly curve.

Polarity of current

KTY83, 84 and 85 sensors are marked with a coloured band to indicate polarity. The published characteristics of the sensors will only be obtained if the current polarity is correct. In events where the current polarity is incorrect, the curve $R = f(T_{amb})$ differs in the upper temperature range significantly from the published form.
Note: Light, especially infrared light, also has an influence on the sensor characteristics when the current polarity is incorrect.

Linearization

The resistance/temperature characteristics of the silicon temperature sensors are nearly linear, but in some applications further linearization becomes necessary, e.g. control systems requiring high accuracy.

A simple way to do this is to shunt the sensor resistance 'R_T' with a fixed resistor 'R_L' (see Fig.11a). The resistance '$R_L \times R_T/(R_L + R_T)$' of the parallel combination then effectively becomes a linear function of temperature, and the output voltage 'V_T' of the linearized circuit can be used to regulate the control system.

If the circuit is powered by a constant-voltage source (see Fig.11b), a linearization resistor R_L can be connected in series with the sensor. The voltages across the sensor and across the resistor will then again be approximately linear functions of temperature.

The value of the series or parallel resistor depends on the required operating temperature range of the sensor.
A method for finding this resistance is described below, giving zero temperature error at three equidistant points T_a, T_b and T_c.

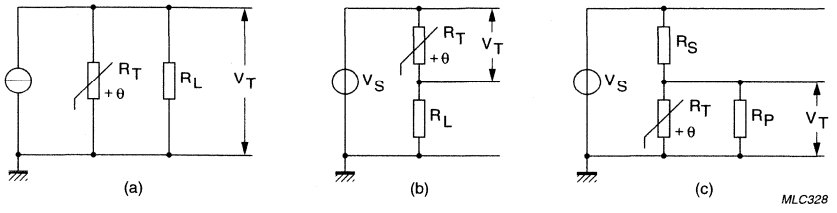

(a) With a resistor 'R_L' shunted across the sensor.
(b) With a resistor 'R_L' in series with the sensor and system powered by a constant-voltage source.
(c) With a series 'R_S' and parallel resistor 'R_P' and system powered by a constant-voltage source.

Fig.11 Linearization of sensor characteristics.

Consider the parallel arrangement. With the resistance of the sensor at three points R_a, R_b and R_c, the requirement for linearity at the three points is:

$$\frac{R_L \times R_a}{R_L + R_a} - \frac{R_L \times R_b}{R_L + R_b} = \frac{R_L \times R_b}{R_L + R_b} - \frac{R_L \times R_c}{R_L + R_c}$$

so

$$R_L = \frac{R_b \times (R_a + R_c) - 2R_a \times R_c}{R_a + R_c - 2R_b}.$$

The same resistor will also be suitable for the series arrangement.

In practice, a current source is too expensive and a fixed supply voltage, e.g. 5 or 12 V is used for a specific operating current, e.g. 1 or 0.1mA. In this case, linearization can be achieved by a series/parallel resistor combination to the sensor (see Fig.11c). The resistance of the parallel combination (R_P, R_T) and series resistor R_S is equal to the optimum linearization resistor R_L, calculated previously. Starting with the value of resistor R and with the desired current I_S through the sensor at a reference temperature T (preferably in the middle of the measured range), the resistor R_S and R_P can be calculated as follows:

$$\text{series resistor: } R_S = \frac{V_S}{I_S \times \left(\frac{R_T}{R_L} + 1\right)}$$

$$\text{parallel resistor: } R_P = \frac{1}{\frac{1}{R_L} - \frac{1}{R_S}}.$$

As an example, Fig.12 shows the deviation from linearity to be expected from a nominal KTY81 sensor, linearized over the temperature range 0 to 100 °C with a linearizing resistance of R_L = 2870 Ω.

Figure 19 shows an application example using a series/parallel combination for the KTY81 (I_S = 1 mA).

Effect of tolerances on linearized sensor characteristics

In practical applications with an arbitrary sensor, the total uncertainty in the sensor reading will be a combination of spread due to manufacturing tolerances and linearization errors.

As an example, Fig.14 shows the combined effects of manufacturing tolerances and linearization errors for the KTY81 sensor linearized over the temperature range 0 to 100 °C. Calibration of the subsequent circuitry (op-amp, control circuitry, etc.) can reduce this error significantly.

Figure 15 shows the temperature error of the system with (linear) output circuitry calibrated at 50 °C, and Fig.16 shows the error of the same system calibrated at 0 and 100 °C.

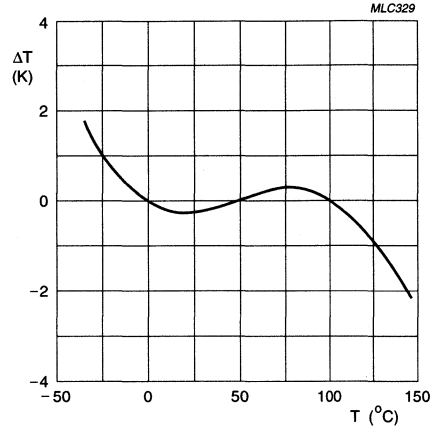

Sensor linearized over the temperature range 0 to 100 °C (linearizing resistance 2870 Ω).

Fig.12 Linearization error 'ΔT' to be expected from a nominal KTY81 sensor.

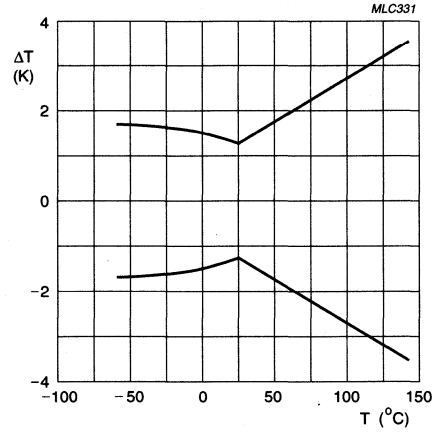

Fig.13 Maximum temperature error 'ΔT' due to manufacturing tolerances expected of a KTY81-1 sensor.

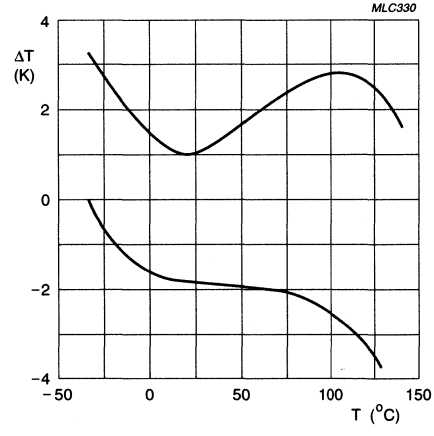

Fig.14 Combined effects of manufacturing tolerances and linearization errors for the KTY81 sensor.

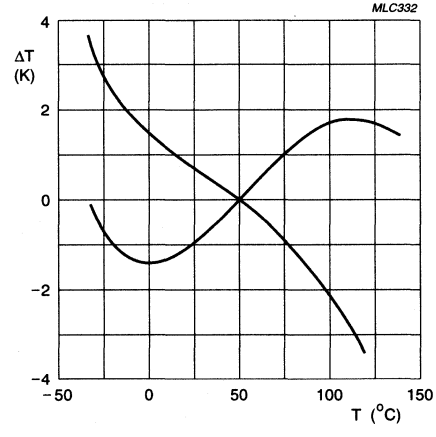

Fig.15 Maximum expected temperature error of a KTY81-1 sensor plus linearization resistor calibrated at 50 °C.

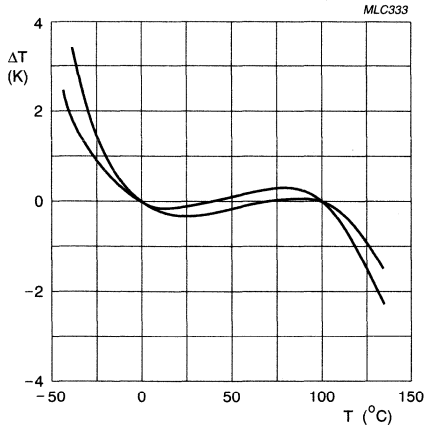

Fig.16 Error of a KTY81-1 sensor (same system as Fig.15) calibrated at 0 and 100 °C.

TEMPERATURE COMPENSATION

In many applications, it is necessary to compensate for the temperature dependency of electronic circuitry. For example, the sensitivity of many magnetic field sensors has a linear drift with temperature. To compensate for this drift, a temperature sensor with linear characteristics is required. The temperature sensors of the KTY series are well suited for this purpose and can be used for compensation of both positive and negative drift.

In many events, as with the magnetoresistive sensor KMZ10B, the temperature drift is negative. For this sensor, two circuits in SMD-technology, which include temperature compensation, are described below. The formulae given can be used to adapt the circuits to other conditions.

Figure 17 shows a simple setup using a single op-amp (NE5230D). The circuit provides the following facilities:

- Compensation of the **average** (sensor-to-sensor) sensitivity drift with temperature via a negative feedback loop incorporating a KTY82-210 silicon temperature sensor
- Offset adjustment by means of potentiometers 'R1' and 'R2'
- Gain adjustment by means of potentiometer 'R7'.

The temperature sensor is part of the amplifier's feedback loop and thus increases the amplification with increasing temperature.

With the resistor as shown in Fig.17 the temperature dependent amplification 'A' is given by:

$$A = \frac{R7}{R4 + \frac{R_B}{2}}\left(1 + 2\frac{R_T}{R_S}\right) \qquad (2)$$

and the temperature coefficient of the amplification can be calculated to be:

$$TC_A = \frac{R_T \times TC_{KTY}}{R_T + \frac{R_S}{2}}$$

with:

R_T = temperature dependent resistance of the KTY82.

TC_{KTY} = temperature coefficient of the KTY82 at reference temperature (0.79 %/K at 25 °C).

R_B = bridge resistance of the magnetoresistive sensor.

The temperature coefficient of amplification must be equal and opposite to the magnetic field sensor's 'TC' of sensitivity.

The value of the resistor 'R_S', which determines the positive 'TC' of the amplification is:

$$R_S = 2 \times R_T\left(\frac{TC_{KTY}}{TC_A} - 1\right).$$

The resistance of the feedback resistor can be derived from equation (2):

$$R7 = R4 \times \left(\frac{A}{1 + 2\frac{R_T}{R_S}}\right).$$

The temperature dependent values 'R_T' and 'A' are taken for a certain reference temperature, usually 25 °C, but in other applications a different reference temperature may be more suitable.

Figure 18 shows an example with a commonly used instrumentation amplifier. The circuit can be divided into two stages: a differential amplifier stage that produces a symmetrical output signal derived from the

magnetoresistive sensor, and an output stage that also provides a reference to ground for the amplification stage.

To compensate the negative sensor drift, the amplification is again given an equal but positive temperature coefficient by means of a KTY81-110 silicon temperature sensor in the feedback loop of the differential amplifier.

The amplification of the input stage ('OP1' and 'OP2') is given by:

$$A1 = 1 + \frac{R_T + R_B}{R_A}$$

and the amplification of the complete amplifier by:

$$A = A1 \times \frac{R14}{R10}.$$

The positive temperature coefficient of the amplification is:

$$TC_A = \frac{R_T \times TC_{KTY}}{R_A + R_B + R_T}.$$

For the given negative 'TC' of the magnetoresistive sensor and the required amplification of the input stage 'A1', the resistance 'R_A' and 'R_B' can be calculated by:

$$R_B = R_T \times \left(\frac{TC_{KTY}}{TC_A} \times \left(1 - \frac{1}{A1} \right) - 1 \right)$$

$$R_A = \frac{R_T + R_B}{A1 - 1}.$$

The circuit provides for adjustment of gain and offset voltage of the magnetic-field sensor. The calculated resistance 'R_A' consists of the fixed resistor 'R5' and trimming resistor 'R6' provided for amplification adjustment. Amplification adjustment only negligibly influences the 'TC' of the amplifier. The output stage 'OP3' gives an output voltage of $^2/_5$ of the supply voltage (2 V for V_S = 5 V) for zero output voltage of the magnetic field sensor and an output voltage of ±1 V for V_S = 5 V. For other supply voltages the circuit has a ratiometric behaviour.

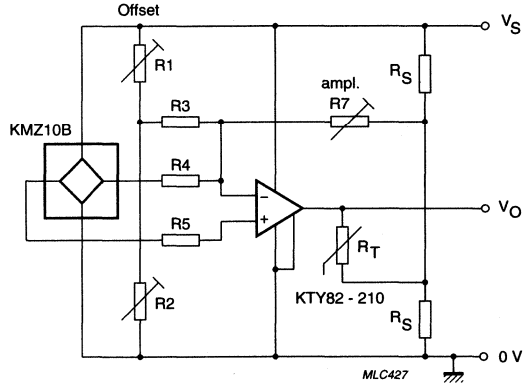

Example: A = 50 (typ.), TC_A = 0.004 K^{-1}.

Fig.17 Temperature compensation circuit.

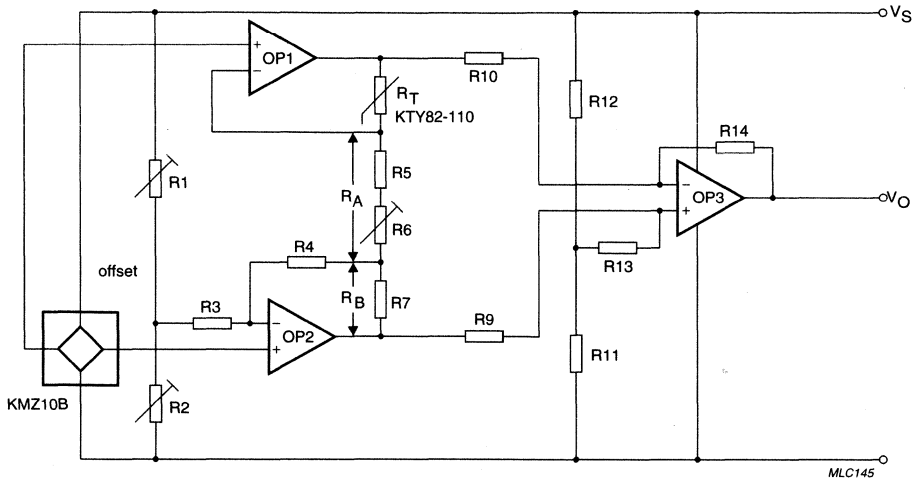

Example: A = 50 (typ.), TC_A = 0.004 K^{-1}.

Fig.18 KMZ10B evaluation circuit with instrumentation amplifier.

TYPICAL APPLICATION CIRCUIT

Figure 19 shows a typical and versatile temperature measuring circuit using silicon temperature sensors. This example is designed for the KTY81-110 (or the KTY82-110) and a temperature range from 0 to 100 °C.

With resistors 'R1' and 'R2', the sensor forms one arm of a bridge, the other arm being formed by resistor 'R3', potentiometer 'P1' and resistor 'R4'. The values of 'R1' and 'R2' are chosen to supply the sensor with the proper current of ≈1 mA, and to linearize the sensor characteristic over the temperature range of interest: in this event, between 0 and 100 °C. Over this temperature range, the output voltage V_O will vary linearly between $0.2V_S$ and $0.6V_S$, i.e. between 1 V and 3 V for a supply of V_S = 5 V.

To calibrate the circuit, adjust 'P1' to set 'V_O' to 1 V, with the sensor at 0 °C. Then, at a temperature of 100 °C, adjust 'P2' to set 'V_O' to the corresponding output voltage, in this example 3 V. With this circuit, adjustment of 'P2' has no effect on the zero adjustment.

The measurement accuracy obtained by this two-point calibration is shown in Fig.16. If the application can tolerate a temperature deviation of ±2 K at the temperature extremes (see Fig.15), costs can be reduced by replacing 'P2' with a 1.8 kΩ fixed resistor and adjusting 'V_O' at one temperature (the middle of the range, for example), using 'P1'.

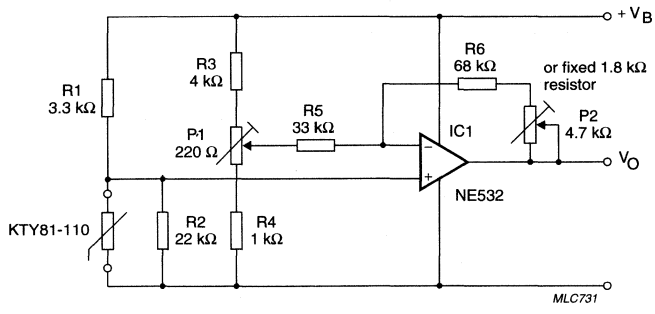

A KTY82-110 sensor would be equally suitable.
Temperature range 0 to 100 °C; $V_O = 0.2V_S$ to $0.6V_S$.
For $V_S = 5$ V: $V_O = 1$ to 3 V.
All resistors metal film; tolerance ±1%.

Fig.19 Temperature measuring circuit using a KTY81-110 sensor.

HIGH TEMPERATURE MEASUREMENT WITH KTY84

The operating range of silicon temperature sensors normally is limited to about 150 °C (an exception is the KTY83 with an upper temperature limit of 175 °C). This is due to the temperature stability of the package and the increasing intrinsic conductivity of the silicon die above 150 °C. The measuring range of the KTY84 silicon temperature sensors, however, is extended up to 300 °C.

The SOD68 (DO-34) diode housing together with special contacts between leads and sensor die give the necessary temperature resistivity for the package. The influence of the intrinsic conductivity can be suppressed by a sufficiently high operating current flowing in the correct direction.

Figure 20 shows the nominal characteristic for the recommended operating current of 2 mA and the effect of operating the sensor with a lower, and especially, a reverse current. The sensor resistance at the high temperature end makes it impossible to draw the current of 2 mA through the sensor in a common bridge circuit as in the previously suggested circuits. This is due to the usually limited supply voltage and the fact that the value of the series resistor may not be less than the linearization resistor of ≈5 kΩ. A solution is to supply the sensor by a constant current source.

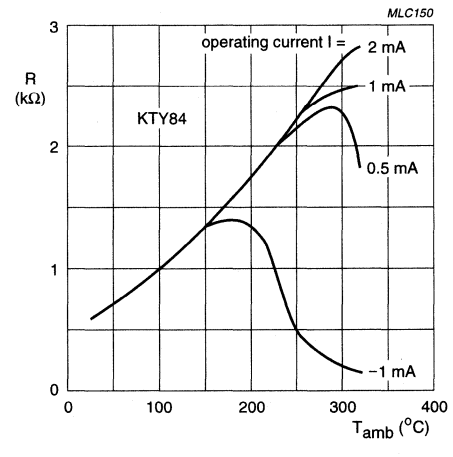

Fig.20 Sensor characteristic of the KTY84.

Figure 21 gives an example with internal voltage stabilization, a supply voltage of 8 to 24 V and for the full measuring range up to 300 °C. Operational amplifier 'OP1' and transistor 'TR1' form a current source to feed the temperature sensor. 'OP2' amplifies the bridge signal to the output voltage range. The circuit provides adjustment for a 'zero point'; 100 °C equals V_O = 2 V ('P1'), and full range ('P2').

A second example for a KTY84 evaluation circuit takes into consideration that in some electronic systems a supply voltage of only 5 V may be used. Under such circumstances it would be impossible to obtain the recommended current of 2 mA. A compromise is suggested by the circuit in Fig.22. A low drop current source supplies the temperature sensor and the linearization resistor. The maximum attainable current at 300 °C is 1.5 mA. This value is below the nominal operating current, but as Fig.20 shows, at up to 250 °C this will not cause any additional measuring error. Between 250 °C and 300 °C, however, a slightly decreasing slope of the sensor characteristic has to be taken into account.

The KTY84 silicon temperature sensor is a reliable and cost effective alternative to more expensive options such as Pt100-resistors or thermocouplers.

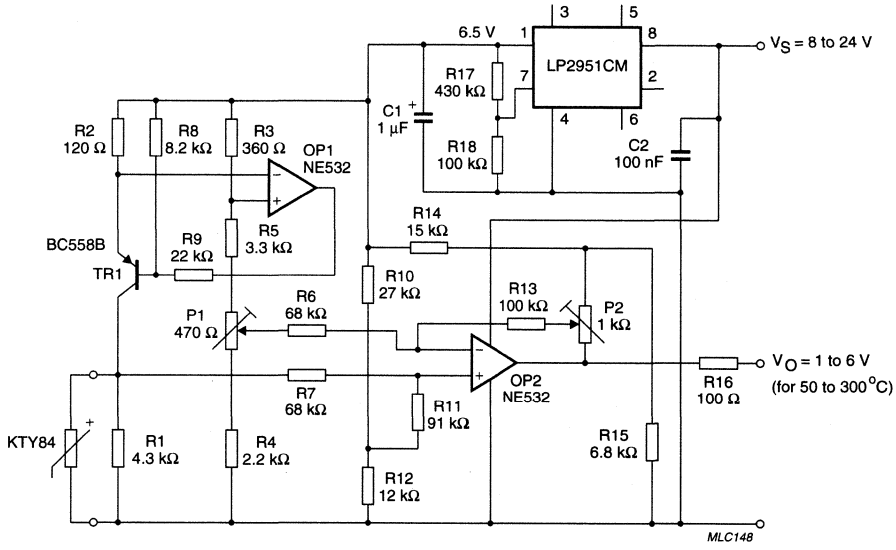

Fig.21 Evaluation circuit for KTY 84 with voltage regulation.

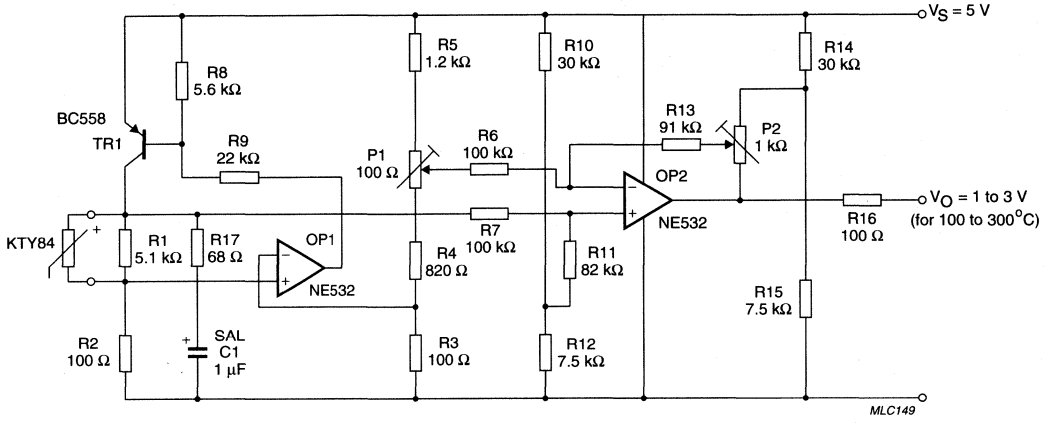

Fig.22 KTY84 evaluation circuit for 5 V power supply.

A/D CONVERTER TEMPERATURE COMPENSATION

When an A/D converter is integrated with a microcontroller, temperature compensation is required.

Figure 23 shows a suitable configuration, using a KTY81-210 temperature sensor in series with linearization resistor R_S. This voltage divider provides a linear temperature dependent voltage V_T of between 1.127 V and 1.886 V over the range 0 to 100 °C. This voltage is used as a reference for the A/D converter. The linear slope 'S' of V_T = 7.59 mV/ K.

ADDITIONAL TEMPERATURE SENSOR APPLICATIONS

Philips temperature sensors are also suitable for use in a number of other applications, for which information can be supplied on request:

- Electronic circuit protection
- Protection for power supplies
- Domestic appliances
- The white goods industry
- The automotive industry.

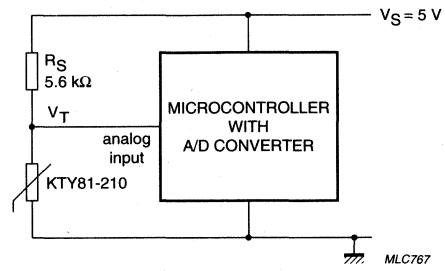

Fig.23 Temperature compensation for A/D converters.

MOUNTING AND HANDLING RECOMMENDATIONS

Mounting

KTY81

When potting techniques for KTY81 sensors are used for assembling, care has to be taken to ensure that mechanical stress and temperature development during curing of epoxy resin do not overstress the devices.

KTY83 AND 84

Excessive forces applied to a sensor may cause serious damage. To avoid this, the following recommendations should be adhered to:

- No perpendicular forces must be applied to the body
- During bending, the leads must be supported
- Bending close to the body must be done very carefully
- Axial forces to the body can influence the accuracy of the sensor and should be avoided
- These sensors can be mounted on a minimum pitch of 5 mm (2E).

Handling

ELECTROSTATIC DISCHARGE (ESD) SENSITIVITY

Electrostatic discharges above a certain energy can lead to irreversible changes of the sensor characteristic. In extreme events, sensors can even be destroyed. In accordance with the test methods described in IEC 47 (CO)955, temperature sensors are classified as sensitive components with respect to ESD. During handling (testing, transporting, fitting), the common rules for handling of ESD sensitive components should be observed.

If necessary, the ESD sensitivity in the practical application can be further reduced by connecting a 10 nF capacitor in parallel to the sensor.

Soldering

KTY81

The common rules for soldering components in TO-92 packages should be observed.

KTY 82

The common rules for soldering SMD components in SOT23 packages should be observed.

KTY83

Avoid any force on the body or leads during, or just after, soldering. Do not correct the position of an already soldered sensor by pushing, pulling or twisting the body. Prevent fast cooling after soldering. For hand soldering, where mounting is not on a printed-circuit board, the soldering temperature should be <300 °C, the soldering time <3 s and the distance between body and soldering point >1.5 mm. For hand soldering, dip, wave or other bath soldering, mounted on a printed-circuit board, the soldering temperature should be <300 °C, the soldering time <5 s and the distance between body and soldering point >1.5 mm.

KTY85

The common rules for surface mounted devices in SOD80 packages should be observed. Hand soldering is not recommended, because there is a great risk of damaging the glass body or the inner construction by uncontrolled temperature and time.

Welding

The KTY84 sensors are manufactured with nickel plated leads suitable for welding. The distance between the body and the welding point should be >0.5 mm. Care should be taken to ensure that welding current never passes through the sensor.

TAPE AND REEL PACKAGING

Tape and reel packaging meets the feed requirements of automatic pick and place equipment. It is also an ideal shipping container.

Table 4 Packaging quantities

TYPE	PACKAGE OUTLINE	PACKAGING METHOD	SPQ	PQ	12NC NUMBER XXXX XXX XX...
KTY81	SOD70	bulk pack	500	4000	112
		reel pack, radial	2000	10000	116
KTY82	SOT23	bulk pack	500	25000	212
		reel pack, SMD low profile 7"	3000	3000	215
		reel pack, SMD low profile 11¼"	10000	10000	235
KTY83, 84	SOD68 (DO-34)	reel pack axial 52 mm	10000	10000	113
		ammopack axial small size	1000	1000	153
KTY85	SOD80	bulk pack	1000	10000	112
		reel pack, SMD, 7"	2500	2500	115

DEVICE DATA

in alphanumeric sequence

Silicon temperature sensors KTY81-1 series

DESCRIPTION

The temperature sensors in the KTY81-1 series have a positive temperature coefficient of resistance and are suitable for use in measurement and control systems. The sensors are encapsulated in the SOD70 leaded plastic package.

Tolerances of 0.5% or other special selections are available on request.

PINNING

PIN	DESCRIPTION
1	electrical contact
2	electrical contact
3	not to be connected to a potential

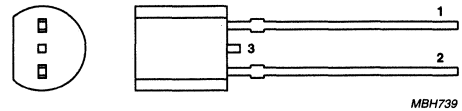

Fig.1 Simplified outline (SOD70).

MARKING

TYPE NUMBER	CODE
KTY81-110	110
KTY81-120	120
KTY81-121	121
KTY81-122	122
KTY81-150	150
KTY81-151	151
KTY81-152	152

QUICK REFERENCE DATA

SYMBOL	PARAMETER	CONDITIONS	MIN.	MAX.	UNIT
R_{25}	sensor resistance	T_{amb} = 25 °C; I_{cont} = 1 mA			
	KTY81-110		990	1010	Ω
	KTY81-120		980	1020	Ω
	KTY81-121		980	1000	Ω
	KTY81-122		1000	1020	Ω
	KTY81-150		950	1050	Ω
	KTY81-151		950	1000	Ω
	KTY81-152		1000	1050	Ω
T_{amb}	ambient operating temperature		−55	+150	°C

LIMITING VALUES

In accordance with the Absolute Maximum Rating System (IEC 134).

SYMBOL	PARAMETER	CONDITIONS	MIN.	MAX.	UNIT
I_{cont}	continuous sensor current	in free air; T_{amb} = 25 °C	–	10	mA
		in free air; T_{amb} = 150 °C	–	2	mA
T_{amb}	ambient operating temperature		−55	+150	°C

CHARACTERISTICS

T_{amb} = 25 °C, in liquid, unless otherwise specified.

SYMBOL	PARAMETER	CONDITIONS	MIN.	TYP.	MAX.	UNIT
R_{25}	sensor resistance	I_{cont} = 1 mA				
	KTY81-110		990	–	1010	Ω
	KTY81-120		980	–	1020	Ω
	KTY81-121		980	–	1000	Ω
	KTY81-122		1000	–	1020	Ω
	KTY81-150		950	–	1050	Ω
	KTY81-151		950	–	1000	Ω
	KTY81-152		1000	–	1050	Ω
TC	temperature coefficient		–	0.79	–	%/K
R_{100}/R_{25}	resistance ratio	T_{amb} = 100 °C and 25 °C	1.676	1.696	1.716	
R_{-55}/R_{25}	resistance ratio	T_{amb} = −55 °C and 25 °C	0.480	0.490	0.500	
τ	thermal time constant; note 1	in still air	–	30	–	s
		in still liquid; note 2	–	5	–	s
		in flowing liquid; note 2	–	3	–	s
	rated temperature range		−55	–	+150	°C

Notes

1. The thermal time constant is the time taken for the sensor to reach 63.2% of the total temperature difference. For example, if a sensor with a temperature of 25 °C is moved to an environment with an ambient temperature of 100 °C, the time for the sensor to reach a temperature of 47.4 °C is the thermal time constant.
2. Inert liquid, e.g. FC43 manufactured by the 3M company.

Table 1 Ambient temperature, corresponding resistance, temperature coefficient and maximum expected temperature error for KTY81-110 and KTY81-120

I_{cont} = 1 mA.

AMBIENT TEMPERATURE		TEMP. COEFF.	KTY81-110				KTY81-120			
(°C)	(°F)	(%/K)	RESISTANCE (Ω)			TEMP. ERROR (K)	RESISTANCE (Ω)			TEMP. ERROR (K)
			MIN.	TYP.	MAX.		MIN.	TYP.	MAX.	
−55	−67	0.99	475	490	505	±3.02	470	490	510	±4.02
−50	−58	0.98	500	515	530	±2.92	495	515	535	±3.94
−40	−40	0.96	552	567	582	±2.74	547	567	588	±3.78
−30	−22	0.93	609	624	638	±2.55	603	624	645	±3.62
−20	−4	0.91	669	684	698	±2.35	662	684	705	±3.45
−10	14	0.88	733	747	761	±2.14	726	747	769	±3.27
0	32	0.85	802	815	828	±1.91	793	815	836	±3.08
10	50	0.83	874	886	898	±1.67	865	886	907	±2.88
20	68	0.80	950	961	972	±1.41	941	961	982	±2.66
25	77	0.79	990	1000	1010	±1.27	980	1000	1020	±2.54
30	86	0.78	1029	1040	1051	±1.39	1018	1040	1061	±2.68
40	104	0.75	1108	1122	1136	±1.64	1097	1122	1147	±2.97
50	122	0.73	1192	1209	1225	±1.91	1180	1209	1237	±3.28
60	140	0.71	1278	1299	1319	±2.19	1265	1299	1332	±3.61
70	158	0.69	1369	1392	1416	±2.49	1355	1392	1430	±3.94
80	176	0.67	1462	1490	1518	±2.8	1447	1490	1532	±4.3
90	194	0.65	1559	1591	1623	±3.12	1543	1591	1639	±4.66
100	212	0.63	1659	1696	1733	±3.46	1642	1696	1750	±5.05
110	230	0.61	1762	1805	1847	±3.83	1744	1805	1865	±5.48
120	248	0.58	1867	1915	1963	±4.33	1848	1915	1982	±6.07
125	257	0.55	1919	1970	2020	±4.66	1899	1970	2040	±6.47
130	266	0.52	1970	2023	2077	±5.07	1950	2023	2097	±6.98
140	284	0.45	2065	2124	2184	±6.28	2043	2124	2205	±8.51
150	302	0.35	2145	2211	2277	±8.55	2123	2211	2299	±11.43

Table 2 Ambient temperature, corresponding resistance, temperature coefficient and maximum expected temperature error for KTY81-121 and KTY81-122

I_{cont} = 1 mA.

AMBIENT TEMPERATURE		TEMP. COEFF.	KTY81-121				KTY81-122			
(°C)	(°F)	(%/K)	RESISTANCE (Ω)			TEMP. ERROR (K)	RESISTANCE (Ω)			TEMP. ERROR (K)
			MIN.	TYP.	MAX.		MIN.	TYP.	MAX.	
−55	−67	0.99	471	485	500	±3.02	480	495	510	±3.02
−50	−58	0.98	495	510	524	±2.92	505	520	535	±2.92
−40	−40	0.96	547	562	576	±2.74	558	573	588	±2.74
−30	−22	0.93	603	617	632	±2.55	615	630	645	±2.55
−20	−4	0.91	662	677	691	±2.35	676	690	705	±2.35
−10	14	0.88	726	740	754	±2.14	741	755	769	±2.14
0	32	0.85	794	807	820	±1.91	810	823	836	±1.91
10	50	0.83	865	877	889	±1.67	883	895	907	±1.67
20	68	0.80	941	951	962	±1.41	960	971	982	±1.41
25	77	0.79	980	990	1000	±1.27	1000	1010	1020	±1.27
30	86	0.78	1018	1029	1041	±1.39	1039	1050	1062	±1.39
40	104	0.75	1097	1111	1125	±1.64	1120	1134	1148	±1.64
50	122	0.73	1180	1196	1213	±1.91	1204	1221	1238	±1.91
60	140	0.71	1266	1286	1305	±2.19	1291	1312	1332	±2.19
70	158	0.69	1355	1378	1402	±2.49	1382	1406	1430	±2.49
80	176	0.67	1447	1475	1502	±2.8	1477	1505	1533	±2.8
90	194	0.65	1543	1575	1607	±3.12	1574	1607	1639	±3.12
100	212	0.63	1642	1679	1716	±3.46	1676	1713	1750	±3.46
110	230	0.61	1745	1786	1828	±3.83	1780	1823	1865	±3.83
120	248	0.58	1849	1896	1943	±4.33	1886	1934	1982	±4.33
125	257	0.55	1900	1950	2000	±4.66	1938	1989	2041	±4.66
130	266	0.52	1950	2003	2056	±5.07	1989	2044	2098	±5.07
140	284	0.45	2044	2103	2162	±6.28	2085	2146	2206	±6.28
150	302	0.35	2124	2189	2254	±8.55	2167	2233	2299	±8.55

Table 3 Ambient temperature, corresponding resistance, temperature coefficient and maximum expected temperature error for KTY81-150 and KTY81-151

I_{cont} = 1 mA.

AMBIENT TEMPERATURE		TEMP. COEFF.	KTY81-150				KTY81-151			
(°C)	(°F)	(%/K)	RESISTANCE (Ω)			TEMP. ERROR (K)	RESISTANCE (Ω)			TEMP. ERROR (K)
			MIN.	TYP.	MAX.		MIN.	TYP.	MAX.	
−55	−67	0.99	456	490	524	±7.04	456	478	499	±4.52
−50	−58	0.98	479	515	550	±6.99	480	502	524	±4.45
−40	−40	0.96	530	567	605	±6.91	530	553	576	±4.3
−30	−22	0.93	584	624	663	±6.84	584	608	632	±4.16
−20	−4	0.91	642	684	725	±6.77	642	667	691	±4.01
−10	14	0.88	703	747	791	±6.69	704	729	753	±3.84
0	32	0.85	769	815	861	±6.61	770	794	819	±3.67
10	50	0.83	838	886	934	±6.51	839	864	889	±3.48
20	68	0.80	912	961	1010	±6.41	912	937	962	±3.28
25	77	0.79	950	1000	1050	±6.35	950	975	1000	±3.18
30	86	0.78	987	1040	1093	±6.55	988	1014	1040	±3.33
40	104	0.75	1064	1122	1181	±6.97	1064	1094	1124	±3.64
50	122	0.73	1143	1209	1274	±7.4	1144	1178	1212	±3.97
60	140	0.71	1226	1299	1371	±7.85	1227	1266	1305	±4.31
70	158	0.69	1313	1392	1472	±8.31	1314	1357	1401	±4.67
80	176	0.67	1402	1490	1577	±8.79	1404	1453	1501	±5.05
90	194	0.65	1495	1591	1687	±9.29	1497	1551	1606	±5.43
100	212	0.63	1591	1696	1801	±9.81	1593	1654	1714	±5.84
110	230	0.61	1690	1805	1919	±10.4	1692	1759	1827	±6.3
120	248	0.58	1791	1915	2039	±11.28	1792	1867	1942	±6.94
125	257	0.55	1840	1970	2099	±11.91	1842	1920	1999	±7.38
130	266	0.52	1889	2023	2158	±12.72	1891	1973	2055	±7.94
140	284	0.45	1980	2124	2269	±15.21	1982	2071	2161	±9.63
150	302	0.35	2057	2211	2365	±20.09	2059	2156	2252	±12.88

Table 4 Ambient temperature, corresponding resistance, temperature coefficient and maximum expected temperature error for KTY81-152

I_{cont} = 1 mA.

AMBIENT TEMPERATURE			KTY81-152			
(°C)	(°F)	(%/K)	RESISTANCE (Ω)			TEMP. ERROR (K)
			MIN.	TYP.	MAX.	
−55	−67	0.99	480	502	525	±4.52
−50	−58	0.98	505	528	551	±4.45
−40	−40	0.96	558	582	606	±4.3
−30	−22	0.93	614	639	664	±4.16
−20	−4	0.91	675	701	726	±4.01
−10	14	0.88	740	766	792	±3.84
0	32	0.85	809	835	861	±3.67
10	50	0.83	882	908	934	±3.48
20	68	0.80	959	985	1011	±3.28
25	77	0.79	1000	1025	1050	±3.18
30	86	0.78	1038	1066	1093	±3.33
40	104	0.75	1119	1150	1182	±3.64
50	122	0.73	1203	1239	1275	±3.97
60	140	0.71	1290	1331	1372	±4.31
70	158	0.69	1381	1427	1473	±4.67
80	176	0.67	1476	1527	1578	±5.05
90	194	0.65	1573	1631	1688	±5.43
100	212	0.63	1674	1738	1802	±5.84
110	230	0.61	1779	1850	1921	±6.3
120	248	0.58	1884	1963	2041	±6.94
125	257	0.55	1937	2019	2101	±7.38
130	266	0.52	1988	2074	2160	±7.94
140	284	0.45	2084	2178	2271	±9.63
150	302	0.35	2165	2266	2367	±12.88

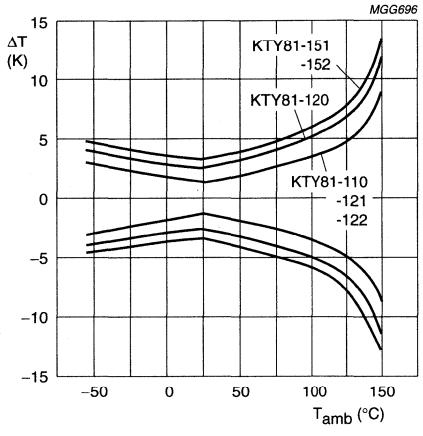

Fig.2 Maximum expected temperature error (ΔT).

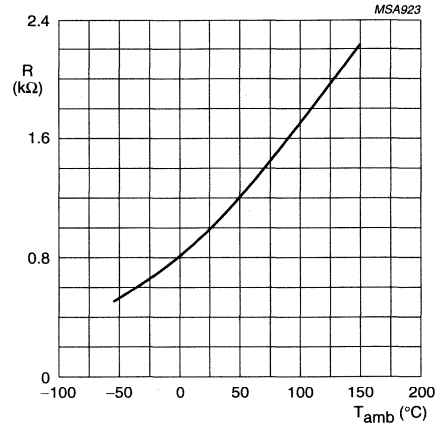

I_{cont} = 1 mA.

Fig.3 Sensor resistance as a function of ambient temperature; average values.

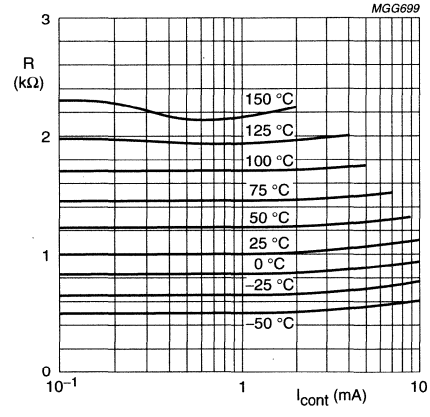

To keep the temperature error low, an operating current of I_{cont} = 1 mA is recommended for temperatures above 100 °C.

Fig.4 Sensor resistance as a function of operating current.

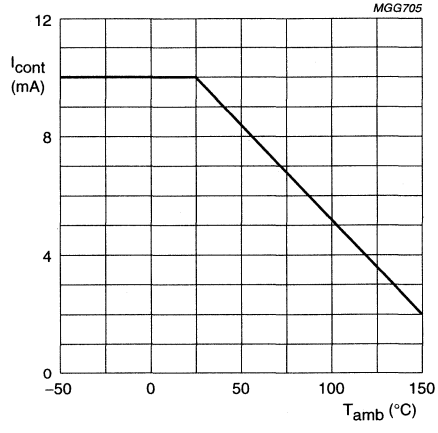

Fig.5 Maximum operating current for safe operation.

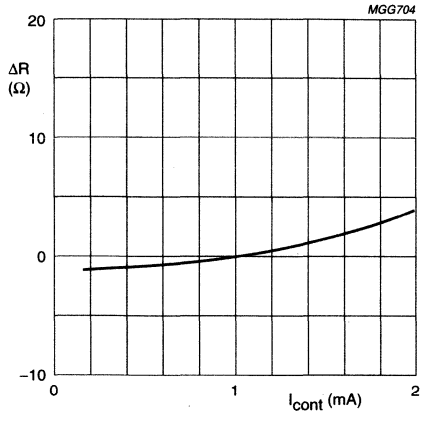

T_{amb} = 25 °C.

Fig.6 Deviation of sensor resistance as a function of operating current in still liquid.

APPLICATION INFORMATION

SYMBOL	PARAMETER	CONDITIONS	TYP.	UNIT
ΔR_{25}	drift of sensor resistance at 25 °C	10000 hours continuous operation; T_{amb} = 150 °C	1.6	Ω

PACKAGING

Sensors in SOD70 encapsulation are delivered in bulk packaging and also in reel packaging for automatic placement on hybrid circuits and printed-circuit boards (see Fig.7).

Note: Types in bulk packaging have a lead-to-lead distance of 2.54 millimetres, whereas the distance for types packaged on reel is 5.08 millimetres.

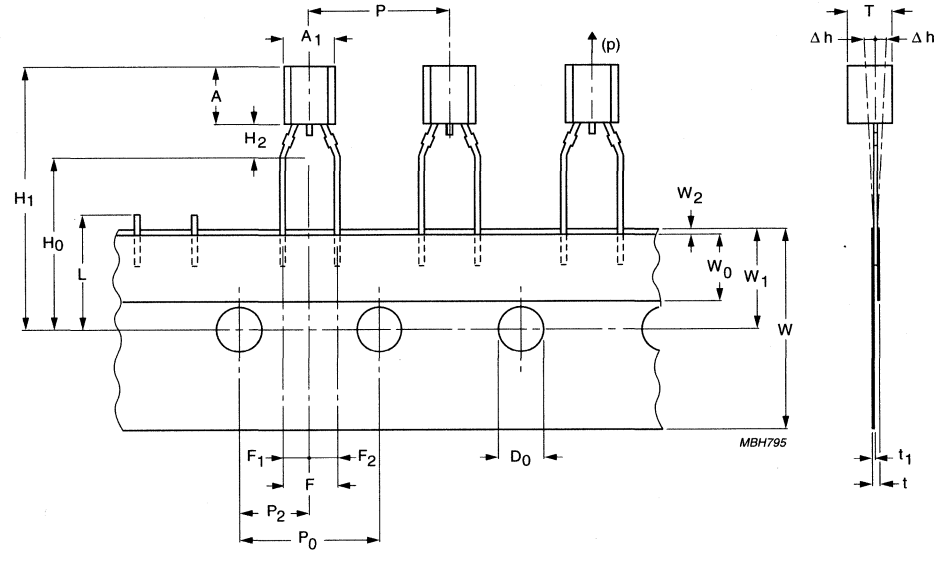

Fig.7 Configuration of bandolier.

Table 5 Tape specification

SYMBOL	DIMENSION	SPECIFICATIONS					REMARKS
		MIN.	NOM.	MAX.	TOL.	UNIT	
A_1	body width	4.4	–	4.8	–	mm	
A	body height	5	–	5.2	–	mm	
T	body thickness	3.6	–	3.9	–	mm	
P	pitch of component	–	12.7	–	±1	mm	
P_0	feed hole pitch	–	12.7	–	±0.3	mm	
	cumulative pitch error	–	–	–	±0.1		note 1
P_2	feed hole centre to component centre	–	6.35	–	±0.4	mm	to be measured at bottom of clinch
F	lead-to-lead distance	–	5.08	–	+0.6/–0.2	mm	
Δh	component alignment	–	0	1	–	mm	at top of body
W	tape width	–	18	–	±0.5	mm	
W_0	hold-down tape width	–	6	–	±0.2	mm	
W_1	hole position	–	9	–	+0.7/–0.5	mm	
W_2	hold-down tape position	–	0.5	–	±0.2	mm	
H_0	lead wire clinch height	–	16.5	–	±0.5	mm	
H_1	component height	–	–	23.25	–	mm	
L	length of snipped leads	–	–	11	–	mm	
D_0	feed hole diameter	–	4	–	±0.2	mm	
t	total tape thickness	–	–	1.2	–	mm	t_1 = 0.3 to 0.6
F_1, F_2	lead to snipped lead distance	–	2.54	–	+0.4/–0.2	mm	
H_2	clinch height	–	2.5	–	+0.5/0	mm	
(p)	pull-out force	6	–	–	–	N	

Note

1. Measured over 20 devices.

PACKAGE OUTLINE

Plastic near cylindrical single-ended package; 2 in-line leads **SOD70**

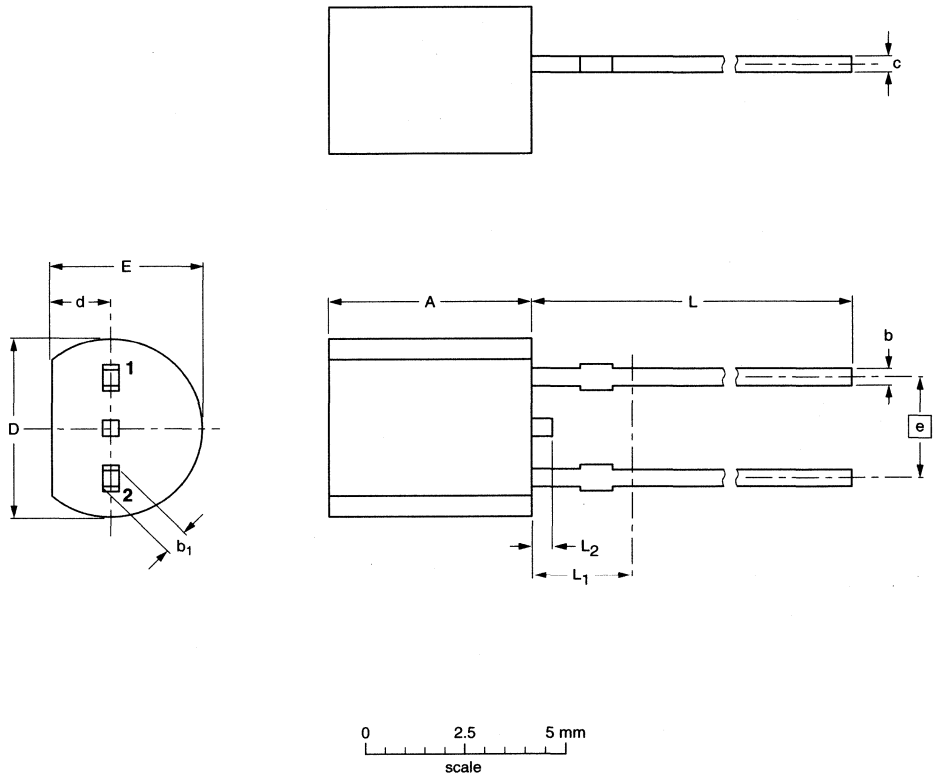

DIMENSIONS (mm are the original dimensions)

UNIT	A	b	b_1	c	D	d	E	e	L	L_1(1) max.	L_2
mm	5.2 5.0	0.48 0.40	0.66 0.56	0.45 0.40	4.8 4.4	1.7 1.4	4.2 3.6	2.54	14.5 12.7	2.5	0.7 0.5

Note

1. Terminal dimensions within this zone are uncontrolled to allow for flow of plastic and terminal irregularities.

OUTLINE VERSION	REFERENCES				EUROPEAN PROJECTION	ISSUE DATE
	IEC	JEDEC	EIAJ			
SOD70						98-05-25

Silicon temperature sensors KTY81-2 series

DESCRIPTION

The temperature sensors in the KTY81-2 series have a positive temperature coefficient of resistance and are suitable for use in measurement and control systems. The sensors are encapsulated in the SOD70 leaded plastic package.

Tolerances of 0.5% or other special selections are available on request.

PINNING

PIN	DESCRIPTION
1	electrical contact
2	electrical contact
3	not to be connected to a potential

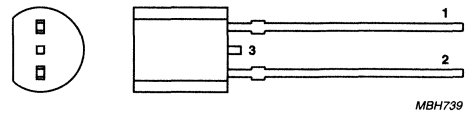

Fig.1 Simplified outline (SOD70).

MARKING

TYPE NUMBER	CODE
KTY81-210	210
KTY81-220	220
KTY81-221	221
KTY81-222	222
KTY81-250	250
KTY81-251	251
KTY81-252	252

QUICK REFERENCE DATA

SYMBOL	PARAMETER	CONDITIONS	MIN.	MAX.	UNIT
R_{25}	sensor resistance	T_{amb} = 25 °C; I_{cont} = 1 mA			
	KTY81-210		1980	2020	Ω
	KTY81-220		1960	2040	Ω
	KTY81-221		1960	2000	Ω
	KTY81-222		2000	2040	Ω
	KTY81-250		1900	2100	Ω
	KTY81-251		1900	2000	Ω
	KTY81-252		2000	2100	Ω
T_{amb}	ambient operating temperature		−55	+150	°C

LIMITING VALUES

In accordance with the Absolute Maximum Rating System (IEC 134).

SYMBOL	PARAMETER	CONDITIONS	MIN.	MAX.	UNIT
I_{cont}	continuous sensor current	in free air; T_{amb} = 25 °C	–	10	mA
		in free air; T_{amb} = 150 °C	–	2	mA
T_{amb}	ambient operating temperature		−55	+150	°C

CHARACTERISTICS

T_{amb} = 25 °C, in liquid, unless otherwise specified.

SYMBOL	PARAMETER	CONDITIONS	MIN.	TYP.	MAX.	UNIT
R_{25}	sensor resistance	I_{cont} = 1 mA				
	KTY81-210		1980	–	2020	Ω
	KTY81-220		1960	–	2040	Ω
	KTY81-221		1960	–	2000	Ω
	KTY81-222		2000	–	2040	Ω
	KTY81-250		1900	–	2100	Ω
	KTY81-251		1900	–	2000	Ω
	KTY81-252		2000	–	2100	Ω
TC	temperature coefficient		–	0.79	–	%/K
R_{100}/R_{25}	resistance ratio	T_{amb} = 100 °C and 25 °C	1.676	1.696	1.716	
R_{-55}/R_{25}	resistance ratio	T_{amb} = −55 °C and 25 °C	0.480	0.490	0.500	
τ	thermal time constant; note 1	in still air	–	30	–	s
		in still liquid; note 2	–	5	–	s
		in flowing liquid; note 2	–	3	–	s
	rated temperature range		−55	–	+150	°C

Notes

1. The thermal time constant is the time taken for the sensor to reach 63.2% of the total temperature difference. For example, if a sensor with a temperature of 25 °C is moved to an environment with an ambient temperature of 100 °C, the time for the sensor to reach a temperature of 72.4 °C is the thermal time constant.
2. Inert liquid, e.g. FC43 manufactured by the 3M company.

Table 1 Ambient temperature, corresponding resistance, temperature coefficient and maximum expected temperature error for KTY81-210 and KTY81-220

I_{cont} = 1 mA.

AMBIENT TEMPERATURE		TEMP. COEFF.	KTY81-210				KTY81-220			
(°C)	(°F)	(%/K)	RESISTANCE (Ω)			TEMP. ERROR (K)	RESISTANCE (Ω)			TEMP. ERROR (K)
			MIN.	TYP.	MAX.		MIN.	TYP.	MAX.	
−55	−67	0.99	951	980	1009	±3.02	941	980	1019	±4.02
−50	−58	0.98	1000	1030	1059	±2.92	990	1030	1070	±3.94
−40	−40	0.96	1105	1135	1165	±2.74	1094	1135	1176	±3.78
−30	−22	0.93	1218	1247	1277	±2.55	1205	1247	1289	±3.62
−20	−4	0.91	1338	1367	1396	±2.35	1325	1367	1410	±3.45
−10	14	0.88	1467	1495	1523	±2.14	1452	1495	1538	±3.27
0	32	0.85	1603	1630	1656	±1.91	1587	1630	1673	±3.08
10	50	0.83	1748	1772	1797	±1.67	1730	1772	1814	±2.88
20	68	0.80	1901	1922	1944	±1.41	1881	1922	1963	±2.66
25	77	0.79	1980	2000	2020	±1.27	1960	2000	2040	±2.54
30	86	0.78	2057	2080	2102	±1.39	2036	2080	2123	±2.68
40	104	0.75	2217	2245	2272	±1.64	2194	2245	2295	±2.97
50	122	0.73	2383	2417	2451	±1.91	2359	2417	2475	±3.28
60	140	0.71	2557	2597	2637	±2.19	2531	2597	2663	±3.61
70	158	0.69	2737	2785	2832	±2.49	2709	2785	2860	±3.94
80	176	0.67	2924	2980	3035	±2.8	2894	2980	3065	±4.3
90	194	0.65	3118	3182	3246	±3.12	3086	3182	3278	±4.66
100	212	0.63	3318	3392	3466	±3.46	3284	3392	3500	±5.05
110	230	0.59	3523	3607	3691	±3.93	3487	3607	3728	±5.61
120	248	0.53	3722	3817	3912	±4.7	3683	3817	3950	±6.59
125	257	0.49	3815	3915	4016	±5.26	3775	3915	4055	±7.31
130	266	0.44	3901	4008	4114	±6	3861	4008	4154	±8.27
140	284	0.33	4049	4166	4283	±8.45	4008	4166	4325	±11.46
150	302	0.20	4153	4280	4407	±14.63	4110	4280	4450	±19.56

Table 2 Ambient temperature, corresponding resistance, temperature coefficient and maximum expected temperature error for KTY81-221 and KTY81-222

I_{cont} = 1 mA.

AMBIENT TEMPERATURE		TEMP. COEFF.	KTY81-221				KTY81-222			
(°C)	(°F)	(%/K)	RESISTANCE (Ω)			TEMP. ERROR (K)	RESISTANCE (Ω)			TEMP. ERROR (K)
			MIN.	TYP.	MAX.		MIN.	TYP.	MAX.	
−55	−67	0.99	941	970	999	±3.02	960	990	1020	±3.02
−50	−58	0.98	990	1019	1049	±2.92	1010	1040	1070	±2.92
−40	−40	0.96	1094	1123	1153	±2.74	1116	1146	1176	±2.74
−30	−22	0.93	1205	1235	1264	±2.55	1230	1260	1290	±2.55
−20	−4	0.91	1325	1354	1382	±2.35	1352	1381	1410	±2.35
−10	14	0.88	1452	1480	1508	±2.14	1481	1510	1538	±2.14
0	32	0.85	1587	1613	1640	±1.91	1619	1646	1673	±1.91
10	50	0.83	1730	1754	1779	±1.67	1765	1790	1815	±1.67
20	68	0.80	1882	1903	1924	±1.41	1920	1941	1963	±1.41
25	77	0.79	1960	1980	2000	±1.27	2000	2020	2040	±1.27
30	86	0.78	2037	2059	2081	±1.39	2078	2100	2123	±1.39
40	104	0.75	2195	2222	2250	±1.64	2239	2267	2295	±1.64
50	122	0.73	2360	2393	2426	±1.91	2407	2441	2475	±1.91
60	140	0.71	2531	2571	2611	±2.19	2582	2623	2664	±2.19
70	158	0.69	2710	2757	2804	±2.49	2764	2812	2860	±2.49
80	176	0.67	2895	2950	3005	±2.8	2953	3009	3065	±2.8
90	194	0.65	3086	3150	3214	±3.12	3149	3214	3279	±3.12
100	212	0.63	3285	3358	3431	±3.46	3351	3426	3501	±3.46
110	230	0.59	3488	3571	3655	±3.93	3558	3643	3728	±3.93
120	248	0.53	3684	3779	3873	±4.7	3759	3855	3951	±4.7
125	257	0.49	3776	3876	3976	±5.26	3853	3955	4056	±5.26
130	266	0.44	3862	3967	4073	±6	3940	4048	4155	±6
140	284	0.33	4009	4125	4241	±8.45	4090	4208	4326	±8.45
150	302	0.20	4112	4237	4363	±14.63	4195	4323	4451	±14.63

Table 3 Ambient temperature, corresponding resistance, temperature coefficient and maximum expected temperature error for KTY81-250 and KTY81-251

I_{cont} = 1 mA.

AMBIENT TEMPERATURE		TEMP. COEFF.	KTY81-250				KTY81-251			
(°C)	(°F)	(%/K)	RESISTANCE (Ω)			TEMP. ERROR (K)	RESISTANCE (Ω)			TEMP. ERROR (K)
			MIN.	TYP.	MAX.		MIN.	TYP.	MAX.	
−55	−67	0.99	911	980	1049	±7.04	913	956	999	±4.52
−50	−58	0.98	959	1030	1101	±6.99	960	1004	1048	±4.45
−40	−40	0.96	1060	1135	1210	±6.91	1061	1106	1152	±4.3
−30	−22	0.93	1168	1247	1327	±6.84	1169	1216	1263	±4.16
−20	−4	0.91	1283	1367	1451	±6.77	1285	1333	1381	±4.01
−10	14	0.88	1407	1495	1583	±6.69	1408	1457	1507	±3.84
0	32	0.85	1538	1630	1721	±6.61	1539	1589	1639	±3.67
10	50	0.83	1677	1772	1867	±6.51	1678	1728	1778	±3.48
20	68	0.80	1824	1922	2021	±6.41	1825	1874	1923	±3.28
25	77	0.79	1900	2000	2100	±6.35	1900	1950	2000	±3.18
30	86	0.78	1974	2080	2185	±6.55	1975	2028	2080	±3.33
40	104	0.75	2127	2245	2362	±6.97	2129	2189	2248	±3.64
50	122	0.73	2287	2417	2547	±7.4	2289	2357	2425	±3.97
60	140	0.71	2453	2597	2741	±7.85	2455	2532	2609	±4.31
70	158	0.69	2626	2785	2943	±8.31	2628	2715	2802	±4.67
80	176	0.67	2805	2980	3154	±8.79	2807	2905	3003	±5.05
90	194	0.65	2990	3182	3374	±9.29	2993	3102	3212	±5.43
100	212	0.63	3182	3392	3602	±9.81	3185	3307	3429	±5.84
110	230	0.59	3379	3607	3836	±10.65	3382	3517	3652	±6.45
120	248	0.53	3569	3817	4065	±12.25	3573	3721	3870	±7.53
125	257	0.49	3658	3915	4173	±13.45	3662	3817	3973	±8.33
130	266	0.44	3741	4008	4274	±15.06	3745	3907	4070	±9.4
140	284	0.33	3883	4166	4450	±20.49	3887	4062	4237	±12.96
150	302	0.20	3982	4280	4578	±34.35	3987	4173	4359	±22.02

Table 4 Ambient temperature, corresponding resistance, temperature coefficient and maximum expected temperature error for KTY81-252

I_{cont} = 1 mA.

AMBIENT TEMPERATURE		TEMP. COEFF.	KTY81-252			
(°C)	(°F)	(%/K)	RESISTANCE (Ω)			TEMP. ERROR (K)
			MIN.	TYP.	MAX.	
−55	−67	0.99	959	1005	1050	±4.52
−50	−58	0.98	1009	1055	1102	±4.45
−40	−40	0.96	1115	1163	1211	±4.3
−30	−22	0.93	1229	1278	1328	±4.16
−20	−4	0.91	1351	1401	1452	±4.01
−10	14	0.88	1480	1532	1584	±3.84
0	32	0.85	1618	1670	1723	±3.67
10	50	0.83	1764	1817	1869	±3.48
20	68	0.80	1919	1970	2022	±3.28
25	77	0.79	2000	2050	2100	±3.18
30	86	0.78	2077	2132	2187	±3.33
40	104	0.75	2238	2301	2364	±3.64
50	122	0.73	2406	2478	2549	±3.97
60	140	0.71	2581	2662	2743	±4.31
70	158	0.69	2763	2854	2946	±4.67
80	176	0.67	2951	3054	3157	±5.05
90	194	0.65	3147	3262	3376	±5.43
100	212	0.63	3349	3477	3605	±5.84
110	230	0.59	3556	3697	3839	±6.45
120	248	0.53	3756	3912	4068	±7.53
125	257	0.49	3850	4013	4177	±8.33
130	266	0.44	3937	4108	4278	±9.4
140	284	0.33	4087	4271	4455	±12.96
150	302	0.20	4191	4387	4583	±22.02

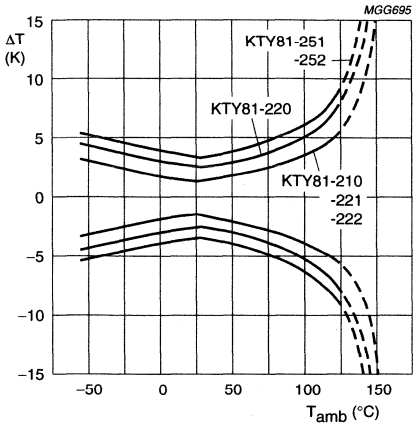

Fig.2 Maximum expected temperature error (ΔT).

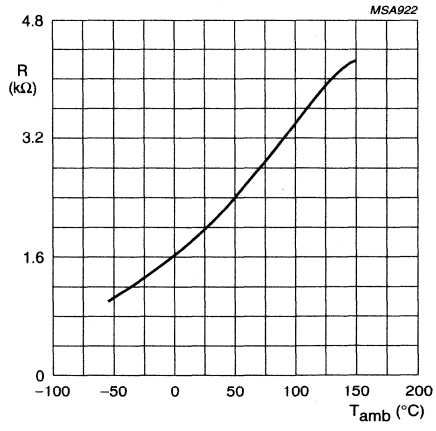

I_{cont} = 1 mA.

Fig.3 Sensor resistance as a function of ambient temperature; average values.

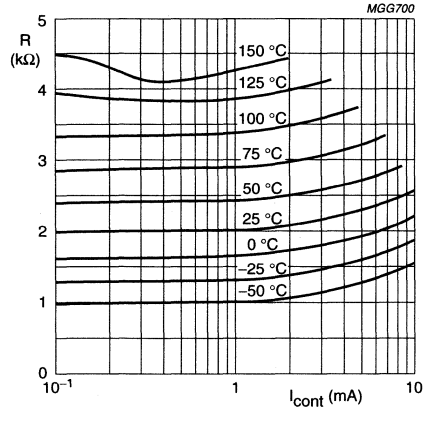

To keep the temperature error low, an operating current of I_{cont} = 1 mA is recommended for temperatures above 100 °C.

Fig.4 Sensor resistance as a function of operating current.

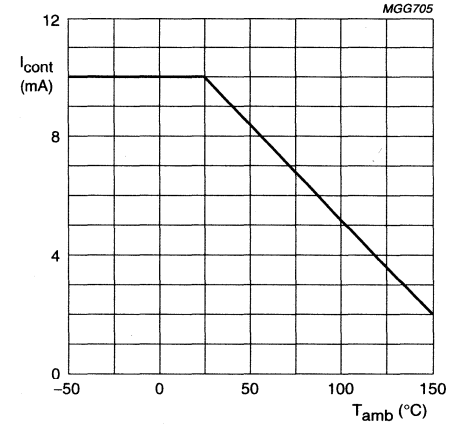

Fig.5 Maximum operating current for safe operation.

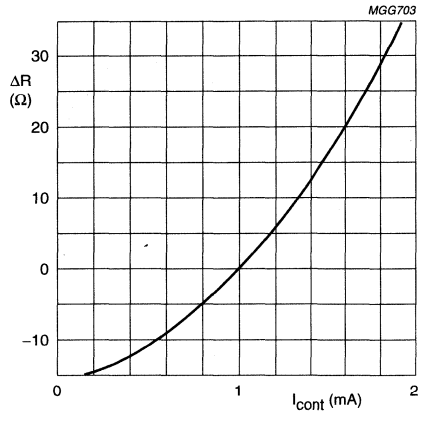

T_{amb} = 25 °C.

Fig.6 Deviation of sensor resistance as a function of operating current in still liquid.

APPLICATION INFORMATION

SYMBOL	PARAMETER	CONDITIONS	TYP.	UNIT
ΔR_{25}	drift of sensor resistance at 25 °C	10000 hours continuous operation; T_{amb} = 150 °C	0.5	Ω

PACKAGING

Sensors in SOD70 encapsulation are delivered in bulk packaging, and also reel packaging for automatic placement on hybrid circuits and printed-circuit boards (see Fig.7).

Note: Types in bulk packaging have a lead-to-lead distance of 2.54 millimetres, whereas the distance for types packaged on reel is 5.08 millimetres.

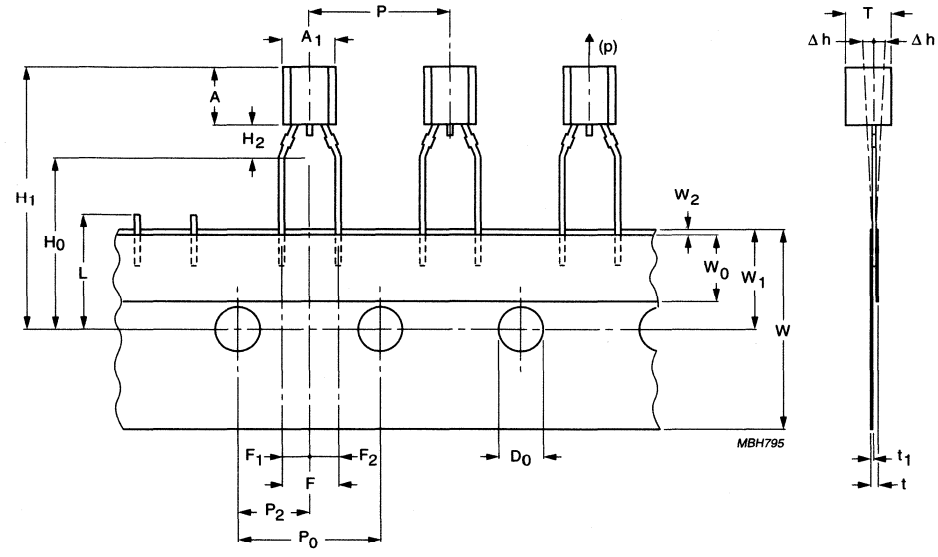

Fig.7 Configuration of bandolier.

Table 5 Tape specification

SYMBOL	DIMENSION	SPECIFICATIONS					REMARKS
		MIN.	NOM.	MAX.	TOL.	UNIT	
A_1	body width	4.4	–	4.8	–	mm	
A	body height	5	–	5.2	–	mm	
T	body thickness	3.6	–	3.9	–	mm	
P	pitch of component	–	12.7	–	±1	mm	
P_0	feed hole pitch	–	12.7	–	±0.3	mm	
	cumulative pitch error	–	–	–	±0.1		note 1
P_2	feed hole centre to component centre	–	6.35	–	±0.4	mm	to be measured at bottom of clinch
F	lead-to-lead distance	–	5.08	–	+0.6/–0.2	mm	
Δh	component alignment	–	0	1	–	mm	at top of body
W	tape width	–	18	–	±0.5	mm	
W_0	hold-down tape width	–	6	–	±0.2	mm	
W_1	hole position	–	9	–	+0.7/–0.5	mm	
W_2	hold-down tape position	–	0.5	–	±0.2	mm	
H_0	lead wire clinch height	–	16.5	–	±0.5	mm	
H_1	component height	–	–	23.25	–	mm	
L	length of snipped leads	–	–	11	–	mm	
D_0	feed hole diameter	–	4	–	±0.2	mm	
t	total tape thickness	–	–	1.2	–	mm	t_1 = 0.3 to 0.6
F_1, F_2	lead to snipped lead distance	–	2.54	–	+0.4/–0.2	mm	
H_2	clinch height	–	2.5	–	+0.5/0	mm	
(p)	pull-out force	6	–	–	–	N	

Note

1. Measured over 20 devices.

PACKAGE OUTLINE

Plastic near cylindrical single-ended package; 2 in-line leads **SOD70**

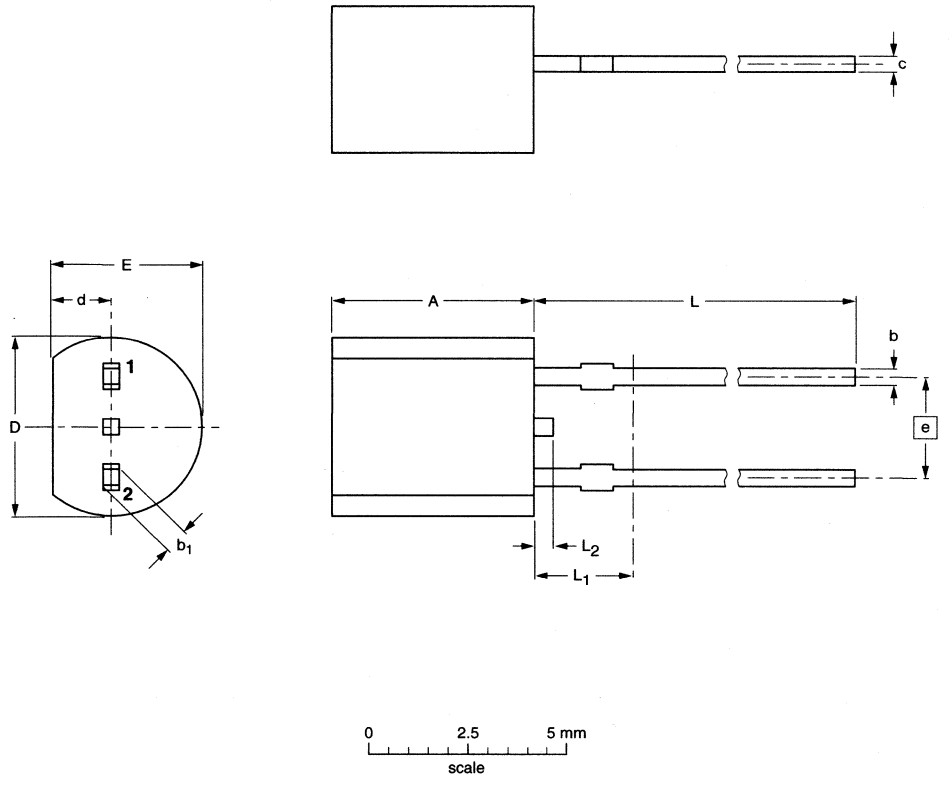

DIMENSIONS (mm are the original dimensions)

UNIT	A	b	b_1	c	D	d	E	e	L	L_1(1) max.	L_2
mm	5.2 5.0	0.48 0.40	0.66 0.56	0.45 0.40	4.8 4.4	1.7 1.4	4.2 3.6	2.54	14.5 12.7	2.5	0.7 0.5

Note

1. Terminal dimensions within this zone are uncontrolled to allow for flow of plastic and terminal irregularities.

OUTLINE VERSION	REFERENCES				EUROPEAN PROJECTION	ISSUE DATE
	IEC	JEDEC	EIAJ			
SOD70						98-05-25

Silicon temperature sensors KTY82-1 series

DESCRIPTION

The temperature sensors in the KTY82-1 series have a positive temperature coefficient of resistance and are suitable for use in measurement and control systems. The sensors are encapsulated in the small plastic SMD SOT23 package.

Tolerances of 0.5% or other special selections are available on request.

PINNING

PIN	DESCRIPTION
1	electrical contact
2	electrical contact
3	substrate (must remain potential free)

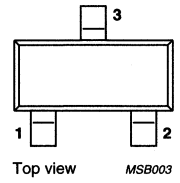

Fig.1 Simplified outline (SOT23).

MARKING

TYPE NUMBER	CODE
KTY82-110	110
KTY82-120	120
KTY82-121	121
KTY82-122	122
KTY82-150	150
KTY82-151	151
KTY82-152	152

QUICK REFERENCE DATA

SYMBOL	PARAMETER	CONDITIONS	MIN.	MAX.	UNIT
R_{25}	sensor resistance	T_{amb} = 25 °C; I_{cont} = 1 mA			
	KTY82-110		990	1010	Ω
	KTY82-120		980	1020	Ω
	KTY82-121		980	1000	Ω
	KTY82-122		1000	1020	Ω
	KTY82-150		950	1050	Ω
	KTY82-151		950	1000	Ω
	KTY82-152		1000	1050	Ω
T_{amb}	ambient operating temperature		−55	+150	°C

LIMITING VALUES

In accordance with the Absolute Maximum Rating System (IEC 134).

SYMBOL	PARAMETER	CONDITIONS	MIN.	MAX.	UNIT
I_{cont}	continuous sensor current	in free air; T_{amb} = 25 °C	–	10	mA
		in free air; T_{amb} = 150 °C	–	2	mA
T_{amb}	ambient operating temperature		−55	+150	°C

CHARACTERISTICS

T_{amb} = 25 °C, in liquid, unless otherwise specified.

SYMBOL	PARAMETER	CONDITIONS	MIN.	TYP.	MAX.	UNIT
R_{25}	sensor resistance	I_{cont} = 1 mA				
	KTY82-110		990	–	1010	Ω
	KTY82-120		980	–	1020	Ω
	KTY82-121		980	–	1000	Ω
	KTY82-122		1000	–	1020	Ω
	KTY82-150		950	–	1050	Ω
	KTY82-151		950	–	1000	Ω
	KTY82-152		1000	–	1050	Ω
TC	temperature coefficient		–	0.79	–	%/K
R_{100}/R_{25}	resistance ratio	T_{amb} = 100 °C and 25 °C	1.676	1.696	1.716	
R_{-55}/R_{25}	resistance ratio	T_{amb} = −55 °C and 25 °C	0.480	0.490	0.500	
τ	thermal time constant; note 1	in still air	–	7	–	s
		in still liquid; note 2	–	1	–	s
		in flowing liquid; note 2	–	0.5	–	s
	rated temperature range		−55	–	+150	°C

Notes

1. The thermal time constant is the time taken for the sensor to reach 63.2% of the total temperature difference. For example, if a sensor with a temperature of 25 °C is moved to an environment with an ambient temperature of 100 °C, the time for the sensor to reach a temperature of 72.4 °C is the thermal time constant.
2. Inert liquid, e.g. FC43 manufactured by the 3M company.

Table 1 Ambient temperature, corresponding resistance, temperature coefficient and maximum expected temperature error for KTY82-110 and KTY82-120

I_{cont} = 1 mA.

AMBIENT TEMPERATURE		TEMP. COEFF.	KTY82-110				KTY82-120			
(°C)	(°F)	(%/K)	RESISTANCE (Ω)			TEMP. ERROR (K)	RESISTANCE (Ω)			TEMP. ERROR (K)
			MIN.	TYP.	MAX.		MIN.	TYP.	MAX.	
−55	−67	0.99	475	490	505	±3.02	470	490	510	±4.02
−50	−58	0.98	500	515	530	±2.92	495	515	535	±3.94
−40	−40	0.96	552	567	582	±2.74	547	567	588	±3.78
−30	−22	0.93	609	624	638	±2.55	603	624	645	±3.62
−20	−4	0.91	669	684	698	±2.35	662	684	705	±3.45
−10	14	0.88	733	747	761	±2.14	726	747	769	±3.27
0	32	0.85	802	815	828	±1.91	793	815	836	±3.08
10	50	0.83	874	886	898	±1.67	865	886	907	±2.88
20	68	0.80	950	961	972	±1.41	941	961	982	±2.66
25	77	0.79	990	1000	1010	±1.27	980	1000	1020	±2.54
30	86	0.78	1029	1040	1051	±1.39	1018	1040	1061	±2.68
40	104	0.75	1108	1122	1136	±1.64	1097	1122	1147	±2.97
50	122	0.73	1192	1209	1225	±1.91	1180	1209	1237	±3.28
60	140	0.71	1278	1299	1319	±2.19	1265	1299	1332	±3.61
70	158	0.69	1369	1392	1416	±2.49	1355	1392	1430	±3.94
80	176	0.67	1462	1490	1518	±2.8	1447	1490	1532	±4.3
90	194	0.65	1559	1591	1623	±3.12	1543	1591	1639	±4.66
100	212	0.63	1659	1696	1733	±3.46	1642	1696	1750	±5.05
110	230	0.61	1762	1805	1847	±3.83	1744	1805	1865	±5.48
120	248	0.58	1867	1915	1963	±4.33	1848	1915	1982	±6.07
125	257	0.55	1919	1970	2020	±4.66	1899	1970	2040	±6.47
130	266	0.52	1970	2023	2077	±5.07	1950	2023	2097	±6.98
140	284	0.45	2065	2124	2184	±6.28	2043	2124	2205	±8.51
150	302	0.35	2145	2211	2277	±8.55	2123	2211	2299	±11.43

Table 2 Ambient temperature, corresponding resistance, temperature coefficient and maximum expected temperature error for KTY82-121 and KTY82-122

I_{cont} = 1 mA.

AMBIENT TEMPERATURE		TEMP. COEFF.	KTY82-121				KTY82-122			
(°C)	(°F)	(%/K)	RESISTANCE (Ω)			TEMP. ERROR (K)	RESISTANCE (Ω)			TEMP. ERROR (K)
			MIN.	TYP.	MAX.		MIN.	TYP.	MAX.	
−55	−67	0.99	471	485	500	±3.02	480	495	510	±3.02
−50	−58	0.98	495	510	524	±2.92	505	520	535	±2.92
−40	−40	0.96	547	562	576	±2.74	558	573	588	±2.74
−30	−22	0.93	603	617	632	±2.55	615	630	645	±2.55
−20	−4	0.91	662	677	691	±2.35	676	690	705	±2.35
−10	14	0.88	726	740	754	±2.14	741	755	769	±2.14
0	32	0.85	794	807	820	±1.91	810	823	836	±1.91
10	50	0.83	865	877	889	±1.67	883	895	907	±1.67
20	68	0.80	941	951	962	±1.41	960	971	982	±1.41
25	77	0.79	980	990	1000	±1.27	1000	1010	1020	±1.27
30	86	0.78	1018	1029	1041	±1.39	1039	1050	1062	±1.39
40	104	0.75	1097	1111	1125	±1.64	1120	1134	1148	±1.64
50	122	0.73	1180	1196	1213	±1.91	1204	1221	1238	±1.91
60	140	0.71	1266	1286	1305	±2.19	1291	1312	1332	±2.19
70	158	0.69	1355	1378	1402	±2.49	1382	1406	1430	±2.49
80	176	0.67	1447	1475	1502	±2.8	1477	1505	1533	±2.8
90	194	0.65	1543	1575	1607	±3.12	1574	1607	1639	±3.12
100	212	0.63	1642	1679	1716	±3.46	1676	1713	1750	±3.46
110	230	0.61	1745	1786	1828	±3.83	1780	1823	1865	±3.83
120	248	0.58	1849	1896	1943	±4.33	1886	1934	1982	±4.33
125	257	0.55	1900	1950	2000	±4.66	1938	1989	2041	±4.66
130	266	0.52	1950	2003	2056	±5.07	1989	2044	2098	±5.07
140	284	0.45	2044	2103	2162	±6.28	2085	2146	2206	±6.28
150	302	0.35	2124	2189	2254	±8.55	2167	2233	2299	±8.55

Table 3 Ambient temperature, corresponding resistance, temperature coefficient and maximum expected temperature error for KTY82-150 and KTY82-151

I_{cont} = 1 mA.

AMBIENT TEMPERATURE		TEMP. COEFF.	KTY82-150				KTY82-151			
(°C)	(°F)	(%/K)	RESISTANCE (Ω)			TEMP. ERROR (K)	RESISTANCE (Ω)			TEMP. ERROR (K)
			MIN.	TYP.	MAX.		MIN.	TYP.	MAX.	
−55	−67	0.99	456	490	524	±7.04	456	478	499	±4.52
−50	−58	0.98	479	515	550	±6.99	480	502	524	±4.45
−40	−40	0.96	530	567	605	±6.91	530	553	576	±4.3
−30	−22	0.93	584	624	663	±6.84	584	608	632	±4.16
−20	−4	0.91	642	684	725	±6.77	642	667	691	±4.01
−10	14	0.88	703	747	791	±6.69	704	729	753	±3.84
0	32	0.85	769	815	861	±6.61	770	794	819	±3.67
10	50	0.83	838	886	934	±6.51	839	864	889	±3.48
20	68	0.80	912	961	1010	±6.41	912	937	962	±3.28
25	77	0.79	950	1000	1050	±6.35	950	975	1000	±3.18
30	86	0.78	987	1040	1093	±6.55	988	1014	1040	±3.33
40	104	0.75	1064	1122	1181	±6.97	1064	1094	1124	±3.64
50	122	0.73	1143	1209	1274	±7.4	1144	1178	1212	±3.97
60	140	0.71	1226	1299	1371	±7.85	1227	1266	1305	±4.31
70	158	0.69	1313	1392	1472	±8.31	1314	1357	1401	±4.67
80	176	0.67	1402	1490	1577	±8.79	1404	1453	1501	±5.05
90	194	0.65	1495	1591	1687	±9.29	1497	1551	1606	±5.43
100	212	0.63	1591	1696	1801	±9.81	1593	1654	1714	±5.84
110	230	0.61	1690	1805	1919	±10.4	1692	1759	1827	±6.3
120	248	0.58	1791	1915	2039	±11.28	1792	1867	1942	±6.94
125	257	0.55	1840	1970	2099	±11.91	1842	1920	1999	±7.38
130	266	0.52	1889	2023	2158	±12.72	1891	1973	2055	±7.94
140	284	0.45	1980	2124	2269	±15.21	1982	2071	2161	±9.63
150	302	0.35	2057	2211	2365	±20.09	2059	2156	2252	±12.88

Table 4 Ambient temperature, corresponding resistance, temperature coefficient and maximum expected temperature error for KTY82-152

I_{cont} = 1 mA.

AMBIENT TEMPERATURE		TEMP. COEFF.	KTY82-152			
			RESISTANCE (Ω)			TEMP. ERROR (K)
(°C)	(°F)	(%/K)	MIN.	TYP.	MAX.	
−55	−67	0.99	480	502	525	±4.52
−50	−58	0.98	505	528	551	±4.45
−40	−40	0.96	558	582	606	±4.3
−30	−22	0.93	614	639	664	±4.16
−20	−4	0.91	675	701	726	±4.01
−10	14	0.88	740	766	792	±3.84
0	32	0.85	809	835	861	±3.67
10	50	0.83	882	908	934	±3.48
20	68	0.80	959	985	1011	±3.28
25	77	0.79	1000	1025	1050	±3.18
30	86	0.78	1038	1066	1093	±3.33
40	104	0.75	1119	1150	1182	±3.64
50	122	0.73	1203	1239	1275	±3.97
60	140	0.71	1290	1331	1372	±4.31
70	158	0.69	1381	1427	1473	±4.67
80	176	0.67	1476	1527	1578	±5.05
90	194	0.65	1573	1631	1688	±5.43
100	212	0.63	1674	1738	1802	±5.84
110	230	0.61	1779	1850	1921	±6.3
120	248	0.58	1884	1963	2041	±6.94
125	257	0.55	1937	2019	2101	±7.38
130	266	0.52	1988	2074	2160	±7.94
140	284	0.45	2084	2178	2271	±9.63
150	302	0.35	2165	2266	2367	±12.88

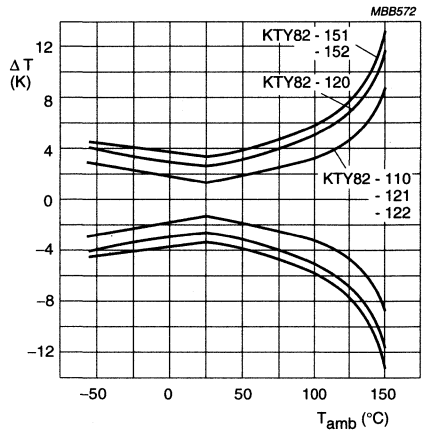

Fig.2 Maximum expected temperature error (ΔT).

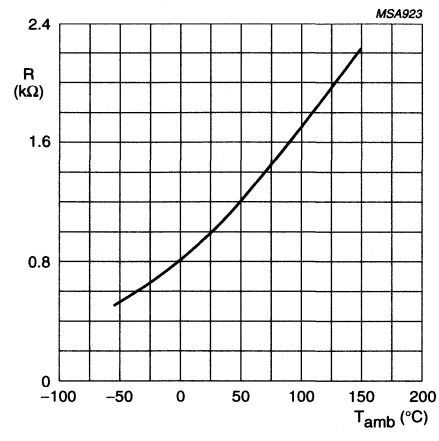

I_{cont} = 1 mA.

Fig.3 Sensor resistance as a function of ambient temperature; average values.

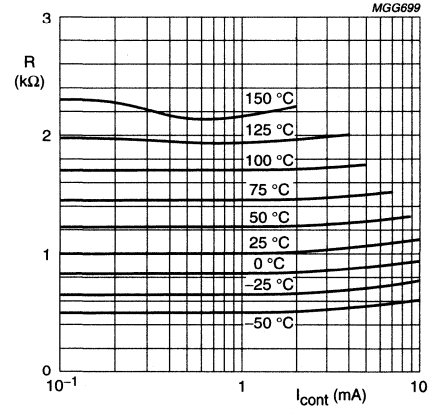

To keep the temperature error low, an operating current of I_{cont} = 1 mA is recommended for temperatures above 100 °C.

Fig.4 Sensor resistance as a function of operating current.

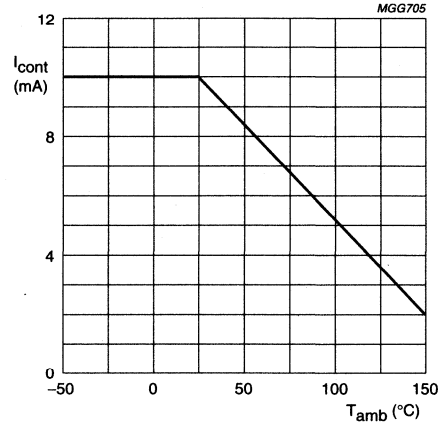

Fig.5 Maximum operating current for safe operation.

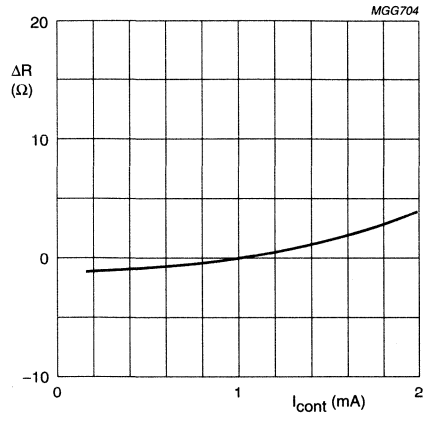

T_{amb} = 25 °C.

Fig.6 Deviation of sensor resistance as a function of operating current in still liquid.

APPLICATION INFORMATION

SYMBOL	PARAMETER	CONDITIONS	TYP.	UNIT
ΔR_{25}	drift of sensor resistance at 25 °C	10000 hours continuous operation; T_{amb} = 150 °C	1.6	Ω

PACKAGING

Tape specification

Sensors in SOT23 encapsulation are delivered in reel packaging for automatic placement on hybrid circuits and printed-circuit boards. The devices are placed with the mounting side downwards in the compartments.

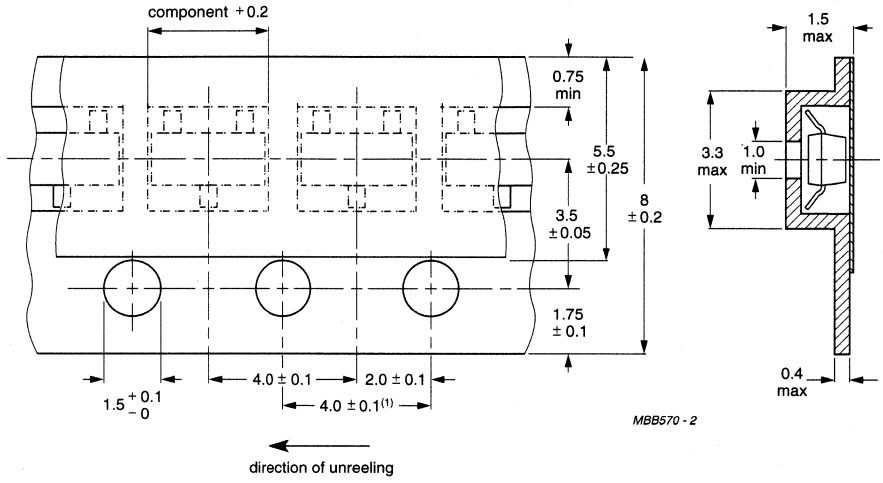

Dimension in mm.

(1) Tolerance over any 10 pitches: ±0.2 mm.

Fig.7 Configuration of bandolier.

PACKAGE OUTLINE

Plastic surface mounted package; 3 leads **SOT23**

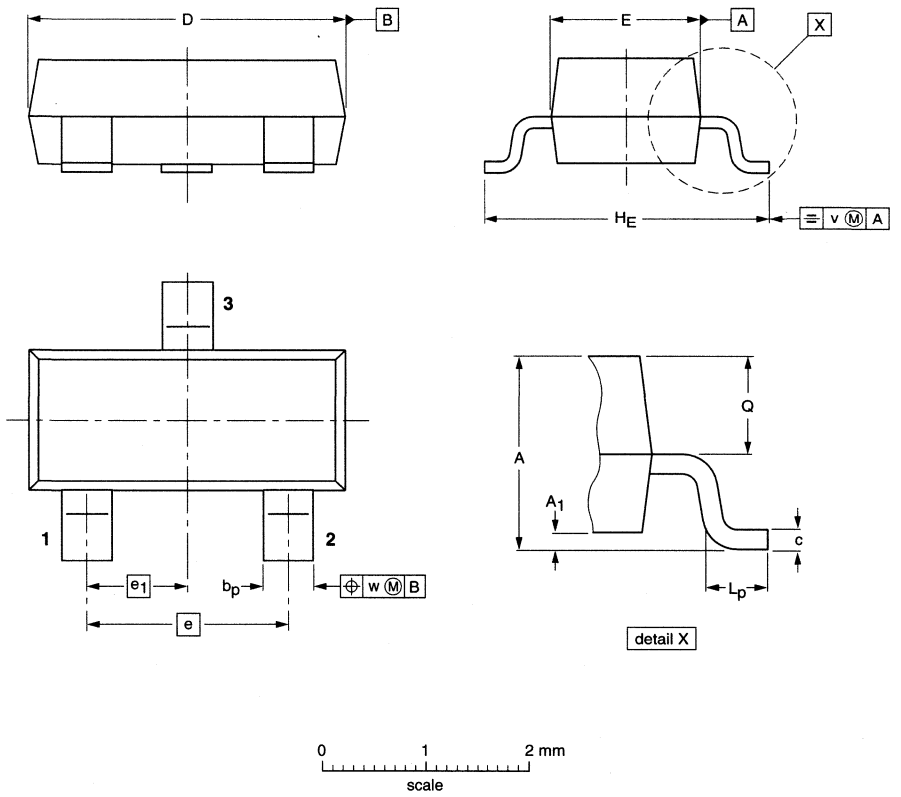

DIMENSIONS (mm are the original dimensions)

UNIT	A	A_1 max.	b_p	c	D	E	e	e_1	H_E	L_p	Q	v	w
mm	1.1 0.9	0.1	0.48 0.38	0.15 0.09	3.0 2.8	1.4 1.2	1.9	0.95	2.5 2.1	0.45 0.15	0.55 0.45	0.2	0.1

OUTLINE VERSION	REFERENCES				EUROPEAN PROJECTION	ISSUE DATE
	IEC	JEDEC	EIAJ			
SOT23						97-02-28

Silicon temperature sensors KTY82-2 series

DESCRIPTION

The temperature sensors in the KTY82-2 series have a positive temperature coefficient of resistance and are suitable for use in measurement and control systems. The sensors are encapsulated in the small plastic SMD SOT23 package.

Tolerances of 0.5% or other special selections are available on request.

PINNING

PIN	DESCRIPTION
1	electrical contact
2	electrical contact
3	substrate (must remain potential free)

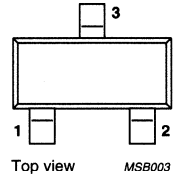

Fig.1 Simplified outline (SOT23).

MARKING

TYPE NUMBER	CODE
KTY82-210	210
KTY82-220	220
KTY82-221	221
KTY82-222	222
KTY82-250	250
KTY82-251	251
KTY82-252	252

QUICK REFERENCE DATA

SYMBOL	PARAMETER	CONDITIONS	MIN.	MAX.	UNIT
R_{25}	sensor resistance	T_{amb} = 25 °C; I_{cont} = 1 mA			
	KTY82-210		1980	2020	Ω
	KTY82-220		1960	2040	Ω
	KTY82-221		1960	2000	Ω
	KTY82-222		2000	2040	Ω
	KTY82-250		1900	2100	Ω
	KTY82-251		1900	2000	Ω
	KTY82-252		2000	2100	Ω
T_{amb}	ambient operating temperature		−55	+150	°C

LIMITING VALUES

In accordance with the Absolute Maximum Rating System (IEC 134).

SYMBOL	PARAMETER	CONDITIONS	MIN.	MAX.	UNIT
I_{cont}	continuous sensor current	in free air; T_{amb} = 25 °C	–	10	mA
		in free air; T_{amb} = 150 °C	–	2	mA
T_{amb}	ambient operating temperature		−55	+150	°C

CHARACTERISTICS

T_{amb} = 25 °C, in liquid, unless otherwise specified.

SYMBOL	PARAMETER	CONDITIONS	MIN.	TYP.	MAX.	UNIT
R_{25}	sensor resistance	I_{cont} = 1 mA				
	KTY82-210		1980	–	2020	Ω
	KTY82-220		1960	–	2040	Ω
	KTY82-221		1960	–	2000	Ω
	KTY82-222		2000	–	2040	Ω
	KTY82-250		1900	–	2100	Ω
	KTY82-251		1900	–	2000	Ω
	KTY82-252		2000	–	2100	Ω
TC	temperature coefficient		–	0.79	–	%/K
R_{100}/R_{25}	resistance ratio	T_{amb} = 100 °C and 25 °C	1.676	1.696	1.716	
R_{-55}/R_{25}	resistance ratio	T_{amb} = –55 °C and 25 °C	0.480	0.490	0.500	
τ	thermal time constant; note 1	in still air	–	7	–	s
		in still liquid; note 2	–	1	–	s
		in flowing liquid; note 2	–	0.5	–	s
	rated temperature range		–55	–	+150	°C

Notes

1. The thermal time constant is the time taken for the sensor to reach 63.2% of the total temperature difference. For example, if a sensor with a temperature of 25 °C is moved to an environment with an ambient temperature of 100 °C, the time for the sensor to reach a temperature of 72.4 °C is the thermal time constant.
2. Inert liquid, e.g. FC43 manufactured by the 3M company.

Table 1 Ambient temperature, corresponding resistance, temperature coefficient and maximum expected temperature error for KTY82-210 and KTY82-220

I_{cont} = 1 mA.

AMBIENT TEMPERATURE		TEMP. COEFF.	KTY82-210				KTY82-220			
(°C)	(°F)	(%/K)	RESISTANCE (Ω)			TEMP. ERROR (K)	RESISTANCE (Ω)			TEMP. ERROR (K)
			MIN.	TYP.	MAX.		MIN.	TYP.	MAX.	
−55	−67	0.99	951	980	1009	±3.02	941	980	1019	±4.02
−50	−58	0.98	1000	1030	1059	±2.92	990	1030	1070	±3.94
−40	−40	0.96	1105	1135	1165	±2.74	1094	1135	1176	±3.78
−30	−22	0.93	1218	1247	1277	±2.55	1205	1247	1289	±3.62
−20	−4	0.91	1338	1367	1396	±2.35	1325	1367	1410	±3.45
−10	14	0.88	1467	1495	1523	±2.14	1452	1495	1538	±3.27
0	32	0.85	1603	1630	1656	±1.91	1587	1630	1673	±3.08
10	50	0.83	1748	1772	1797	±1.67	1730	1772	1814	±2.88
20	68	0.80	1901	1922	1944	±1.41	1881	1922	1963	±2.66
25	77	0.79	1980	2000	2020	±1.27	1960	2000	2040	±2.54
30	86	0.78	2057	2080	2102	±1.39	2036	2080	2123	±2.68
40	104	0.75	2217	2245	2272	±1.64	2194	2245	2295	±2.97
50	122	0.73	2383	2417	2451	±1.91	2359	2417	2475	±3.28
60	140	0.71	2557	2597	2637	±2.19	2531	2597	2663	±3.61
70	158	0.69	2737	2785	2832	±2.49	2709	2785	2860	±3.94
80	176	0.67	2924	2980	3035	±2.8	2894	2980	3065	±4.3
90	194	0.65	3118	3182	3246	±3.12	3086	3182	3278	±4.66
100	212	0.63	3318	3392	3466	±3.46	3284	3392	3500	±5.05
110	230	0.59	3523	3607	3691	±3.93	3487	3607	3728	±5.61
120	248	0.53	3722	3817	3912	±4.7	3683	3817	3950	±6.59
125	257	0.49	3815	3915	4016	±5.26	3775	3915	4055	±7.31
130	266	0.44	3901	4008	4114	±6	3861	4008	4154	±8.27
140	284	0.33	4049	4166	4283	±8.45	4008	4166	4325	±11.46
150	302	0.20	4153	4280	4407	±14.63	4110	4280	4450	±19.56

Table 2 Ambient temperature, corresponding resistance, temperature coefficient and maximum expected temperature error for KTY82-221 and KTY82-222

I_{cont} = 1 mA.

AMBIENT TEMPERATURE		TEMP. COEFF.	KTY82-221				KTY82-222			
(°C)	(°F)	(%/K)	RESISTANCE (Ω)			TEMP. ERROR (K)	RESISTANCE (Ω)			TEMP. ERROR (K)
			MIN.	TYP.	MAX.		MIN.	TYP.	MAX.	
−55	−67	0.99	941	970	999	±3.02	960	990	1020	±3.02
−50	−58	0.98	990	1019	1049	±2.92	1010	1040	1070	±2.92
−40	−40	0.96	1094	1123	1153	±2.74	1116	1146	1176	±2.74
−30	−22	0.93	1205	1235	1264	±2.55	1230	1260	1290	±2.55
−20	−4	0.91	1325	1354	1382	±2.35	1352	1381	1410	±2.35
−10	14	0.88	1452	1480	1508	±2.14	1481	1510	1538	±2.14
0	32	0.85	1587	1613	1640	±1.91	1619	1646	1673	±1.91
10	50	0.83	1730	1754	1779	±1.67	1765	1790	1815	±1.67
20	68	0.80	1882	1903	1924	±1.41	1920	1941	1963	±1.41
25	77	0.79	1960	1980	2000	±1.27	2000	2020	2040	±1.27
30	86	0.78	2037	2059	2081	±1.39	2078	2100	2123	±1.39
40	104	0.75	2195	2222	2250	±1.64	2239	2267	2295	±1.64
50	122	0.73	2360	2393	2426	±1.91	2407	2441	2475	±1.91
60	140	0.71	2531	2571	2611	±2.19	2582	2623	2664	±2.19
70	158	0.69	2710	2757	2804	±2.49	2764	2812	2860	±2.49
80	176	0.67	2895	2950	3005	±2.8	2953	3009	3065	±2.8
90	194	0.65	3086	3150	3214	±3.12	3149	3214	3279	±3.12
100	212	0.63	3285	3358	3431	±3.46	3351	3426	3501	±3.46
110	230	0.59	3488	3571	3655	±3.93	3558	3643	3728	±3.93
120	248	0.53	3684	3779	3873	±4.7	3759	3855	3951	±4.7
125	257	0.49	3776	3876	3976	±5.26	3853	3955	4056	±5.26
130	266	0.44	3862	3967	4073	±6	3940	4048	4155	±6
140	284	0.33	4009	4125	4241	±8.45	4090	4208	4326	±8.45
150	302	0.20	4112	4237	4363	±14.63	4195	4323	4451	±14.63

Table 3 Ambient temperature, corresponding resistance, temperature coefficient and maximum expected temperature error for KTY82-250 and KTY82-251

I_{cont} = 1 mA.

AMBIENT TEMPERATURE		TEMP. COEFF.	KTY82-250				KTY82-251			
(°C)	(°F)	(%/K)	RESISTANCE (Ω)			TEMP. ERROR (K)	RESISTANCE (Ω)			TEMP. ERROR (K)
			MIN.	TYP.	MAX.		MIN.	TYP.	MAX.	
−55	−67	0.99	911	980	1049	±7.04	913	956	999	±4.52
−50	−58	0.98	959	1030	1101	±6.99	960	1004	1048	±4.45
−40	−40	0.96	1060	1135	1210	±6.91	1061	1106	1152	±4.3
−30	−22	0.93	1168	1247	1327	±6.84	1169	1216	1263	±4.16
−20	−4	0.91	1283	1367	1451	±6.77	1285	1333	1381	±4.01
−10	14	0.88	1407	1495	1583	±6.69	1408	1457	1507	±3.84
0	32	0.85	1538	1630	1721	±6.61	1539	1589	1639	±3.67
10	50	0.83	1677	1772	1867	±6.51	1678	1728	1778	±3.48
20	68	0.80	1824	1922	2021	±6.41	1825	1874	1923	±3.28
25	77	0.79	1900	2000	2100	±6.35	1900	1950	2000	±3.18
30	86	0.78	1974	2080	2185	±6.55	1975	2028	2080	±3.33
40	104	0.75	2127	2245	2362	±6.97	2129	2189	2248	±3.64
50	122	0.73	2287	2417	2547	±7.4	2289	2357	2425	±3.97
60	140	0.71	2453	2597	2741	±7.85	2455	2532	2609	±4.31
70	158	0.69	2626	2785	2943	±8.31	2628	2715	2802	±4.67
80	176	0.67	2805	2980	3154	±8.79	2807	2905	3003	±5.05
90	194	0.65	2990	3182	3374	±9.29	2993	3102	3212	±5.43
100	212	0.63	3182	3392	3602	±9.81	3185	3307	3429	±5.84
110	230	0.59	3379	3607	3836	±10.65	3382	3517	3652	±6.45
120	248	0.53	3569	3817	4065	±12.25	3573	3721	3870	±7.53
125	257	0.49	3658	3915	4173	±13.45	3662	3817	3973	±8.33
130	266	0.44	3741	4008	4274	±15.06	3745	3907	4070	±9.4
140	284	0.33	3883	4166	4450	±20.49	3887	4062	4237	±12.96
150	302	0.20	3982	4280	4578	±34.35	3987	4173	4359	±22.02

Table 4 Ambient temperature, corresponding resistance, temperature coefficient and maximum expected temperature error for KTY82-252

I_{cont} = 1 mA.

AMBIENT TEMPERATURE		TEMP. COEFF.	KTY82-252			
			RESISTANCE (Ω)			TEMP. ERROR (K)
(°C)	(°F)	(%/K)	MIN.	TYP.	MAX.	
−55	−67	0.99	959	1005	1050	±4.52
−50	−58	0.98	1009	1055	1102	±4.45
−40	−40	0.96	1115	1163	1211	±4.3
−30	−22	0.93	1229	1278	1328	±4.16
−20	−4	0.91	1351	1401	1452	±4.01
−10	14	0.88	1480	1532	1584	±3.84
0	32	0.85	1618	1670	1723	±3.67
10	50	0.83	1764	1817	1869	±3.48
20	68	0.80	1919	1970	2022	±3.28
25	77	0.79	2000	2050	2100	±3.18
30	86	0.78	2077	2132	2187	±3.33
40	104	0.75	2238	2301	2364	±3.64
50	122	0.73	2406	2478	2549	±3.97
60	140	0.71	2581	2662	2743	±4.31
70	158	0.69	2763	2854	2946	±4.67
80	176	0.67	2951	3054	3157	±5.05
90	194	0.65	3147	3262	3376	±5.43
100	212	0.63	3349	3477	3605	±5.84
110	230	0.59	3556	3697	3839	±6.45
120	248	0.53	3756	3912	4068	±7.53
125	257	0.49	3850	4013	4177	±8.33
130	266	0.44	3937	4108	4278	±9.4
140	284	0.33	4087	4271	4455	±12.96
150	302	0.20	4191	4387	4583	±22.02

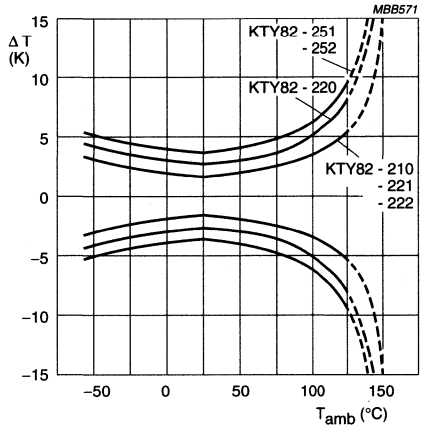

Fig.2 Maximum expected temperature error (ΔT).

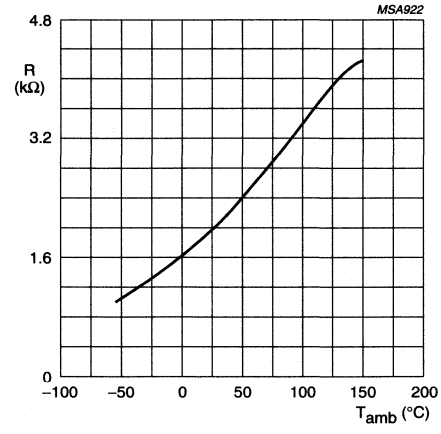

I_{cont} = 1 mA.

Fig.3 Sensor resistance as a function of ambient temperature; average values.

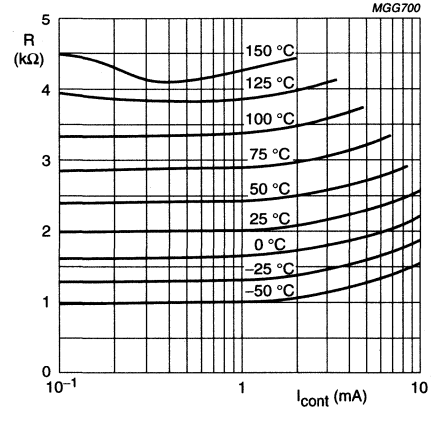

To keep the temperature error low, an operating current of I_{cont} = 1 mA is recommended for temperatures above 100 °C.

Fig.4 Sensor resistance as a function of operating current.

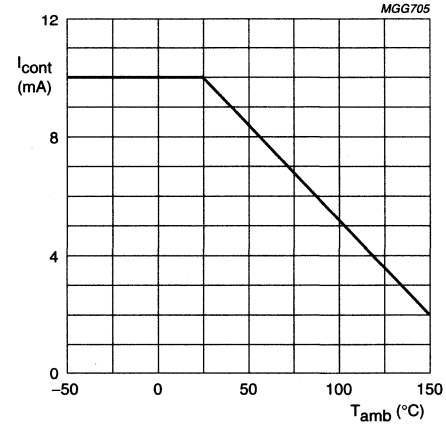

Fig.5 Maximum operating current for safe operation.

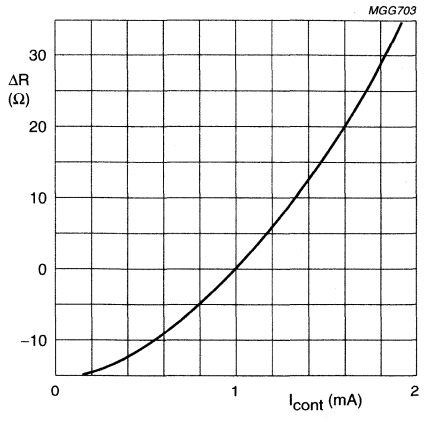

T_{amb} = 25 °C.

Fig.6 Deviation of sensor resistance as a function of operating current in still liquid.

APPLICATION INFORMATION

SYMBOL	PARAMETER	CONDITIONS	TYP.	UNIT
ΔR_{25}	drift of sensor resistance at 25 °C	10000 hours continuous operation; T_{amb} = 150 °C	3.2	Ω

PACKAGING

Tape specification

Sensors in SOT23 encapsulation are delivered in reel packaging for automatic placement on hybrid circuits and printed-circuit boards. The devices are placed with the mounting side downwards in the compartments.

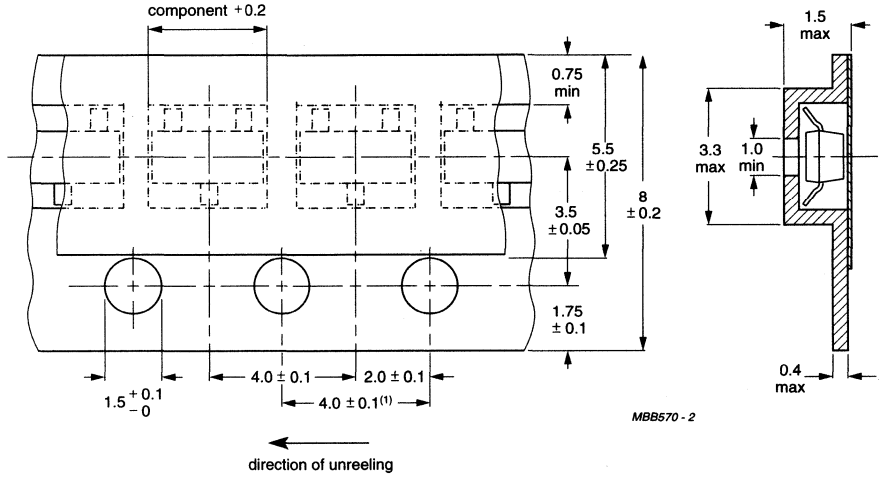

Dimension in mm.

(1) Tolerance over any 10 pitches: ±0.2 mm.

Fig.7 Configuration of bandolier.

PACKAGE OUTLINE

Plastic surface mounted package; 3 leads **SOT23**

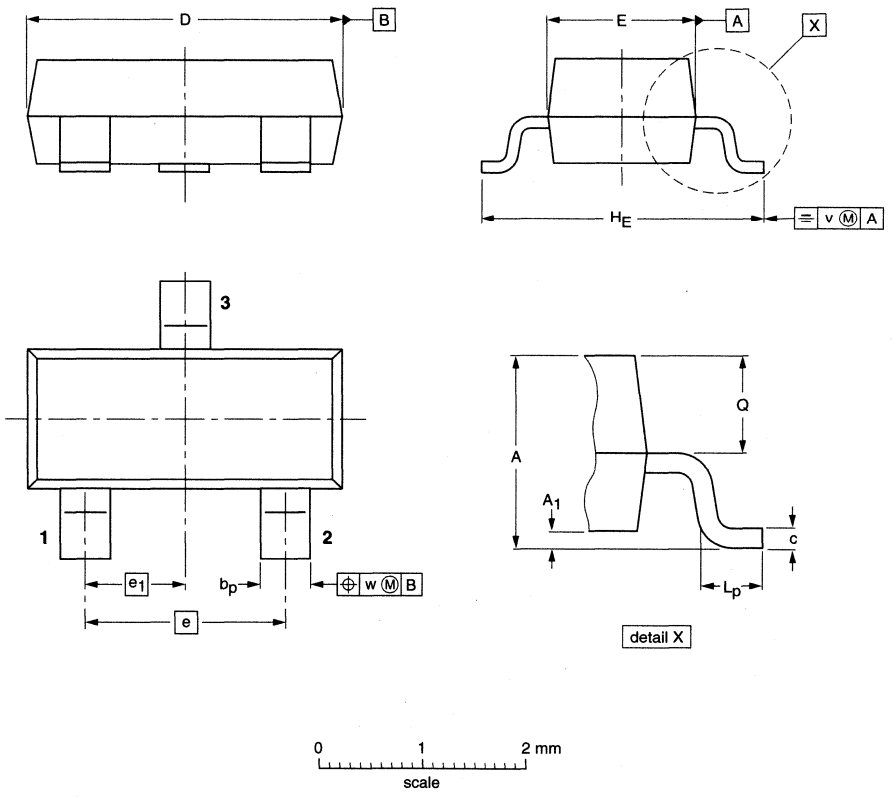

DIMENSIONS (mm are the original dimensions)

UNIT	A	A_1 max.	b_p	c	D	E	e	e_1	H_E	L_p	Q	v	w
mm	1.1 0.9	0.1	0.48 0.38	0.15 0.09	3.0 2.8	1.4 1.2	1.9	0.95	2.5 2.1	0.45 0.15	0.55 0.45	0.2	0.1

OUTLINE VERSION	REFERENCES				EUROPEAN PROJECTION	ISSUE DATE
	IEC	JEDEC	EIAJ			
SOT23						97-02-28

Silicon temperature sensors KTY83-1 series

DESCRIPTION

The temperature sensors in the KTY83-1 series have a positive temperature coefficient of resistance and are suitable for use in measurement and control systems. The sensors are encapsulated in the SOD68 (DO-34) leaded package.

Tolerances of 0.5% or other special selections are available on request.

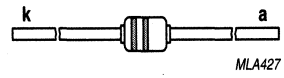

The first (black) band indicates the negative connection.
The second (coloured) band provides type identity.
The sensor must be operated with the lower potential at the marked connection.

Fig.1 Simplified outline (SOD68; DO34).

MARKING

TYPE NUMBER	MARKING BAND COLOUR
KTY83-110	yellow
KTY83-120	red
KTY83-121	white
KTY83-122	green
KTY83-150	grey
KTY83-151	black
KTY83-152	blue

QUICK REFERENCE DATA

SYMBOL	PARAMETER	CONDITIONS	MIN.	MAX.	UNIT
R_{25}	sensor resistance	T_{amb} = 25 °C; I_{cont} = 1 mA			
	KTY83-110		990	1010	Ω
	KTY83-120		980	1020	Ω
	KTY83-121		980	1000	Ω
	KTY83-122		1000	1020	Ω
	KTY83-150		950	1050	Ω
	KTY83-151		950	1000	Ω
	KTY83-152		1000	1050	Ω
T_{amb}	ambient operating temperature		−55	+175	°C

LIMITING VALUES

In accordance with the Absolute Maximum Rating System (IEC 134).

SYMBOL	PARAMETER	CONDITIONS	MIN.	MAX.	UNIT
I_{cont}	continuous sensor current	in free air; T_{amb} = 25 °C	–	10	mA
		in free air; T_{amb} = 175 °C	–	2	mA
T_{amb}	ambient operating temperature		−55	+175	°C

CHARACTERISTICS

T_{amb} = 25 °C, in liquid, unless otherwise specified.

SYMBOL	PARAMETER	CONDITIONS	MIN.	TYP.	MAX.	UNIT
R_{25}	sensor resistance	I_{cont} = 1 mA				
	KTY83-110		990	–	1010	Ω
	KTY83-120		980	–	1020	Ω
	KTY83-121		980	–	1000	Ω
	KTY83-122		1000	–	1020	Ω
	KTY83-150		950	–	1050	Ω
	KTY83-151		950	–	1000	Ω
	KTY83-152		1000	–	1050	Ω
TC	temperature coefficient		–	0.76	–	%/K
R_{100}/R_{25}	resistance ratio	T_{amb} = 100 °C and 25 °C	1.65	1.67	1.69	
R_{-55}/R_{25}	resistance ratio	T_{amb} = −55 °C and 25 °C	0.49	0.50	0.51	
τ	thermal time constant; note 1	in still air	–	20	–	s
		in still liquid; note 2	–	1	–	s
		in flowing liquid; note 2	–	0.5	–	s
	rated temperature range		−55	–	+175	°C

Notes

1. The thermal time constant is the time taken for the sensor to reach 63.2% of the total temperature difference. For example, if a sensor with a temperature of 25 °C is moved to an environment with an ambient temperature of 100 °C, the time for the sensor to reach a temperature of 72.4 °C is the thermal time constant.
2. Inert liquid, e.g. FC43 manufactured by the 3M company.

Table 1 Ambient temperature, corresponding resistance, temperature coefficient and maximum expected temperature error for KTY83-110 and KTY83-120

I_{cont} = 1 mA.

AMBIENT TEMPERATURE		TEMP. COEFF.	KTY83-110				KTY83-120			
(°C)	(°F)	(%/K)	RESISTANCE (Ω)			TEMP. ERROR (K)	RESISTANCE (Ω)			TEMP. ERROR (K)
			MIN.	TYP.	MAX.		MIN.	TYP.	MAX.	
−55	−67	0.97	485	500	515	±3.08	480	500	520	±4.11
−50	−58	0.96	510	525	540	±2.99	504	525	545	±4.04
−40	−40	0.93	562	577	592	±2.81	556	577	598	±3.88
−30	−22	0.91	617	632	647	±2.62	611	632	654	±3.72
−20	−4	0.88	677	691	706	±2.42	670	691	713	±3.56
−10	14	0.85	740	754	768	±2.2	732	754	776	±3.37
0	32	0.83	807	820	833	±1.97	798	820	841	±3.18
10	50	0.80	877	889	902	±1.72	868	889	910	±2.97
20	68	0.78	951	962	973	±1.45	942	962	983	±2.74
25	77	0.76	990	1000	1010	±1.31	980	1000	1020	±2.62
30	86	0.75	1027	1039	1050	±1.44	1017	1039	1060	±2.77
40	104	0.73	1105	1118	1132	±1.7	1093	1118	1143	±3.07
50	122	0.71	1185	1202	1219	±1.98	1173	1202	1231	±3.39
60	140	0.69	1268	1288	1309	±2.27	1255	1288	1321	±3.73
70	158	0.67	1355	1379	1402	±2.58	1341	1379	1416	±4.08
80	176	0.65	1445	1472	1500	±2.9	1430	1472	1515	±4.44
90	194	0.63	1537	1569	1601	±3.24	1522	1569	1617	±4.82
100	212	0.61	1633	1670	1707	±3.59	1617	1670	1723	±5.22
110	230	0.60	1732	1774	1816	±3.95	1714	1774	1834	±5.63
120	248	0.58	1834	1882	1929	±4.34	1815	1882	1948	±6.06
125	257	0.57	1886	1937	1987	±4.53	1867	1937	2006	±6.28
130	266	0.57	1939	1993	2046	±4.73	1919	1993	2066	±6.5
140	284	0.55	2047	2107	2167	±5.14	2026	2107	2188	±6.96
150	302	0.54	2158	2225	2292	±5.57	2136	2225	2314	±7.43
160	320	0.52	2272	2346	2420	±6.02	2249	2346	2444	±7.92
170	338	0.51	2389	2471	2553	±6.47	2364	2471	2578	±8.43
175	347	0.51	2449	2535	2621	±6.71	2423	2535	2646	±8.68

Table 2 Ambient temperature, corresponding resistance, temperature coefficient and maximum expected temperature error for KTY83-121 and KTY83-122

I_{cont} = 1 mA.

AMBIENT TEMPERATURE		TEMP. COEFF.	KTY83-121				KTY83-122			
(°C)	(°F)	(%/K)	RESISTANCE (Ω)			TEMP. ERROR (K)	RESISTANCE (Ω)			TEMP. ERROR (K)
			MIN.	TYP.	MAX.		MIN.	TYP.	MAX.	
−55	−67	0.97	480	495	510	±3.08	490	505	520	±3.08
−50	−58	0.96	505	519	534	±2.99	515	530	545	±2.99
−40	−40	0.93	556	571	586	±2.81	567	583	598	±2.81
−30	−22	0.91	611	626	641	±2.62	624	639	654	±2.62
−20	−4	0.88	670	685	699	±2.42	684	698	713	±2.42
−10	14	0.85	732	746	760	±2.2	747	762	776	±2.2
0	32	0.83	799	812	825	±1.97	815	828	842	±1.97
10	50	0.80	868	880	893	±1.72	886	898	911	±1.72
20	68	0.78	942	953	963	±1.45	961	972	983	±1.45
25	77	0.76	980	990	1000	±1.31	1000	1010	1020	±1.31
30	86	0.75	1017	1028	1039	±1.44	1038	1049	1060	±1.44
40	104	0.73	1094	1107	1121	±1.7	1116	1130	1144	±1.7
50	122	0.71	1173	1190	1206	±1.98	1197	1214	1231	±1.98
60	140	0.69	1256	1276	1295	±2.27	1281	1301	1322	±2.27
70	158	0.67	1341	1365	1388	±2.58	1368	1392	1416	±2.58
80	176	0.65	1430	1458	1485	±2.9	1459	1487	1515	±2.9
90	194	0.63	1522	1554	1585	±3.24	1553	1585	1617	±3.24
100	212	0.61	1617	1653	1690	±3.59	1650	1687	1724	±3.59
110	230	0.60	1715	1756	1798	±3.95	1750	1792	1834	±3.95
120	248	0.58	1816	1863	1910	±4.34	1853	1900	1948	±4.34
125	257	0.57	1867	1917	1967	±4.53	1905	1956	2007	±4.53
130	266	0.57	1920	1973	2025	±4.73	1959	2012	2066	±4.73
140	284	0.55	2027	2086	2145	±5.14	2068	2128	2188	±5.14
150	302	0.54	2137	2203	2269	±5.57	2180	2247	2314	±5.57
160	320	0.52	2249	2323	2396	±6.02	2295	2370	2444	±6.02
170	338	0.51	2365	2446	2527	±6.47	2413	2496	2578	±6.47
175	347	0.51	2424	2509	2595	±6.71	2473	2560	2647	±6.71

Table 3 Ambient temperature, corresponding resistance, temperature coefficient and maximum expected temperature error for KTY83-150 and KTY83-151

I_{cont} = 1 mA.

AMBIENT TEMPERATURE		TEMP. COEFF.	KTY83-150				KTY83-151			
(°C)	(°F)	(%/K)	RESISTANCE (Ω)			TEMP. ERROR (K)	RESISTANCE (Ω)			TEMP. ERROR (K)
			MIN.	TYP.	MAX.		MIN.	TYP.	MAX.	
−55	−67	0.97	465	500	535	±7.19	466	487	509	±4.92
−50	−58	0.96	489	525	561	±7.16	489	512	534	±4.56
−40	−40	0.93	539	577	615	±7.1	539	562	586	±4.42
−30	−22	0.91	592	632	673	±7.04	593	617	641	±4.28
−20	−4	0.88	649	691	734	±6.97	650	674	699	±4.12
−10	14	0.85	710	754	798	±6.9	710	735	760	±3.96
0	32	0.83	774	820	866	±6.81	774	799	824	±3.79
10	50	0.80	842	889	937	±6.72	842	867	892	±3.59
20	68	0.78	913	962	1012	±6.61	914	938	963	±3.39
25	77	0.76	950	1000	1050	±6.55	950	975	1000	±3.27
30	86	0.75	986	1039	1091	±6.76	987	1013	1039	±3.43
40	104	0.73	1060	1118	1177	±7.19	1061	1090	1120	±3.76
50	122	0.71	1137	1202	1267	±7.63	1138	1172	1206	±4.1
60	140	0.69	1217	1288	1360	±8.1	1218	1256	1295	±4.45
70	158	0.67	1300	1379	1457	±8.58	1301	1344	1387	±4.83
80	176	0.65	1386	1472	1559	±9.07	1387	1435	1484	±5.21
90	194	0.63	1475	1569	1664	±9.59	1476	1530	1584	±5.62
100	212	0.61	1566	1670	1773	±10.12	1568	1628	1688	±6.04
110	230	0.60	1661	1774	1887	±10.66	1663	1730	1796	±6.47
120	248	0.58	1759	1882	2004	±11.282	1761	1835	1908	±6.92
125	257	0.57	1809	1937	2064	±11.51	1811	1888	1966	±7.15
130	266	0.57	1859	1993	2126	±11.8	1862	1943	2024	±7.38
140	284	0.55	1963	2107	2251	±12.4	1965	2054	2143	±7.87
150	302	0.54	2069	2225	2380	±13.01	2072	2169	2267	±8.36
160	320	0.52	2178	2346	2514	±13.64	2181	2288	2394	±8.87
170	338	0.51	2290	2471	2652	±14.28	2293	2409	2525	±9.4
175	347	0.51	2347	2535	2722	±14.61	2350	2471	2592	±9.67

Table 4 Ambient temperature, corresponding resistance, temperature coefficient and maximum expected temperature error for KTY83-152

I_{cont} = 1 mA.

AMBIENT TEMPERATURE		TEMP. COEFF.	KTY83-152			
(°C)	(°F)	(%/K)	RESISTANCE (Ω)			TEMP. ERROR (K)
			MIN.	TYP.	MAX.	
−55	−67	0.97	489	512	536	±4.92
−50	−58	0.96	514	538	561	±4.56
−40	−40	0.93	567	591	616	±4.42
−30	−22	0.91	623	648	673	±4.28
−20	−4	0.88	683	709	734	±4.12
−10	14	0.85	747	773	799	±3.96
0	32	0.83	814	840	867	±3.79
10	50	0.80	885	912	938	±3.59
20	68	0.78	960	986	1012	±3.39
25	77	0.76	1000	1025	1050	±3.27
30	86	0.75	1037	1065	1092	±3.43
40	104	0.73	1115	1146	1178	±3.76
50	122	0.71	1196	1232	1267	±4.1
60	140	0.69	1280	1321	1361	±4.45
70	158	0.67	1368	1413	1459	±4.83
80	176	0.65	1458	1509	1560	±5.21
90	194	0.63	1552	1609	1666	±5.62
100	212	0.61	1648	1712	1775	±6.04
110	230	0.60	1748	1818	1889	±6.47
120	248	0.58	1851	1929	2006	±6.92
125	257	0.57	1904	1985	2066	±7.15
130	266	0.57	1957	2042	2128	±7.38
140	284	0.55	2066	2160	2253	±7.87
150	302	0.54	2178	2280	2383	±8.36
160	320	0.52	2293	2405	2517	±8.87
170	338	0.51	2411	2533	2655	±9.4
175	347	0.51	2471	2598	2725	±9.67

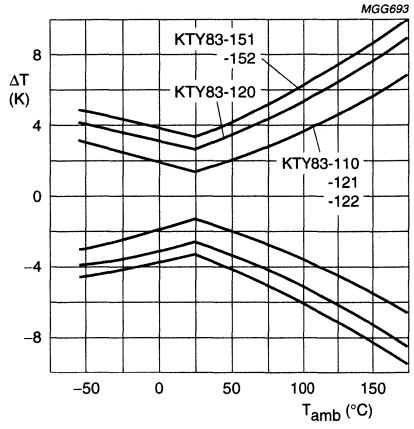

Fig.2 Maximum expected temperature error (ΔT).

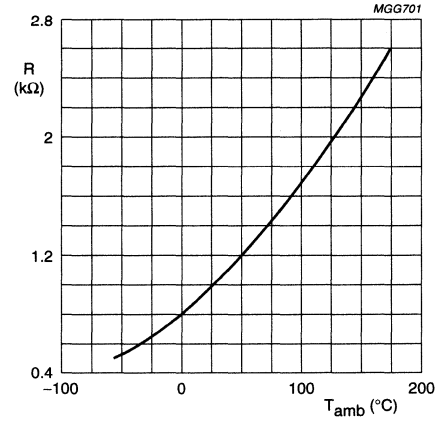

I_{cont} = 1 mA.

Fig.3 Sensor resistance as a function of ambient temperature; average values.

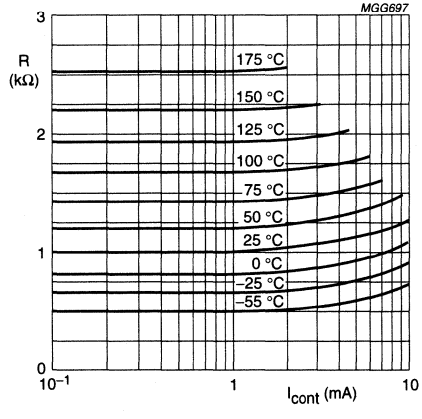

To keep the temperature error low, an operating current of I_{cont} = 1 mA is recommended for temperatures above 100 °C.

Fig.4 Sensor resistance as a function of operating current.

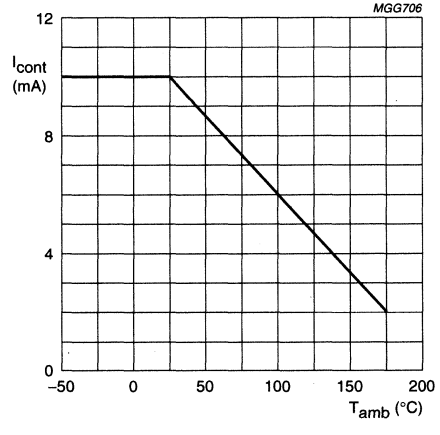

Fig.5 Maximum operating current for safe operation.

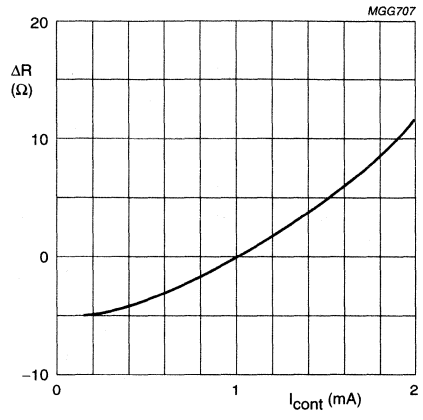

T_{amb} = 25 °C.

Fig.6 Deviation of sensor resistance as a function of operating current in still liquid.

APPLICATION INFORMATION

SYMBOL	PARAMETER	CONDITIONS	TYP.	UNIT
ΔR_{25}	drift of sensor resistance at 25 °C	10000 hours continuous operation; T_{amb} = 175 °C	1	Ω

PACKAGE OUTLINE

Hermetically sealed glass package; axial leaded; 2 leads **SOD68**

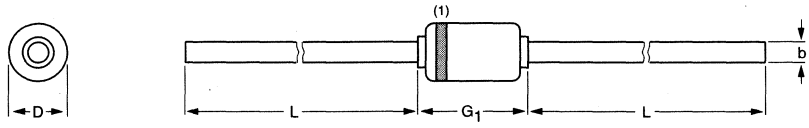

DIMENSIONS (mm are the original dimensions)

UNIT	b max.	D max.	G_1 max.	L min.
mm	0.55	1.6	3.04	25.4

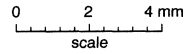

Note

1. The marking band indicates the cathode.

OUTLINE VERSION	REFERENCES				EUROPEAN PROJECTION	ISSUE DATE
	IEC	JEDEC	EIAJ			
SOD68		DO-34				97-06-09

Silicon temperature sensors KTY84-1 series

DESCRIPTION

The temperature sensors in the KTY84-1 series have a positive temperature coefficient of resistance and are suitable for use in measurement and control systems over a temperature range of −40 to +300 °C. The sensors are encapsulated in the SOD68 (DO-34) leaded package.

Tolerances of 0.5% or other special selections are available on request.

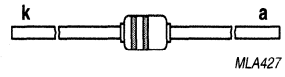

The first (green) band indicates the negative connection.
The second (coloured) band provides type identity.
The sensor must be operated with the lower potential at the marked connection.

Fig.1 Simplified outline (SOD68; DO-34).

MARKING

TYPE NUMBER	MARKING BAND COLOUR
KTY84-130	yellow
KTY84-150	grey
KTY84-151	black
KTY84-152	blue

QUICK REFERENCE DATA

SYMBOL	PARAMETER	CONDITIONS	MIN.	MAX.	UNIT
R_{100}	sensor resistance	T_{amb} = 100 °C; I_{cont} = 2 mA			
	KTY84-130		970	1030	Ω
	KTY84-150		950	1050	Ω
	KTY84-151		950	1000	Ω
	KTY84-152		1000	1050	Ω
T_{amb}	ambient operating temperature		−40	+300	°C

LIMITING VALUES

In accordance with the Absolute Maximum Rating System (IEC 134).

SYMBOL	PARAMETER	CONDITIONS	MIN.	MAX.	UNIT
I_{cont}	continuous sensor current	in free air; T_{amb} = 25 °C; note 1	–	10	mA
		in free air; T_{amb} = 300 °C	–	2	mA
T_{amb}	ambient operating temperature		−40	+300	°C
T_{stg}	storage temperature		−55	+300	°C

Note

1. For temperatures greater than 200 °C, a sensor current of I_{cont} = 2 mA must be used.

CHARACTERISTICS

T_{amb} = 100 °C, in liquid, unless otherwise specified.

SYMBOL	PARAMETER	CONDITIONS	MIN.	TYP.	MAX.	UNIT
R_{100}	sensor resistance	I_{cont} = 2 mA				
	KTY84-130		970	–	1030	Ω
	KTY84-150		950	–	1050	Ω
	KTY84-151		950	–	1000	Ω
	KTY84-152		1000	–	1050	Ω
TC	temperature coefficient		–	0.61	–	%/K
R_{250}/R_{100}	resistance ratio	T_{amb} = 250 °C and 100 °C	2.111	2.166	2.221	
R_{25}/R_{100}	resistance ratio	T_{amb} = 25 °C and 100 °C	0.595	0.603	0.611	
τ	thermal time constant; note 1	in still air	–	20	–	s
		in still liquid; note 2	–	1	–	s
		in flowing liquid; note 2	–	0.5	–	s
	rated temperature range		−40	–	+300	°C

Notes

1. The thermal time constant is the time taken for the sensor to reach 63.2% of the total temperature difference. For example, if a sensor with a temperature of 25 °C is moved to an environment with an ambient temperature of 100 °C, the time for the sensor to reach a temperature of 72.4 °C is the thermal time constant.
2. Inert liquid, e.g. FC43 manufactured by the 3M company.

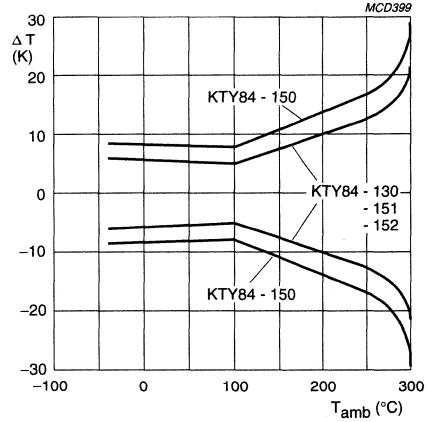

Fig.2 Maximum expected temperature error (ΔT).

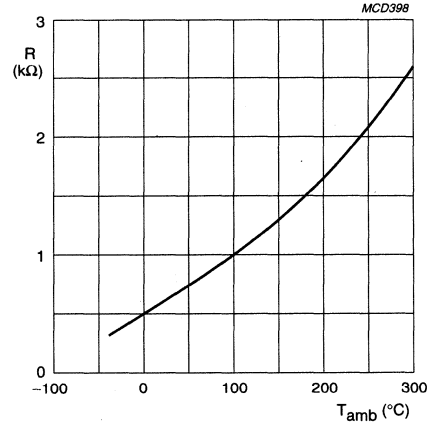

I_{cont} = 2 mA.

Fig.3 Sensor resistance as a function of ambient temperature; average values.

Table 1 Ambient temperature, corresponding resistance, temperature coefficient and maximum expected temperature error for KTY84-130 and KTY84-150

I_{cont} = 2 mA.

AMBIENT TEMPERATURE		TEMP. COEFF.	KTY84-130				KTY84-150			
(°C)	(°F)	(%/K)	RESISTANCE (Ω)			TEMP. ERROR (K)	RESISTANCE (Ω)			TEMP. ERROR (K)
			MIN.	TYP.	MAX.		MIN.	TYP.	MAX.	
−40	−40	0.84	340	359	379	±6.48	332	359	386	±8.85
−30	−22	0.83	370	391	411	±6.36	362	391	419	±8.76
−20	−4	0.82	403	424	446	±6.26	394	424	455	±8.7
−10	14	0.80	437	460	483	±6.16	428	460	492	±8.65
0	32	0.79	474	498	522	±6.07	464	498	532	±8.61
10	50	0.77	514	538	563	±5.98	503	538	574	±8.58
20	68	0.75	555	581	607	±5.89	544	581	618	±8.55
25	77	0.74	577	603	629	±5.84	565	603	641	±8.54
30	86	0.73	599	626	652	±5.79	587	626	665	±8.53
40	104	0.71	645	672	700	±5.69	632	672	713	±8.5
50	122	0.70	694	722	750	±5.59	679	722	764	±8.46
60	140	0.68	744	773	801	±5.47	729	773	817	±8.42
70	158	0.66	797	826	855	±5.34	781	826	872	±8.37
80	176	0.64	852	882	912	±5.21	835	882	929	±8.31
90	194	0.63	910	940	970	±5.06	891	940	989	±8.25
100	212	0.61	970	1000	1030	±4.9	950	1000	1050	±8.17
110	230	0.60	1029	1062	1096	±5.31	1007	1062	1117	±8.66
120	248	0.58	1089	1127	1164	±5.73	1067	1127	1187	±9.17
130	266	0.57	1152	1194	1235	±6.17	1128	1194	1259	±9.69
140	284	0.55	1216	1262	1309	±6.63	1191	1262	1334	±10.24
150	302	0.54	1282	1334	1385	±7.1	1256	1334	1412	±10.8
160	320	0.53	1350	1407	1463	±7.59	1322	1407	1492	±11.37
170	338	0.52	1420	1482	1544	±8.1	1391	1482	1574	±11.96
180	356	0.51	1492	1560	1628	±8.62	1461	1560	1659	±12.58
190	374	0.49	1566	1640	1714	±9.15	1533	1640	1747	±13.2
200	392	0.48	1641	1722	1803	±9.71	1607	1722	1837	±13.85
210	410	0.47	1719	1807	1894	±10.28	1683	1807	1931	±14.51
220	428	0.46	1798	1893	1988	±10.87	1760	1893	2026	±15.19
230	446	0.45	1879	1982	2085	±11.47	1839	1982	2125	±15.88
240	464	0.44	1962	2073	2184	±12.09	1920	2073	2226	±16.59
250	482	0.44	2046	2166	2286	±12.73	2003	2166	2329	±17.32
260	500	0.42	2132	2261	2390	±13.44	2087	2261	2436	±18.15
270	518	0.41	2219	2357	2496	±14.44	2172	2357	2543	±19.36
280	536	0.38	2304	2452	2600	±15.94	2255	2452	2650	±21.21
290	554	0.34	2384	2542	2700	±18.26	2333	2542	2751	±24.14
300	572	0.29	2456	2624	2791	±22.12	2404	2624	2844	±29.05

Table 2 Ambient temperature, corresponding resistance, temperature coefficient and maximum expected temperature error for KTY84-151 and KTY84-152

I_{cont} = 2 mA.

AMBIENT TEMPERATURE		TEMP. COEFF.	KTY84-151				KTY84-152			
(°C)	(°F)	(%/K)	RESISTANCE (Ω)			TEMP. ERROR (K)	RESISTANCE (Ω)			TEMP. ERROR (K)
			MIN.	TYP.	MAX.		MIN.	TYP.	MAX.	
–40	–40	0.84	332	350	368	±5.97	350	368	386	±5.82
–30	–22	0.83	362	381	399	±5.84	381	400	419	±5.69
–20	–4	0.82	394	414	433	±5.72	415	435	455	±5.57
–10	14	0.80	428	449	469	±5.62	451	472	492	±5.46
0	32	0.79	464	486	507	±5.51	489	511	532	±5.35
10	50	0.77	503	525	547	±5.41	530	552	574	±5.25
20	68	0.75	544	566	589	±5.31	573	595	618	±5.14
25	77	0.74	565	588	611	±5.25	595	618	641	±5.08
30	86	0.73	587	610	633	±5.2	618	641	665	±5.03
40	104	0.71	632	656	679	±5.08	665	689	713	±4.91
50	122	0.70	679	704	728	±4.96	715	740	764	±4.78
60	140	0.68	729	754	778	±4.83	767	792	817	±4.64
70	158	0.66	781	806	831	±4.68	822	847	872	±4.5
80	176	0.64	835	860	885	±4.53	879	904	929	±4.34
90	194	0.63	891	916	942	±4.37	938	963	989	±4.17
100	212	0.61	950	975	1000	±4.19	1000	1025	1050	±3.99
110	230	0.60	1007	1036	1064	±4.58	1060	1089	1117	±4.37
120	248	0.58	1067	1099	1131	±4.99	1123	1155	1187	±4.77
130	266	0.57	1128	1164	1199	±5.41	1187	1223	1259	±5.19
140	284	0.55	1191	1231	1271	±5.84	1254	1294	1334	±5.62
150	302	0.54	1256	1300	1345	±6.3	1322	1367	1412	±6.07
160	320	0.53	1322	1372	1421	±6.77	1392	1442	1492	±6.53
170	338	0.52	1391	1445	1500	±7.25	1464	1519	1574	±7.01
180	356	0.51	1461	1521	1581	±7.75	1538	1599	1659	±7.51
190	374	0.49	1533	1599	1664	±8.27	1614	1681	1747	±8.02
200	392	0.48	1607	1679	1751	±8.81	1692	1765	1837	±8.55
210	410	0.47	1683	1761	1839	±9.36	1772	1852	1931	±9.09
220	428	0.46	1760	1846	1931	±9.93	1854	1940	2026	±9.66
230	446	0.45	1839	1932	2024	±10.51	1937	2031	2125	±10.23
240	464	0.44	1920	2021	2121	±11.11	2022	2125	2226	±10.83
250	482	0.44	2003	2112	2220	±11.73	2110	2220	2329	±11.44
260	500	0.42	2087	2205	2321	±12.42	2198	2318	2436	±12.12
270	518	0.41	2172	2298	2424	±13.37	2288	2416	2543	±13.06
280	536	0.38	2257	2391	2525	±14.79	2376	2513	2650	±14.46
290	554	0.34	2335	2479	2622	±16.98	2459	2606	2751	±16.61
300	572	0.29	2406	2558	2710	±20.61	2533	2689	2844	±20.18

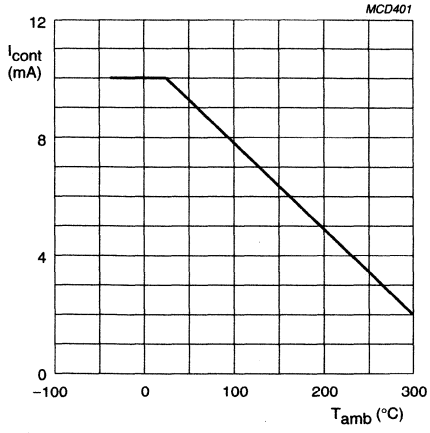

Fig.4 Maximum operating current for safe operation.

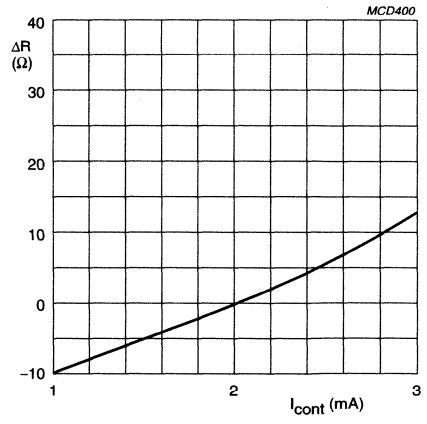

T_{amb} = 100 °C.

Fig.5 Deviation of sensor resistance as a function of operating current in still liquid.

PACKAGE OUTLINE

Hermetically sealed glass package; axial leaded; 2 leads **SOD68**

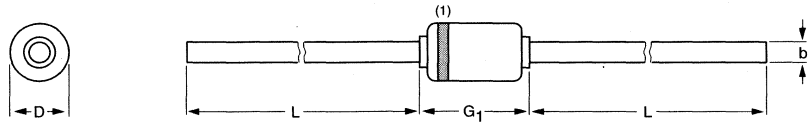

DIMENSIONS (mm are the original dimensions)

UNIT	b max.	D max.	G_1 max.	L min.
mm	0.55	1.6	3.04	25.4

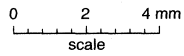

Note

1. The marking band indicates the cathode.

OUTLINE VERSION	REFERENCES				EUROPEAN PROJECTION	ISSUE DATE
	IEC	JEDEC	EIAJ			
SOD68		DO-34				97-06-09

Silicon temperature sensors KTY85-1 series

DESCRIPTION

The temperature sensors in the KTY85-1 series have a positive temperature coefficient of resistance and are suitable for use in measurement and control systems. The sensors are encapsulated in the SOD80 glass SMD package.

Tolerances of 0.5% or other special selections are available on request.

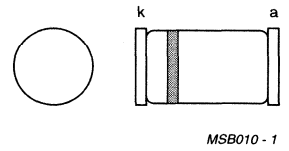

MSB010 - 1

The coloured marking band indicates the negative connection and the product type.

The sensor must be operated with the lower potential at the marked connection.

Fig.1 Simplified outline (SOD80).

MARKING

TYPE NUMBER	MARKING BAND COLOUR
KTY85-110	yellow
KTY85-120	red
KTY85-121	white
KTY85-122	green
KTY85-150	grey
KTY85-151	black
KTY85-152	blue

QUICK REFERENCE DATA

SYMBOL	PARAMETER	CONDITIONS	MIN.	MAX.	UNIT
R_{25}	sensor resistance	T_{amb} = 25 °C; I_{cont} = 1 mA			
	KTY85-110		990	1010	Ω
	KTY85-120		980	1020	Ω
	KTY85-121		980	1000	Ω
	KTY85-122		1000	1020	Ω
	KTY85-150		950	1050	Ω
	KTY85-151		950	1000	Ω
	KTY85-152		1000	1050	Ω
T_{amb}	ambient operating temperature		−40	+125	°C

LIMITING VALUES

In accordance with the Absolute Maximum Rating System (IEC 134).

SYMBOL	PARAMETER	CONDITIONS	MIN.	MAX.	UNIT
I_{cont}	continuous sensor current	in free air; T_{amb} = 25 °C	–	10	mA
		in free air; T_{amb} = 125 °C	–	2	mA
T_{amb}	ambient operating temperature		−40	+125	°C

CHARACTERISTICS

T_{amb} = 25 °C, in liquid, unless otherwise specified.

SYMBOL	PARAMETER	CONDITIONS	MIN.	TYP.	MAX.	UNIT
R_{25}	sensor resistance	I_{cont} = 1 mA				
	KTY85-110		990	–	1010	Ω
	KTY85-120		980	–	1020	Ω
	KTY85-121		980	–	1000	Ω
	KTY85-122		1000	–	1020	Ω
	KTY85-150		950	–	1050	Ω
	KTY85-151		950	–	1000	Ω
	KTY85-152		1000	–	1050	Ω
TC	temperature coefficient		–	0.76	–	%/K
R_{100}/R_{25}	resistance ratio	T_{amb} = 100 °C and 25 °C	1.65	1.67	1.69	
R_{-40}/R_{25}	resistance ratio	T_{amb} = −40 °C and 25 °C	0.569	0.577	0.585	
τ	thermal time constant; note 1	in still air	–	20	–	s
		in still liquid; note 2	–	1	–	s
		in flowing liquid; note 2	–	0.5	–	s
	rated temperature range		−40	–	+125	°C

Notes

1. The thermal time constant is the time taken for the sensor to reach 63.2% of the total temperature difference. For example, if a sensor with a temperature of 25 °C is moved to an environment with an ambient temperature of 100 °C, the time for the sensor to reach a temperature of 72.4 °C is the thermal time constant.
2. Inert liquid, e.g. FC43 manufactured by the 3M company.

Table 1 Ambient temperature, corresponding resistance, temperature coefficient and maximum expected temperature error for KTY85-110 and KTY85-120

I_{cont} = 1 mA.

AMBIENT TEMPERATURE		TEMP. COEFF.	KTY85-110				KTY85-120			
(°C)	(°F)	(%/K)	RESISTANCE (Ω)			TEMP. ERROR (K)	RESISTANCE (Ω)			TEMP. ERROR (K)
			MIN.	TYP.	MAX.		MIN.	TYP.	MAX.	
−40	−40	0.93	562	577	592	±2.81	556	577	598	±3.88
−30	−22	0.91	617	632	647	±2.62	611	632	654	±3.72
−20	−4	0.88	677	691	706	±2.42	670	691	713	±3.56
−10	14	0.85	740	754	768	±2.2	732	754	776	±3.37
0	32	0.83	807	820	833	±1.97	798	820	841	±3.18
10	50	0.80	877	889	902	±1.72	868	889	910	±2.97
20	68	0.78	951	962	973	±1.45	942	962	983	±2.74
25	77	0.76	990	1000	1010	±1.31	980	1000	1020	±2.62
30	86	0.75	1027	1039	1050	±1.44	1017	1039	1060	±2.77
40	104	0.73	1105	1118	1132	±1.7	1093	1118	1143	±3.07
50	122	0.71	1185	1202	1219	±1.98	1173	1202	1231	±3.39
60	140	0.69	1268	1288	1309	±2.27	1255	1288	1321	±3.73
70	158	0.67	1355	1379	1402	±2.58	1341	1379	1416	±4.08
80	176	0.65	1445	1472	1500	±2.9	1430	1472	1515	±4.44
90	194	0.63	1537	1569	1601	±3.24	1522	1569	1617	±4.82
100	212	0.61	1633	1670	1707	±3.59	1617	1670	1723	±5.22
110	230	0.60	1732	1774	1816	±3.95	1714	1774	1834	±5.63
120	248	0.58	1834	1882	1929	±4.34	1815	1882	1948	±6.06
125	257	0.57	1886	1937	1987	±4.53	1867	1937	2006	±6.28

Table 2 Ambient temperature, corresponding resistance, temperature coefficient and maximum expected temperature error for KTY85-121 and KTY85-122

I_{cont} = 1 mA.

AMBIENT TEMPERATURE		TEMP. COEFF.	KTY85-121				KTY85-122			
(°C)	(°F)	(%/K)	RESISTANCE (Ω)			TEMP. ERROR (K)	RESISTANCE (Ω)			TEMP. ERROR (K)
			MIN.	TYP.	MAX.		MIN.	TYP.	MAX.	
−40	−40	0.93	556	571	586	±2.81	567	583	598	±2.81
−30	−22	0.91	611	626	641	±2.62	624	639	654	±2.62
−20	−4	0.88	670	685	699	±2.42	684	698	713	±2.42
−10	14	0.85	732	746	760	±2.2	747	762	776	±2.2
0	32	0.83	799	812	825	±1.97	815	828	842	±1.97
10	50	0.80	868	880	893	±1.72	886	898	911	±1.72
20	68	0.78	942	953	963	±1.45	961	972	983	±1.45
25	77	0.76	980	990	1000	±1.31	1000	1010	1020	±1.31
30	86	0.75	1017	1028	1039	±1.44	1038	1049	1060	±1.44
40	104	0.73	1094	1107	1121	±1.7	1116	1130	1144	±1.7
50	122	0.71	1173	1190	1206	±1.98	1197	1214	1231	±1.98
60	140	0.69	1256	1276	1295	±2.27	1281	1301	1322	±2.27
70	158	0.67	1341	1365	1388	±2.58	1368	1392	1416	±2.58
80	176	0.65	1430	1458	1485	±2.9	1459	1487	1515	±2.9
90	194	0.63	1522	1554	1585	±3.24	1553	1585	1617	±3.24
100	212	0.61	1617	1653	1690	±3.59	1650	1687	1724	±3.59
110	230	0.60	1715	1756	1798	±3.95	1750	1792	1834	±3.95
120	248	0.58	1816	1863	1910	±4.34	1853	1900	1948	±4.34
125	257	0.57	1867	1917	1967	±4.53	1905	1956	2007	±4.53

Table 3 Ambient temperature, corresponding resistance, temperature coefficient and maximum expected temperature error for KTY85-150 and KTY85-151

I_{cont} = 1 mA.

AMBIENT TEMPERATURE		TEMP. COEFF.	KTY85-150				KTY85-151			
(°C)	(°F)	(%/K)	RESISTANCE (Ω)			TEMP. ERROR (K)	RESISTANCE (Ω)			TEMP. ERROR (K)
			MIN.	TYP.	MAX.		MIN.	TYP.	MAX.	
−40	−40	0.93	539	577	615	±7.1	539	562	586	±4.42
−30	−22	0.91	592	632	673	±7.04	593	617	641	±4.28
−20	−4	0.88	649	691	734	±6.97	650	674	699	±4.12
−10	14	0.85	710	754	798	±6.9	710	735	760	±3.96
0	32	0.83	774	820	866	±6.81	774	799	824	±3.79
10	50	0.80	842	889	937	±6.72	842	867	892	±3.59
20	68	0.78	913	962	1012	±6.61	914	938	963	±3.39
25	77	0.76	950	1000	1050	±6.55	950	975	1000	±3.27
30	86	0.75	986	1039	1091	±6.76	987	1013	1039	±3.43
40	104	0.73	1060	1118	1177	±7.19	1061	1090	1120	±3.76
50	122	0.71	1137	1202	1267	±7.63	1138	1172	1206	±4.1
60	140	0.69	1217	1288	1360	±8.1	1218	1256	1295	±4.45
70	158	0.67	1300	1379	1457	±8.58	1301	1344	1387	±4.83
80	176	0.65	1386	1472	1559	±9.07	1387	1435	1484	±5.21
90	194	0.63	1475	1569	1664	±9.59	1476	1530	1584	±5.62
100	212	0.61	1566	1670	1773	±10.12	1568	1628	1688	±6.04
110	230	0.60	1661	1774	1887	±10.66	1663	1730	1796	±6.47
120	248	0.58	1759	1882	2004	±11.22	1761	1835	1908	±6.92
125	257	0.57	1809	1937	2064	±11.51	1811	1888	1966	±7.15

Table 4 Ambient temperature, corresponding resistance, temperature coefficient and maximum expected temperature error for KTY85-152

I_{cont} = 1 mA.

AMBIENT TEMPERATURE		TEMP. COEFF.	KTY85-152			
(°C)	(°F)	(%/K)	RESISTANCE (Ω)			TEMP. ERROR (K)
			MIN.	TYP.	MAX.	
−40	−40	0.93	567	591	616	±4.42
−30	−22	0.91	623	648	673	±4.28
−20	−4	0.88	683	709	734	±4.12
−10	14	0.85	747	773	799	±3.96
0	32	0.83	814	840	867	±3.79
10	50	0.80	885	912	938	±3.59
20	68	0.78	960	986	1012	±3.39
25	77	0.76	1000	1025	1050	±3.27
30	86	0.75	1037	1065	1092	±3.43
40	104	0.73	1115	1146	1178	±3.76
50	122	0.71	1196	1232	1267	±4.1
60	140	0.69	1280	1321	1361	±4.45
70	158	0.67	1368	1413	1459	±4.83
80	176	0.65	1458	1509	1560	±5.21
90	194	0.63	1552	1609	1666	±5.62
100	212	0.61	1648	1712	1775	±6.04
110	230	0.60	1748	1818	1889	±6.47
120	248	0.58	1851	1929	2006	±6.92
125	257	0.57	1904	1985	2066	±7.15

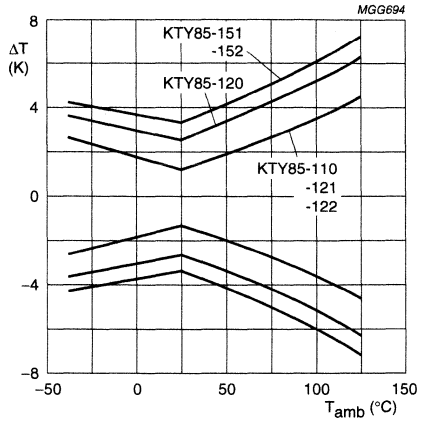

Fig.2 Maximum expected temperature error (ΔT).

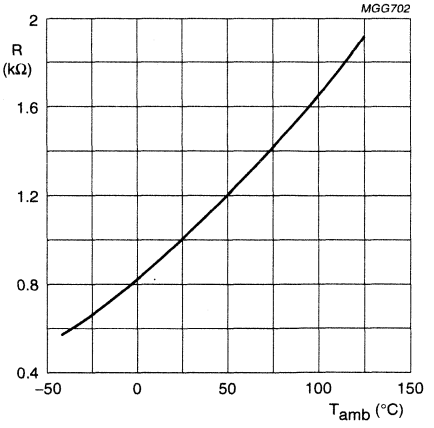

I_{cont} = 1 mA.

Fig.3 Sensor resistance as a function of ambient temperature; average values.

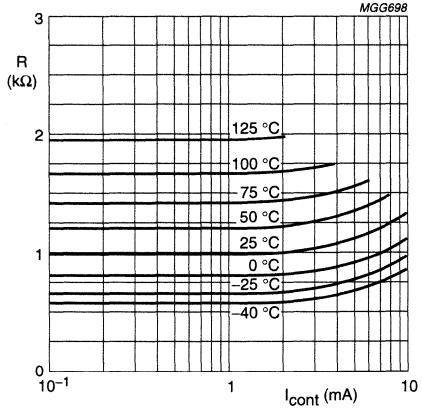

To keep the temperature error low, an operating current of I_{cont} = 1 mA is recommended for temperatures above 100 °C.

Fig.4 Sensor resistance as a function of operating current.

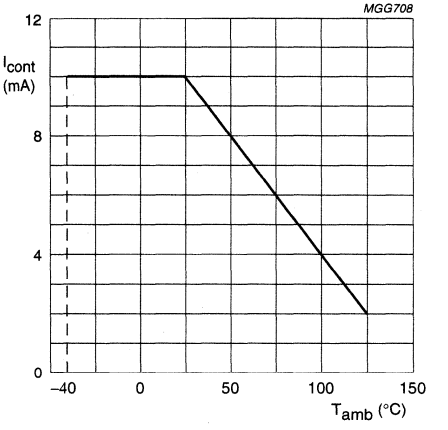

Fig.5 Maximum operating current for safe operation.

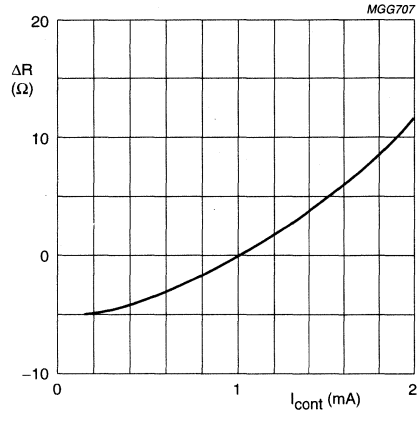

T_{amb} = 25 °C.

Fig.6 Deviation of sensor resistance as a function of operating current in still liquid.

APPLICATION INFORMATION

SYMBOL	PARAMETER	CONDITIONS	TYP.	UNIT
ΔR_{25}	drift of sensor resistance at 25 °C	10000 hours continuous operation; T_{amb} = 125 °C	1	Ω

PACKAGE OUTLINE

Hermetically sealed glass surface mounted package; 2 connectors **SOD80**

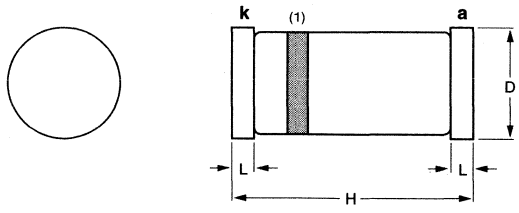

DIMENSIONS (mm are the original dimensions)

UNIT	D	H	L
mm	1.7 1.5	3.7 3.3	0.3

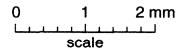

Note

1. The marking band indicates the cathode.

OUTLINE VERSION	REFERENCES				EUROPEAN PROJECTION	ISSUE DATE
	IEC	JEDEC	EIAJ			
SOD80	100H02					97-06-20

DATA HANDBOOK SYSTEM

Data handbook system

DATA HANDBOOK SYSTEM

Philips Semiconductors data handbooks contain all pertinent data available at the time of publication and each is revised and reissued regularly.

Loose data sheets are sent to subscribers to keep them up-to-date on additions or alterations made during the lifetime of a data handbook.

Catalogues are available for selected product ranges (some catalogues are also on floppy discs).

Our data handbook titles are listed here.

Integrated circuits

Book	*Title*
IC01	Semiconductors for Radio, Audio and CD/DVD Systems
IC02	Semiconductors for Television and Video Systems
IC03	Semiconductors for Wired Telecom Systems
IC04	HE4000B Logic Family CMOS
IC05	Advanced Low-power Schottky (ALS) Logic
IC06	High-speed CMOS Logic Family
IC11	General-purpose/Linear ICs
IC12	I^2C Peripherals
IC13	Programmable Logic Devices (PLD)
IC14	8048-based 8-bit Microcontrollers
IC15	FAST TTL Logic Series
IC16	CMOS ICs for Clocks, Watches and Real Time Clocks
IC17	Semiconductors for Wireless Communications
IC18	Semiconductors for In-Car Electronics
IC19	ICs for Data Communications
IC20	80C51-based 8-bit Microcontrollers
IC22	Multimedia ICs
IC23	BiCMOS Bus Interface Logic
IC24	Low Voltage CMOS & BiCMOS Logic
IC25	16-bit 80C51XA Microcontrollers (eXtended Architecture)
IC26	Integrated Circuit Packages
IC27	Complex Programmable Logic Devices

Discrete semiconductors

Book	*Title*
SC01	Small-signal and Medium-power Diodes
SC02	Power Diodes
SC03	Power Thyristors and Triacs
SC04	Small-signal Transistors
SC05	Video Transistors and Modules for Monitors
SC06	High-voltage and Switching NPN Power Transistors
SC07	Small-signal Field-effect Transistors
SC13	PowerMOS Transistors
SC14	RF Wideband Transistors
SC16	Wideband Hybrid Amplifier Modules for CATV
SC17	Semiconductor Sensors
SC18	Discrete Semiconductor Packages
SC19	RF & Microwave Power Transistors, RF Power Modules and Circulators/Isolators

MORE INFORMATION FROM PHILIPS SEMICONDUCTORS?

For more information about Philips Semiconductors data handbooks, catalogues and subscriptions contact your nearest Philips Semiconductors national organization, select from the **address list on the back cover of this handbook.** Product specialists are at your service and enquiries are answered promptly.

OVERVIEW OF PHILIPS COMPONENTS DATA HANDBOOKS

Our sister product division, Philips Components, also has a comprehensive data handbook system to support their products. Their data handbook titles are listed here.

Display components

Book	*Title*
DC01	Colour Television Tubes
DC02	Monochrome Monitor Tubes and Deflection Units
DC03	Television Tuners, Coaxial Aerial Input Assemblies
DC04	Colour Monitor and Multimedia Tubes
DC05	Wire Wound Components

Magnetic products

MA01	Soft Ferrites
MA03	Piezoelectric Ceramics Specialty Ferrites
MA04	Dry-reed Switches

Passive components

PA01	Electrolytic Capacitors
PA02	Varistors, Thermistors and Sensors
PA03	Potentiometers
PA04	Variable Capacitors
PA05	Film Capacitors
PA06	Ceramic Capacitors
PA06a	Surface Mounted Ceramic Multilayer Capacitors
PA06b	Leaded Ceramic Capacitors
PA08	Fixed Resistors
PA10	Quartz Crystals
PA11	Quartz Oscillators

MORE INFORMATION FROM PHILIPS COMPONENTS?

For more information contact your nearest Philips Components national organization shown in the following list.

Australia: North Ryde, Tel. +61 2 9805 4455, Fax. +61 2 9805 4466
Austria: Wien, Tel. +43 1 60 101 12 41, Fax. +43 1 60 101 12 11
Belarus: Minsk, Tel. +375 172 200 924/733, Fax. +375 172 200 773
Benelux: Eindhoven, Tel. +31 40 2783 749, Fax. +31 40 2788 399
Brazil: São Paolo, Tel. +55 11 821 2333, Fax. +55 11 829 1849
Canada: Scarborough, Tel. 1 416 292 5161, Fax. 1 416 754 6248
China: Shanghai, Tel. +86 21 6354 1088, Fax. +86 21 6354 1060
Denmark: Copenhagen, Tel. +45 32 883 333, Fax. +45 31 571 949
Finland: Espoo, Tel. 358 9 615 800, Fax. 358 9 615 80510
France: Suresnes, Tel. +33 1 4099 6161, Fax. +33 1 4099 6493
Germany: Hamburg, Tel. +49 40 2489-0, Fax. +49 40 2489 1400
Greece: Tavros, Tel. +30 1 4894 339/+30 1 4894 239, Fax. +30 1 4814 240
Hong Kong: Kowloon, Tel. +852 2784 3000, Fax. +852 2784 3003
India: Mumbai, Tel. +91 22 4930 311, Fax. +91 22 4930 966/4950 304
Indonesia: Jakarta, Tel. +62 21 794 0040, Fax. +62 21 794 0080
Ireland: Dublin, Tel. +353 1 7640 203, Fax. +353 1 7640 210
Israel: Tel Aviv. Tel. +972 3 6450 444, Fax. +972 3 6491 007
Italy: Milano, Tel. +39 2 6752 2531, Fax. +39 2 6752 2557
Japan: Tokyo, Tel. +81 3 3740 5135, Fax. +81 3 3740 5035
Korea (Republic of): Seoul, Tel. +82 2 709 1472, Fax. +82 2 709 1480
Malaysia: Pulau Pinang, Tel. +60 3 750 5213, Fax. +60 3 757 4880
Mexico: El Paso, Tel. +52 915 772 4020, Fax. +52 915 772 4332
New Zealand: Auckland, Tel. +64 9 815 4000, Fax. +64 9 849 7811
Norway: Oslo, Tel. +47 22 74 8000, Fax. +47 22 74 8341
Pakistan: Karachi, Tel. +92 21 587 4641-49,
Fax. +92 21 577 035/+92 21 587 4546
Philippines: Manila, Tel. +63 2 816 6345, Fax. +63 2 817 3474
Poland: Warszawa, Tel. +48 22 612 2594, Fax. +48 22 612 2327
Portugal: Linda-A-Velha, Tel. +351 1 416 3160/416 3333,
Fax. +351 1 416 3174/416 3366
Russia: Moscow, Tel. +7 95 755 6918, Fax. +7 95 755 6919
Singapore: Singapore, Tel. +65 350 2000, Fax. +65 355 1758
South Africa: Johannesburg, Tel. +27 11 470 5911, Fax. +27 11 470 5494
Spain: Barcelona, Tel. +34 3 301 63 12, Fax. +34 3 301 42 43
Sweden: Stockholm, Tel. +46 8 5985 2000, Fax. +46 8 5985 2745
Switzerland: Zürich, Tel. +41 1 488 22 11, Fax. +41 1 481 7730
Taiwan: Taipei, Tel. +886 2 2134 2900, Fax. +886 2 2134 2929
Thailand: Bangkok, Tel. +66 2 745 4090, Fax. +66 2 398 0793
Turkey: Istanbul, Tel. +90 212 279 2770, Fax. +90 212 282 6707
United Kingdom: Dorking, Tel. +44 1306 512 000, Fax. +44 1306 512 345
United States:

- Ann Arbor, Tel. +1 734 996 9400, Fax. +1 734 761 2776
- Saugerties, Tel. +1 914 246 2811, Fax. +1 914 246 0487
- San Jose, Tel. +1 408 570 5600, Fax. +1 408 570 5700

Yugoslavia (Federal Republic of): Belgrade,
Tel. +381 11 625 344/373, Fax. +381 11 635 777
Internet:

- Passive Components: www.passives.comp.philips.com

For all other countries apply to:
Philips Components, Marketing Communications, Building BF-1,
P.O. Box 218, 5600 MD EINDHOVEN, The Netherlands,
Fax. +31-40-2724547.

North American Sales Offices, Representatives and Distributors

PHILIPS SEMICONDUCTORS
811 East Arques Avenue
P.O. Box 3409
Sunnyvale, CA 94088-3409

ALABAMA
Huntsville
Philips Semiconductors
Phone: (256) 464-9101
(256) 464-0111

Elcom, Inc.
Phone: (256) 830-4001

ARIZONA
Scottsdale
Thom Luke Sales, Inc.
Phone: (602) 451-5400

Tempe
Philips Semiconductors
Phone: (602) 820-2225

CALIFORNIA
Calabasas
Philips Semiconductors
Phone: (818) 880-6304

Centaur Corporation
Phone: (818) 878-5800

Granite Bay
B.A.E. Sales, Inc.
Phone: (916) 652-6777

Irvine
Philips Semiconductors
Phone: (714) 453-0770

Centaur Corporation
Phone: (714) 261-2123

San Diego
Philips Semiconductors
Phone: (619) 560-0242

Centaur Corporation
Phone: (619) 278-4950

San Jose
B.A.E. Sales, Inc.
Phone: (408) 452-8133

Sunnyvale
Philips Semiconductors
Phone: (408) 991-3737

COLORADO
Englewood
Philips Semiconductors
Phone: (303) 792-9011

Thom Luke Sales, Inc.
Phone: (303) 649-9717

CONNECTICUT
Wallingford
JEBCO, Inc.
Phone: (203) 265-1318

FLORIDA
(Norcross, Georgia)
Elcom, Inc.
Phone: (770) 447-8200

GEORGIA
Norcross
Elcom, Inc.
Phone: (770) 447-8200

IDAHO
(Englewood, Colorado)
Thom Luke Sales, Inc.
Phone: (303) 649-9717

ILLINOIS
Itasca
Philips Semiconductors
Phone: (630) 250-0050

INDIANA
Indianapolis
Mohrfield Marketing, Inc.
Phone: (317) 546-6969

Kokomo
Philips Semiconductors
Phone: (765) 459-5355

Leo
Mohrfield Marketing, Inc.
Phone: (219) 627-5355

KANSAS
(Bloomington, Minnesota)
High Technology Sales, Inc.
Phone: (612) 844-9933

KENTUCKY
(Indianapolis, Indiana)
Mohrfield Marketing, Inc.
Phone: (317) 546-6969

MARYLAND
(Rockville Centre, New York)
S-J Associates, Inc.
Phone: (516) 536-4242

MASSACHUSETTS
Chelmsford
JEBCO, Inc.
Phone: (978) 256-5800

Westford
Philips Semiconductors
Phone: (978) 692-6211

MICHIGAN
Farmington Hills
Philips Semiconductors
Phone: (248) 848-7600

Novi
Mohrfield Marketing, Inc.
Phone: (248) 380-8100

MINNESOTA
Bloomington
High Technology Sales, Inc.
Phone: (612) 844-9933

MISSOURI
(Bloomington, Minnesota)
High Technology Sales, Inc.
Phone: (612) 844-9933

NEBRASKA
(Bloomington, Minnesota)
High Technology Sales, Inc.
Phone: (612) 844-9933

NEW JERSEY
Toms River
Philips Semiconductors
Phone: (732) 505-1200
(732) 240-1479

NEW MEXICO
(Scottsdale, Arizona)
Thom Luke Sales, Inc.
Phone: (602) 451-5400

NEW YORK
Rockville Centre
S-J Associates, Inc.
Phone: (516) 536-4242

(Chelmsford, Massachusetts)
JEBCO, Inc.
Phone: (978) 256-5800

NORTH CAROLINA
Cary
Philips Semiconductors
Phone: (919) 462-1332
(919) 462-6361

Raleigh
Elcom, Inc.
Phone: (919) 743-5200

OHIO
(Indianapolis, Indiana)
Mohrfield Marketing, Inc.
Phone: (317) 546-6969

OKLAHOMA
(Richardson, Texas)
OM Associates, Inc.
Phone: (972) 690-96746

OREGON
Beaverton
Philips Semiconductors
Phone: (503) 627-0110

Cascade-Tech
Phone: (503) 645-9660

PENNSYLVANIA
(Indianapolis, Indiana)
Mohrfield Marketing, Inc.
Phone: (317) 546-6969

(Rockville Centre, New York)
S-J Associates, Inc.
Phone: (516) 536-4242

TENNESSEE
Dandridge
Philips Semiconductors
Phone: (423) 397-5557

TEXAS
Austin
OM Associates, Inc.
Phone: (512) 794-9971

Houston
Philips Semiconductors
Phone: (281) 999-1316

OM Associates, Inc.
Phone: (281) 376-6400

Richardson
Philips Semiconductors
Phone: (972) 644-1610

OM Associates, Inc.
Phone: (972) 690-6746

VIRGINIA
(Rockville Centre, New York)
S-J Associates, Inc.
Phone: (516) 536-4242

WISCONSIN
(Bloomington, Minnesota)
High Technology Sales, Inc.
Phone: (612) 844-9933

WASHINGTON
Kirkland
Cascade-Tech
Phone: (425) 822-7299

CANADA
PHILIPS SEMICONDUCTORS CANADA, LTD.

Calgary, Alberta
Tech-Trek, Ltd.
Phone: (403) 291-6866

Kanata, Ontario
Tech-Trek, Ltd.
Phone: (613) 599-8787

Mississauga, Ontario
Tech-Trek, Ltd.
Phone: (905) 238-0366

Richmond, B.C.
Tech-Trek, Ltd.
Phone: (604) 276-8735

Ville St. Laurent, Quebec
Tech-Trek, Ltd.
Phone: (514) 337-7540

MEXICO
Guadalajara
Mepco Centralab, Inc./Philips
Phone: 8-011-52-3-122-2325

Monterrey
Mepco Centralab, Inc./Philips
Phone: 8-011-52-8-399-0164

El Paso, TX
Philips Components
Phone: (915) 772-4020

PUERTO RICO
(Norcross, Georgia)
Elcom, Inc.
Phone: (770) 447-8200

DISTRIBUTORS

Contact one of our local distributors:
Allied Electronics
Arrow Electronics
Future Electronics
Hamilton Hallmark
Marshall Industries
Newark Electronics
Penstock
Richardson Electronics
Zeus Electronics

06/11/98

Philips Semiconductors – a worldwide company

Argentina: see South America

Australia: 34 Waterloo Road, NORTH RYDE, NSW 2113,
Tel. +61 2 9805 4455, Fax. +61 2 9805 4466

Austria: Computerstr. 6, A-1101 WIEN, P.O. Box 213, Tel. +43 160 1010,
Fax. +43 160 101 1210

Belarus: Hotel Minsk Business Center, Bld. 3, r. 1211, Volodarski Str. 6,
220050 MINSK, Tel. +375 172 200 733, Fax. +375 172 200 773

Belgium: see The Netherlands

Brazil: see South America

Bulgaria: Philips Bulgaria Ltd., Energoproject, 15th floor,
51 James Bourchier Blvd., 1407 SOFIA,
Tel. +359 2 689 211, Fax. +359 2 689 102

Canada: PHILIPS SEMICONDUCTORS/COMPONENTS, Tel. +1 800 234 7381

China/Hong Kong: 501 Hong Kong Industrial Technology Centre,
72 Tat Chee Avenue, Kowloon Tong, HONG KONG,
Tel. +852 2319 7888, Fax. +852 2319 7700

Colombia: see South America

Czech Republic: see Austria

Denmark: Prags Boulevard 80, PB 1919, DK-2300 COPENHAGEN S,
Tel. +45 32 88 2636, Fax. +45 31 57 0044

Finland: Sinikalliontie 3, FIN-02630 ESPOO,
Tel. +358 9 615800, Fax. +358 9 61580920

France: 51 Rue Carnot, BP317, 92156 SURESNES Cedex,
Tel. +33 1 40 99 6161, Fax. +33 1 40 99 6427

Germany: Hammerbrookstraße 69, D-20097 HAMBURG,
Tel. +49 40 23 53 60, Fax. +49 40 23 536 300

Greece: No. 15, 25th March Street, GR 17778 TAVROS/ATHENS,
Tel. +30 1 4894 339/239, Fax. +30 1 4814 240

Hungary: see Austria

India: Philips INDIA Ltd, Band Box Building, 2nd floor,
254-D, Dr. Annie Besant Road, Worli, MUMBAI 400 025,
Tel. +91 22 493 8541, Fax. +91 22 493 0966

Indonesia: PT Philips Development Corporation, Semiconductors Division,
Gedung Philips, Jl. Buncit Raya Kav.99-100, JAKARTA 12510,
Tel. +62 21 794 0040 ext. 2501, Fax. +62 21 794 0080

Ireland: Newstead, Clonskeagh, DUBLIN 14,
Tel. +353 1 7640 000, Fax. +353 1 7640 200

Israel: RAPAC Electronics, 7 Kehilat Saloniki St, PO Box 18053,
TEL AVIV 61180, Tel. +972 3 645 0444, Fax. +972 3 649 1007

Italy: PHILIPS SEMICONDUCTORS, Piazza IV Novembre 3, 20124 MILANO,
Tel. +39 2 6752 2531, Fax. +39 2 6752 2557

Japan: Philips Bldg 13-37, Kohnan 2-chome, Minato-ku, TOKYO 108-8507,
Tel. +81 3 3740 5130, Fax. +81 3 3740 5077

Korea: Philips House, 260-199 Itaewon-dong, Yongsan-ku, SEOUL,
Tel. +82 2 709 1412, Fax. +82 2 709 1415

Malaysia: No. 76 Jalan Universiti, 46200 PETALING JAYA, SELANGOR,
Tel. +60 3 750 5214, Fax. +60 3 757 4880

Mexico: 5900 Gateway East, Suite 200, EL PASO, TEXAS 79905,
Tel. +9-5 800 234 7381

Middle East: see Italy

Netherlands: Postbus 90050, 5600 PB EINDHOVEN, Bldg. VB,
Tel. +31 40 27 82785, Fax. +31 40 27 88399

New Zealand: 2 Wagener Place, C.P.O. Box 1041, AUCKLAND,
Tel. +64 9 849 4160, Fax. +64 9 849 7811

Norway: Box 1, Manglerud 0612, OSLO,
Tel. +47 22 74 8000, Fax. +47 22 74 8341

Pakistan: see Singapore

Philippines: Philips Semiconductors Philippines Inc.,
106 Valero St. Salcedo Village, P.O. Box 2108 MCC, MAKATI, Metro MANILA,
Tel. +63 2 816 6380, Fax. +63 2 817 3474

Poland: Ul. Lukiska 10, PL 04-123 WARSZAWA,
Tel. +48 22 612 2831, Fax. +48 22 612 2327

Portugal: see Spain

Romania: see Italy

Russia: Philips Russia, Ul. Usatcheva 35A, 119048 MOSCOW,
Tel. +7 095 755 6918, Fax. +7 095 755 6919

Singapore: Lorong 1, Toa Payoh, SINGAPORE 319762,
Tel. +65 350 2538, Fax. +65 251 6500

Slovakia: see Austria

Slovenia: see Italy

South Africa: S.A. PHILIPS Pty Ltd., 195-215 Main Road Martindale,
2092 JOHANNESBURG, P.O. Box 7430 Johannesburg 2000,
Tel. +27 11 470 5911, Fax. +27 11 470 5494

South America: Al. Vicente Pinzon, 173, 6th floor, 04547-130 SÃO PAULO, SP,
Brazil, Tel. +55 11 821 2333, Fax. +55 11 821 2382

Spain: Balmes 22, 08007 BARCELONA,
Tel. +34 93 301 6312, Fax. +34 93 301 4107

Sweden: Kottbygatan 7, Akalla, S-16485 STOCKHOLM,
Tel. +46 8 5985 2000, Fax. +46 8 5985 2745

Switzerland: Allmendstrasse 140, CH-8027 ZÜRICH,
Tel. +41 1 488 2741 Fax. +41 1 488 3263

Taiwan: Philips Semiconductors, 6F, No. 96, Chien Kuo N. Rd., Sec. 1, TAIPEI,
Taiwan Tel. +886 2 2134 2865, Fax. +886 2 2134 2874

Thailand: PHILIPS ELECTRONICS (THAILAND) Ltd.,
209/2 Sanpavuth-Bangna Road Prakanong, BANGKOK 10260,
Tel. +66 2 745 4090, Fax. +66 2 398 0793

Turkey: Talatpasa Cad. No. 5, 80640 GÜLTEPE/ISTANBUL,
Tel. +90 212 279 2770, Fax. +90 212 282 6707

Ukraine: PHILIPS UKRAINE, 4 Patrice Lumumba str., Building B, Floor 7,
252042 KIEV, Tel. +380 44 264 2776, Fax. +380 44 268 0461

United Kingdom: Philips Semiconductors Ltd., 276 Bath Road, Hayes,
MIDDLESEX UB3 5BX, Tel. +44 181 730 5000, Fax. +44 181 754 8421

United States: 811 East Arques Avenue, SUNNYVALE, CA 94088-3409,
Tel. +1 800 234 7381

Uruguay: see South America

Vietnam: see Singapore

Yugoslavia: PHILIPS, Trg N. Pasica 5/v, 11000 BEOGRAD,
Tel. +381 11 625 344, Fax.+381 11 635 777

For all other countries apply to: Philips Semiconductors, International Marketing & Sales Communications, Building BE-p, P.O. Box 218, 5600 MD EINDHOVEN, The Netherlands, Fax. +31 40 27 24825

Internet: http://www.semiconductors.philips.com

Printed in USA

115105/24.7M/ed04/pp312

Date of release: July 1998

Document order number: 9397 750 03589